Deltares

Enabling Delta Life

Comparative Assessment of Drought Hazard and Risk Modeling Tools

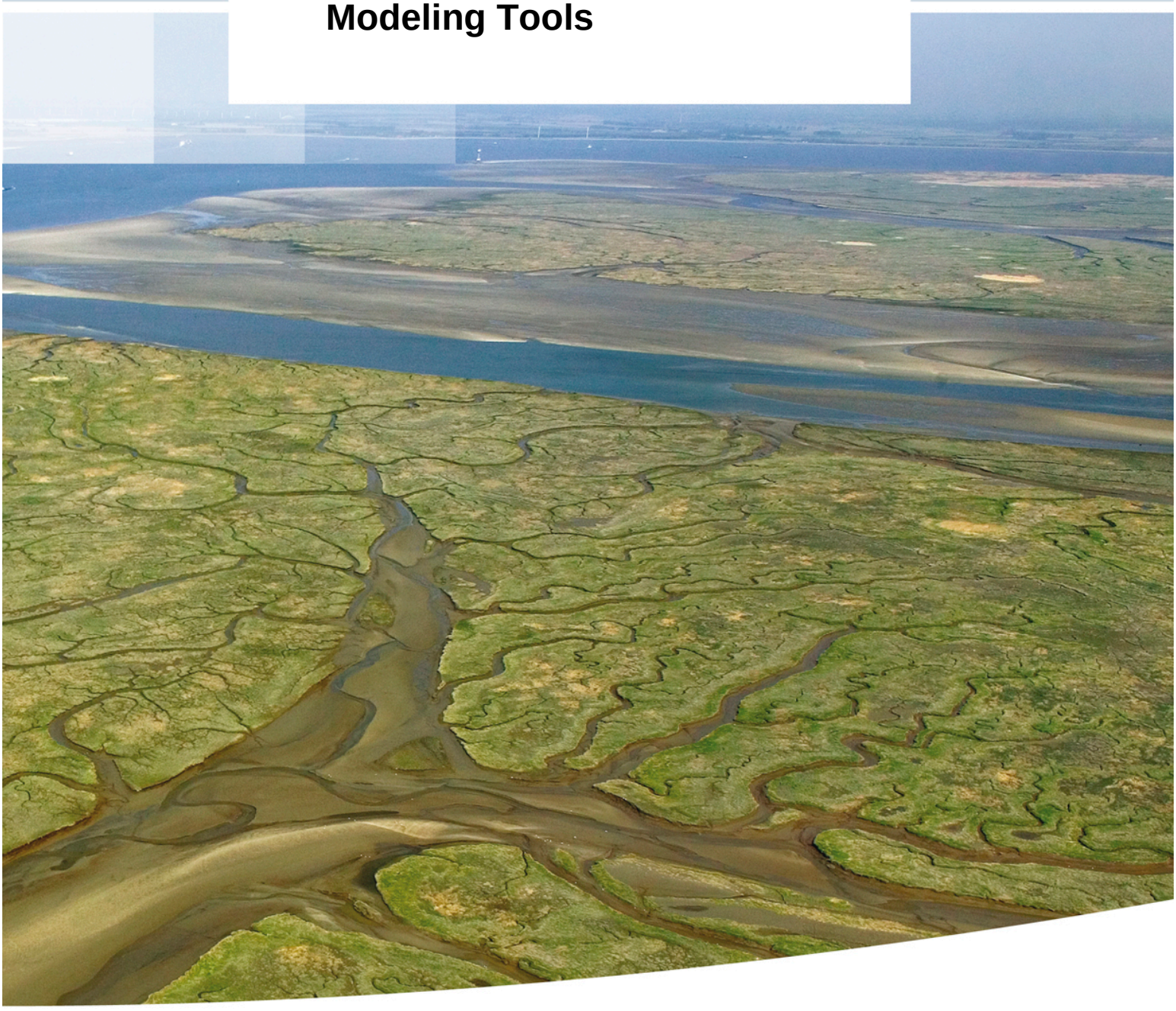

Deltares

Comparative Assessment of Drought Hazard and Risk Modeling Tools

11200758-002

© Deltares, 2018, B

Deltares

Title
Comparative Assessment of Drought Hazard and Risk Modeling Tools

Project	Attribute	Pages
11200758-002	11200758-002-ZWS-0003	4

Keywords
Drought, risk, hazard, global, Afghanistan, Colombia, Ethiopia, Fiji, Malawi, indices, modeling tools, big data, detection and forecasting

Version	Date	Author	Initials	Review	Initials	Approval	Initials
	Nov. 2018	dr. D.M.D. Hendriks (Deltares)		Sophie Vermooten			
		dr. P. Trambauer (Deltares)					
		dr. M. Mens (Deltares)					
		S. Galvis Rodriguez (Deltares)					
		dr. M. Werner (IHE-Delft)					
		dr. S. Maskey (IHE-Delft)					
		dr. M. Svoboda (NDMC)					
		dr. T. Tadesse (NDMC)					
		dr. T. Veldkamp (VU-IVM)					
		dr. C. Funk (UCSB)					
		dr. S. Shukla (UCSB)					

Status
final

Abbreviations

A&L	Agricultural crop and livestock production
ADB	Asian Development Bank
ADO	African Drought Observatory
ANDMA	Afghanistan National Disaster Management Authority
ASI	Agricultural Stress Index
BCM	Billion cubic meters
CA	Central Asia
CAF	Corporación Andina de Fomento, Latin American development bank
CFSv2	Coupled forecast system model version 2
CHIRPS	Climate Hazards Group InfraRed Precipitation with Station data
CPC	Climate Prediction Center
CRU	Climate Research Unit
CSC	Climate Services Centre
CSIRO	Commonwealth Scientific and Industrial Research Organisation
CVC	Corporación Autonoma del Valle de Cauca
DIR	Drought impact reporter
DVI	Drought Vulnerability Index
eMODIS	EROS Moderate Resolution Imaging Spectroradiometer
ECMWF	European Centre for Medium-Range Weather Forecasts
ECON	Overall economy
EM-DAT	Emergency Events Database
EN	El Niño
ENA	Estudio Nacional de Agua
ENSO	El Niño–Southern Oscillation
ERA	Evaluación Regional de Agua
ESP	Ensemble Streamflow Prediction
ET	Evapotranspiration
EU-WATCH	EU FP6 Project Water and Global Change
FAO	Food and Agriculture Organization of the United Nations
FEWS	Flood Early Warning System
FEWS NET	Famine Early Warning Systems Network
GCM's	Global Circulation Models
GDP	Gross domestic product
GeoCLIM	Climdata climate data archive format
GET-D	GOES Evapotranspiration and drought
GFDRR	Global Facility for Disaster Reduction and Recovery
GFS	Global Forecast System
GHACOF	Greater Horn of Africa Climate Outlook Forum
GHMs	Global Hydrological Models
GLS	Global Land Surface

GOES	Geostationary Operational Environmental Satellite system
GRDC	Global Runoff Data Centre
HEC-HMS	Hydrologic Modeling System
HYDR	Hydropower production
ICPAC	IGAD Climate Prediction and Application Centre
IDEAM	Colombian national Institute of Meteorology, hydrology and environmental studies
IGAD	Inter-Governmental Authority on Development
IOD	Indian Ocean dipole
IRI	International Research Institute for Climate and Society
ITHACA	Information Technology for Humanitarian Assistance, Cooperation and Action
ITCZ	Inter-Tropical Convergence Zone
IWMI	International Water Management Institute
JAS	July-August-September
JFM	January-February-March
JJA	June-July-August
JMA	Japan Meteorological Agency
JRC	Joint Research Centre
LN	La Niña
m.s.l	Mean sea level
M&IWN	Municipal and industrial water needs
MJO	Madden-Julian Oscillation
MODIS	Moderate Resolution Imaging Spectroradiometer
N	Neutral
NCAR	National Center for Atmospheric Research
NDVI	Normalized Difference Vegetation Index
NDMC	National Disaster Management Commission
NDMO	National Disaster Management Office
NDRRP	National Disaster Risk Reduction Platform
NMA	National Meteorology Agency
NMME	National Multi-model Ensemble
NOAA	National Oceanic and Atmospheric Administration
PCR-GLOBWB	PCRaster Global Water Balance
PDSI	Palmer Drought Severity Index
POP	Impact category population
QBO	Quasi Biennial Oscillation
SADC	Southern African Development
SARCOF	Southern African Regional Climate Outlook Forum
sc-PDSI	Self-Calibrated Palmer Drought Severity Index
SMDI	Soil moisture deficit index
SNAP	Strategic National Action Plan
SPCZ	South Pacific Climate Zone
SPEI	Standardized Precipitation Evapotranspiration Index
SPI	Standardized Precipitation Index

SSEBop	Simplified Surface Energy Balance model
SSFI	Standardized Streamflow Index
SST	Sea surface temperature
UCAR	University Corporation for Atmospheric Research
UNGRD	Unidad Nacional para la Gestión del Riesgo de Desastres
USAID	United States Agency for International Development
USGS	United States Geological Survey
VegDRI	Vegetation Drought Response Index
VPA	Vegetation Productivity Anomaly
WASP	Weighted Anomaly Standardized Precipitation Index
WaterGAP	Water - Global Analysis and Prognosis
WCI	Water Cycle Integrator
WRI	World Resources Institute
WSI	Water scarcity index

Contents

1. Executive summary

1.1 Introduction

Multiple models, methods and tools are available for hazard monitoring and risk assessment. This is especially true for drought. Over the past few years, numerous new products have been developed that enable the monitoring of drought from satellite observations; map drought levels using hydrological models; and compute physical, economic and humanitarian impacts of drought. In spite of all these possibilities, there is currently no comprehensive inventory and comparison of the available data and tools. It is, therefore, currently very difficult to decide on the appropriate model or tool for a specific drought-related application, and to find these models and underlying data to perform the assessment. As a result, drought hazard monitoring programs and drought risk assessment studies may often use sub-optimal approaches and spend substantial resources on finding the appropriate modeling tools.

The main purpose of this report is an evaluation of available drought hazard and risk modeling tools and other resources that are available at the global scale for their suitability to be applied for drought hazard mapping and hotspot identification, drought risk assessments and drought detection and forecasting. This report describes a quantitative and qualitative comparative assessment of a selection of drought hazard and risk modeling tools and resources that are available from the global drought inventory as developed by the GFDRR (Deltares, 2018). Not all modeling tools and resources collected in the global drought inventory were taken up in these analyses. Only modeling tools and resources that are available online, free of cost, and have global coverage were assessed. The reason for these selection criteria is that the results of this study should be applicable for all users in all countries of the world. However, for the review and qualitative comparison of drought monitoring and forecasting systems, regional and national systems were also assessed.

1.2 Methods

The comparative assessment of drought hazard and risk modelling tools and resources consisted of the following components:

- A comparative spatial time-series analysis of drought hazard models.
    - Country scale comparison of global data sets.
    - Validation of global data with local time series.
    - Sensitivity to ENSO-driven hydro-climatic variability.
- A qualitative comparison of drought impact models.
- A review and qualitative comparison of drought detection and forecasting systems.

These analyses have been applied for the following five low- and medium-income case study countries: Afghanistan, Colombia, Ethiopia, Fiji, and Malawi. These countries were selected for their varying hydro-climatic, socioeconomic, and geographical characteristics. The methods of this assessment are applied to the selected countries, but are applicable to the entire world. For this purpose, the approach therefore relies to a large extent on globally available modelling tools and resources. Prior to the analyses listed above, each case study country was subjected to an assessment of drought related country characteristics and the Falkenmark index for water stress was computed. This information was required to interpret and validate the results of the analyses based on global modeling tools and resources.

1.2.1 Spatial time series analysis of global datasets

To assess the performance of meteorological and hydrological drought hazard indices available from online global datasets at a national and sub-national scale, comparative spatial time series analyses were done. First, the global datasets providing hazard indices are subjected to a spatio-temporal comparison. This was done for 16 available dataset-index combinations, covering 5 different datasets (Global Land Surface (GLS) from NCAR-UCAR, IRI data library, Global Drought Monitor, PCR-GLOBWB from Earth2Observe database, and WaterGAP from Earth2Observe database) and five drought indices (SPI3, SPI12, SPEI3, SPEI12, SSFI). Next, the two best performing global datasets (PCR-GLOBWB and WaterGap) were validated with local discharge measurement data. Finally, an analysis of ENSO on the frequency and intensity of the drought events was done.

1.2.2 Assessment of drought impact and risk platforms and data

With this assessment, we reviewed the quality and applicability of online available drought impact and risk platforms and datasets. Five available online platforms and datasets were assessed for their capacity to provide spatial drought impact and/or risk information: Global map of drought risk (JRC), IWMI water data portal, the Aqueduct Water Risk Atlas, the FAO Agricultural Stress Index, and the African Drought Observatory. The online platforms and datasets providing impact and risk information based on historical data were compared with information from the country descriptions and, where possible, with each other.

1.2.3 Qualitative assessment of forecasting and monitoring products

The forecasting and monitoring products used in the five case study countries were described and subjected to a qualitative analysis. We focussed on assessing the currently available operational systems that support decision processes on the management of drought conditions. We concentrate primarily on operational systems used at the national level either for monitoring drought conditions, as well as those available systems providing forecasts at the seasonal scale. Where relevant, forecasting systems at the regional scale (where region indicates a geographic region, such as Southern Africa) are included. The objective of this section is to provide insight into current practices in drought monitoring and forecasting in the case study countries, how these are used to support the management of drought events, the data and systems used and the efficiency and availability of information during drought events.

1.3 Conclusions and recommendations

1.3.1 Country characteristics and reported droughts

A concise but complete description of drought related country characteristics is an important starting point for a drought hazard and risk assessment as it provides much needed background information to interpret analyses results or for further drought risk assessments. In addition it reveals the existing level of drought knowledge in the country. The following characteristics provide the context for a drought assessment: socio-economic country characteristics, meteorological and hydrological characteristics, key characteristics of the natural environment and land use, information about water resources and demand, as well as historical droughts and drought impacts.

1.3.2 Comparison of global datasets

The various drought hazard indices based on the global datasets showed varying correspondence to the registered drought events. Also, the comparability of dataset-index combinations in detecting droughts varies between the case study countries. Based on our analysis, the SPEI3 index based on the WaterGAP dataset shows the best match with

registered droughts, followed by SPEI3 and indices based on the Global Drought Monitor and PCR-GLOBWB datasets.

Interestingly, the dataset-index combinations assessed in this project showed more or other drought hazards than were registered (45% false alarms). The dataset-index combination GLS-SPI3 and GLS-SPI12 resulted in a high level of false alarms for 3 out of the 5 case study countries, while the false alarm rate for WaterGAP-SSFI was relatively low. The overestimation of drought hazards can be caused by the specific critical threshold values set for the drought hazard indices or by a mismatch in the timing of the modelled drought hazards and the registered events. Moreover, the modelled droughts only represent the hazard aspect of drought risk, while for the registered droughts the exposure and vulnerability to drought are also important. Hence, a drought does not necessarily have to result in adverse impacts.

At the time of this research only meteorological drought and hydrological drought global spatio-temporal datasets were available. It is recommended that a similar analysis is made for agricultural drought and socio-economic drought if and when such datasets become available.

1.3.3 Validation of global datasets with local time series

Using the two global models in the different country scale case studies to validate its results with local time-series we do not find large consistent differences in performance. No single best model exists across all case study countries or even within each case study country. Overall, the global models perform well in representing the relative variability of droughts while the performance on simulating the absolute values is less good. Having such knowledge at hand, the global models can be safely applied in drought event detection and monitoring, but should be handled with care when applying them for water resources management purposes.

1.3.4 ENSO analysis

For most case study countries we find significant differences in drought frequency and exposure between El Niño/La Niña phases. Despite the significant anomalies in drought frequency and exposure, we do not always find a strong correlation between the continuous drought indicator values and the Japan Meteorological Agency (JMA SST) index. Low correlation results indicate that the identified variability in drought conditions cannot be explained merely by variations in the JMA SST; here drought variability is the result of a composite of actors. This is the case for example for Ethiopia and Malawi.

Whereas the country-scale anomalies are shown to be consistent across the two models investigated when looking at the meteorological drought indicators (SPI, SPEI), the results differ in most case studies for the SSFI indicator. This can be explained by the differences in routing routines and calibration between the two models and the level of variability incorporated within the two models. Looking at the spatially explicit anomalies in exposure and the spatial patterns of correlation we do see, however, that for most case studies investigated both models show a similar spatial pattern and that the choice of model does not significantly affect the outcomes.

In this assessment we only coupled the exposure to drought with the ENSO signal. However, ENSO is part of an ocean–atmospheric climate variability system that constitutes many more sub-regional systems and local circulation patterns like the Indian monsoon, Pacific/North America pattern, North Atlantic Oscillation, East Atlantic/West Russia pattern, Scandinavia pattern, which modulate the ENSO signal (Hannaford et al., 2011). Future research should

therefore look into the sensitivity of drought exposure to combinations of these systems, especially in areas that provide a relative low ENSO signal.

1.3.5 Assessment of drought impact and risk models

The five online platforms and datasets assessed for their capacity to provide spatial drought impact and/or risk information showed advantages and disadvantages. It was found that a diversity of approaches, underlying data, and spatial scales are used to create and present impact and risk. Some platforms/datasets show high spatial detail and focus on one or several specific drought impact indices (*IMWI, FAO platform*), while other platforms provide more generic and large scale information of abstract impact indices (*Global map of drought risk from JRC, African Drought Observatory),* and/or sectors (*Aqueduct)*. It is recommended that more uniformity in drought impact and risk indices and visualisation is promoted in order to increase comparability of products. Moreover, this will probably increase the level of understanding and utilization of the drought impact and risk information.

An important general observation during this project was the *unavailability of data about drought related impacts for relevant impact categories on a sub-national scale*. As a result, actual validation of the maps from the online platforms and datasets was not possible. For Malawi, an analysis of national and sub-national agricultural data could be made available based on information from FEWS NET. However, also in the case of Malawi, drought impact data on hydro-power and data on other relevant impact categories were not available. It is advised that a *separate investigation* is started to develop a methodology for collection of sub-national drought impacts in the main sectors and that effort is put into building a database for such data (historic impacts as well as exposure and vulnerability information). Such information could be added to the (existing) online platforms and databases to increase the reliability and relevance of the impact and risk maps.

1.3.6 Qualitative assessment of forecasting and monitoring products

Based on the qualitative analysis of existing drought monitoring and forecasting systems in the five case study countries, the following *key conclusions* are provided:

- Despite the existence of several global scale drought monitoring and forecasting systems, it is found that these systems are most mature in the countries where there are one or more national or regional agencies tasked with providing monitoring and forecasting information and where there are national or regionally focused versions of the global datasets.
- Of the five countries analysed, drought monitoring and forecasting systems are most limited in Afghanistan and most mature in Ethiopia.
- In general, most of the national and regional monitoring systems in the case study countries rely on FEWS data products among other products, and forecasting systems combine consensus forecasts (based on local experts assessments and statistics) with forecasts from global dynamical forecasts.

Based on this assessment, the following *recommendations* are provided for starting up or improving drought detection/early warning and forecasting systems:

- Appoint one or, preferably, several national and regional agencies with providing monitoring and forecasting information to authorities and the public. A strong national or regional agency mandated to provide operational drought monitoring and early warning products, is key.
- It is important that governments commit to multi-year collaboration so that the operational demonstration of monitoring and forecasting products has been realized.

Make sure that local agencies have the skill and infrastructure they need to keep the system operationally sustainable.

- In case there is a lack of understanding of the climate and drought sensitivity and exposure to different sectors, it is important that research is conducted to assess the drought characteristics and the level of drought predictability for a given country or region.
- Global systems are extremely valuable as they provide first cut monitoring and early warning product for the national and regional agencies, without them spending their computational resources. Here it is important that local/regional agencies have knowledge as well as easy and smooth access to global products.
- Monitoring and forecasting products should be developed in close collaboration with the local/regional agencies. The agencies should be provided with the right tools, skills and datasets needed so they can best utilize their local expertise on monitoring and early warning. Assistance from international experts could be requested to set up and/or improve drought detection and forecasting systems.
- Importantly, drought detection and monitoring systems should connect closely to the questions and needs of local/regional agencies and other stakeholders. In doing so, data and derivative products from such a system can be packaged into usable impact information.

1 Introduction

1.4 Background

Multiple models, methods and tools are available for hazard monitoring and risk assessment. This is especially true for drought. Over the past few years, numerous new products have been developed that enable the monitoring of drought from satellite observations; map drought levels using hydrological models; and compute physical, economic and humanitarian impacts of drought. The products include academically published papers, online web platforms and operational tools.

In spite of all these possibilities, there is currently no comprehensive inventory and comparison of the available data and tools. It is, therefore, currently very difficult to decide on the appropriate model or tool for a specific drought-related application, and to find these models and underlying data to perform the assessment. As a result, drought hazard monitoring programs and drought risk assessment studies may often use sub-optimal approaches and spend substantial resources on finding the appropriate modeling tools.

The GFDRR aims to support professionals in assessing the drought hazard and risk in data-scarce environments with clear information and guidance documents. This is realized with the project “Global Inventory and Comparative Assessment of Drought Risk Modeling Tools”. The project starts with a thorough inventory of all relevant online platforms, newsletters/bulletins, datasets, indices and other relevant tools that can be used to detect and monitor drought risk in data scarce areas. In this project phase the drought risk models are subjected to a more detailed analysis. This analysis comprises a quantitative and qualitative comparative assessment of the ability of the models in capturing drought impacts for different impact categories: (i) population; (ii) municipal and industrial water needs; (iii) agricultural crop and livestock production; (iv) hydropower production; and (v) the overall economy (e.g. GDP). The analysis will be completed for five low- and medium-income countries that are subject to diverse climatic and socio-economic conditions (Afghanistan, Colombia, Ethiopia, Fiji, and Malawi). Subsequently, a set of representative drought events is defined, reflecting the typical drought type and severity in the case study countries, and covering the range of possible socioeconomic impacts and frequencies.

1.5 Purpose and use of this document

The main purpose of this report is an evaluation of available drought hazard and risk modeling tools and other resources that are available at the global scale for their suitability to be applied for drought hazard mapping and hotspot identification, drought risk assessments and drought detection and forecasting. This report describes a quantitative and qualitative comparative assessment of a selection of drought hazard and risk modeling tools and resources that are available from the global drought inventory as developed by the GFDRR (Deltares, 2018). This global inventory includes online platforms, newsletters/bulletins, datasets, indices, tools and modelling software. The collected drought risk modeling tools and resources cover a range of applications, including drought detection and forecasting, drought hazard mapping, as well as assessments of drought impacts and risks.

The comparative assessment described in this report consisted of the following components:

- A comparative spatial time-series analysis of drought hazard models;
- A qualitative comparison of drought impact models;
- A review and qualitative comparison of drought monitoring and forecasting systems.

Not all modeling tools and resources collected in the global drought inventory were taken up in these analyses. Only modeling tools and resources that are available online, free of cost, and have global coverage were assessed. The reason for this selection criteria is that the results of this study should be applicable for all users in all countries of the world. For the review and qualitative comparison of drought monitoring and forecasting systems, regional and national systems were also assessed.

These analyses have been applied for the following five low- and medium-income case study countries: Afghanistan, Colombia, Ethiopia, Fiji, and Malawi. These countries were selected for their varying hydro-climatic, socioeconomic and geographical characteristics. The methodology and results of this assessment were developed for the selected countries, but are applicable to the entire world. Therefore, for our purposes, the approach relies to a large extent on globally available data.

1.6 Reading guide

Chapter 2 describes the methods and data that were used to perform the comparative assessment of the pros and cons of the drought risk models identified within the global inventory of drought risk modeling tools. In the subsequent chapters (3-7), this approach is demonstrated for the five case study countries and the results of the various quantitative and qualitative comparative assessments are presented for each country. In Chapter 8 conclusions are drawn and recommendations are provided. In addition, the applicability of the results of the quantitative and qualitative comparative assessment described in this report for all countries in the world is explained.

2 Approach and Methods

This chapter describes the approach for the comparative assessment of the pros and cons of the drought risk models identified by the global inventory of drought hazard and risk modeling tools and resources (Deltares, 2018). The approach consists of several aspects and methods of drought risk analyses, which are described in the consecutive sections of this chapter:

1. Assessment of drought risk related country characteristics
2. Assessment of available drought hazard models
    - Comparison and validation of global drought hazard models at the country scale
    - Comparison of global drought hazard models with observed local data
    - ENSO analysis
3. Assessment of drought impact and risk platforms and datasets
4. Evaluation of forecasting and monitoring systems

2.1 Assessment of drought related country characteristics

The first step in a drought risk assessment consists of a concise description of drought related country characteristics, based on easily available information and expert knowledge. The goal is to assess the primary characteristics of the severity and frequency of droughts, drought exposure (water demand), water stress and drought vulnerability (potential economic losses, potential to cope with drought). An assessment contains information regarding the countries general characteristics, (location, size, population, governance aspects, economic activities), description of hydrogeology and water resources/water use, climate and an overview of reported historic drought events. For the five case study countries, the water availability relative to the water demand was evaluated using the Falkenmark Index (see section 2.1.1). Information about subnational levels of water stress can be taken from the Aqueduct Water Risk Atlas (Baseline Water Stress). An overview of reported historical droughts was based on the disaster impact database EM-DAT, which was also supplemented with online searches of historic droughts as reported by official institutions like the national meteorological institutes.

2.1.1 Relative water availability - Falkenmark Index

When describing water availability in a country, the Falkenmark Water Stress Indicator, which was developed by the Swedish water expert Falkenmark in 1989, is one of the most commonly used indicators. This index consists of the sum of the total yearly local runoff per country compared to estimates of population density. Hence, any influences of temperature on water demand are not taken into account. Water availability of more than 1,700 m^3/capita/year is defined as the threshold above which water shortage occurs only irregularly or locally. Below this level, water scarcity arises in different levels of severity. Below 1,700 m^3/capita/year water stress appears regularly, below 1,000m^3/capita/year water scarcity is a limitation to economic development and human health and well-being, and below 500 m^3/capita/year water availability is a primary constraint to life. Despite its global acceptance, this indicator has numerous shortcomings. First of all, only the renewable surface and groundwater flows in a country are considered. As such, transboundary water fluxes are not taken into account in this analysis. Moreover, the water availability per person is calculated as an average with regard to both the temporal and the spatial scale and thereby neglects water shortages in dry seasons or in certain regions within a country. A more detailed analysis on water scarcity conditions would require the use of the Water Scarcity Index (WSI, Liu et al.,

2017). However, computing this index requires the availability of (modelled) water demand estimates. Such estimates are usually not publicly available.

For our analysis, we used the Falkenmark Index with a threshold of 1700 m^3/cap/yr as a general indication to identify whether countries are in a (population-based) water scarcity status. The analysis was done for the five case study countries using both the PCR-GLOBWB and the WaterGAP spatio-temporal datasets. Historical population estimates for these countries for the period 1979-2010 were taken from Wada et al. (2011a, b), who derived yearly gridded population maps (0.5x0.5 degree) from yearly country-scale FAOSTAT data in combination with decadal gridded global population maps (Klein Goldewijk and van Drecht, 2006). Furthermore, it does not take water quality into account nor does it give information about a country's ability to use the resources. Even if a country has sufficient water according to the Falkenmark Indicator, these water resources may possibly be unused because of pollution or insufficient access. Values of water availability and water demand for selected countries are depicted in Figure 2.1Figure 2.1.

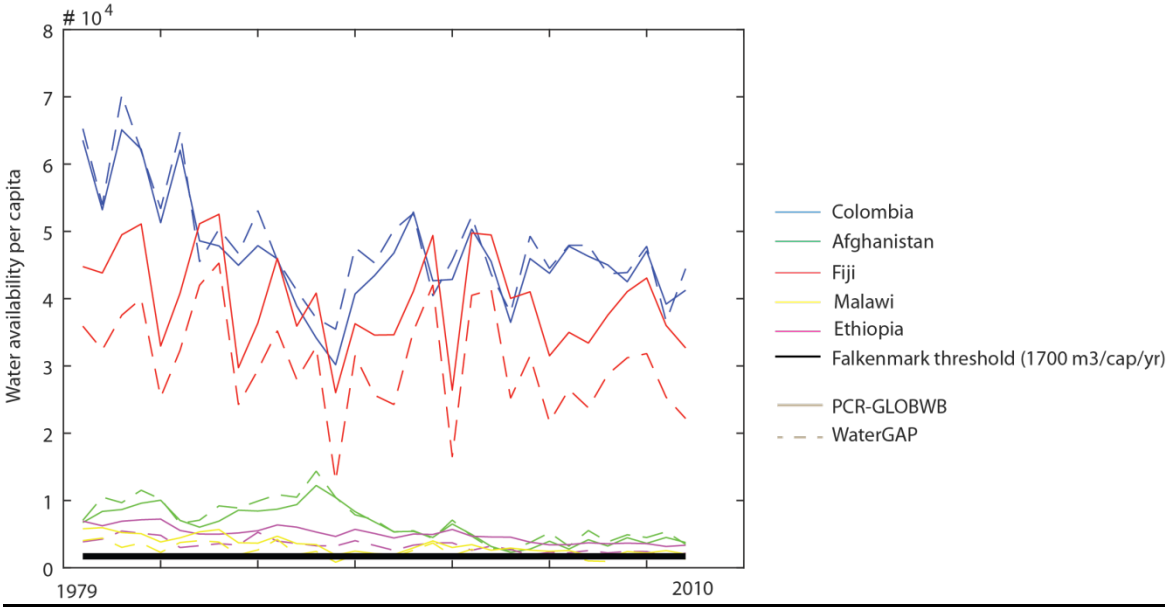

Figure 2.1 Time line of country-wide water scarcity estimates using the Falkenmark Index. Lines show the yearly water availability per capita in m3 whereas the coloured lines show the water availability for the different countries and the black line indicates the threshold for water scarcity: 1700 m3/cap/year. Dashed lines show the estimated values for WaterGAP whereas normal lines show the estimates for PCR-GLOBWB.

Figure 2.1Figure 2.1 shows the Falkenmark index on a yearly basis for the period 1979 to 2010. When looking at the graph we see that large variations exist in the available volume of water per capita per year. Whilst Colombia and Fiji have a relatively large source of water availability per capita, water availability per capita per year is significantly less for Afghanistan, Malawi and Ethiopia. These latter three countries are approaching or already crossing the critical threshold value of 1700 m3/cap/year when using the country-total values. All countries show, moreover, a decreasing trend, with less water availability per capita per year in more recent years compared to the start of the time-line for this analysis. This is due to a combination of increases in population density per country and changes in total yearly water availability. What can also be seen from the graph is that both Fiji and Colombia have a strong inter-annual fluctuation in their water availability per capita per year caused by the inter-annual variability in total water availability for these countries; influenced by large scale

atmospheric patterns like ENSO, whereas the water availability is relatively constant for the other countries. Estimates from the two model-inputs differ slightly with the WaterGAP (dashed lines) having relatively lower estimates for Fiji, Ethiopia, and Malawi. Estimates for Afghanistan and Colombia are very similar for the two models.

2.2 Spatial time series analysis of global datasets

In the second section, comparative spatial time series analyses are performed for the meteorological and hydrological hazard drought indices available online from global datasets. First, the global datasets providing hazard indices are subjected to a spatio-temporal comparison. Next, the global datasets are validated with local measurement data. Finally, an analysis of ENSO on the frequency and intensity of the drought events was done. The three elements of the spatial time series analysis are described in more detail below.

2.2.1 Country scale comparison of global datasets

National and sub-national droughts can be assessed based on available online spatio-temporal global datasets of drought indices. Here, we made a comparison of the drought hazard characteristics based on drought indices from five datasets that are freely available over the 30-year period 1983 - 2013: Standard precipitation Index (SPI) from Global Land Surface (NCAR-UCAR; Keyantash and John, 2018), SPI from the IRI data library, Standardised Precipitation-Evapotranspiration Index (SPEI) (Vincente et al., 2010) from the Global Drought Monitor, and SPI, SPEI, and Standardized Streamflow Index (SSFI) (Telesca et al, 2007) from PCR-GLOBWB (eg. Van Beek, 2007; Biekens and Van Beek, 2009) and WaterGap (eg. Lehner et al., 2006) (both available through the Earth2Observe WCI portal). Table 2.1Table 2.1 gives an overview of the 22 datasets and indices used in the analysis. The choice for these datasets was based on practical criteria ‘easy to obtain’, ‘widely used’, and ‘most promising – expert judgement’. More information about the specific drought indices, datasets, and platforms can be found through the online catalogue of drought hazard and risk modelling tools and resources[1].

Table 2.1 Overview of indicators available as global spatio-temporal dataset from five various platforms that were assessed.

	Global Land Surface (NCAR-UCAR)	IRI data library	Global Drought Monitor	PCR-GLOBWB (Earth2Observe)	WaterGAP (Earth2Observe)
SPI1		x		x	x
SPI3	x	x		x	x
SPI12	x	x		x	x
SPEI1			x	x	x
SPEI3			x	x	x
SPEI12			x	x	x
SSFI				x	x

For each country, we estimated the severity of droughts by computing the index levels at a monthly time scale for each grid cell: moderately dry (index value below -1), severely dry (index value below -1.5) and extremely dry (index value below -2) (McKee et al., 1993). Next, the percentage-area of the country falling into these drought classes was calculated. This

[1] *https://droughtcatalogue.com/*

gives an indication of the drought hazard in terms of both the severity and spatial extent of the drought hazard. The resulting time series were evaluated in two ways:

- Assessment of the overlap with droughts reported by EM-DAT and national services, providing a basic validation of the drought hazard models of the different datasets and indices:
  - Hit rate (percentage of registered drought events computed by the dataset-index combinations)
  - False alarm (percentage of droughts computed by the dataset-index combinations that do not match with a registered drought event)

- Assessment of the comparability of the indices between the different datasets, showing the level of agreement between datasets.

For this purpose the computed drought hazards were assigned to three categories:

- Pronounced drought (+): covering over 40% area of the country with extreme or severe drought for at least 3 months
- Moderate drought: (+/-): covering between 20% and 40% area of the country with extreme or severe drought for at least 3 months
- Limited drought (-): covering less than 20% area of the country with extreme or severe drought and/or for less than 3 months.

The analysis was done for all combinations of datasets and indices listed in Table 2.1Table 2.1, except for the SSP1 and SPEI1.

2.2.2 Validation of global data with local time series

For each of the selected countries we evaluated the performance of the datasets from the global repository with observational-based reference data. Here, we evaluated monthly discharge estimates from PCR-GLOBWB and WaterGAP against historical discharge observations from the Global Runoff Data Centre (GRDC)[2]. An assessment of monthly discharge estimates instead of monthly drought indicator values was performed in this evaluation since the drought indicator estimates need at least 30 years of data as input, which are often not available by the historical observations period of record. Comparing simulated drought indicators having a 30-year basis with observed drought indicators that use a different reference time-period would result in biased performance metrics.

As a reference dataset, we used all available discharge stations provided by the GRDC for each of the countries. Since length of the monitored time-series of each of the discharge observation stations varies, we applied a pair-wise comparison of the data. In doing so, some stations having more data-points may have been used to calculate the performance metrics compared to other stations. Table 2.2Table 2.2 provides an overview of the number of stations used for each of the countries and their mean, minimum and maximum length of time-series covered. As such, Table 2.2 shows that the length of available time-series varies significantly between the countries with a minimum of only two months of data-availability for one station in Afghanistan. Although stations with a limited number of data-points may not always be able to represent trends or variability correctly, they still give an insight into the overall correctness of the discharge estimates and how ‘off’ the models are when compared

[2] *http://www.bafg.de/GRDC/EN/Home/homepage_node.html*

to observations. Hence, we have taken all available data points into account when evaluating the performance of the models, despite their limited temporal availability.

Table 2.2 Overview of the availability of reference discharge data per country. The numbers between brackets indicate the number of stations with an upstream catchment area larger than 9,000 km2.

Country	**Number of stations**	**Mean length time-series (months)**	**Maximum length time-series (months)**	**Minimum length time-series (months)**
Afghanistan	9 (5)	16.6	21	2
Colombia	46 (-)	112.7	120	84
Ethiopia	38 (3)	84.7	327	24
Fiji	2 (-)	24	24	24
Malawi	47 (4)	95.1	11	154

Performance metrics that were used to evaluate the ability of the datasets that come from the global repository are the Pearson correlation coefficient and the Percent Bias. Although a multitude of performance metrics are available, these two indicators are widely used in the scientific literature and are good indicators aimed at giving a good indication of the ability of the model-datasets to: (1) give a good reflection of the seasonal and inter-annual variability of hydrological conditions (Pearson correlation coefficient); and (2) estimate the absolute discharges correctly (Percent Bias). Whilst for the purpose of drought identification and characterization having a good correlation coefficient might be sufficient, water managers dealing with the absolute deficits and measures to cope with it might be more interested in the ability of models to represent the actual values correctly.

2.2.3 ENSO analysis

Hydro-climatic variability linked by large scale oscillation mechanisms partly determines the temporal variations in hydrological conditions, which influences the occurrence and severity of droughts. Here we evaluated each of the selected countries to determine their sensitivity to ENSO-driven hydro-climatic variability. ENSO was chosen as an indicator for hydro-climatic variability as it is the most dominant signal of inter-annual climate variability (McPhaden et al., 2006). Moreover, different studies suggest that ENSO can be predicted with reasonable skill up to several seasons beforehand (Cheng et al., 2011; Ludescher et al, 2014), hence it can provide useful information for adaptation management to account for inter-annual variability in blue water resources and drought (Veldkamp et al., 2015). Different global studies have assessed the impacts of ENSO on drought before (Vicente-Serrano et al., 2011; Davey et al., 2014; Kumar et al., 2017; Wang-Chun Lai et al., 2018).

A country's sensitivity to ENSO driven hydro-climatic variability was assessed in multiple ways. First, we quantified the 'per country median area' exposed to droughts (SPI/SPEI/SSFI <-1) during El Niño, La Niña, or neutral years. Subsequently, we evaluated whether or not significant anomalies exist between these estimates of areas exposed to droughts during El Niño versus non-El Niño years, and during La Niña versus non-La Niña years. Secondly, we assessed per country in a spatially explicit manner whether or not the frequency of drought months differs significantly between El Niño and non-El Niño years and between La Niña and non-La Niña years. Differences within the frequency of drought months larger than 5% were considered here to be significant. Finally, we tested each country in a spatially explicit manner as to whether or not significant correlations exists between the continuous values of the different drought indicators (ranging from -3 to +3) and the monthly ENSO conditions. In order to do so we investigated various lag-time periods, ranging from 1 to 12 months. Results shown here are only for those months having the best correlation results.

We examined the relationship between drought conditions and ENSO driven climate variability by means of their correlation with the Japan Meteorological Agency's (JMA) Sea Surface Temperature (SST) anomaly index. To distinguish between El Niño, La Niña and neutral years, we used the classification of ENSO years from the Centre for Ocean-Atmospheric Prediction Studies based on the JMA SST values. Years are assigned as El Niño or La Niña years when their 5-month moving average JMA SST index values are + 0.5 ^{o}C or greater (El Niño) / - 0.5 ^{o}C or greater (La Niña) for at least six consecutive months (including October-December). Continuous JMA-SST values were used for the correlation analysis (Table 2.3Table 2.3).

Table 2.3 Hydrological years that fall under the El Niño and La Niña phases. Other years are classified as ENSO neutral.

ENSO phase	Hydrological year
El Niño	1982,1986,1987,1991,1997,2002,2006,2009
La Niña	1988,1998,1999,2007,2010

All calculations were made for multiple drought indicators (SPI, SPEI, and SSFI) over multiple accumulation time periods (1, 3, 12) by using the data-inputs from two GHMs (WaterGAP, PCR-GLOBWB). For the sake of simplicity, a selection of results is shown here. All underlying data and figures (providing information on the other indicators, datasets, or accumulation periods used) are provided as a supplement. Results are presented by country.

2.3 Assessment of drought impact and risk platforms and datasets

Exposure and vulnerability to droughts are an important aspect of drought risk assessment. Based on the global inventory of drought hazard and risk models, an overview was made for online platforms, datasets and newsletters/bulletins that provide information on drought impacts (Table 2.4Table 2.4). We distinguish between the following impacts categories: population; municipal and industrial water needs; agricultural crop and livestock production; hydropower production; and the overall economy. In general, these platforms and datasets can be used for a first assessment of drought impacts and risks in a country or region thereby giving an indication of drought impact hotspots. This information may help to identify hotspots and prioritize more detailed efforts for drought risk analysis.

Seven models provide drought impact information for the whole world. From these models, four include information on temporal aggregated information historic drought impacts and/or risk at sub-national levels. Two other models focus on providing real-time drought impact information and the EM-DAT database does not provide sub-national information. These models are not taken up in this analysis of impact models. Two models provide drought impact information for Africa. From these models, one includes temporal aggregated information on historic drought impacts and/or risk, while the other model focusses on providing real-time drought impact information. The models for Europe and North America are not considered in the assessment, because they do not cover any of the case study countries.

A qualitative assessment of the five models that provide historical information at sub-national levels was performed. For each of the case study countries the relevant impact and/or risk models are presented and compared with available knowledge and information of impacts. For Malawi, the assessment is extended with an analysis of the impact data collected from FEWS-NET projects. Platforms that provide (near) real-time and forecasting information are evaluated in the sections about monitoring and forecasting products (see section 2.4 of this

chapter). Below, a short description of the five drought impact models that are taken up in the qualitative assessment. Information on all of these models can be found in the report "Drought hazard and risk modeling tools" (Hendriks, 2017).

Table 2.4 Overview of online platforms, datasets, and newsletters/bulletins that provide historical drought impact information about the impact categories population (POP), municipal and industrial water needs (M&IWN), agricultural crop and livestock production (A&L), hydropower production (HYDR), and the overall economy (ECON). Other applications of the drought risk models are provided in the overview.

		Region	Impact Mapping	Risk Mapping	Historical information	Monitoring/ forecasting	Aggregated impact information
PLATFORMS	**Aqueduct Water Risk Atlas**	Global	--	ECO	X	--	X
	IWMI water data portal	Global	--	POP, M&IWN, A&L, HYDR, ECO	X	--	X
	Agricultural Stress Index and precipitation anomalies (FAO)	Global	A&L	--	X	X	X
	Global Agricultural Drought Monitoring and Forecasting System	Global	A&L	--	--	X	--
	GEOGLAM Crop Monitor	Global	A&L	--	X	X	--
	Canadian agroclimate impact reporter	North America	A&L	--	X	--	X
	US Drought Impact Reporter (DIR)	North America	POP, M&IWN, A&L, HYDR, ECO	--	X	X	X
	Vegetation Drought Response Index (VegDRI)	North America	A&L	--	X	--	X
	GOES Evapotranspiration and Drought (GET-D)	North America	A&L	--	X	--	--
	European Drought Centre Impact Report Inventory	Europe	ECO, A&L, M&IWN	--	X	--	X
	ITHACA Drought Monitoring	Africa	--	A&L, POP	X	X	--
	African Drought Observatory	Africa	A&L, ECO	A&L, ECO	X	X	X
DATASET	**Global map of drought risk (JRC)**	Global	POP, M&IWN, A&L, ECO	POP, M&IWN, A&L, ECO	X	X	X
	EM-DAT	Global	ECO, POP	--	X	--	--
	European Drought Centre Reference Database	Europe	POP, M&IWN, A&L, HYDR, ECO	--	X	--	X

2.3.1 Global map of drought risk (Global)

A global drought risk map was developed at the JRC based on a relatively simple and data-driven method (Carrão et al., 2016). This global map of drought risk has been developed at the sub-national administrative level for the period 2000–2014, using the product of three independent determinants: hazard, exposure and vulnerability. Drought hazard is determined here by means of the weighted anomaly of the standardized precipitation index (WASP). Drought exposure takes into account the spatial distribution of population and the amount of numerous physical elements (proxy indicators) characterizing agriculture and primary sector activities, namely: crop areas (agricultural drought), livestock (agricultural drought), industrial/ domestic water stress (hydrological drought), and human population (socioeconomic drought). The relative exposure of each region to drought was obtained from a multidimensional set of indicators by its statistical positioning and normalized multivariate distance to a performance frontier. Drought vulnerability was computed as a 2-step composite model that is derived from the aggregation of proxy indicators representing the economic, social and infrastructural factors of vulnerability at each geographic location, as similar as for the Drought Vulnerability Index (DVI) (Naumann et al., 2014). The proxy indicators of

exposure and vulnerability that have been used as input for the respective models were compiled for 170 countries and 2,515 sub-national administrative regions. Subsequently, both exposure and vulnerability indicators have been normalized in this study, enabling for a comparison between regions while at the same time limiting the evaluation of absolute drought risk levels.

2.3.2 Aqueduct Water Risk Atlas (Global)

The Aqueduct Water Risk Atlas is a global platform[3] that can be used to obtain static global information of meteorological, hydrological, agricultural, socio-economic drought hazards as well as drought risk to the overall economy. The information is available for historical and future (2020 and 2040) periods at the spatial scale of countries and river basins. The platform presents the following 12 indicators and indices related to drought: overall water risk, baseline water stress, inter-annual variability, seasonal variability, flood occurrence, drought severity, upstream storage, groundwater stress, return flow ration upstream protected land, media coverage, access to water, threatened amphibians. The umbrella index "Overall Water Stress" identifies areas with higher exposure to water-related risks and is an aggregated measure of all selected indicators from the Physical Quantity, Quality and Regulatory & Reputational Risk categories.

2.3.3 IWMI water data portal (Global)

This platform[4] can be used to obtain historic information of socio-economic drought hazards for the world. Indices providing drought impact and drought risk information included are socioeconomic drought vulnerability index, drought risk index with respect to monthly precipitation, drought risk index with respect to monthly river discharge, mean drought run duration (months), storage-drought duration (length) index, and the storage-drought deficit index. The information is available for a historical period with a spatial scale of 0.5^{o}.

2.3.4 FAO Agricultural Stress Index and precipitation anomalies (Global)

The FAO-platform "Agricultural Stress Index and precipitation anomalies"[5] can be used to obtain historical (annual summaries) and near real-time information of agricultural drought hazards and drought impact to agriculture and livestock. The data on crop conditions are available at a global and country scale on a decadal basis since 1984 up to the month previous to the current month. Annual summaries are available as well. The provided impact indices (NDVI, Agricultural Stress Index, Vegetation Health Index, and Vegetation Condition Index) are mapped at a gridded resolution of 1 km. Country scale graphs with time series of the indices are also provided. The indices provided through this platform are described in in the report "Drought hazard and risk modeling tools and resources" (Hendriks, 2017).

2.3.5 African Drought Observatory[6] (Africa)

This platform[7] can be used to obtain information about meteorological, hydrological and agricultural drought hazards as well as drought impact to the overall economy on a near real-time and forecast (SPI3 only) basis for Africa. Indices that are presented are precipitation anomalies (percent of normal), SPI3, Vegetation Productivity Anomaly (VPA), Drought Hazard Index, Drought Vulnerability Index, and the Drought Risk Index. The precipitation anomalies, SPI3, and the Vegetation Productivity Anomaly are available at a 1^{o} spatial

[3] *http://www.wri.org/resources/maps/aqueduct-water-risk-atlas*

[4] *http://waterdata.iwmi.org/Applications/Drought_Patterns_Map/*

[5] *http://www.fao.org/giews/earthobservation/asis/index_1.jsp?lang=en*

[6] *The African Drought Observatory will be will be fully integrated into the Global Drought Observatory.*

[7] *http://edo.jrc.ec.europa.eu/ado/*

resolution. The JRC Drought Hazard Index, JRC Drought Vulnerability Index, and JRC Drought Risk Index are available at country and sub-basin scales.

2.4 Qualitative assessment of forecasting and monitoring products

This section presents an analysis of the products used in each of the five case study countries for monitoring and forecasting drought conditions. For each of these countries, we focus on assessing the currently available operational systems that support decision processes on the management of drought conditions. We concentrate primarily on operational systems used at the national level either for monitoring drought conditions, as well as those available systems providing forecasts at the seasonal scale. Where relevant, forecasting systems at the regional scale (where region indicates a geographic region, such as Southern Africa) are included. The objective of this section is to provide insight into current practices in drought monitoring and forecasting in the case study countries, how these are used to support the management of drought events, the data and systems used and the efficiency and availability of information during drought events.

For each of the five focus countries the following aspects are described:

- A brief résumé on the occurrence of drought events within the country;
- A description of currently available monitoring and forecasting information and systems, how the process is organized and how these systems are used in support of decision making.
- For each of the systems discussed relevant details are provided in tabular format;
- When information is available, a short review is also provided describing the potential for seasonal forecasts in the case study countries, including relevant literature and current initiatives to improve drought monitoring and forecasting capabilities where these factors are known.

3 Results - Afghanistan

3.1 Drought risk related country characteristics

3.1.1 Introduction to the country

Afghanistan is a large, mountainous country in South-Asia. The Hindu Kush Mountains, running northeast to southwest across the country divide it into three major regions: the Central Highlands, the Southwestern Plateau, and the Northern Plains area. Kabul is the capital and largest city of the country, located in the province of Kabul (International Business Publications, 2013; Figure 3.1). The population has been significantly increasing over the past two decades, reaching 34.66 million people in 2016 (World Bank Country Profile Afghanistan). An overview of the spatial variation of the population density (total and rural population) between the districts can be viewed in Figure 3.2. Table 3.1Table 3.1 shows an overview of relevant country characteristics.

Figure 3.1 Map of Afghanistan (source: Wikipedia).

Table 3.1 Afghanistan country characteristics

Geography	
Total Area	652,230 km^2
Land	652,230 km^2
Water	
Highest Elevation	7,492 m (24,580 ft)
Land Use	
Arable	15%
Permanent cropland	0.28%
Other	84.99% (2016-17)
People	
Population	34.66 million (2016)
Population Growth Rate	2.7 %
Economy	
GDP per capita (PPP)	596.30 US Dollar
Hydrology	
Average rainfall (country average)	250 mm per annum

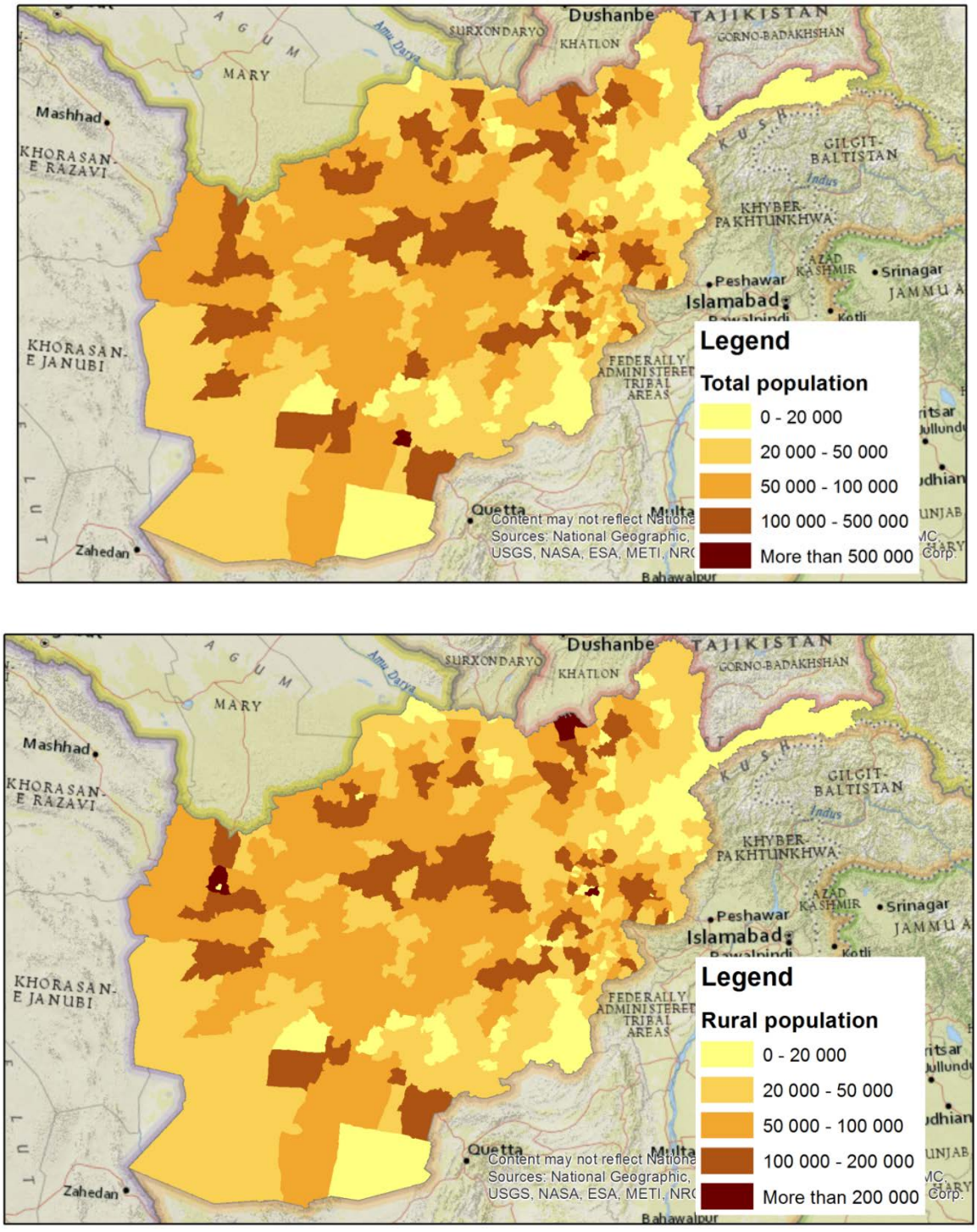

Figure 3.2 Total population (top) and rural population per province in Afghanistan (source Deltares, 2016).

Afghanistan is still a conflicted zone and the deteriorating security continues to have a negative impact on the livelihood, business confidence, and economic activity. In the past decade we can observe big fluctuations in its economic growth, which was busted by the international aid and the goods and services that the troops consumed. The drawdown of international troops had an impact on the economic performance, slowing growth down from

14% in 2012 to less than 2% in 2014 and 2015.[8] In 2016 there has been a slight improvement as the growth rate has increased from 1.1 % in 2015 to 2.2 % in 2016, mainly due to the strong growth of the agricultural sector.[9]

The agricultural sector, including livestock and related activities, represents 21% of the GDP (Figure 3.3Figure 3.3)[10], but given its high importance for the livelihood of the predominant rural population in the country (72% of the population), the sector represents the backbone of Afghanistan's economy. In 2011/12 for example, agriculture provided income for nearly half of the households in the country, was the main source of income for 30% while employing 40% of the total workforce.[11]

Of Afghanistan's land area of 65 million hectares, only 15% corresponds to arable land (Table 3.2Table 3.2); most of the country is comprised by mountains and deserts and the continental climate is predominantly arid or semi-arid, receiving only 400 mm of rain per year for the cultivable lands. Therefore, irrigation is the base of Afghanistan's agriculture where it represents 26% (Table 3.2Table 3.2)[12] of the agricultural land. This is especially true in the mountainous areas, where agriculture centres around rain-fed and mountain spring irrigated lands with wheat being the predominant crop.[13] The irrigation is sourced from snowmelt in the high mountains in the spring and summer months. In the mountainous areas in eastern Badghis and western Hirat, there is an extensive belt of primarily rain-fed land on which most agricultural activity takes place, estimated at 90% and 60%, respectively, for the two provinces (Bhattacharyya et al., 2004).

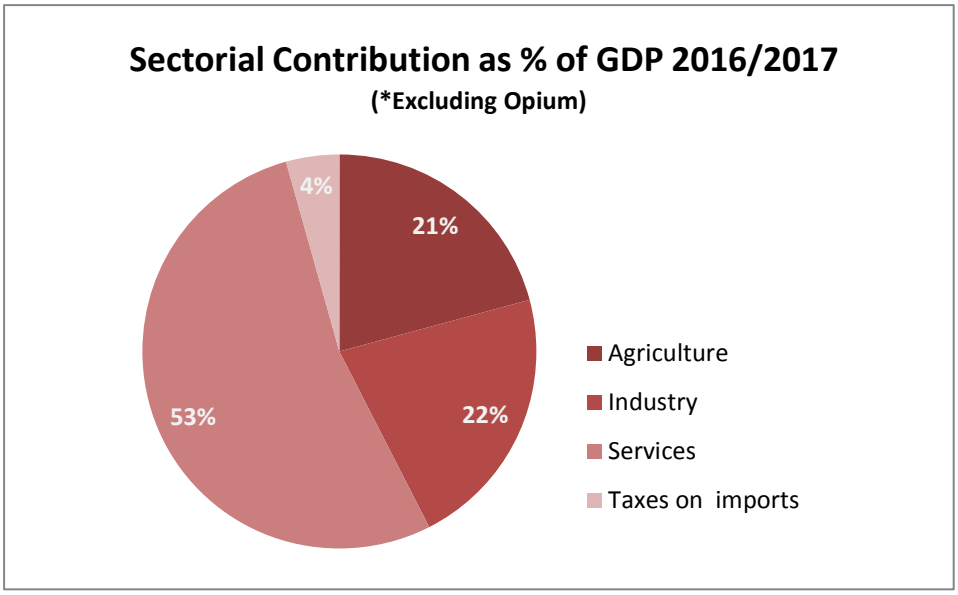

*Figure 3.3 Sectorial Contribution as % of GDP 2016/2017 (*Excluding Opium). Source: Central Statistics Organization, Statistical Yearbook 2016-17 – National Account.*

[8] *https://www.imf.org/external/np/country/notes/afghanistan.htm*

[9] *http://www.worldbank.org/en/country/afghanistan/publication/afghanistan-development-update-may-2107*

[10] *http://cso.gov.af/en/page/1500/4722/2016-17*

[11] *http://documents.worldbank.org/curated/en/245541467973233146/pdf/AUS9779-REVISED-WP-PUBLIC-Box391431B-Final-Afghanistan-ASR-web-October-31-2014.pdf*

[12] *http://cso.gov.af/en/page/economy-statistics/economy/agriculture*

[13] *http://documents.worldbank.org/curated/en/245541467973233146/pdf/AUS9779-REVISED-WP-PUBLIC-Box391431B-Final-Afghanistan-ASR-web-October-31-2014.pdf).*

Table 3.2 Agricultural Land use 2016-17. Source: Central Statistics Organization, Agricultural Statistics 2008-2016

Land use 2016-17		
	Thousand Hectares	**% of agricultural land per use**
Total land area	65,223	
Agricultural area (a+b+c+d)	9,610	(15% of total land)
a - Forests and woodland	1,781	19%
b-Fallow land	4,228	44%
c-Irrigated crops area	2,457	26%
d- Cultivated rain fed area	1,144	12%

3.1.2 Hydrology and water resources

Afghanistan has an arid to semi-arid climate. Rainfall in Afghanistan is very scarce, and mainly only affects the northern highlands. Most of the annual precipitation occurs in winter and spring from Jan to April. Rainfall in the more arid lowlands is rare and can be very unpredictable[14]. The average annual precipitation (rain and snow) is approximately 250 mm; and varies from 60 mm in the south-western parts of the country to 1200 mm in the north-eastern Hindu Kush Mountains (Bhattacharyya et al., 2004). Afghanistan receives snow during winter, providing base flow for numerous rivers, lakes, and streams, most of which flows into neighbouring countries. Currently, about two-third of the water generated in Afghanistan drains to neighbouring countries (Pakistan, Iran, Tajikistan, Uzbekistan and Turkmenistan).

Afghanistan has 5 major river basins (Figure 3.4Figure 3.4):

- Endorheic Aral Sea basin, including the Panj and Amu Darya Rivers;
- Endorheic Karakum Desert with Harirud and Murghab Rivers;
- Endorheic Sistan basin with Harut, Farah, Helmand and Ghazni Rivers;
- Indus River basin flowing into Arabian Sea with the Kabul River; and
- Endorheic Northern basin with Shirin Tagab, Sare Pul, Balkh and Khulm Rivers.

Although Afghanistan is located in a half desert-like environment, it is still rich in water resources mainly due to the series of high mountains such as Wakhan, Hindu Kush and Baba, which are covered by snow. The annual per capita water availability is approximately 2500 cubic meters, which is comparable with other countries of the region[15]. More than 80% of the irrigation water from Afghanistan comes from river and streams (surface water) and the main supply for surface water is derived from precipitation and seasonal melting of snow and glaciers in the highland areas (Habib, 2014) .

In the early 2000s the potential of water resources for the country was estimated at 75 billion cubic meters (BCM), of which 55 BCM correspond to surface water and 20 BCM reflect groundwater resources. The annual volume of water used in irrigation was estimated at 20 BCM, nearly 85% of which came from rivers and superficial streams, while 15% was derived

[14] *UNDP Climate Change Country Profiles: https://digital.library.unt.edu/ark:/67531/metadc226769/m2/1/high_res_d/Afghanistan.hires.report.pdf*

[15] *IWMI Working paper 49. Pakistan Country Series No. 14. Water Resourecs Management in Afghanistan: the issues and options. https://cropwatch.unl.edu/documents/Water%20Resource%20Issues%20In%20Afghanistan.pdf*

from groundwater extraction (alluvial groundwater aquifers, springs, and shallow and deep wells). However, a more recent assessment of water resources shows that Afghanistan has 4.4 million ha of potentially irrigable land, but to develop this potential would require significant new investment in infrastructure and agreements with the downstream countries (World Bank, 2014). Moreover, a qualitative assessment carried out in the early 2000s shows that Afghanistan's water resources are still largely underused (Table 3.3Table 3.3). Recent data from the Central Statistics Organization of Afghanistan shows that at present the annual freshwater withdrawal is 43% of the total internal resources available[16]

Table 3.3 Estimated Surface and Groundwater balance (BCM per year). Source: International Water Management Institute, 2002.

	Estimated Surface and Ground Water Balance (BCM per year)		
Water resources	**Potential**	**Present**	**Balance**
Surface water	57	17	40
Groundwater	18	3	15
Total	75	20	55

Figure 3.4 Afghanistan major river basins (Deltares, 2016)

Many parts of Afghanistan, with the exception of north-eastern highlands, are facing frequent droughts. From 21 wetlands in Afghanistan, three are of international importance. Due to the widespread degradation of natural resource, these wetlands have almost completely dried up, causing trans-boundary problems. Moreover, less than 20% of Afghan people have access to safe water, which is worsened by the severe, historic drought that the country has experienced (Deltares, 2016).

3.1.3 Historic droughts

Deltares (2015) carried out a multi-hazard risk assessment (including droughts) for Afghanistan for the World Bank. Meteorological drought was quantified based on the EU-WATCH precipitation dataset from 1959-1998. Figure 3.5Figure 3.5 shows a time series of

[16] *http://cso.gov.af/en/page/economy-statistics/economy/agriculture*

the annual precipitation sum for the whole of Afghanistan. It also shows the moving average (Two year window) and the average over the entire period. It follows from this figure that over a period of 40 years (1959-1998) three nation-wide meteorological droughts occurred: 1969-1970, 1982-1985 and 1996-1998.

SPI maps and values are available per catchment. As an example, we show the SPI maps for the dry years 1970 and 1998, when the entire country was in a drought (Figure 3.6). Figure 3.7 shows two examples of regional droughts: 1962 was a dry year for the Southwest, and 1968 was a dry year for some catchments in southern Afghanistan. The 1968 map also shows that the North can be very wet while the South is dry (Deltares, 2016).

A time lag between meteorological drought and drought losses was observed. The reported losses in 1971-1973 may stem from the lack of precipitation in 1969-1970. Likewise, the reported losses in 2000-2002 may stem from the lack of precipitation starting in 1996-1998. An explanation for this time-lag may be found in over-year storage capacity in reservoirs. Another explanation could be that some of the reported losses stem from water shortage from groundwater wells, in which water levels drop after a few years of precipitation deficit, and/or that farmers have some financial reserves to survive one or two drought years (Deltares, 2016).

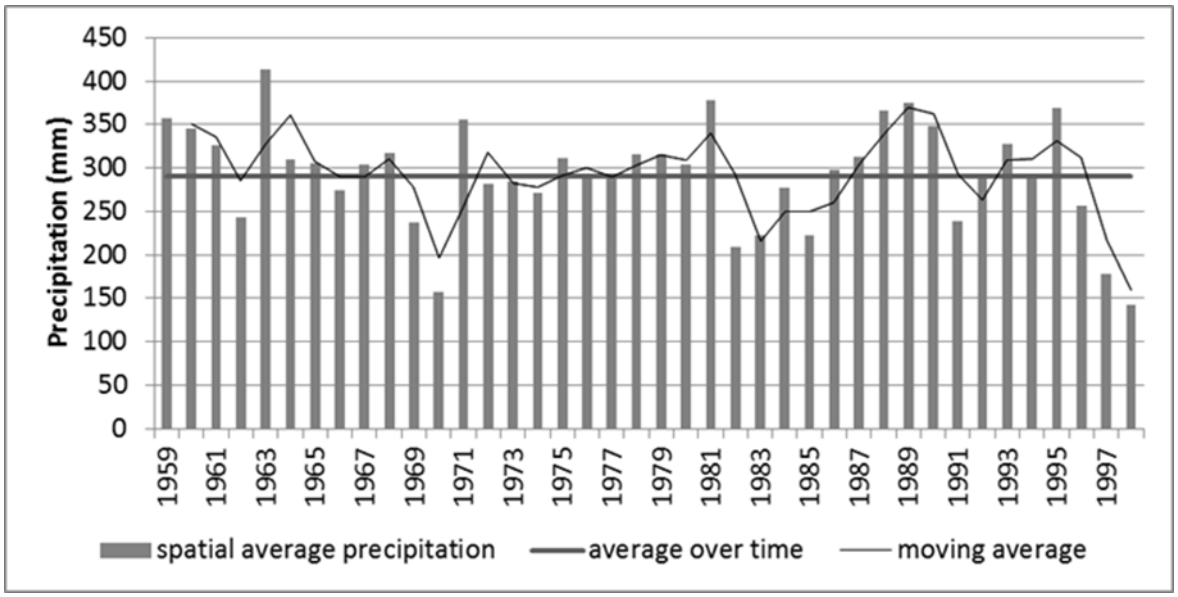

Figure 3.5 Annual and moving average precipitation over all Afghanistan river basins compared to average precipitation over time. Source: Deltares, 2016.

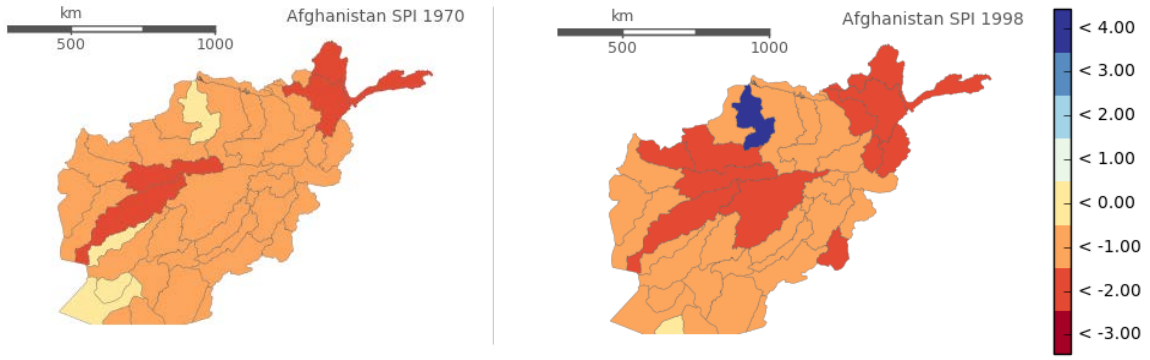

Figure 3.6 SPI1 maps of two dry years with a large extent: 1970 and 1998

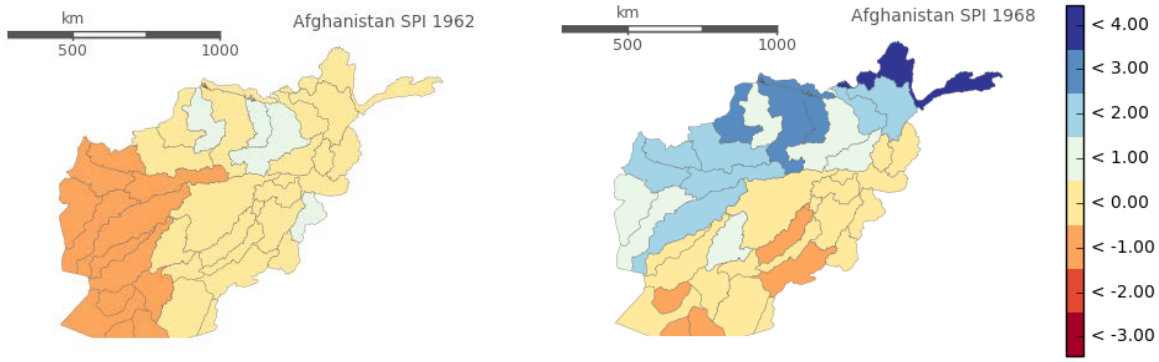

Figure 3.7 SPI1 maps of a dry year in the South-West (1962, left) and a dry year in the South (1968, right)

Droughts registered by EM-DAT and Reliefweb are shown in Figure 3.8Figure 3.8. It is striking that the meteorological drought in the period 1982-1985 is not registered by these organisations. This may be due to the war in Afghanistan during that period (1979-1989). In more recent years, several sources (EM-DAT, Reliefweb, etc.) have reported severe droughts from 1998-2006, 2008-2009, and another in 2011 (Figure 3.8Figure 3.8). These frequent droughts put the country in a difficult position, which is worsened by dry spells that have serious consequences for food security.

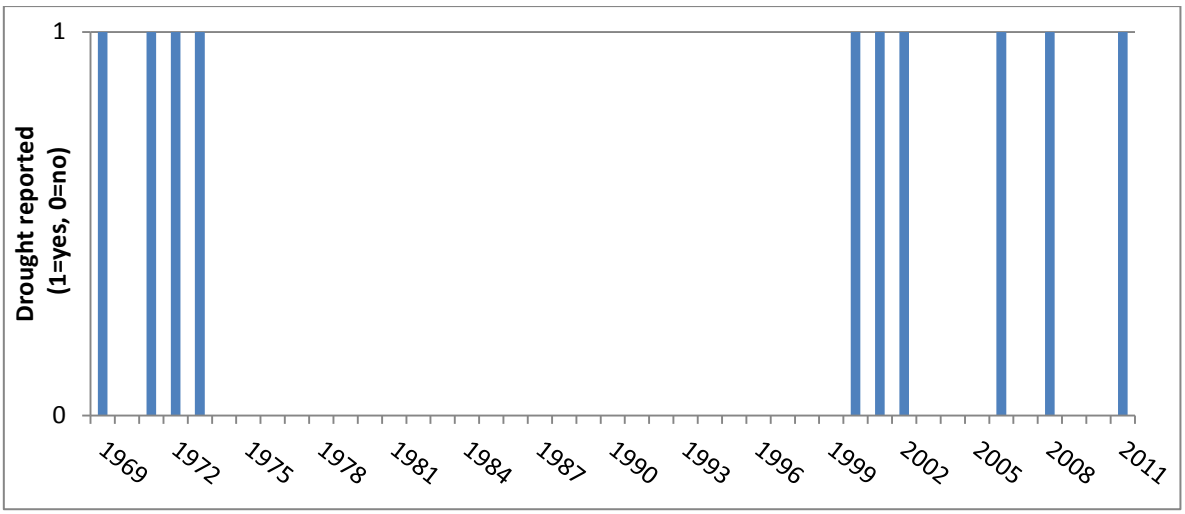

Figure 3.8 - Drought events in Afghanistan recorded by EM-DAT, Reliefweb, and others.

3.2 Assessment of available drought hazard models

3.2.1 Comparison and validation at the country scale

For the relevant drought hazard indices obtained from available global datasets (section 2.2.1), graphs were produced of the percentage-area of the country experiencing drought conditions for three drought levels: moderately dry (index value below -1), severely dry (index value below -1.5) and extremely dry (index value below -2). All graphs are shown in Appendix A1. In these graphs, the registered droughts from EM-DAT are plotted as well. Based on the graphs, the overlap of global drought hazards with reported droughts was assessed as well as the comparability of datasets and indices. SPI1 was left out of the comparison because the results are relatively spikey and could not be compared to drought events at a yearly time scale.

Table 3.4Table 3.4 gives an overview of the results for Afghanistan, showing that the reported droughts are generally well detected by most drought hazard indices from the global datasets, mainly the indices SPI3 (except for the Global Land Surface dataset), SPEI3, and SPEI12 showed pronounced drought signals in the six years with reported drought events.

For the years with registered drought events, the comparability of the drought hazards shown by the different dataset-index combinations was high. In the 30 year period that was assessed, the global models indicated nine other drought years that were not registered as drought events by EM-DAT. False alarm rates of individual dataset-index combinations range between 14% (WaterGap-SSFI) to 63% (GLS-SPI3). For the drought years detected by the drought hazard indices from the global datasets, the comparability of drought hazards was much lower.

Table 3.4 Results of the country-scale assessment of globally available drought hazard dataset-index combinations. In the table, years with registered drought events are shown in black and years without registered drought events but drought hazards shown by the dataset-index combinations, are shown in red. Corresponding graphs can be found in Appendix A1.

drought events		EM-DAT (6)	'84	'86	'87	'89	'95	'97	'98	'99	'00	'01	'02	'04	'06	'08	'11	Summary of hits			Summary of false alarms	
		Global data																regist. events		global data		
																		(+)	(+, +/-)	(+)	(+, +/-)	(+)	(+, +/-)
SPI 3		IRI	+	+	+/-	+/-	-	+	-	+	+	+	+/-	+	+	+	+	83%	100%	56%	78%	50%	54%
		GLS	+	+	+/-	+/-	-	+	-	+	+	+	+/-	+	+/-	+/-	+	50%	100%	56%	78%	63%	54%
		PRCGWB	+/-	+/-	+/-	+/-	-	+	+	-	+	+	+/-	+	+	+	+	83%	100%	44%	78%	44%	54%
		WaterGap	+/-	+/-	+/-	+/-	-	+	+	-	+	+	+/-	+	+	+	+	83%	100%	33%	78%	38%	54%
SPI 12		IRI	+	+	+/-	+/-	-	+/-	-	+/-	+	+	+	+	+	+	+	100%	100%	33%	78%	33%	54%
		GLS	+	+	+/-	+/-	-	-	+	+	+	+	+	+/-	+/-	-	+	67%	83%	44%	78%	50%	58%
		PRCGWB	+/-	+/-	+/-	+/-	-	+/-	-	-	+	+	+/-	+	+/-	+/-	+/-	33%	100%	11%	67%	33%	50%
		WaterGap	+/-	+/-	+/-	+/-	-	+/-	-	-	+	+	+/-	+	+/-	+/-	+/-	33%	100%	11%	67%	33%	50%
SPEI 3		GDM	+	+/-	-	-	-	+	+	-	+	+	+	+	+	+	+	100%	100%	44%	56%	40%	45%
		PRCGWB	+	+/-	-	-	-	+	+	-	+	+	+	+	+	+	+	100%	100%	44%	56%	40%	45%
		WaterGap	+	+/-	-	-	+	+	+	+/-	+	+	+	+	+	+	+	100%	100%	56%	78%	45%	54%
SPEI 12		GDM	+	+	+/-	+/-	-	-	-	-	+	+	+	+	+	+	+	100%	100%	33%	56%	33%	45%
		PRCGWB	+/-	+	-	-	-	-	-	-	+	+	+	+	+	+	+	100%	100%	22%	33%	25%	33%
		WaterGap	+	+	-	-	+/-	-	+/-	-	+	+	+	+	+	+	+	100%	100%	33%	56%	33%	45%
SSFI 1		PRCGWB	-	+/-	-	-	-	-	-	-	+	+	+	+	-	+/-	-	50%	67%	11%	22%	25%	33%
		WaterGap	-	-	-	-	-	-	-	-	+	+	+	+	+/-	+/-	+/-	50%	100%	11%	11%	25%	14%
Summary of hits		(+)	56%	44%	0%	0%	6%	19%	38%	19%	100%	100%	63%	94%	69%	63%	75%	**77%**	--	**34%**	--	**38%**	--
		(+, +/-)	88%	94%	56%	56%	13%	38%	44%	31%	100%	100%	100%	100%	100%	94%	94%	--	**97%**	--	**60%**	--	**47%**

3.2.2 Validation with local data

For Afghanistan, nine river discharge measurement stations were available for use with 16.6 months being the average length of the time-series. As shown in Figure 3.9Figure 3.9 the observation stations available for use were not equally distributed over the country but centred towards the northeast. As such, the evaluation should not be interpreted as being representative for the whole country.

Figure 3.9Figure 3.9 shows for both global models evaluated the results for the two performance metrics taking into account all available stations. PCR-GLOBWB shows a median correlation coefficient value of 0.48 when using all stations, compared to a value of 0.51 for WaterGAP. For PCR-GLOBWB thecorrelation ceofficient values range from 0.08 up to 1. For WaterGAP we find correlation coefficient values that range from 0.23 up to 1. Median percent bias for PCR-GLOBWB in Afghanistan is 108.0%. Median percent bias values (62.9%) are lower with the WaterGAP output.

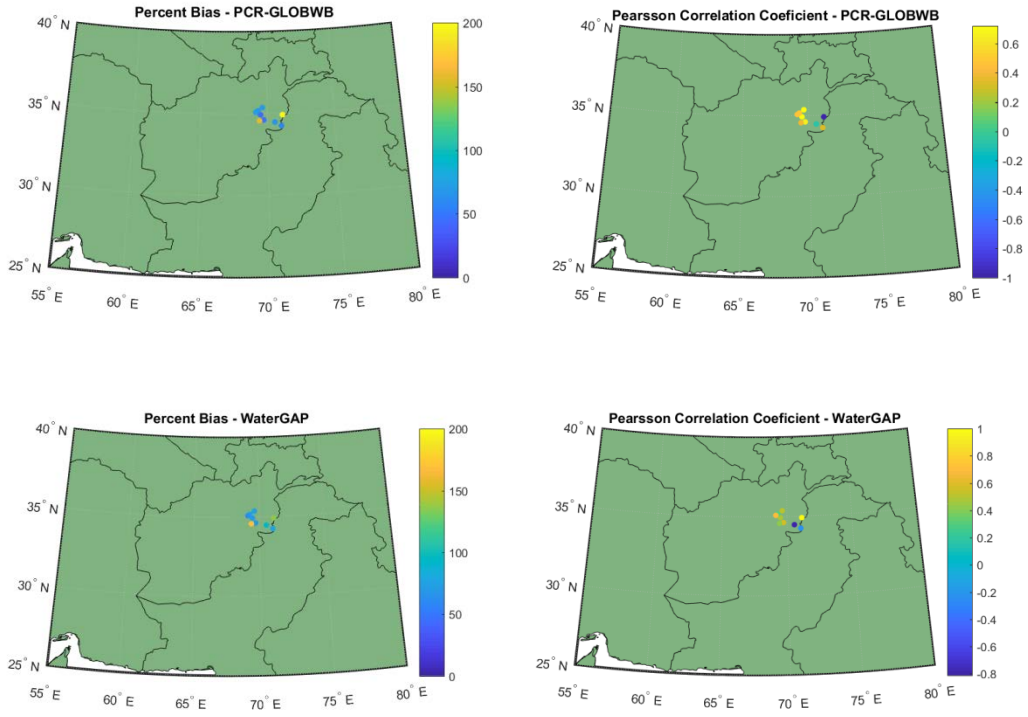

Figure 3.9 Spatial distribution of GRDC measurement stations available for use in Afghanistan and their performance values for the percent bias and the Pearson correlation coefficient.

Figure 3.10Figure 3.10 shows the hydrograph for a selected discharge observation station in Afganistan with 21 months of data available. As shown in the graph, both models represent the observed seasonal and interannual variability relatively well. Correlation coefficient values for this particular station are 0.72 (PCR-GLOBWB) and 0.47 (WaterGAP). Although WaterGAP is able to reflect the yearly peaks in the hydrograph relatively well, the timing is a bit off, which results in a lower correlation coefficient value compared to that of PCR-GLOBWB. Percent bias values are within the moderate range at 42.4% for PCR-GLOBWB and 68.4% for WaterGAP. Whereas PCR-GLOBWB misses the yearly peaks, it represents the yearly low-flow conditions relatively well. On the othe hand, WaterGAP is too early with

its peak and too low in its low-flow estimates. Hydrographs for all other stations in Afghanistan are available as a supplement to this document.

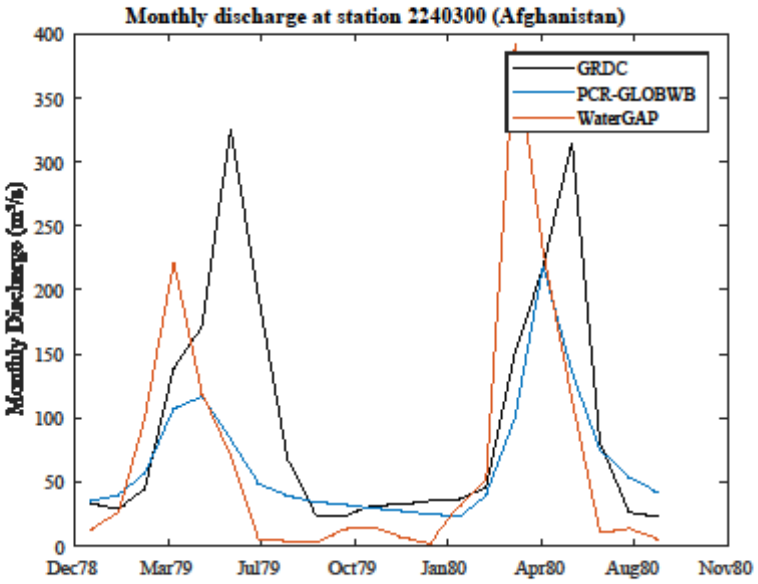

Figure 3.10 Hydrograph visualizing the performance of PCR-GLOBWB and WaterGAP relative to the historical observations from GRDC.

3.2.3 ENSO analysis

Figure 3.11Figure 3.11 visualizes the median share of total land area in drought conditions for Afghanistan during El Niño (EN), La Niña (LN), and Neutral (N) years using the different drought indicators, various accumulation time-periods and the inputs from both PCR-GLOBWB and WaterGAP. Results for both the SPI and SPEI indicator show that, at shorter accumulation times (e.g., 1, 3 months), the median area in drought in Afghanistan is significantly higher during LN years, compared to EN and N years. For longer accumulation time-periods, under the SPI and SPEI drought indicators, this signal shifts with a significantly higher median share of land area in drought during EN years, compared to LN and N years. For the SSFI (accumulation period 1) the two models indicate an opposite signal. Whilst the median share of total land area in drought conditions is relatively lower during LN years compared to EN and N years, the PCR-GLOBWB shows an opposite signal. The link between ENSO and droughts in Afghanistan has been studied on a very limited basis. As such, we cannot compare our results with previous studies. Studies performed on the correlation between ENSO and droughts in adjacent regions show a positive relationship between El Niño and hydrological droughts, using the SSFI index in Iran (Hosseinzadeh et al., 2012)

Figure 3.12Figure 3.12 shows, in a spatially explicit manner for Afghanistan, those areas experiencing a significant increase or decrease in frequency of drought months (SSFI < -1) when comparing the EN years with non-EN years (LN and N). Spatial patterns in anomalies in drought frequency months are shown to be roughly similar between PCR-GLOBWB and WaterGAP. During LN years, a vast majority of the land area indicates a significant decrease in the frequency of drought months, compared to non-LN years. During EN years both models indicate that whilst in the southwestern part of the country drought frequency is mostly

elevated compared to non-EN years, drought frequency is significantly lower compared to non-EN years in the north-eastern part of the country.

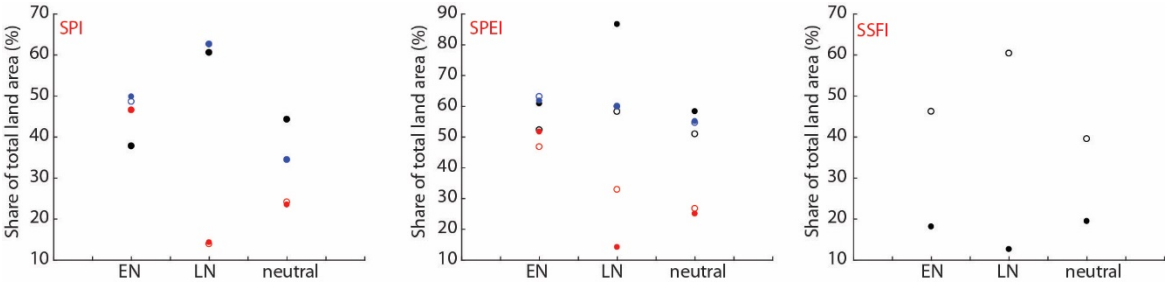

Figure 3.11 Area in drought in Afghanistan during El Nino (EN), La Nina (LN), or neutral years using the SPI, SPEI, and SSFI drought indicator. The open symbols show the results for WaterGAP while the filled symbols show the results for PCR-GLOBWB. Different colors indicate the different accumulation periods used: 1 month (black), 3 months (blue) and 12 months (red).

Despite the significant anomalies in drought frequency and the share of total land area exposed to drought between EN/LN and non-EN/non-LN year's correlations between drought indicators and the continuous JMA SST values seem to be relatively low, with correlation coefficient values around 0.4 for WaterGAP and 0.5 for PCR-GLOBWB. Figure 3.13 shows the spatial distribution in Pearson correlation values between the continuous JMA SST values and the SSFI-1 for both WaterGAP and PCR-GLOBWB. Moreover, it visualized at which lag-time the highest correlation was found. Whereas for the largest part of the total land area of Afghanistan lag-times of 6-9 months are shown to give the best correlation coefficient for PCR-GLOBWB, WaterGAP shows optimal lag-times that are significantly lower (0 – 3 months), especially for the southern and south-eastern part of the country.

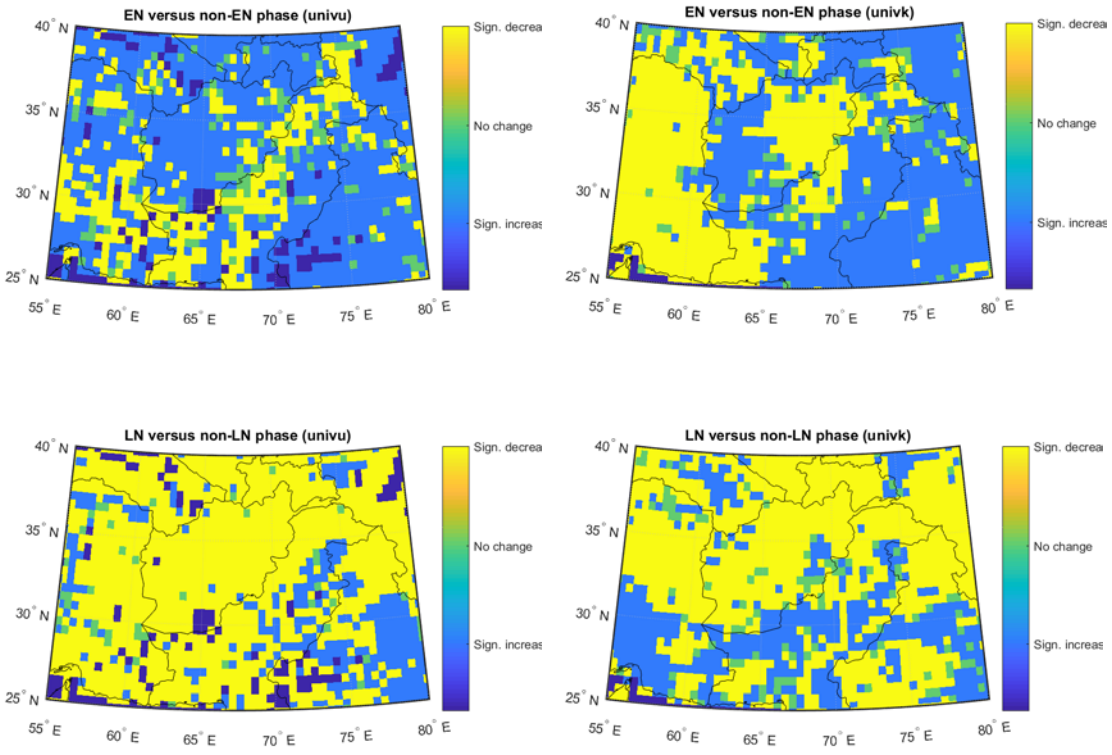

Figure 3.12 Spatial distribution of area with a significant increase, decrease or no change in frequency of drought months when comparing the El Niño years with the non El Niño years and the La Niña years with the non La Niña years. Left sub-plots show the results for PCR-GLOBWB, right sub-plots show the results for WaterGAP.

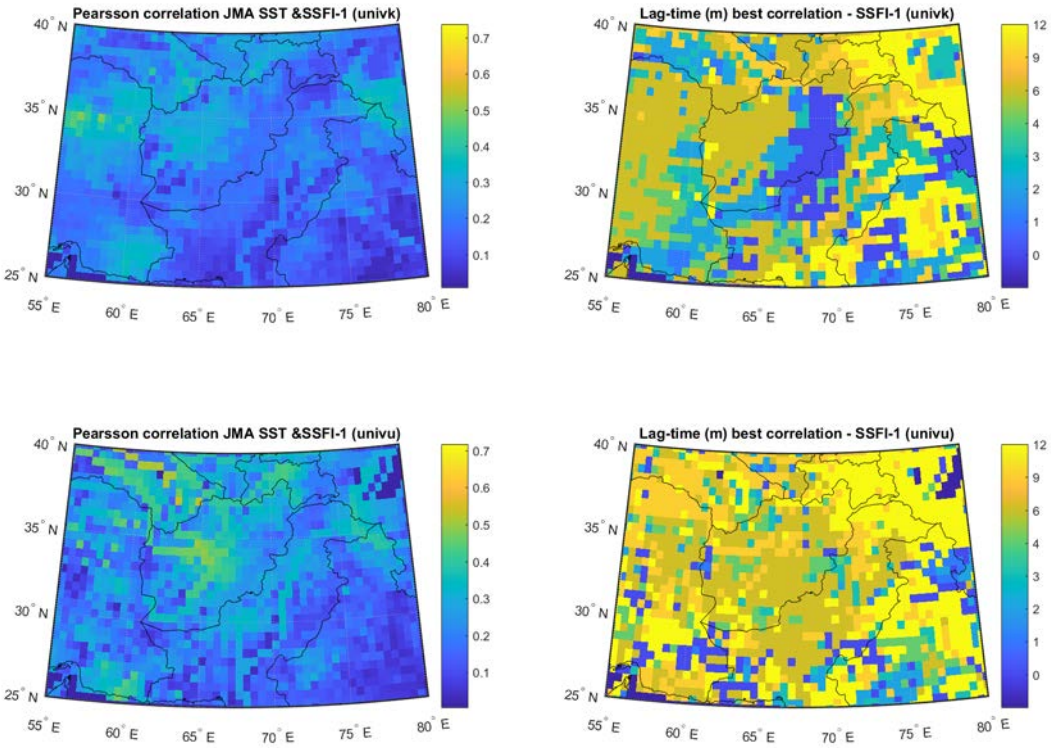

Figure 3.13 Spatial distribution of optimal Pearson correlation coefficient between continuous JMA SST values indicating ENSO conditions and the SSFI-1 drought indicator. Left sub-plots show the optimal correlation coefficient, right sub-plots show the lag-time that corresponds to the best correlation coefficient found. Results for both PCR-GLOBWB and WaterGAP are visualized.

3.3 Assessment of drought impact and risk platforms and datasets

3.3.1 Maps of overall drought impact and risk

Country scale maps are presented that are based on the Global map of drought risk from JRC (Carrão et al., 2016) (Figure 3.14). Although the presented indices of drought hazard, exposure, vulnerability, impact and risk are dimensionless factors based on an aggregation of information and data, they provide a good first impression of the drought risk situation in the country. For Afghanistan drought hazard and exposure are high in large parts of the country, which is in line with the assessments of drought hazards with global models and the descriptive information of the country characteristics. Vulnerability is high in the whole country, which is mainly caused by the fact that Afghanistan is in a conflicted zone. Also, Afghanistan has a low GDP per capita. The combination of relatively high levels of hazard, exposure and vulnerability in large parts of the country, leads to high drought impact and risk levels in the maps produced by the JRC. For an assessment of the spatial variability in the maps, a detailed study including the extensive collection of impact data is required.

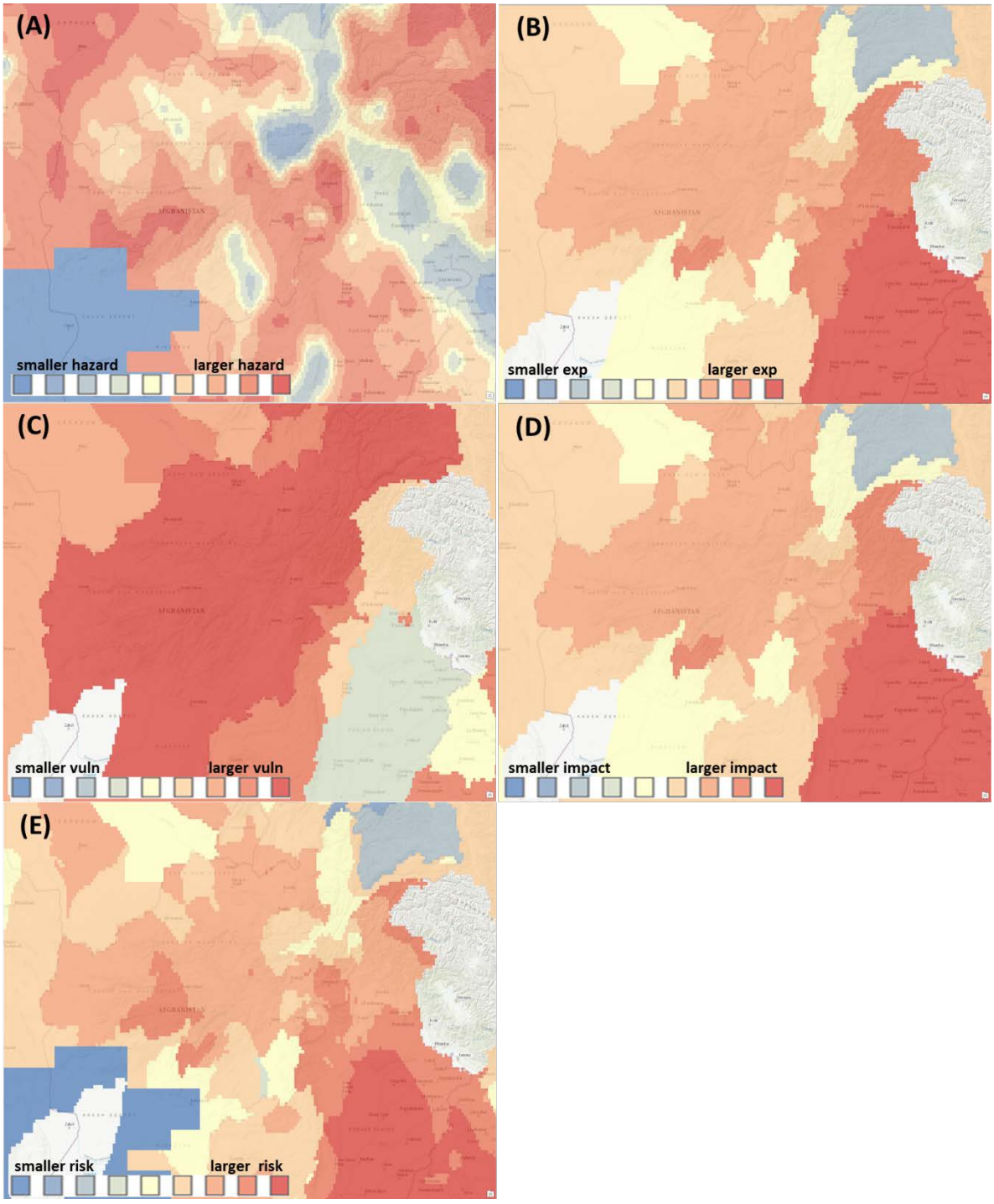

Figure 3.14 Maps from the Global map of drought risk developed by JRC showing the following indices: drought hazard (A), exposure (B), vulnerability (C), impact (exposure x vulnerability) (D), and risk (hazard x impact) (E).

3.3.2 Drought impact on population

The IWMI data portal provides maps with information related to impact drought impact on population for all countries in the world: per capita mean annual river discharge, agricultural water crowding (population per m^3 precipitation) with respect to mean annual precipitation,

and agricultural water crowding with respect to mean annual river discharge (population per m^3 discharge) (Figure 3.15). The spatial resolution of 0.5^o may be too coarse for a country with complex orography and remotely sparse villages such as in Afghanistan. However, the maps show that the annual discharge per person is generally low and in some areas very low in Afghanistan. The amount of people that are dependent on one m^3 precipitation and one m^3 discharge water is in general medium to high, except for some areas in the middle-west and northern regions of the country.
The maps show some comparability with the drought hazard map from JRC, but are not as comparable with the other exposure and impact map from JRC (Figure 3.14). For an assessment of the spatial variability in the maps, a detailed study including extensive collection of impact data is required. Impact data could consist of local data of actual reduction of water availability to the population and agriculture during historical drought periods as well as the effects of such levels of water shortage on economic revenues across various sectors.

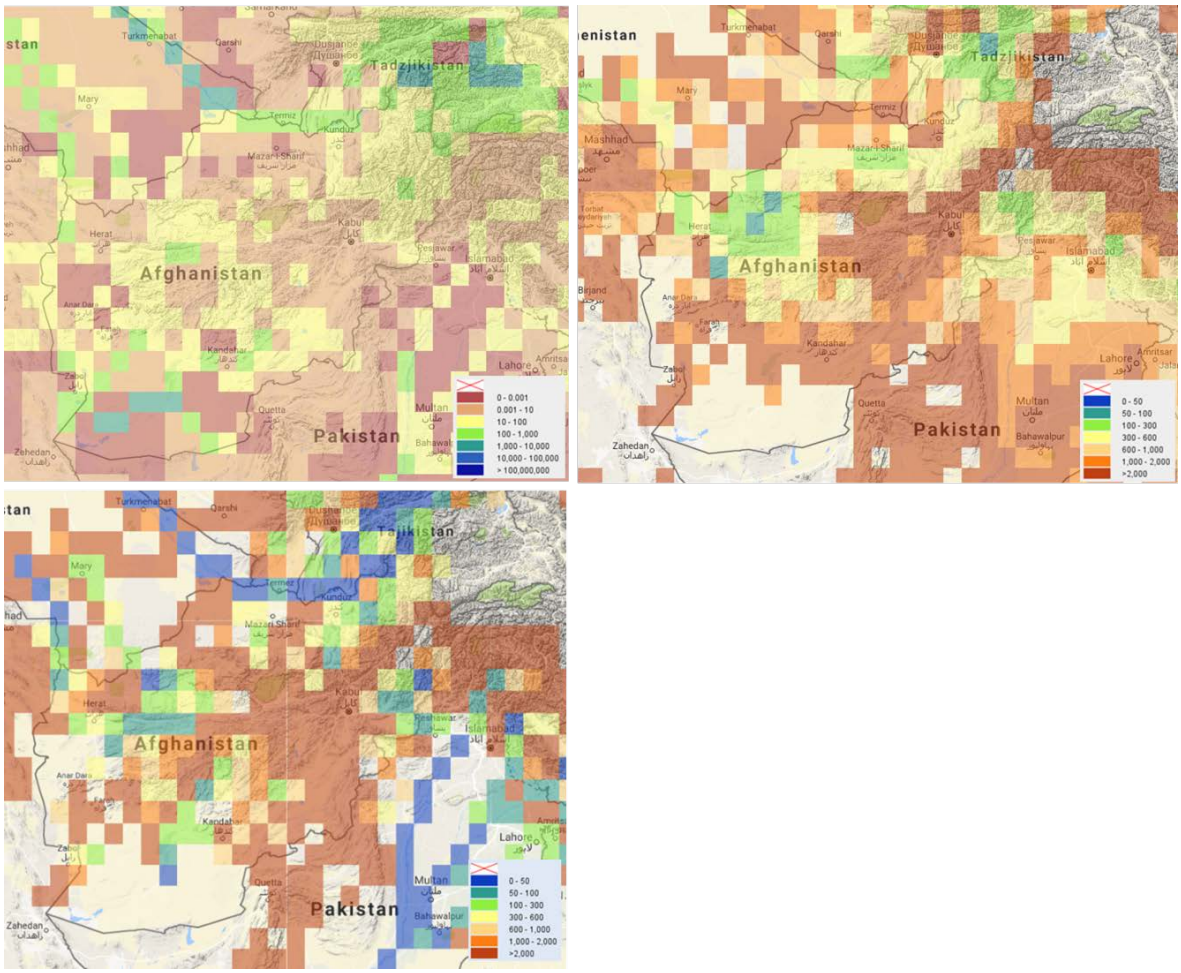

Figure 3.15 Maps providing impact (exposure/vulnerability) to population available from the IWMI water data portal, from left to right: per capita mean annual river discharge (m^3 per person); agricultural water crowding with respect to mean annual precipitation (population m^3); agricultural water crowding with respect to mean annual river discharge (population m^3).

3.3.3 Impact to agriculture

Maps on historical agricultural drought impact are provided by the online Aqueduct Water Risk Atlas (baseline water stress with respect to agriculture) and by the FAO-platform

"Agricultural Stress Index and precipitation anomalies" (Figure 3.16). However, due to the difference in temporal aggregation periods, the maps cannot be compared. The spatial patterns of baseline agricultural water stress in the Aqueduct map show similarities with the impact map from JRC (Figure 3.14). The FAO-platform provides a map with Agricultural Stress Index (ASI; % cropland affected by drought) for each year since 1985. Table 3.5 provides an overview of the years with coverage of approximately 25% the country or more with high to very high ASI levels and matching drought years based on registered droughts and the global drought hazard models (see section 3.2.1). According to the ASI maps, 10 out of the 31 years in the monitoring period show large areas with high levels of agricultural drought stress. Four out of these 10 years were listed as registered drought years. Four other years of these 10 years showed significant drought hazard by the global models. For an assessment of the spatial variability in the maps a detailed study including extensive collection of impact data is required. Impact data could consist of local data of actual reduction of water availability to agriculture during historical drought periods as well as the effects of such levels of water stress on economic revenues.

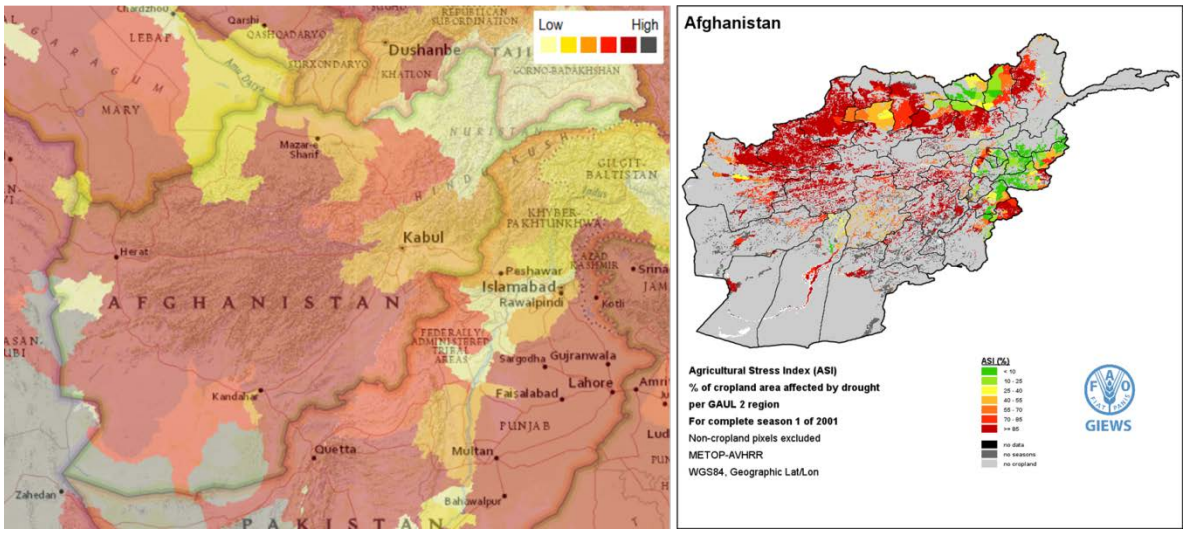

Figure 3.16 Maps on historical agricultural drought impact. Left map from Aqueduct Water Risk Atlas providing baseline water stress with respect to agriculture; right: map from FAO-platform "Agricultural Stress Index and precipitation anomalies" for a relatively dry year.

Table 3.5 Years with high ASI values during first growing season covering 30% or more of the country (FAO platform[17]) compared to registered droughts and drought hazards determined with global models (see section 3.2.1).

years with high ASI (S1)	Registered droughts	Hazard in global models
1985		
1986		x
1989		
1990		
2001	x	
2004		x
2006	x	
2007		
2008	x	x
2011	x	x

3.3.4 Impact on hydropower

The online Aqueduct Water Risk Atlas provides maps with baseline water stress with respect to electric power (Figure 3.17), which is (almost) identical to the map with baseline stress with respect to agriculture. For Afghanistan it can be observed that for a large part of the country the stress level is relatively high. The spatial patterns in the map are in line with the map of overall drought impact from JRC (Figure 3.14). For a more thorough analysis of the drought impact to hydropower, a comparison with local impact data should be performed. Such impact data could consist of locations of hydropower plants and the actual reduction of water availability (e.g. lowered reservoirs levels, reduced river discharge) to these plants during historical drought periods as well as the effects of such levels of water shortage on produced electricity and economic revenues.

Figure 3.17 Map from Aqueduct Water Risk Atlas providing baseline water stress with respect to electric power.

[17] *http://www.fao.org/giews/earthobservation/country/index.jsp?lang=en&type=15&code=AFG*

3.3.5 Impact to the overall economy

A map presenting a socio-economic drought vulnerability index is available from the IWMI-portal and a default baseline water stress map is available from the Aqueduct Water Risk Atlas (both maps in Figure 3.18). The IWMI map shows a high level of socio-economic vulnerability but does not provide any spatial differentiation at the sub-national level. This is more or less similar to the vulnerability map from JRC (Figure 3.14), although that map shows some spatial differentiation with lower vulnerability in the eastern part of the country. It can be observed that for a large part of the country the default water stress level is relatively high, which is (almost) identical to the maps presenting baseline stress with respect to agriculture and electric power. The spatial patterns in the map are in line with the map of overall drought impacts from the JRC (Figure 3.14).

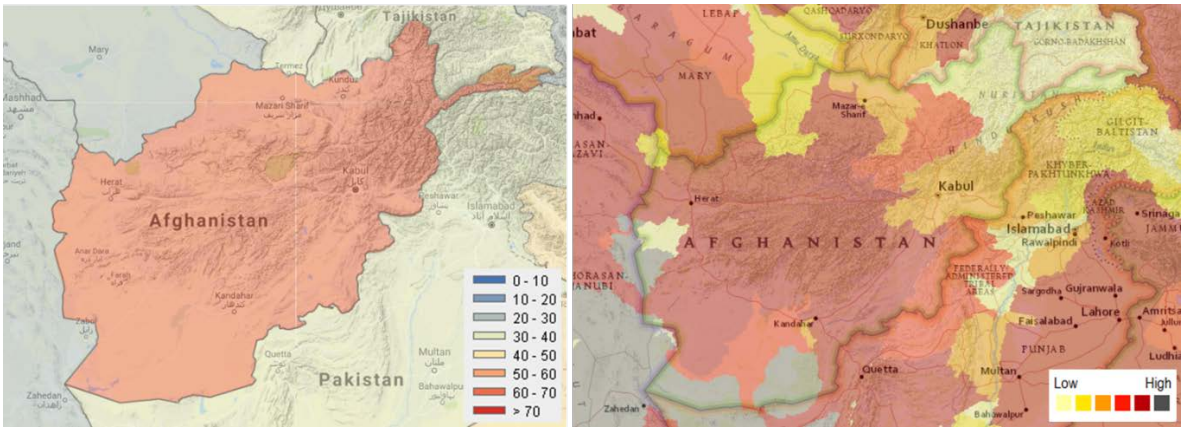

Figure 3.18 Maps with drought impact to the overall economy from different online platforms: Socio-economic drought vulnerability index from IWMI-portal (left); Baseline Water stress – Default form Aqueduct Water Risk Atlas (right).

3.3.6 Impact on municipal and industrial water needs

Various maps are available at the Aqueduct Water Risk Atlas that related baseline water stress to industrial sectors (mining, food & beverage, chemicals, semi-conductor, oil and gas, mining, construction materials, textiles). However, there does not seem to be any variation in base line water stress for the different sectors. It is unclear if any spatial information of the impact sectors was available for Afghanistan at the sub-national scale. Also, no independent drought impact information for these industrial sectors was available for the case study countries during our research. Hence, no further assessment of these impact maps was performed.

3.4 Evaluation of forecasting and monitoring systems

Droughts are a frequently occurring natural hazard in Afghanistan, whose impacts include significant loss of agricultural yields, severe famine and large migrations of population. The multi-year droughts of the 1970s, 2000, 2006 and 2008 are examples of severe droughts recorded in recent decades in Afghanistan. Drought is, however, only one of many natural disasters (e.g. floods, landslides, avalanche and earthquake) that hit this mountainous country every year. Still, droughts affect more people than any other natural disaster. The droughts of 2000, 2006, and 2008 were reported to have affected 2.6, 1.9 and 0.28 million people, respectively (Government of Afghanistan, 2011).

3.4.1 Current drought monitoring and forecasting

The Government of Afghanistan released a Strategic National Action Plan (SNAP) for Disaster Risk and Reduction in 2011. In 2012, the National Disaster Management Low was enacted to establish a National Disaster Management Commission (NDMC), and its secretariat Afghanistan National Disaster Management Authority (ANDMA) (IFRC, 2013). NDMC and ANDMA are the highest level entities for regulation and coordination of disaster preparedness, response, and enforcement in the country. Separate provincial and district level commissions were also established to effectively implement decisions of NDMC. In addition, the National Disaster Risk Reduction Platform (NDRRP) was established aimed at collaboration of disaster risk reduction activities with national/international non-governmental organizations and civil societies, and to achieve synergy of resources and efforts (ADB, 2014).

Despite records of frequent and devastating drought events and existing disaster risk management instruments, Afghanistan seriously lacks the necessary infrastructure (GWP-SA, 2014), resources and well developed drought preparedness and mitigation planning for the country. Only recently, USAID has extended the coverage of the Famine Early Warning Systems Network (FEWS NET) [18] to Central Asian countries including Afghanistan. Currently available FEWS NET data products for Afghanistan include several drought related products, such as the 6-day precipitation forecast (based on NOAA GFL), dekadal anomaly of precipitation, monthly anomaly of evapotranspiration, daily anomaly of snow depth, NDVI (based on MODIS), etc. These data products have not yet been operationally used for decision making and providing early drought warnings in the country.

3.4.2 Available operational systems

Currently, the following data products are available from FEWS NET – CA for Afghanistan:

- Agricultural products
- eMODIS NDVI C6
- Evapotranspiration (ET)
- Irrigated areas
- Rainfall products
- Snow cover products
- Temperature products

Table 3.6Table 3.6 provides an overview of the main characteristics of the Famine Early Warning Systems Network for Central Asia.

The agricultural product contains two maps of agricultural lands in Afghanistan based on 1993 and 2001, and one map of agricultural range lands based on 1993. The eMODIS NDVI C6 product includes maps of decadal (10-day average) values and anomalies of NDVI, agricultural area, rain fed agricultural area and rangeland area. The ET product contains monthly and seasonal evapotranspiration anomalies (Figure 3.19Figure 3.19). The irrigated area product includes annual irrigated areas per major river basins and provinces, which are derived from the eMODIS products.

[18] *FEWS NET – CA (2017): https://earlywarning.usgs.gov/fews/search/Asia/Central%20Asia/Afghanistan; Accessed on 02-Oct-2017.*

The rainfall product includes a 6-day rainfall forecast (Figure 3.20Figure 3.20), decadal rainfall and anomalies, and decadal cumulative rainfall and anomalies. The snow cover product contains three different data maps: daily snow depth and anomaly, daily snow water equivalent and anomaly, and 8-day snow cover (based on MODIS) and anomaly. Similarly the temperature product includes decadal daily mean temperature and anomalies (Figure 3.21Figure 3.21).

The rainfall product is the only forecast product currently available. It gives a daily rainfall forecast for up to a 6-day lead time (forecast horizon) and is updated every day. All other products are monitoring products, which are available up to the last day, decade, month or season, except the agriculture products. The agricultural products are based on 1993 and 2001 with no updates being available. More conventionally used drought indices, such as the SPI and Soil Water Indices are not available for Afghanistan as of yet. Currently these products are only available for Africa.

Table 3.6 Characteristics of drought monitoring and forecasting systems available in Afghanistan.

Characteristics	**Famine Early Warning Systems Network - Central Asia**
Monitoring	Yes
Forecasting	Yes
Region/countries/areas	Central Asia, includes five countries, including Afghanistan
Spatial resolution	Various depending on the data products. Some products are also available per major river basins and provinces.
Datasets used	NOAA GFS, MODIS, etc.
Software and tools used	Various, including GCMs, and MODIS algorithms/tools
Indices presented	6-day precipitation forecast, decadal anomaly of precipitation, monthly anomaly of evapotranspiration, daily anomaly of snow depth, NDVI, etc.
Reflective of impacts	Not available
Forecast horizon	6-Day (The 6-day precipitation forecast is the only forecast product currently available (others are monitoring products).
Update frequency	Daily (for the 6-day precipitation forecast)
Accessibility of forecast	Easy, open access (only maps)
Method of access	Directly through the Internet
Procedure / steps	Final products can be downloaded directly
Resources required	Internet access
Post-processing	None
Hit rate (estimation)	Not known

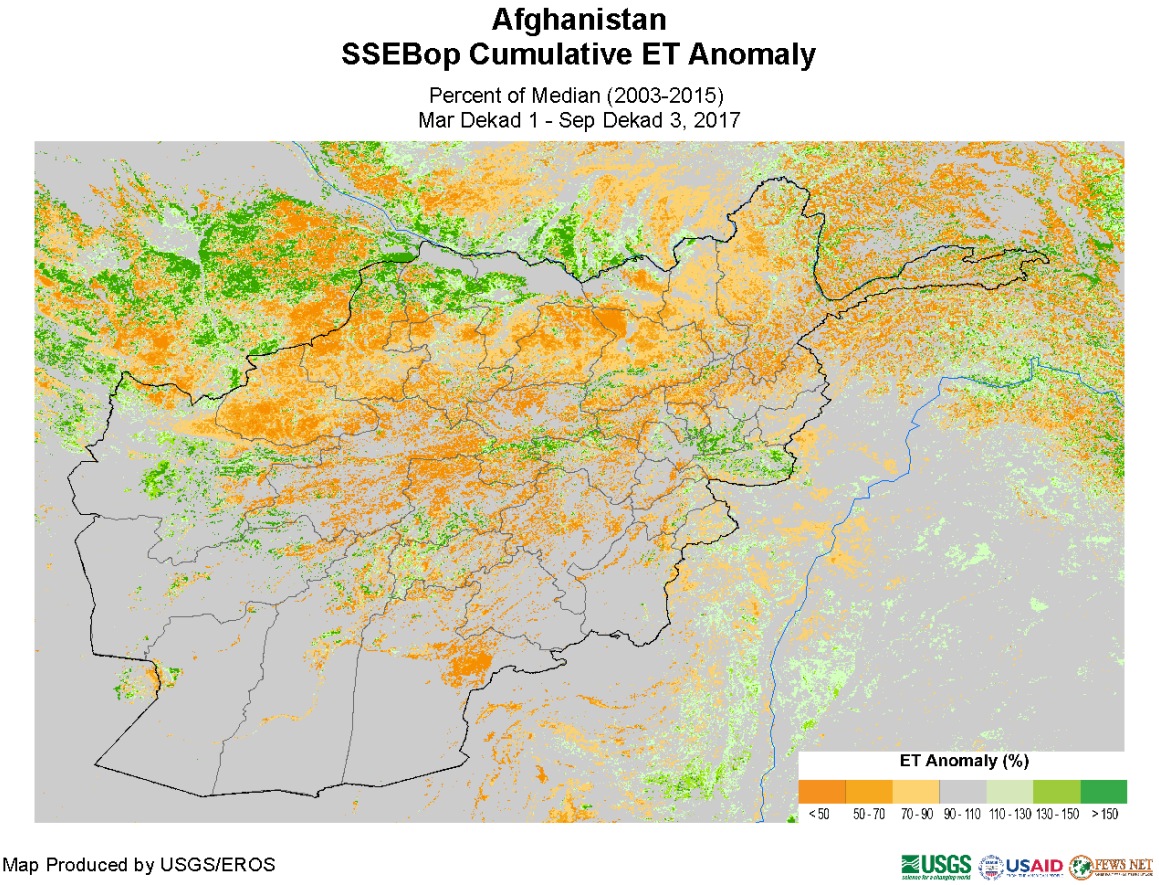

Figure 3.19 Seasonal evapotranspiration anomaly (relative to median of the same period from 2003 to 2015) available from FEWS NET – CA for Afghanistan[19]

[19] *FEWS NET – CA (2017): https://earlywarning.usgs.gov/fews/search/Asia/Central%20Asia/Afghanistan; Accessed on 08-Oct-2017.*

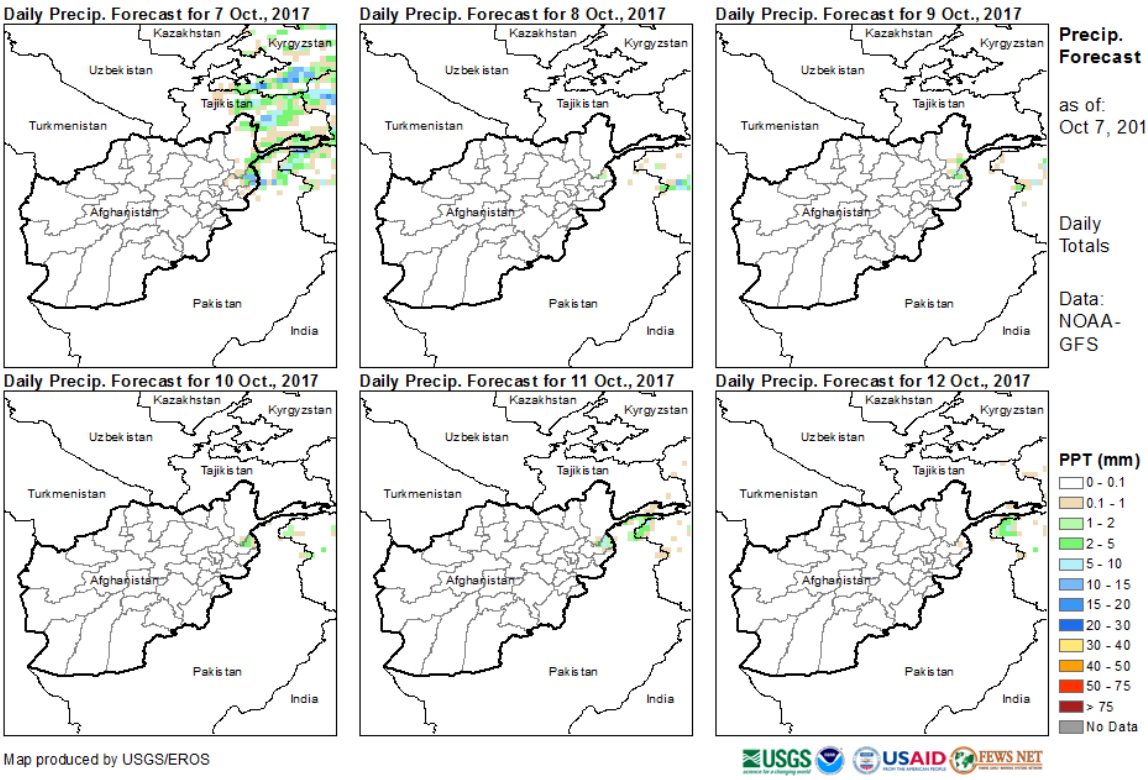

Figure 3.20 6-Day Rainfall Forecasts currently available from FEWS NET – CA for Afghanistan[20]

[20] *FEWS NET – CA (2017): https://earlywarning.usgs.gov/fews/search/Asia/Central%20Asia/Afghanistan; Accessed on 08-Oct-2017.*

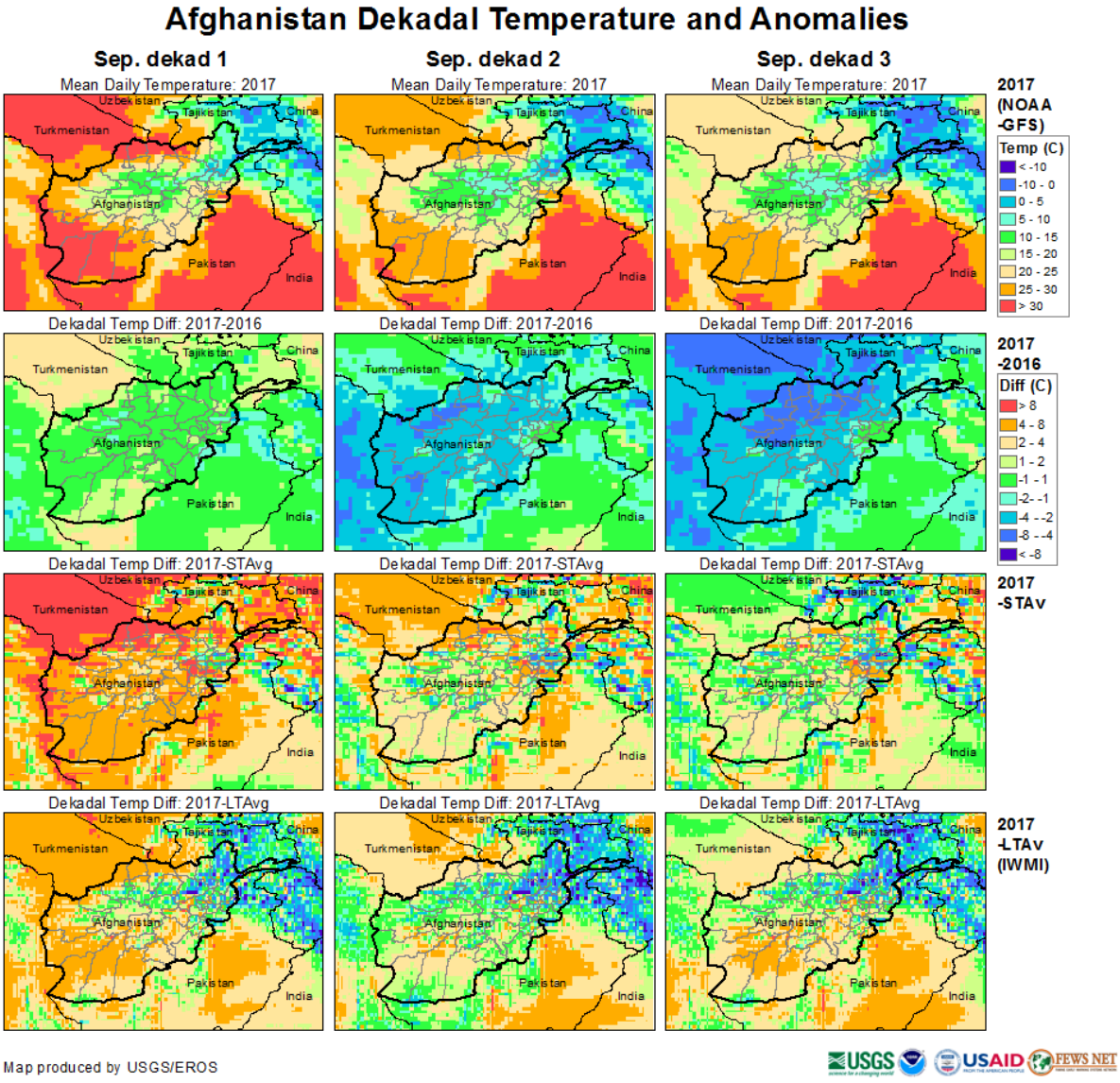

Figure 3.21 Decadal daily mean temperature and anomalies from FEWS NET – CA for Afghanistan[21]

[21] *FEWS NET – CA (2017): https://earlywarning.usgs.gov/fews/search/Asia/Central%20Asia/Afghanistan; Accessed on 08-Oct-2017.*

3.4.3 Predictability of droughts and potential for improved monitoring and forecasting

Afghanistan is characterised by large climate variability. While the majority of the country is semi-arid, the climate varies from arid in the southern part to moderately humid in the high mountain ranges (Qureshi, 2002). A recent study (Hoell et al., 2015) over Southwest Asia, which includes Afghanistan, showed that the long-term trend of sea surface temperatures (SST) are linked to the anti-cyclonic circulation over the region, and that has been shown to decrease precipitation and increase temperature in the region. An earlier study on drought assessment (Muhammad et al., 2011) in northern Afghanistan (part of the Amu Darya Basin) showed good potential of the Palmer Drought Severity Index (PDSI) method (Palmer, 1965) by modifying it to account for snow storage and melt. Similarly, a recent study (Nasery, 2017) in several sub-basins of the Kabul basin showed reasonable accuracies in long-term hydrological simulation using the HEC-HMS model with detailed snowmelt routine. Although the drought related literature is limited for Afghanistan, results of these studies are promising for developing drought monitoring/forecasting systems. Increasingly available meteorological forecasts, remote sensing products and public domain hydrological models will help facilitate such development.

4 Results - Colombia

4.1 Drought risk related country characteristics

4.1.1 Geography and population

Colombia is located in the northwest of South America. It has a total area of 1,141,750 km^2: 1,038,700 km^2 of land and 100,210 km^2 of marine area. Colombia is an equatorial country with a climate determined by trade winds, humidity and altitude. In most of the country, there are two rainy seasons – from April to June and from August to November – and two dry seasons. Table 4.1 summarizes some characteristics of the country.

The geography of Colombia is characterized by its six main natural regions (Figure 4.1 - a): the Andes mountain range region in the centre of the country, the Pacific coastal region towards the west, the Caribbean coastal region in the north, the Orinoquia region in the east, the Amazon Rainforest region in the south, and the insular area, which is comprised of islands in both the Atlantic and Pacific oceans.

Colombia has a total population of about 46.5 million with an average population density of 40.3 inhabitants/km^2. However, the population is not distributed homogenously (Figure 4.1b). Most of the population is concentrated in the Andean highlands and along the Caribbean coast where the main urban centres are located. Traditionally a rural society, movement to urban areas was very heavy in the mid-20th century and Colombia is now one of the most urbanized countries in Latin America. The urban population increased from 31% of the total in population in 1938 to nearly 75% by 2014[22]. The Orinoquia and Amazon regions, which cover about 54% of Colombia's area, contain less than 6% of the population.

Table 4.1 Characteristics of Colombia

Geography	
Total Area	1,141,750 km^2
Land	1,009,500 km^2
Water	132,250 km^2
Highest Elevation	5,700 m
People	
Population	46,653,419
Population Growth Rate	0.9%
Economy	
GDP per capita (PPP)	$14,130 (est. 2016)

[22] *DANE, 2010.*

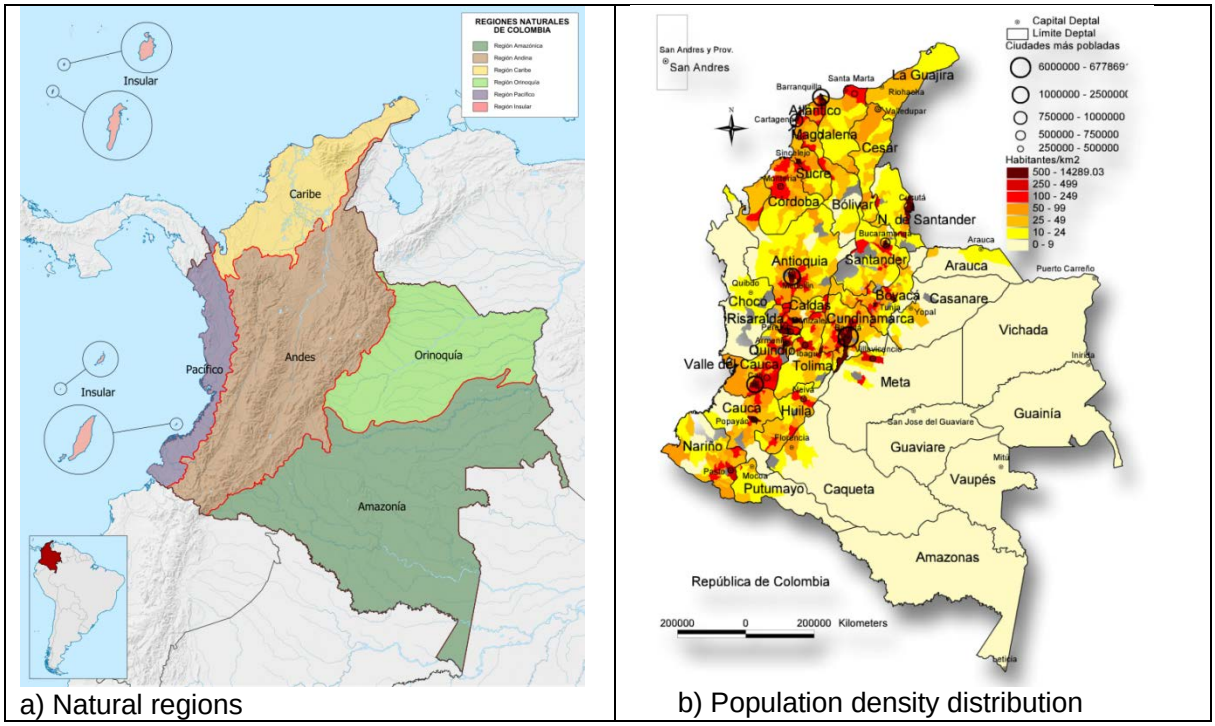

a) Natural regions b) Population density distribution

Figure 4.1 - Colombia population density and natural regions.

4.1.2 Hydrology and water resources

The national meteorology, hydrology and environmental studies institute (IDEAM) divides Colombia into five main hydrographic regions as shown in Figure 4.2. These areas have considerable differences in climate conditions, population density and land use[23].

The *Magdalena – Cauca* region concentrates the large majority of Colombian population and economic activities. Approximately 80% of the Colombian population lives in this region and it produces 85% of the GDP. The Magdalena River is considered to be the main river in the country. It has a length of approximately 1,558 km with1,290 km of it being navigable. It is used to transport goods from the port in Barranquilla in the Caribbean Sea to points inland. The main tributary of the Magdalena River is the Cauca River with both rivers draining parallel from south to north. The annual average rainfall is approximately 2,000 mm in the upper parts of the basin with some areas in the centre of the basin having higher average annual precipitation totals running between 3,000 and 5,000 mm/year. The upper and central part of the basin is used to provide water to the cities and villages, irrigation interests and for hydropower production. The lower part of the basin consists of several interconnected swamps that play an important role in regulating the flows of the river during flooding periods[24].

The *Orinoco* region is located in the eastern part of Colombia and corresponds to a large plains region. Orinoco has large rainfall variability, ranging from 1,500mm/year in the northern part, to 6,000 mm/year in the west given its proximity to the Andean region. On average, rainfall ranges between 2,000 and 3,000 mm/year.

[23] *Atlas climatológico de Colombia. IDEAM 2010.*

[24] *IDEAM – Estudio nacional del agua 2010 – capitulo 3*

The *Amazonas* basin is located in the south part of Colombia and corresponds to the tropical forest that covers one third of the country. Annual precipitation varies approximately between 3,000 and 4,500 mm/year.

The *Pacific* region has an area of approximately 76,500 km^2. The Pacific has the highest average annual precipitation in Colombia, at approximately 6,000 mm/year with some records of up to 12,000 mm/year. It has more than 200 rivers that drain from the western mountainous chain to the Pacific Ocean in the west coast of Colombia. The rivers in this region are short and have large flow discharge rates.

The *Caribe* basin has the lowest annual average rainfall, which varies between 500 and 2,000 mm/year. The lowest annual rainfall occurs towards the north – in the Alta Guajira region- and the highest records are found in the southern parts of the country.

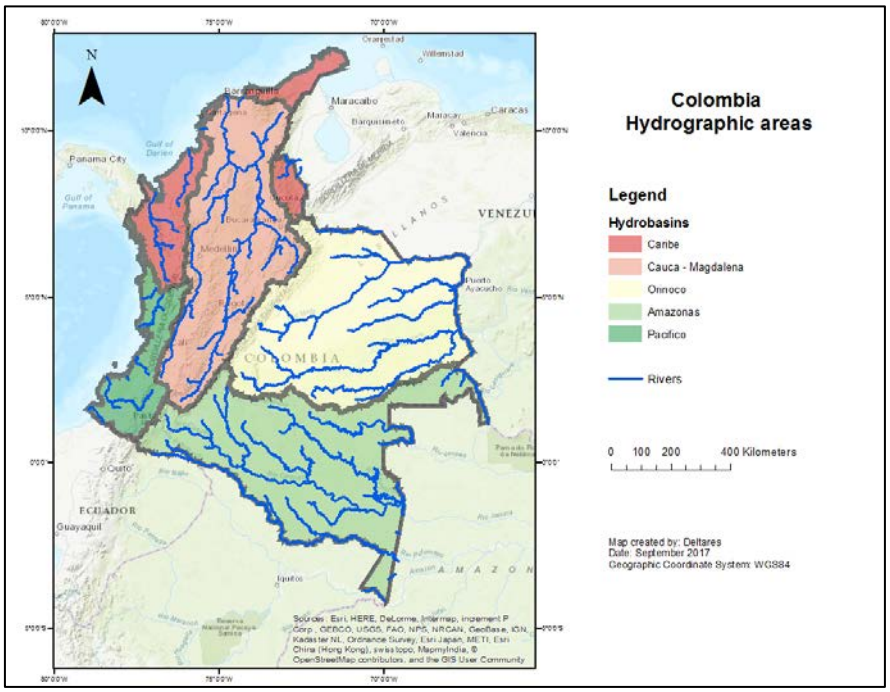

Figure 4.2 Main Colombian hydro basins. Source: IDEAM

Water demand is mainly concentrated in the Magdalena – Cauca and Caribe regions (Figure 4.4) as a result of the population distribution. The highest water demand per year is observed around the large urban centres of Bogota, Cali and Medellin, where it reached up to 1,000 million m^3/year in 2010. The Orinoquia, Amazon and Pacific regions, which normally have abundant water resources have the lowest water demand with less than 20 million m^3 per year.

According to the Aqueduct Water Risk Atlas (Figure 4.3), Colombia has low baseline water stress (equal to the ratio of total annual water withdrawals to total available annual renewable supply, accounting for upstream consumptive use). Higher values indicate more competition among users and more likely that meteorological and hydrological droughts translate into water shortage.

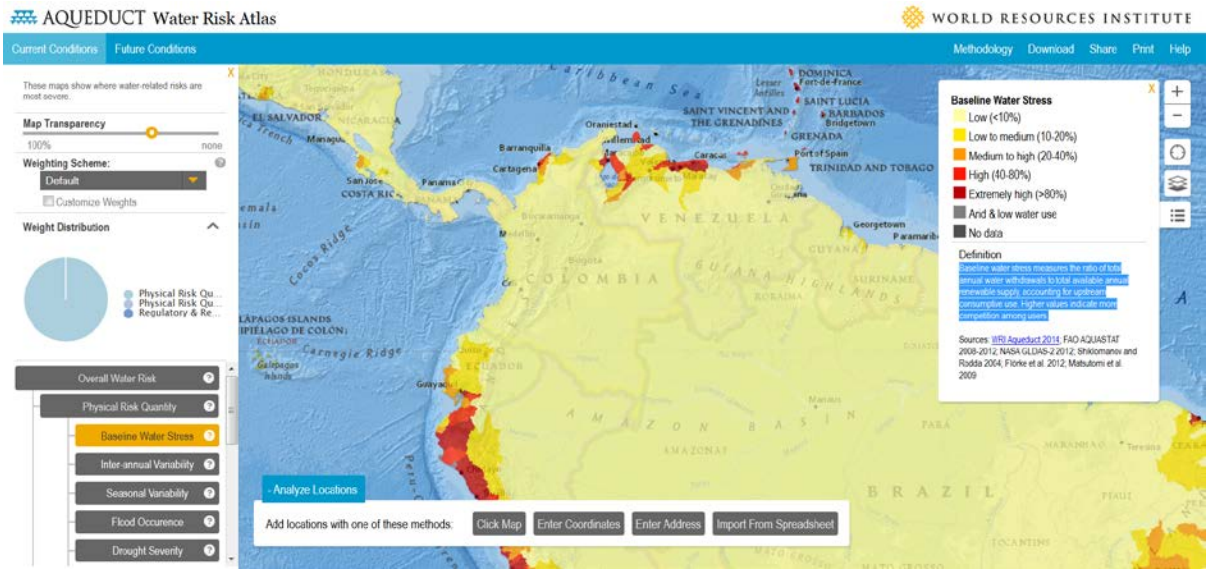

Figure 4.3 Baseline water stress (source: Aqueduct Water Risk Atlas)

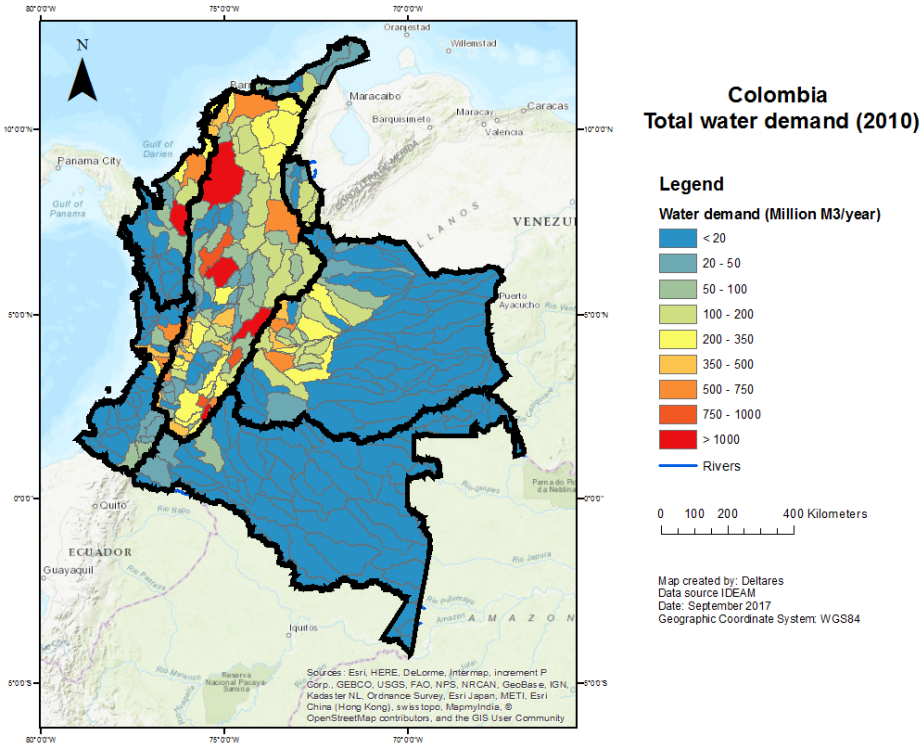

Figure 4.4 Estimated water demand in 2010 aggregating domestic, industrial, agricultural and hydropower generation consumption. Source: IDEAM, National water study 2014.

4.1.3 Historical droughts

According to the EM-DAT Database (Figure 4.5), Colombia experienced droughts having significant impacts (affected population) in 1998 and 2015. The event of 1998 is highlighted as one of the most severe by IDEAM (2014). This event coincides with the occurrence of the strong El Niño registered in 1997-1998. In February 1998, 45% of the territory was under

moderately dry conditions and 2% in very dry conditions. The extremely dry conditions areas were localized within the Magdalena-Cauca basin.

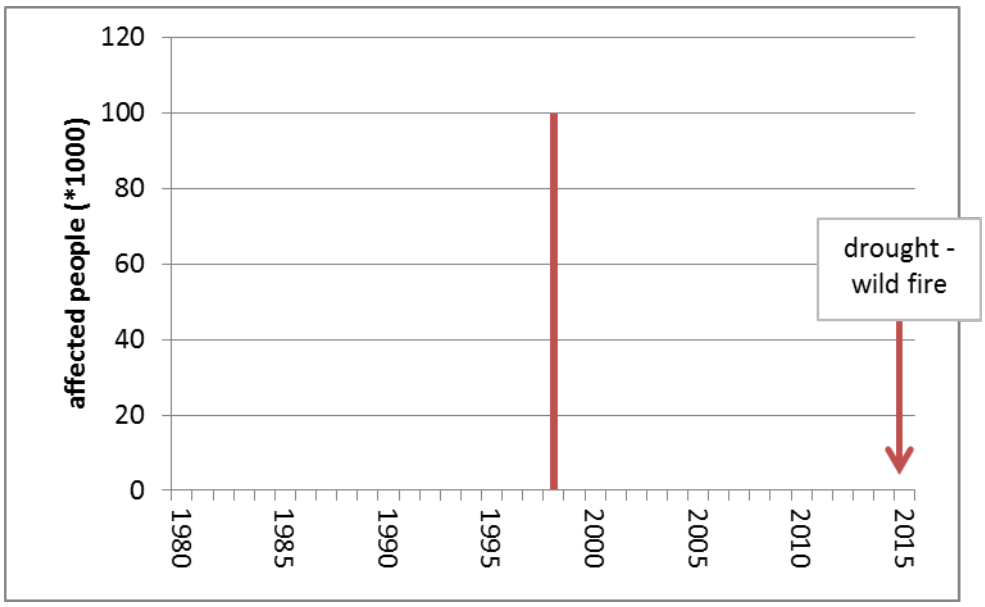

Figure 4.5 Drought events in Colombia recorded by EM-DAT.

IDEAM (2002) conducted an analysis of historical droughts by regions, based on absolute SPI3 values, between 1970 and 2000, including the correlation with El Niño events. IDEAM identified drought periods when SPI3 < - 0.8 for more than 3 consecutive months.

The Magdalena-Cauca region is highly influenced by Niño events (Figure 4.6Figure 4.6). Two extreme droughts, based on the classification used by IDEAM, occurred during the analysed period: 91-92 and 97-98. In terms of duration the most prolonged droughts correspond to 82-83, 91-92 and 97-98. These droughts occurred during strong and very strong Niño years.

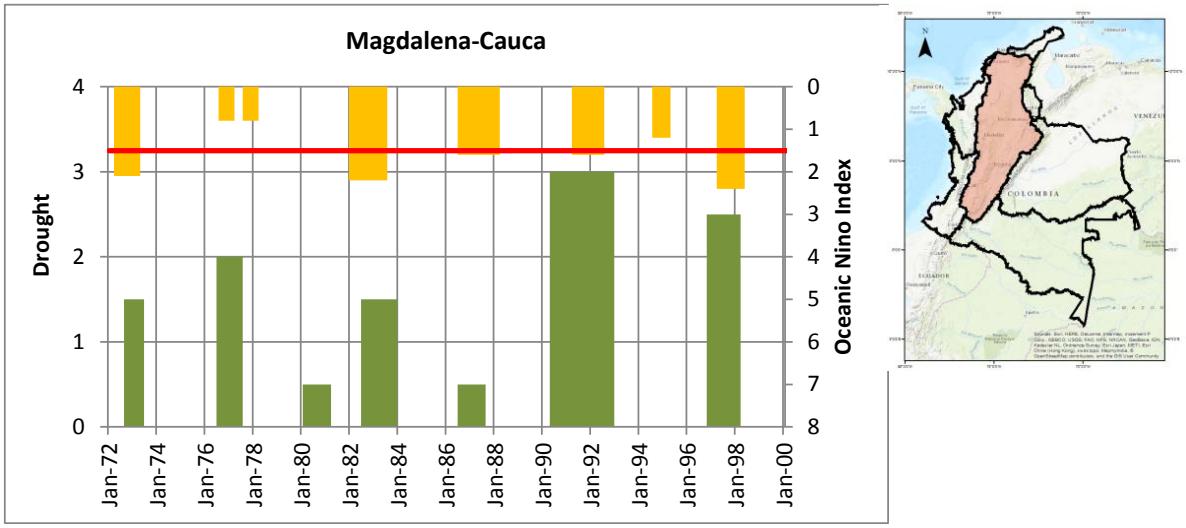

Figure 4.6 Historical droughts and Oceanic Niño Index (ONI) for the Magdalena-Cauca region. Green bars: drought classification; Yellow bars: ONI value, red line: ONI value for very strong Nino events.

The 1998 drought affected various sectors of the economy: agriculture, hydropower production, water supply, and fluvial navigation. The drought affected the most productive regions in Colombia – Magdalena-Cauca, Pacific and Caribe – and caused direct losses of US$56 million (10%) and indirect losses of US$502 million (CAF, 2000).

Water supply: Surface water supply systems were affected mainly in the Magdalena-Cauca and Caribe regions. Almost the entire Magdalena-Cauca region was under water rationing schemes, varying from six hours to two days intervals. Distribution systems were impacted by low pressure, which affected communities that occupy the higher areas where the water pressure was not enough to ensure the distribution. Higher temperatures increased the water demand thereby increasing the water supply issues.

Hydropower production: Almost all reservoirs were affected during the drought period 1997-98. On average, river discharge into the reservoirs in 1997 was 74.9% of the multiannual average. The reduction in hydropower production increased the pressure on the thermal power stations, resulting in an increased price of electricity that was charged to the end users.

Agriculture and livestock: according to CAF (2000), the drought caused a severe reduction in crop and livestock yields. The direct losses for the agriculture sector are estimated at US$101 million and the indirect impacts, related to a decrease in exportations and the negative economic effects, were estimated at US$124 million.

4.2 Assessment of available drought hazard models

4.2.1 Comparison and validation at the country scale

Utilizing the relevant drought hazard indices from the global datasets available (section 2.2.1), graphs were produced for the percent-area of the country experiencing drought conditions for three drought levels: moderately dry (index value below -1), severely dry (index value below -1.5) and extremely dry (index value below -2). All graphs are shown in Appendix A2. In these graphs, the registered droughts from EM-DAT and IDEAM are plotted as well. Based on these graphs, the overlap of global drought hazards with reported droughts was assessed as well as the comparability of datasets and indices. SPI-1 was left out of the comparison because the results are relatively spikey and could not be compared to drought events at a yearly time scale.

Table 4.2Table 4.2 gives an overview of the results for Colombia, showing that the reported droughts are moderately well detected by most drought hazard indices from the global datasets. Only the drought of 1997 was not picked up by the dataset-index combinations used in the analysis. Mainly the indices SPI3 (except for the Global Land Surface dataset), SPEI3, and SPEI12 showed pronounced drought signals in the six years with the reported drought events. The GLS dataset did not show pronounced droughts in the years with registered drought events.

In the 30-year period that was assessed, the global models indicated five other drought years that were not registered as drought events by EM-DAT or IDEAM. Some of them were strong signals (1985-86, 2010, and 2013). False alarm rates of individual dataset-index combinations range between 20% (PCR-GLOBWB-SSFI) to 63% (GLS-SPI3). For both the years with, and without, registered drought events, the comparability of the different dataset-index combinations was variable.

Table 4.2 Results of the country-scale assessment of globally available drought hazard dataset-index combinations. Years with registered drought events are shown in black and years without registered drought events, but drought hazards shown by the dataset-index combinations, are shown in red. Corresponding graphs can be found in Appendix A2.

drought events	EM-DAT (1)														Summary of hits				Summary of false alarms	
	IDEAM (6)	'83		'87	'90	'91/92	'97	'98		'02	'04	'10	'13	registered event		global data			
	Global data		'85/86											(+)	(+, +/-)	(+)	(+, +/-)	(+)	(+, +/-)
SPI 3	IRI	+	+	+/-	+	+	-	+		+/-	+/-	+	+	67%	83%	60%	100%	43%	50%
	GLS	+/-	+	+/-	+/-	+/-	-	+		+/-	+/-	+	+/-	17%	83%	40%	100%	67%	50%
	PRCGWB	+	+	+/-	+	+	-	+		+/-	+/-	+	+	67%	83%	60%	100%	43%	50%
	WaterGap	+	+	+/-	+	+	-	+		+/-	+/-	+	+	67%	83%	60%	100%	43%	50%
SPI 12	IRI	+/-	+	+	+	+	-	+/-		+/-	+/-	+/-	+	50%	83%	40%	100%	40%	50%
	GLS	+/-	+	+	+	+	-	-		+	+	+	+/-	50%	67%	80%	100%	57%	56%
	PRCGWB	+/-	+	+	+	+	-	+		+/-	+/-	+/-	+	67%	83%	40%	100%	33%	50%
	WaterGap	+/-	+	+	+	+	-	+		+/-	+/-	+/-	+	67%	83%	40%	100%	33%	50%
SPEI 3	GDM	+	+/-	+	+	+	+/-	+		+/-	+/-	+	+	83%	100%	40%	100%	29%	45%
	PRCGWB	+	-	+	+	+	+/-	+		+/-	+/-	+	+	83%	100%	40%	80%	29%	40%
	WaterGap	+	-	+	+	+	+/-	+		+/-	+/-	+	+	83%	100%	40%	80%	29%	40%
SPEI 12	GDM	+/-	+	+	+	+	-	+		+	+/-	+/-	+	67%	83%	60%	100%	43%	50%
	PRCGWB	+	+	+	+	+	-	+		+	+/-	+/-	+	83%	83%	60%	100%	38%	50%
	WaterGap	+	+	+	+	+	-	+		+	+/-	+/-	+	83%	83%	60%	100%	38%	50%
SSFI 1	PRCGWB	-	+/-	+	+	+	-	+		-	-	+/-	+	67%	67%	20%	60%	20%	43%
	WaterGap	-	+/-	+/-	+/-	+	-	+		-	-	+	+	33%	67%	40%	60%	50%	43%
Summary of hits	(+)	50%	69%	69%	88%	94%	0%	88%		25%	6%	56%	88%	65%	--	49%	--	40%	--
	(+, +/-)	88%	88%	100%	100%	100%	19%	94%		88%	88%	100%	100%	--	83%	--	93%	--	48%

4.2.2 Validation with local data

For Colombia, 46 streamflow measurement stations were available for use with an average length of 112.7 months for the time-series. As shown in Figure 4.7Figure 4.7, the observation stations available for use are predominantly available in the populated areas while the inland tropical areas (south-east) are not covered.

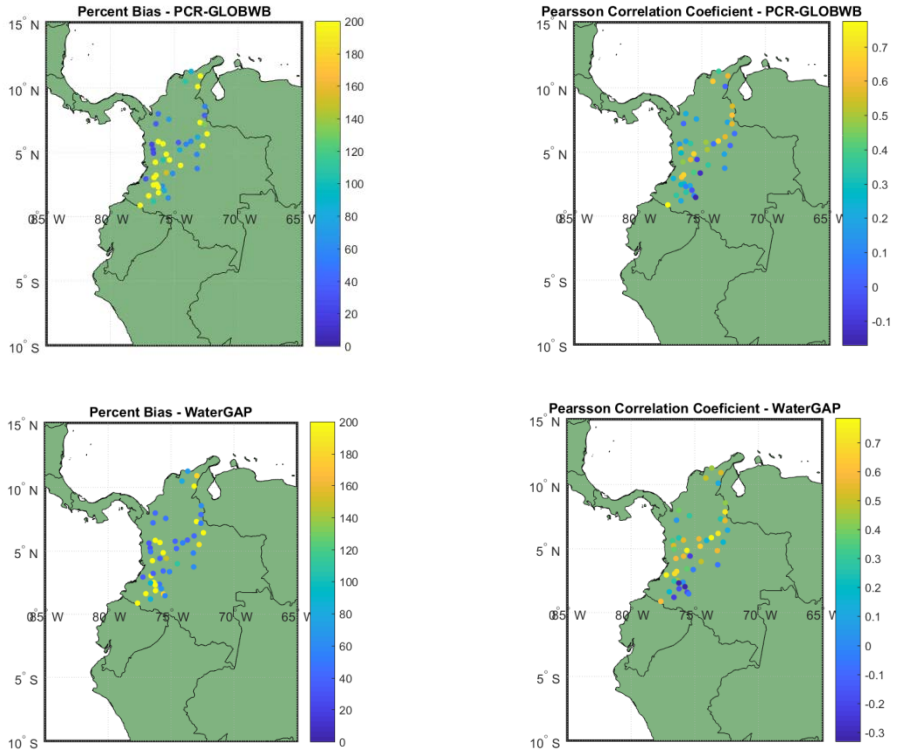

Figure 4.7 Spatial distribution of GRDC measurement stations available for use in Colombia and their performance values for the percent bias, and the Pearson correlation coefficient.

Figure 4.7Figure 4.7 shows for both GHMs evaluated the results for the two performance metrics taking into account all available stations. Overall, PCR-GLOBWB and WaterGAP show a median correlation coefficient value of 0.27 and 0.39, respectively, when using all stations. For PCR-GLOBWB these correlation coefficient values range from 0.02 up to 0.77. For WaterGAP we find correlation coefficient values that range from 0.02 up to 0.78. Median percent bias for PCR-GLOBWB in Colombia is 108% Median percent bias values are lower when looking at the WaterGAP output, 62.9%.

Figure 4.8Figure 4.8 shows the hydrograph for a selected discharge observation station in Colombia with 120 months of data available. As visualized by the the hydrograph, WaterGAP nicely aligns with the observed discharges whilst PCR-GLOBWB shows a structural overestimation of its discharge values for this particular station. This is being reflected in the percent bias values found for both models for this station: 37.39% for WaterGAP compared to 222.8% for PCR-GLOBWB. Despite the relatively large differences in absolute discharge estimates, both models do show relatively good performance when it comes to the correlation coefficient: 0.68 for both PCR-GLOBWB and WaterGAP, indicating that the temporal variability of the river discharge is reflected better than the quantity of the river discharge. Thus, both models are, in general, equally able in reflecting relative dry and wet episodes and

can identify or characterize drought events for this particular location. Hydrographs for all other stations in Colombia are available as a supplement to this document.

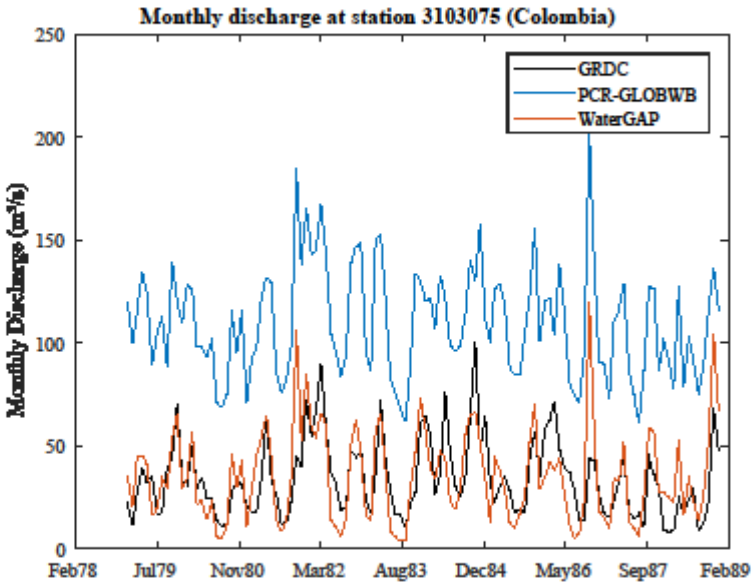

Figure 4.8 Hydrograph visualizing the performance of PCR-GLOBWB and WaterGAP relative to the historical observations at station 310375.

4.2.3 ENSO analysis

Figure 4.9Figure 4.9 visualizes for Colombia the median share of total land area in drought conditions during EN, LN, and N years using the different drought indicators, various accumulation time-periods and the inputs from both PCR-GLOBWB and WaterGAP. Results for the SPI show that it is likely that a higher share of the total land area of Colombia is in drought during La Niña (LN)-years, as compared to El Niño (EN) and Neutral (N) years, and irrespectively of the accumulation period used to identify drought conditions. Results for the SPEI and SSFI show that the two hydrological models show relatively different signals when it comes to the median area in drought. Whilst for the SPEI, the PCR-GLOBWB shows a relatively higher median share of land area in drought under LN conditions, compared to EN and N conditions, WaterGAP shows the opposite signal. For WaterGAP the share of land is in drought is said to be relatively higher under EN conditions, compared to LN and N conditions. For the SSFI, WaterGAP estimates a relatively higher median share of land area in drought under LN years compared to EL and N years, whilst PCR-GLOBWB hints at a relative lower share of the land area in drought during the LN years.

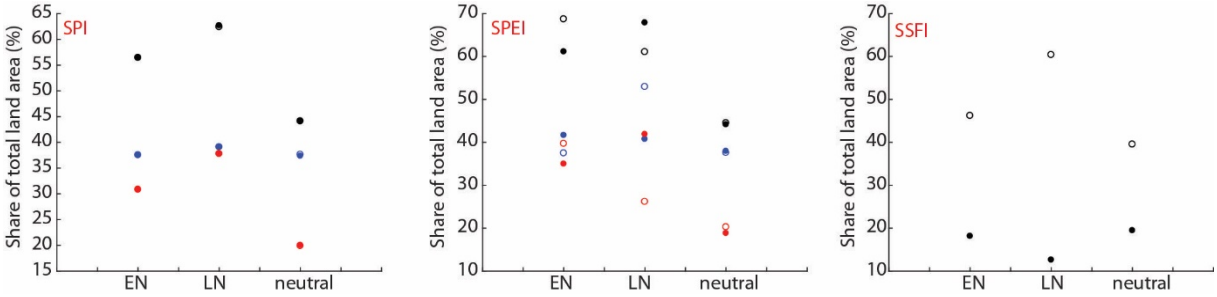

Figure 4.9 Area in drought in Colombia during El Niño (EN), La Niña (LN), or neutral years using the SPI, SPEI, and SSFI drought indicator. The open symbols show the results for WaterGAP while the filled symbols show the results for PCR-GLOBWB. Different colors indicate the different accumulation periods used: 1 month (black), 3 months (blue) and 12 months (red).

Figure 4.10Figure 4.10 shows (in a spatially explicit manner) those areas in Columbia that experience a significant increase or decrease in the frequency of drought months (SSFI < -1) when comparing the EN years with all other years (non-EN: LN and N), and vice versa. Again, spatial patterns in anomalies in drought frequency months show a roughly similar pattern between PCR-GLOBWB and WaterGAP. During LN years, a vast majority of the land area indicates a significant decrease in the frequency of drought months when compared to non-LN years. During EN years, both models indicate that whilst in the central part of the country drought frequency experiences a significant decrease compared to non-EN years, drought frequency is significantly elevated compared to non-EN years in the areas surrounding the central parts.

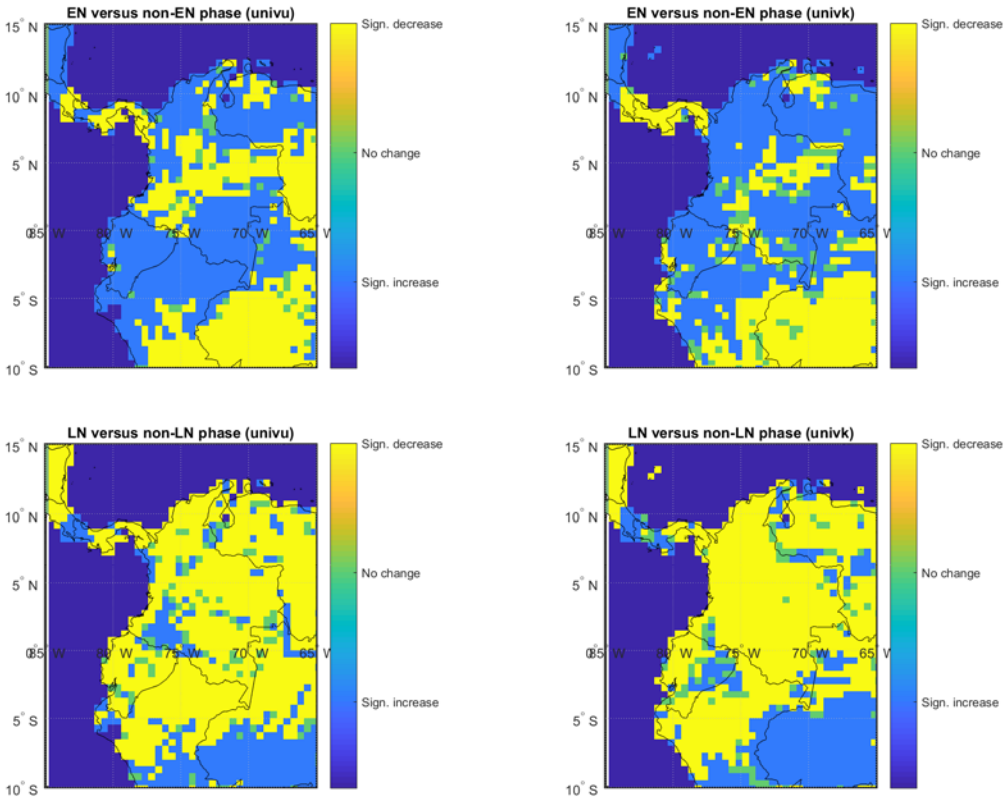

Figure 4.10 Spatial distribution of area with a significant increase, decrease or no change in frequency of drought months when comparing the El Nino years with the non El Niño years and the La Niña years with the

non La Niña years. Left sub-plots show the results for PCR-GLOBWB, right sub-plots show the results for WaterGAP.

Relatively high correlation coefficient values were found for Colombia (see Figure 4.11), especially in the north-western parts of the country, with values ranging up to ~0.8. Both PCR-GLOBWB and WaterGAP show the same spatial distribution in correlation coefficient values although the correlation values themselves seem to be relatively higher for PCR-GLOBWB. The sub-plots visualizing the optimal lag-time indicate that optimal lag-periods for both hydrological models are relatively shorter for Colombia compared to Afghanistan, ~0-3 months for WaterGAP and ~1-4 months for PCR-GLOBWB. Moreover, both models show an inland area (east-central) with consistently high optimal lag-periods of 12 months for both models.

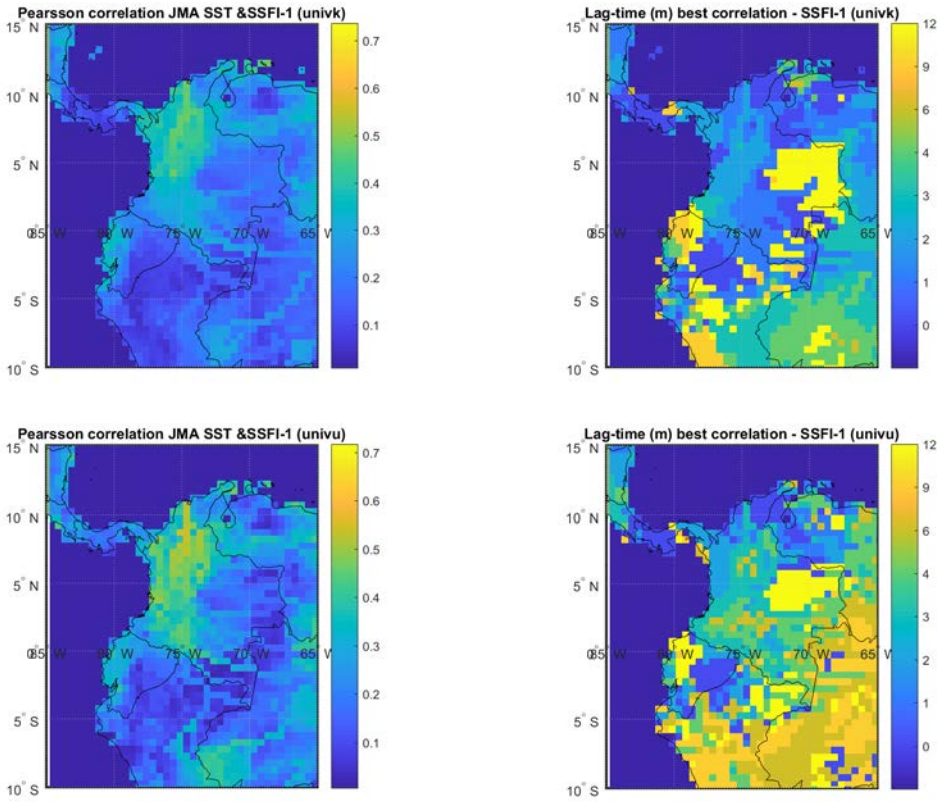

Figure 4.11 Spatial distribution of optimal Pearson correlation coefficient between continuous JMA SST values indicating ENSO conditions and the SSFI-1 drought indicator. Left sub-plots show the optimal correlation coefficient, right sub-plots show the lag-time that corresponds to the best correlation coefficient found. Results for both PCR-GLOBWB and WaterGAP are visualized.

Previous research underpins this result by showing that ENSO has a large influence on the inter-annual variability and water resources availability in Colombia. A large part of Colombian territory, especially towards the Pacific coast and the central region, is sensitive to the effects of droughts and flooding during El Niño and La Niña phases, respectively (World Bank, 2012). In addition, previous research shows that the Orinoquia and Amazonia regions present less severe anomalies, indicating that El Niño has larger impact towards the Pacific Coast.

4.3 Assessment of drought impact and risk platforms and datasets

4.3.1 Maps of overall drought impact and risk

Country scale maps are presented that are based on the Global map of drought risk from JRC (Carrão et a., 2016) (Figure 4.12). Although the presented indices of drought hazard, exposure, vulnerability, impact and risk are dimensionless factors based on an aggregation of information and data, they provide a good first impression of the drought risk situation in the country. For Colombia, drought hazard is relatively low, while exposure and vulnerability are at medium to high levels across large parts of the country. This is in line with the registered drought events (only one national scale, but multiple at the sub-national level) and the descriptive information of the country characteristics. Based on literature, drought hazard and risk are probably higher during dry seasons. This aspect of temporal variability is probably not taken up in the maps from JRC. The high vulnerability to droughts in the country is probably caused by the fact that Colombia has a history of social unrest and a relatively low GDP. The combination of relatively low levels of hazard, but medium to high levels of exposure and vulnerability in large parts of the country, leads to drought impact and risk maps with high spatial variability. The drought risk in Colombia may be higher than shown in the maps during the dry seasons. For an assessment of the spatial variability in the maps a detailed study including extensive collection of impact data is required.

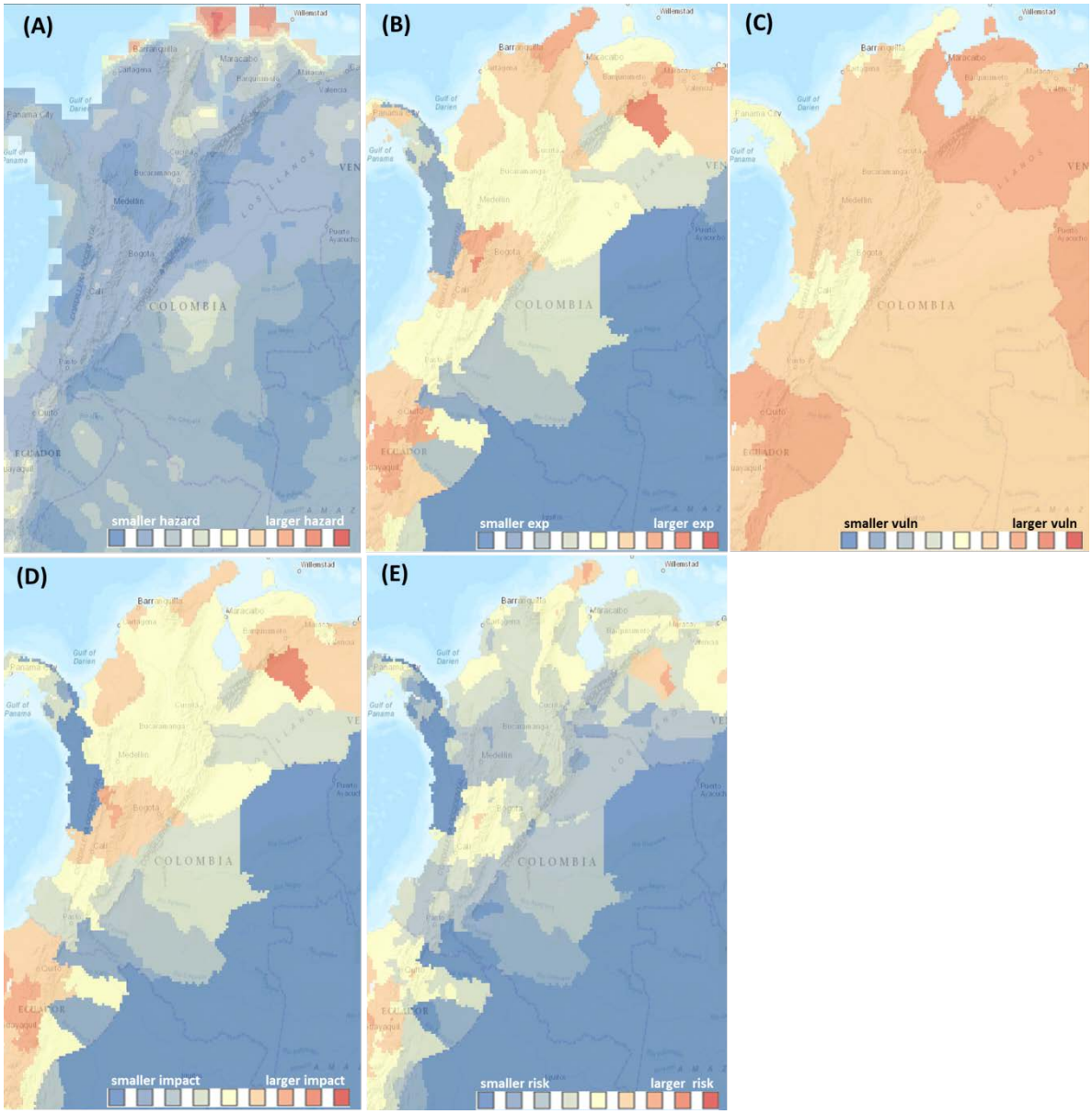

Figure 4.12 Maps from the Global map of drought risk developed by JRC showing the following indices: drought hazard (A), exposure (B), vulnerability (C), impact (exposure x vulnerability) (D), and risk (hazard x impact (E)).

4.3.2 Drought impact on population

The IWMI data portal provides maps with information related to drought impacts on population for all countries in the world: per capita mean annual river discharge, agricultural water crowding with respect to mean annual precipitation and agricultural water crowding with respect to mean annual river discharge (Figure 4.13). For Colombia it shows that the annual discharge per person is low in some mountainous areas, while in the downstream areas it is medium to low. The amount of people that are dependent on one m^3 precipitation and one m^3 discharge water is very diverse across the country, ranging from low to high. The maps show some comparability with the drought exposure and impact maps from JRC (Figure 4.12). For an assessment of the spatial variability in the maps a detailed study including extensive collection of impact data is required.

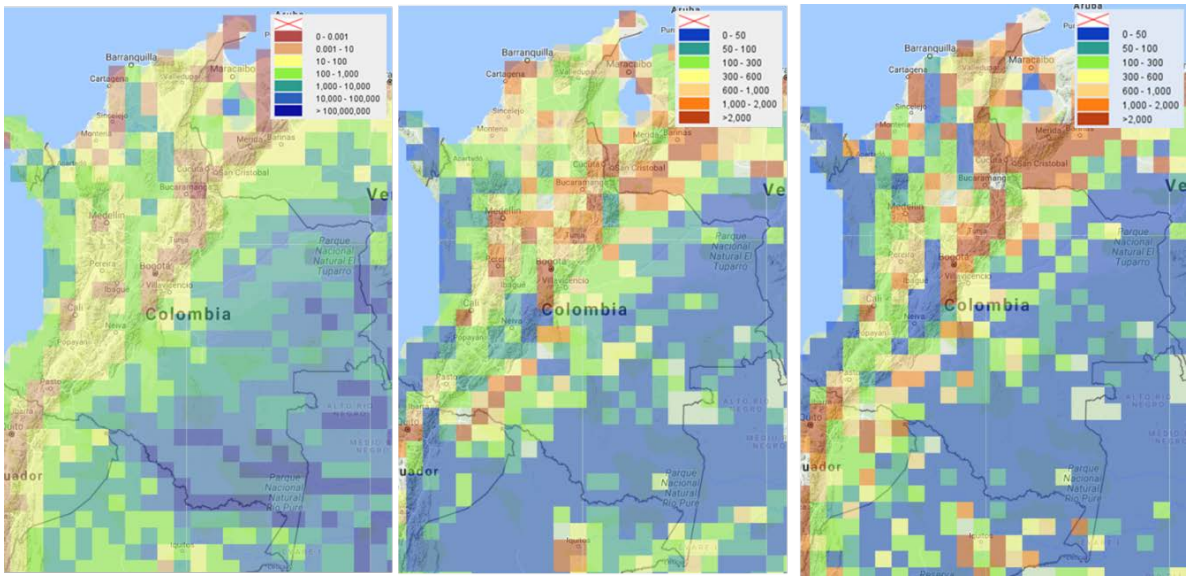

Figure 4.13 Maps providing impact (exposure/vulnerability) on population available from IWMI water data portal, from left to right: per capita mean annual river discharge (m^3 per person); agricultural water crowding with respect to mean annual precipitation (population m^3); agricultural water crowding with respect to mean annual river discharge (population m^3).

4.3.3 Impact on agriculture

Maps of historical agricultural drought impacts are provided by the online Aqueduct Water Risk Atlas (baseline water stress with respect to agriculture) and by the FAO-platform "Agricultural Stress Index and precipitation anomalies" (Figure 4.14). Due to the difference in temporal aggregation periods, the maps cannot be directly compared. The spatial patterns of baseline agricultural water stress in the Aqueduct map do not show large similarity with the impact map from JRC (Figure 4.12). The FAO-platform provides a map with Agricultural Stress Index (ASI; % cropland affected by drought) for each year since 1985. Table 4.3 provides an overview of the years with coverage of approximately 25% the country or more with high to very high ASI levels and matching drought years based on registered droughts and the global drought hazard models (see section 4.2.1). According to the ASI maps, 8 out of 31-year monitoring period show large areas with high levels of agricultural drought stress. Only 2 of these 8 years were listed as registered drought years and 1 of the 8 years showed as being a significant drought hazard from the global models. For an assessment of the spatial variability in the maps, a detailed study including extensive collection of impact data is required. Impact data could consist of local data of actual reduction of water availability to agriculture during historical drought periods as well as the effects of such levels of water stress on economic revenues.

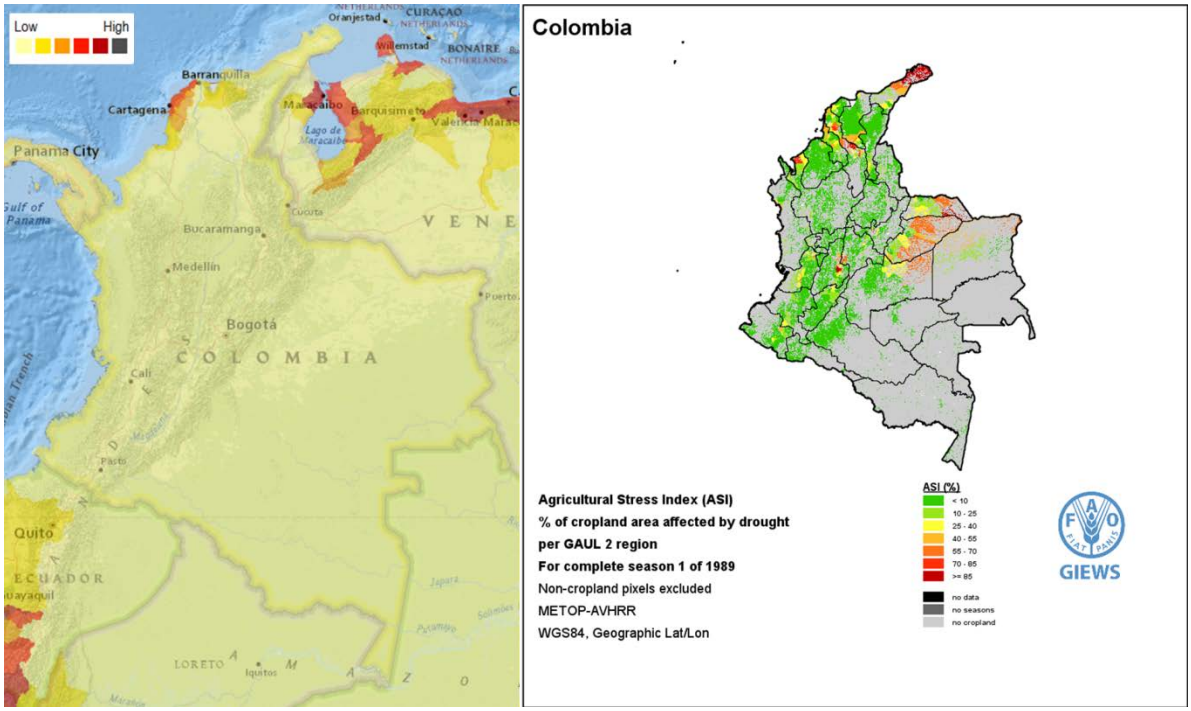

Figure 4.14 Maps of historical agricultural drought impacts. Left: map from the Aqueduct Water Risk Atlas providing baseline water stress with respect to agriculture; Right: map from the FAO-platform "Agricultural Stress Index and precipitation anomalies for a relatively dry year.

years with high ASI (S1)	Registered droughts	Hazard in global models
1985		x
1989		
1991	x	
1992	x	
2001		
2003		
2014	N/A	N/A
2015	N/A	N/A

Table 4.3 Years with high ASI values during first growing season covering 30% or more of the country (FAO platform[25]) compared to registered droughts and drought hazards determined with global models (see section 4.2.1).

4.3.4 Impact to hydropower

The online Aqueduct Water Risk Atlas provides maps with baseline water stress with respect to electric power generation, which is (almost) identical to the map with baseline water stress with respect to agriculture. For Colombia, it can be observed that for a large part of the country the stress level is relatively high. The spatial patterns in the map are not in line with the map of overall drought impact from JRC (Figure 4.12). This may be caused by the different origin of the maps as the maps from JRC are directed at the drought hazard while the Aqueduct map focusses on water stress. In addition, the JRC maps overall drought impacts, while the Aqueduct map has its focus on electrical power. For an assessment of the

[25] *http://www.fao.org/giews/earthobservation/country/index.jsp?lang=en&code=COL*

spatial variability in the maps a detailed study including extensive collection of impact data is required. Impact data could consist of the location of hydropower plants and the actual reduction of water availability (e.g. lowered reservoirs levels, reduced river discharge) to these plants during historical drought periods as well as the effects of such levels of water shortage on produced electricity and economic revenues.

Figure 4.15 Map from the Aqueduct Water Risk Atlas providing baseline water stress with respect to electric power.

4.3.5 Impact on the overall economy

A map presenting a socio-economic drought vulnerability index is available from the IWMI-portal and a default baseline water stress map is available from the Aqueduct Water Risk Atlas (both maps in Figure 4.16). The IWMI map shows a low level of socio-economic vulnerability but does not provide any spatial differentiation at the sub-national level. The low level of socio-economic vulnerability is completely different than the high level of vulnerability shown by the JRC map (Figure 4.12). It can be observed that for the largest part of the country the default water stress level is low, which is very similar to the Aqueduct maps presenting baseline stress with respect to agriculture and electric power. The spatial patterns in the map are not in line with the map of overall drought impact from JRC (Figure 3.14). For an assessment of the spatial variability in the maps a detailed study including extensive collection of impact data is required.

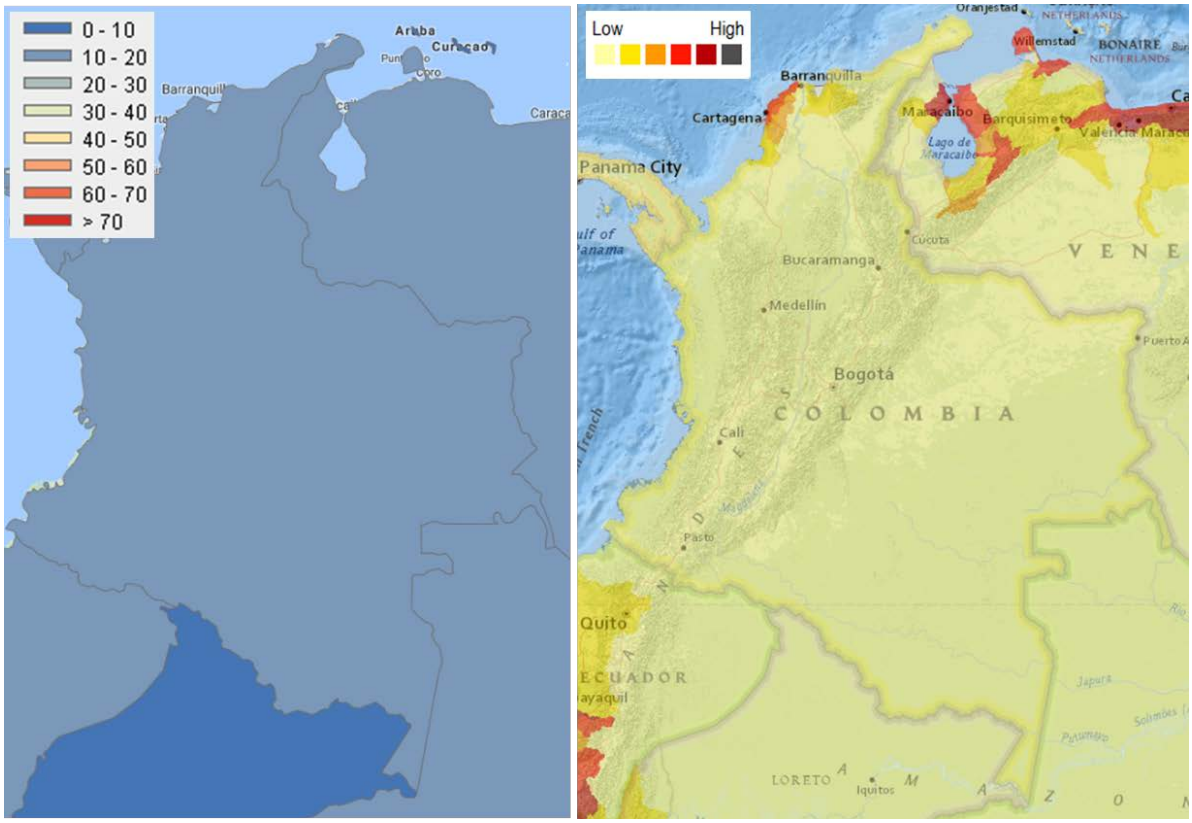

Figure 4.16 Maps with drought impact to the overall economy from different online platforms: Socio-economic drought vulnerability index from IWMI-portal (left); Baseline Water stress – Default form Aqueduct Water Risk Atlas (right).

4.3.6 Impact to municipal and industrial water needs

Various maps are available at the Aqueduct Water Risk Atlas that relate baseline water stress to industrial sectors (mining, food & beverage, chemicals, semi-conductor, oil and gas, mining, construction materials, textiles). However, there does not seem to be any variation in base line water stress for the different sectors. It is unclear if any spatial information of the impact sectors was available for Colombia at the sub-national scale. Also, no independent drought impact information for these industrial sectors was available for the case study countries during our research. Hence, no further assessment of these impact maps was performed.

4.4 Evaluation of forecasting and monitoring systems

Colombia has a tropical climate, which in most of the country has a bimodal regime with two wet seasons (April-May and October-November), interspersed by two dry periods (January-February and June-August). The remaining months are considered transition periods. It is considered as one of countries in the world having the most ample water resources, but due to the complex topography of the Andes, as well as the geographic location between the Pacific and Atlantic Oceans, and the Amazonian basin, the distribution of these resources in time and space is very heterogonous. In the Northwest of the country in the region of Choco, one of the wettest places on Earth can be found with rainfall totals of up to 12 metres annually having being observed. The La Guajira department, some 1000 km away is a hyper arid zone, with up to 200-300 mm of rainfall per annum being observed on average. Additionally, the climate is strongly influenced by the ENSO phenomenon, with El-Niño events typically resulting in drought conditions, while La Niña events may lead to anomalous wet conditions.

This teleconnection is most apparent in the Caribbean and Andean regions of the country, while the signal in the Amazon and Orinoco regions is less clear. Though droughts do occur during El Niño events, there are several other climate signals such as the Madden-Julien oscillation and the Pacific Decadal Oscillation that have influenced the occurrence and spatial distribution of drought. A more complete description can be found in Poveda et al., 2011. Recent droughts that have led to extensive impacts include the 1991/1992, 1994/1995, 1997/1998, 2009/2010 events, and the recent 2015/2016 drought. This most recent event caused extensive impacts to agriculture, livestock (particularly in the Orinoco basin), as well as major issues with failing drinking water supply to urban areas.

4.4.1 Current drought monitoring and forecasting

At the national scale, the monitoring of the climatic and hydrological conditions is the mandate of IDEAM (Instituto de Estudios Ambientales y Meteorlogía), with its main office located in Bogotá, the capital. IDEAM is an agency that falls under the Ministry of Environment and Sustainable Development. The institute operates a nationwide network of meteorological and hydrological stations, including conventional stations that report on a daily basis, as well as telemetered stations. Though the country is reasonably well covered, the density of stations may vary significantly. Data from these stations, complemented by additional information from global resources (for example satellite data such as from GOES) are used to develop a monthly state of the climate bulletin, which reports on a range of meteorological variables such as precipitation and temperature (extremes and anomalies) and drought indicators such as percentage normal precipitation, and the SPI for monthly accumulations ranging from SPI1 to SPI48 months. A climate outlook is also included in the bulletin, primarily based on the six monthly ENSO outlook published by the IRI institute at the University of Columbia in New York. Additionally, consensus seasonal forecasts are made and included in the bulletins available on the IDEAM website. These consensus forecasts are made on a monthly basis, with experts from across IDEAM contributing. Though no other formal seasonal forecasts are included, IDEAM may also issue possible scenarios of precipitation anomalies based on analyses of previous El-Niño events. The declaration of a drought event appears to be done primarily by IDEAM based on El Niño conditions prevailing, although it is not fully clear if a specific threshold is used or if the declaration is based on consensus.

While IDEAM has the mandate to issue bulletins of the climatic situation as well as outlooks, the organisation and coordination of the response at the national level is the mandate of the Unidad Nacional para la Gestión del Riesgo de Desastres (UNGRD, National Unit for Managing Disaster Risk). In the case of drought, this unit may issue a contingency plan to mitigate drought impacts. These contingency plans are developed on a per-event basis. UNGRD will also use assessments of drought vulnerability across the country, such as possible failure of water supply for domestic and agricultural use. Such analyses are based on indicators contained in the National Water Study (Estudio Nacional de Agua, ENA) and the regional water resources evaluation plan (Evaluación Regional de Agua, ERA), which are (or should be) developed for each identified river basin. UNGRD is also currently considering the development of a drought monitoring system at the national level to support their activities.

In addition to the national level agencies, there are 23 regional water management agencies (where regional is synonymous to the departmental level). While most of these agencies depend primarily on the information made available from IDEAM, a selected few also operate their own data networks and forecasting systems. One example is the Corporación Autonoma del Valle de Cauca (CVC), in the Valle del Cauca department. Although they depend on the declaration of drought by IDEAM to enact a local drought contingency plan, they also use a seasonal forecasting system, primarily for the prediction of seasonal inflows to a reservoir in

their area of jurisdiction. This uses an Ensemble Streamflow Prediction (ESP) type approach, as well as statistical forecast models based on selected ENSO indices. These forecasts are run operationally on the national hydrological forecasting system (FEWS Colombia) that is hosted by IDEAM. Its main use is short- to medium-range hydrological forecasting.

4.4.2 Available operational systems

Monthly Climate Bulletin
The Monthly Bulletin is developed by the IDEAM, along with its state of the climate, through selected indices including precipitation and temperature (extremes and anomalies) as well as drought indicators such as percentage-of normal-precipitation and SPI for monthly accumulations ranging from SPI1 to SPI48 months.

FEWS Colombia
The Operational Hydrological Forecasting System is primarily used for issuing short- to medium-range (flood) forecasts, but also includes an Ensemble Streamflow Prediction seasonal forecast for reservoir inflows and statistical forecast models based on ENSO indices.

Table 4.4 provides an overview of the main characteristics of the monitoring and forecasting products available in Colombia.

Table 4.4 Overview of characteristics and performance of drought monitoring and forecasting Models available in Colombia.

	IDEAM Bulletins	**FEWS Colombia**
Monitoring	Yes	Yes
Forecasting	Yes	Yes
Region/countries/areas	Colombia	Colombia
Spatial resolution	N/A	Point
Datasets used	Station data	Station Data
Tools used	-	Delft FEWS
Indices presented	PPA, SPI1-SPI24	Inflow Volume
Reflective of impacts	Limited	No
Forecast horizon	N/A	N/A
Update frequency	Monthly	Monthly
Accessibility of forecast	Good	N/A
Method of access	PDF download	Client system
Procedure / steps	N/A	N/A
Resources required	N/A	N/A
Post-processing	N/A	N/A
Hit-rate (estimation)	N/A	N/A

4.4.3 Predictability of droughts and potential for improvement

The correlations between the ENSO phenomenon and the anonymous meteorological and hydrological conditions, which are stronger for the December-February season and weaker during March-May (Poveda et al., 2001; Poveda et al., 2011), would suggest a reasonable predictability of the onset of drought conditions over Colombia. Dutra et al. (2014) show for the Northern part of South America the improved skill for predicting the onset of drought conditions using ECMWF's System 4 global seasonal forecasting system. Despite this apparent predictability, little effort has been dedicated to date in moving beyond the six

monthly outlooks of El Niño conditions provided by the IRI Institute in New York along with the consensus forecasts from the regional climate outlook forum.

More comprehensive seasonal forecasts could provide significantly more detail on the onset and severity of drought conditions across the country. Such forecasts use either statistical forecasts that have been shown to provide skill in other areas of the world with strong teleconnections such as the Greater Horn of Africa (Funk et al., 2014), using dynamical seasonal prediction models, or mixed approaches (Trambauer et al., 2015; Schepen et al., 2012). The same holds for improved monitoring, where merged station/satellite precipitation products such as CHIRPS could complement station-only based assessments of drought conditions in the area of the country where the monitoring network of IDEAM has low station density. There are some initiatives underway to improve drought monitoring and forecasting through introduction of systems such as GeoCLIM which has been piloted both at IDEAM and at CVC, as well as extending the FEWS Colombia system to provide additional seasonal forecasting functionality.

5 Results - Ethiopia

5.1 Drought risk related country characteristics

5.1.1 Introduction to the country

Ethiopia is a land locked country located in the horn of Africa. The country shares its borders with Sudan in the north and west; Kenya in the south; Somalia and Djibouti in the east. Ethiopia is an ancient country with a unique culture and diversity of people. Since the establishment of the federal administrative structure, there are nine regional governments and two federal city states including the capital city, Addis Ababa. As of August 8, 2017, the population in Ethiopia was 104,571,284, of which 79.3 % of the population lives in rural area[26].

Ethiopia is one of the places that have an extremely varied topography with a complex geological history that began millions of years ago and continues. The country has about 50% percent of the African Mountains, which covers about 371,432 km^2 above 2,000 meters (FAO 1984). The range in altitude varies from 126 meters below sea level (m.s.l.) in the Dalol Depression rising to the highest mountain Ras Dashen in Semien Mountains at about 4,620 m.s.l. The northern half of the country is dissected by the Ethiopian Rift Valley. This valley runs about 600km along the north–northeast Kenyan Border (Awulachew and Yilma, 2007). The country is highly dependent on agriculture, which has suffered from extreme recurring droughts resulting in poor agricultural output. The main characteristics of Ethiopia are listed in Table 5.1.

Table 5.1 The main characteristics of Ethiopia, Sources: UN-Water (2004) and Viste et al., 2013..

Geography	
Total Area	1.13 Million km^2
Land	99.3% (1.122 Million km^2)
Water	0.7% (0,0791 km^2)
Highest Elevation	4000 m
Land Use	
Arable	10.01%
Perm. Crop	0.65%
Other	84.4% (2013)
People	
Population	71.1 Million (2004.)
Population Growth Rate	2.9 % (2004)
Economy	
GDP growth rate	6% (2004 est.)
GDP per capita	72.37 USD Billion in 2016[27]
Water Statistics*	
Lowlands Rainfall	91 - 600 mm per annum
Highlands Rainfall	1,600–2,122 mm per annum

*) Calculated by Awulachew and Yilma (2007) from Global Precipitation Climatology Centre data.

[26] *Ethiopia Population (LIVE) retrieving data: http://www.worldometers.info/world-population/ethiopia-population/; accessed date 09-08-17*

[27] *Trading economics: https://tradingeconomics.com/ethiopia/gdp ; accessed date 09-08-17*

5.1.2 Hydrology and water resources

Ethiopia has 12 major river basins resulting in a total mean annual flow from all rivers of 122 Billion cubic meters (BCM). There are 11 large fresh water lakes, 9 saline lakes, 4 crater lakes and 12 major wetlands and major swamps covering about 7,500km. The majority of the lakes (except for Tana, Ziway, Langano and Chamo) have no surface water outlets and most of these lakes are rich in fish. Shala and Abiyata Lakes located in the southern Ethiopia have high concentrations of chemicals and recently Lake Abiyata is being used for production of soda ash.

Although Ethiopia has relatively low groundwater potential compared to the surface water potential, the total exploitable groundwater potential is still high. It is estimated to be 2.6 BCM (Awulachew and Yilma, 2007).

Figure 5.1 shows that the baseline water stress in Ethiopia is low to medium. Baseline water stress is defined by WRI as the ratio of total annual water withdrawals to total available annual renewable supply, accounting for upstream consumptive use. Higher values indicate more competition among users. If the baseline water stress is low, meteorological and hydrological drought is not likely to translate into water shortage.

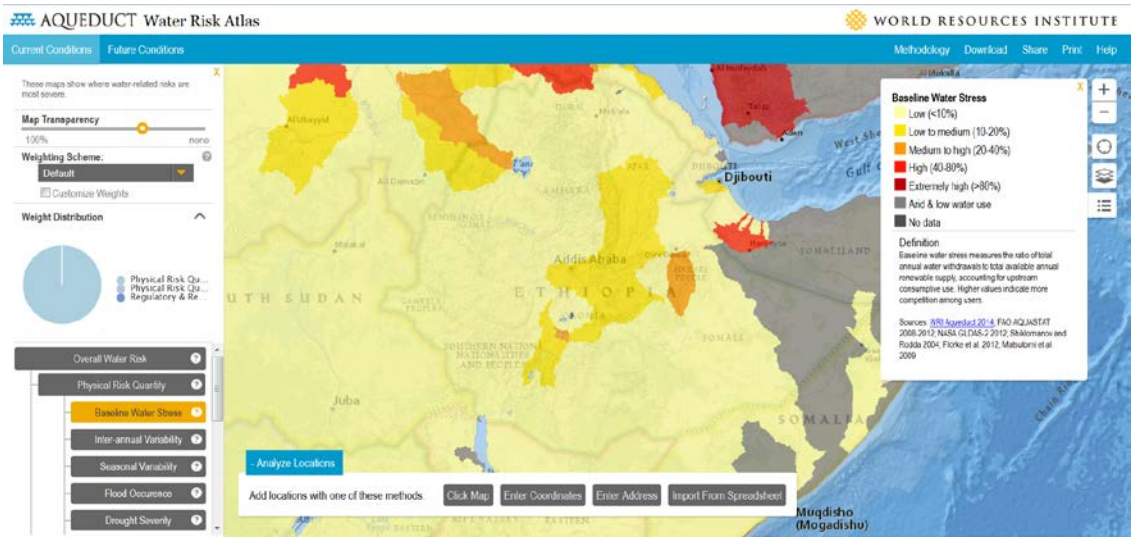

Figure 5.1 Low to medium baseline water stress (= withdrawals divided by renewable supply) in Ethiopia, according to Aqueduct Water Risk Atlas from WRI.

5.1.3 Climate

Most of Ethiopia experiences one main wet season - 'Kiremt' - from mid-June to mid-September (up to 350mm per month in the wettest regions). Parts of northern and central Ethiopia also have a secondary wet season with sporadic and less rainfall from February to May - 'Belg'. The southern regions of Ethiopia experience two distinct wet seasons, here the March to May 'Belg' season is the main rainfall season yielding ~200 mm per month, followed by a lesser rainfall season in October to December called 'Bega' with around 100mm per month. The eastern most corner of Ethiopia receives very little rainfall at any time of year and can be considered dry throughout the entire year. The climate is highly influenced by the Inter-Tropical Convergence Zone (ITCZ).

5.1.4 Drought history

It has been claimed that June 2011 was the driest month over the past 60 years and it was very extreme in some regions of Somalia, northern Kenya and southern Ethiopia. The year

leading up to 2011 was already the driest season in over 60 years and it was very extreme in some regions of Somalia, northern Kenya and southern Ethiopia. The year 2009 was very dry nationally, making it a catastrophic drought next to the 1984 drought (Viste et al., 2013). Yet, the droughts in the years 2015 and 2016 were even more severe. They resulted from very dry rainy seasons and both national and international emergency feeding programs were active to reduce the impacts of the drought[28]. Over the long term, the 1980s have been relatively dry compared to 1990s and 2000s.

In EM-DAT, various drought events have been recorded, including the number of affected people (Figure 5.2). There is little agreement between these figures and the droughts mentioned above except that the period 1990 – 2000 shows relatively small number of droughts.

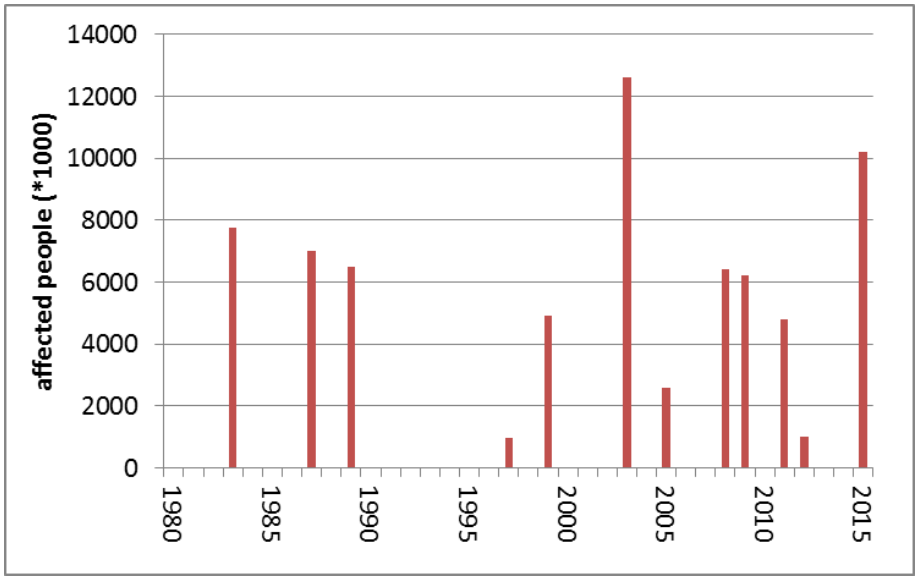

Figure 5.2 Drought events in Ethiopia recorded by EM-DAT

5.1.5 Recent drought study

For Ethiopia, an assessment of spatially varying drought indices has been conducted (Wondie and Terefe, 2016) in which the Palmer Drought Severity Index for the period 1941 to 2010 was calculated using the CRU dataset (Harris et al., 2016). The Palmer Drought Severity Index PDSI (Palmer, 1965) takes into account moisture received (precipitation) as well as moisture stored in the soil, accounting for the potential loss of moisture due to temperature influences. In the assessment, a self-calibrated PDSI was also utilized (ScPDSI, Wells at al. 2004). This overcomes one limitation of the PDSI, which is the use of duration factors that are based on the same precipitation thresholds for different locations. By defining location specific thresholds for the calculation of durations this problem is solved. During the period covered by both sources (1980 – 2010), a limited number of severe drought events occurred (scPDSI < 2) between 1991 and 2000 (Figure 5.3). For this period, EM-DAT shows a relatively small number of drought events in this period. In terms of trends it was found that, for very dry spells with ScPDSI values of -2 to -2.99, no clear trend could be derived at the country scale, but on the regional scale the trend in calculated PDSI values shows that in the western and northern part of Ethiopia extended areas experiencing drought increases with time (Figure 5.4).

[28] *World Food Programme, www.wfp.org, accessed December 2017*

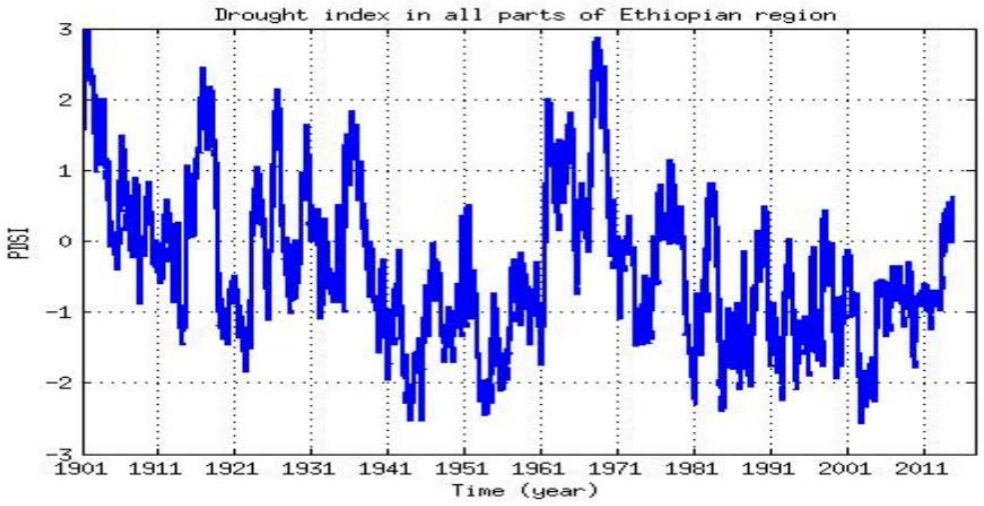

Figure 5.3 PDSI values derived from time-series for the period 1901-2014.

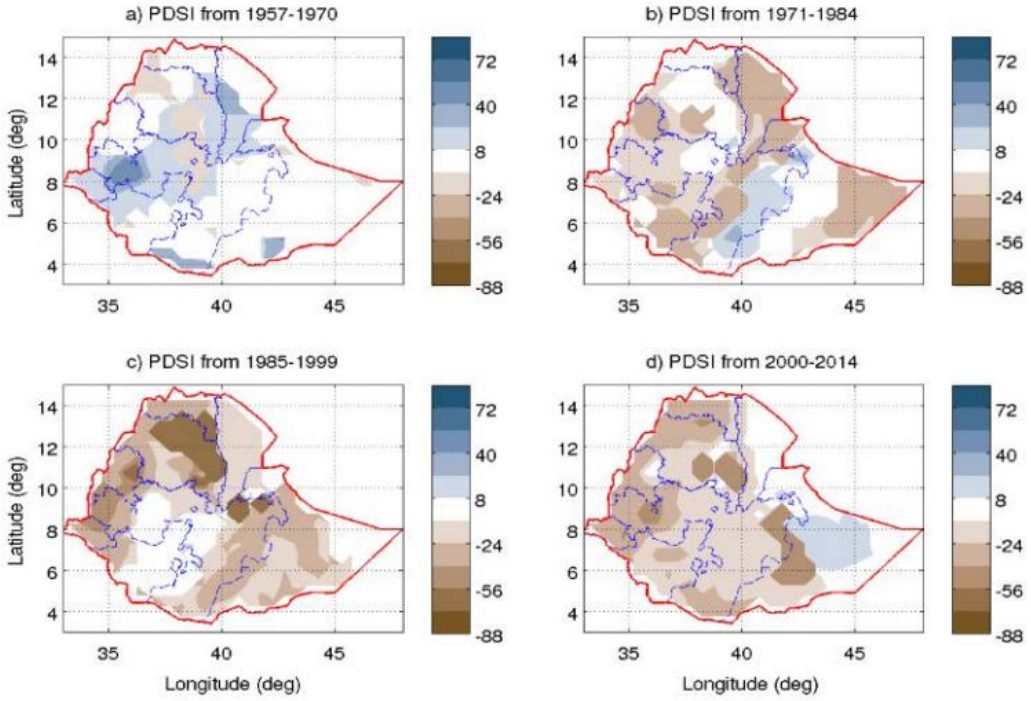

Figure 5.4 Number of months with dry events (PDSI < -2) during the periods as mentioned on top of the graphs, visualising the positive drought trend in the western and northern parts of Ethiopia

5.2 Assessment of available drought hazard models

5.2.1 Comparison and validation at the country scale

For the relevant drought hazard indices available from the global datasets (section 2.2.1), graphs were produced for the percentage-area of the country experiencing drought conditions at three drought levels: moderately dry (index value below -1), severely dry (index value below -1.5) and extremely dry (index value below -2). All graphs are shown in Appendix A3. In these graphs, the registered droughts from EM-DAT are plotted as well. Based on the

graphs, the overlap of global drought hazard with reported droughts was assessed as well as the comparability of datasets and indices. SPI1 was left out of the comparison because the results are relatively spikey and could not be compared to drought events at a yearly time scale.

Table 5.2 gives an overview of the results for Ethiopia, showing that the reported droughts are not always well predicted by the drought hazard indices from the global datasets. For more than 60% of the calculated dataset-index combinations, the calculated drought hazard is not very pronounced, or barely visible if at all. The SPEI3 index based on the WaterGAP database shows a relatively good overlap with registered drought events.

The comparability of the dataset-index combinations is limited. In the 30 year period that was assessed, the global models indicated eight other drought years which were not registered as drought events by EM-DAT. False alarm rates of individual dataset-index combinations range between 36% (WaterGAP-SPEI3) to 63% (GLS-SPI12). For the years without registered drought events, the comparability of the droughts shown by the different dataset-index combinations was relatively high compared to the years with registered drought events.

Table 5.2 Results of the country-scale assessment of globally available drought hazard dataset-index combinations. In the table, years with registered drought events are shown in black and years without registered drought events, but drought hazards shown by the dataset-index combinations, are shown in red. Corresponding graphs can be found in Appendix A3.

drought events	EM-DAT (12)	'83	'84	'85	'86	'87	'88	'89	'91	'93	'94	'97	'98	'99	'00	'03	'05	'08	'09	'11	'12	Summary of hits regist. events (+)	Summary of hits regist. events (+, +/-)	Summary of hits global data (+)	Summary of hits global data (+, +/-)	Summary of false alarms (+)	Summary of false alarms (+, +/-)
	Global data		**'84**	**'85**	**'86**		**'88**		**'91**	**'93**	**'94**				**'00**												
SPI 3	IRI	-	+	-	+	+	+/-	+/-	+	+	+	+	+/-	+	+	+	-	+	+	-	-	50%	67%	75%	88%	50%	47%
	GLS	+/-	+	-	+	+	+/-	+	+	+	+	+/-	+/-	+	-	-	-	-	-	-	-	17%	42%	63%	75%	71%	55%
	PRCGWB	+/-	+	-	+	+	+/-	+/-	+	+	+	+	+/-	+	+	-	-	+	+	-	-	42%	67%	75%	88%	55%	47%
	WaterGap	+/-	+	-	+	+	+/-	+/-	+	+	+	+	+/-	+	+	-	-	+	+	-	-	42%	67%	75%	88%	55%	47%
SPI 12	IRI	+/-	+	-	+	+	+	-	+	+	+	+	+/-	+	+	+	+	-	+/-	-	-	42%	67%	88%	88%	58%	47%
	GLS	+/-	+	+	+	+	+	-	+	+	+	-	-	-	-	-	-	-	-	-	-	8%	17%	88%	88%	88%	78%
	PRCGWB	+/-	+	+	+	+/-	+	+/-	+	+	+	+	-	+	+	+	+	-	-	-	-	33%	58%	100%	100%	67%	53%
	WaterGap	+/-	+	+	+	+/-	+	-	+	+	+	+	-	+	+	+	+	-	-	-	-	33%	50%	100%	100%	67%	57%
SPEI 3	GDM	-	+	+/-	+	+	+/-	+/-	+	+	+	+	+/-	+	+	+/-	-	+/-	+	+	-	25%	58%	75%	100%	67%	53%
	PRCGWB	+/-	+	+	+	+	-	+/-	+	-	+	+	+/-	+	+	+/-	-	+	+	+/-	-	33%	75%	75%	75%	60%	40%
	WaterGap	+	+	+	+	+	-	+/-	+	-	+	+	+	+	+/-	+	+/-	+/-	+	-	-	58%	83%	50%	75%	36%	38%
SPEI 12	GDM	+/-	+	+	+	+	+	-	+	+	+	+	-	+	+	+	+	+	-	-	-	42%	50%	100%	100%	62%	57%
	PRCGWB	+/-	+	+	+	+/-	+	-	+	+	+	+	+/-	+	+	+	+	-	+/-	-	-	33%	67%	100%	100%	67%	50%
	WaterGap	+/-	+	+	+	+	+	-	+/-	+/-	+/-	+	+/-	+	+	+	+	-	-	-	-	33%	58%	63%	100%	56%	53%
SSFI 1	PRCGWB	+	+	+	+	+	+	-	+	+/-	+/-	-	-	+/-	+	+	+	-	-	-	-	33%	42%	63%	100%	56%	62%
	WaterGap	+/-	+	+	+/-	+	+	-	+/-	+/-	+/-	+	-	+	+/-	+	+	-	+/-	-	-	33%	50%	38%	100%	43%	57%
Summary of hits	(+)	13%	100%	81%	94%	75%	56%	6%	75%	69%	81%	81%	6%	81%	75%	63%	44%	25%	38%	0%	0%	**35%**	--	**77%**	--	**60%**	--
	(+, +/-)	88%	100%	88%	100%	100%	88%	50%	100%	88%	100%	88%	63%	88%	88%	75%	56%	38%	56%	6%	0%	--	**57%**	--	**91%**	--	**52%**

5.2.2 Validation with local data

For Ethiopia, 38 streamflow measurement stations were available for use with 84.7 months being the average length of the time-series. As shown in Figure 5.5Figure 5.5, most observation stations available for use are located in the central part of the country with little to no stations being located in the border areas.

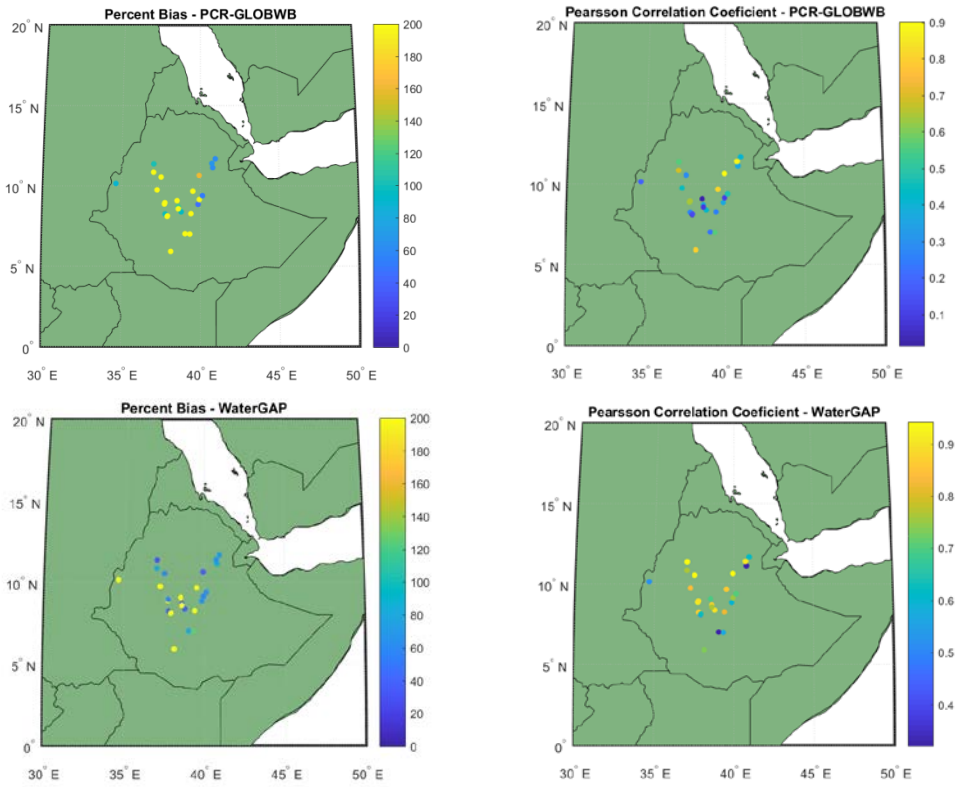

Figure 5.5 Spatial distribution of GRDC measurement stations available for use in Ethiopia and their performance values for the percent bias, and the Pearson correlation coefficient.

Figure 5.6Figure 5.6 shows (for both GHMs) the results for the two performance metrics taking into account all available stations. For Ethiopia, WaterGAP shows a significantly higher median correlation coefficient of 0.66 (ranging between 0.06 – 0.94) compared to a median correlation coefficient of 0.36 for PCR-GLOBWB (ranging between 0.01 – 0.90). When looking at the distribution in correlation coefficient values we find structural differences between the two models (Figure 5.6). Whereas for the percent bias in long-term mean discharges approximately halve of the stations show similar values among the two models, significant differences are found in the correlation coefficient for a majority of the 38 stations evaluated. Regarding the median percent bias, WaterGAP shows on average a better performance with a median percent bias of 73.4% compared to 146.3% for PCR-GLOBWB.

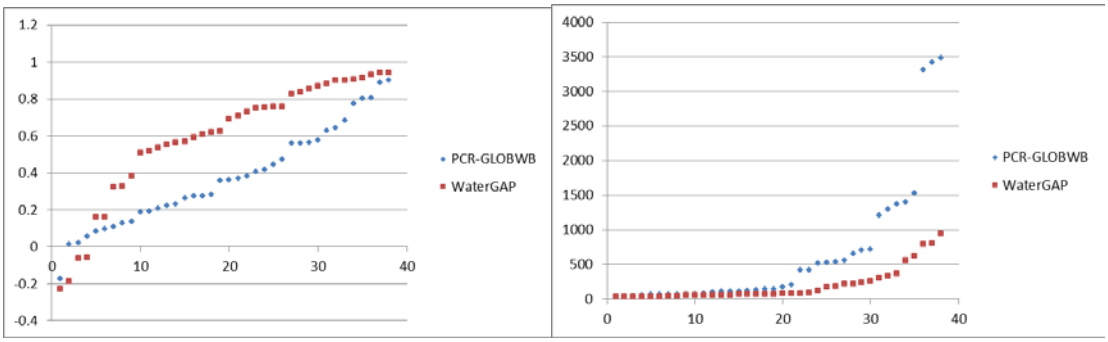

Figure 5.6 Distribution of the correlation coefficient (left) and percent bias (right) values for both PCR-GLOBWB and WaterGAP. X-axis represents all stations available for analysis in Ethiopia. Y-axis represents the correlation coefficient values or the percent bias values.

Figure 5.7Figure 5.7 shows two hydrographs for selected discharge observation stations in Ethiopia with 24 and 108 months of data available. For the first station (visualized on the left) we see that WaterGAP is well able to characteize the hydrological seasonal pattern whereas PCR-GLOBWB has difficulties tin expressing peak- and low-flow discharges. This is relfected in the performance values found for both models. WaterGAP returns a considerably high correlation coefficient value (0.93) and a relatively low percent bias (31.6%). PCR-GLOBWB, on the other hand, returns a correlation coefficient value of 0.56 and a percent bias of 100.8%. For the second station, we see that both models are reasonably able to reflect the seasonal and inter-annual variation in discharges, which is translated into correlation values of 0.189 (PCR-GLOBWB) and 0.56 (WaterGAP) with percent-bias values of 58.15% (PCR-GLOBWB) and 54.9% (WaterGAP), respectively. Although a visual inspection PCR-GLOBWB's ability to reflect the hydrological variation seems to be better in the right sub-plot compared to the left one, correlation coefficient values indicate otherwise. One should take into account here, however, that the left sub-plot uses only two years of data and that a small, but well-timed peak as is shown in August and a correctly timed falling limb might already provide basis for relative high performance values here. This indicates that it is important to not only evaluate the performance values themselves, but to combine this with a visual inspection of the hydrographs. Hydrographs for all other stations in Ethiopia are available as a supplement to this document.

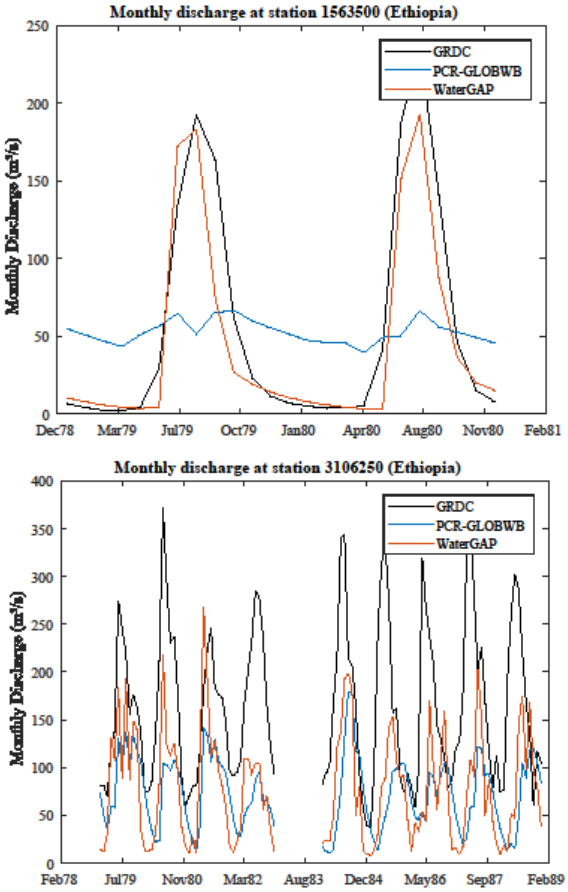

Figure 5.7 Hydrographs visualizing the performance of PCR-GLOBWB and WaterGAP relative to the historical observations.

5.2.3 ENSO analysis

The median share of total land area exposed to drought shows to be significantly lower during La Niña (LN) years, compared to Neutral (N) and El Niño (EN) years for both SPI and SSFI, irrespectively of the accumulation period and the hydrological model used (see Figure 5.8Figure 5.8). At the same time, for these indicators, the share of land area exposed to drought seems to be significantly elevated when selecting only the EN years. For the SPEI indicator, the figure is more dispersed, with results varying between the accumulation periods.

For PCR-GLOBWB we find for the shorter accumulation (1-, 3 months) periods that the share of land area exposed to drought is significantly elevated under EN years and significantly lower under LN years. At longer accumulation times (e.g. 12 months) both EN and LN years show significantly elevated exposure compared to the N years. For WaterGAP we did not find a consistent pattern across the different accumulation periods. Whilst for the 1-month accumulation period median drought exposure is shown to be highest under LN years, no substantial differences were found at the 3-month accumulation period, and even an opposite signal was shown when looking at the 12-month accumulation period.

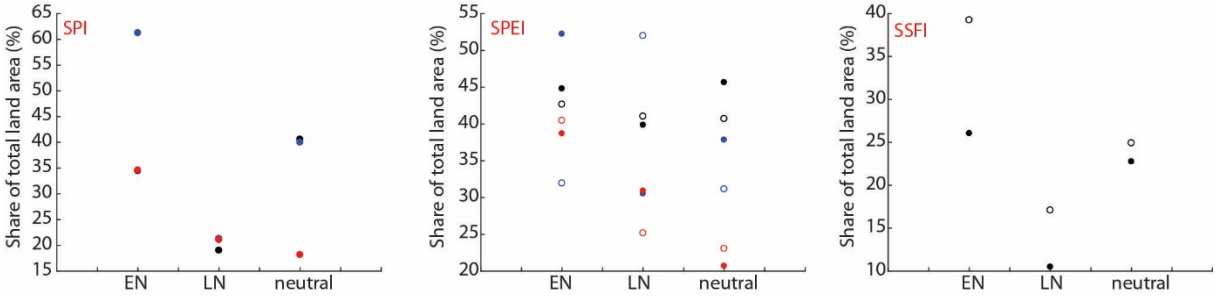

Figure 5.8 Area in drought in Ethiopia during El Niño (EN), La Niña (LN), or neutral years using the SPI, SPEI and SSFI drought indicator. The open symbols show the results for WaterGAP while the filled symbols show the results for PCR-GLOBWB. Different colors indicate the different accumulation periods used: 1 month (black), 3 months (blue) and 12 months (red).

Similar to the spatially explicit results found for Afghanistan and Colombia, we also found in Ethiopia that both models showed (for a vast majority of the land area) that the frequency of drought months significantly decreases during LN years when compared to non-LN years (see Figure 5.9Figure 5.9). Only in the south-eastern parts of the country did we find isolated areas having significant increases in drought frequency during LN years. For EN years the opposite signal is shown. Most of the land area shows a significant increase in drought frequency, while a few spots indicate areas with a significant decrease. However, as shown by Figure 5.9Figure 5.9, this is not a 100% opposite signal. For example, in the northern part of Ethiopia we find places that experience a significant decrease in drought frequency both during EN and LN years.

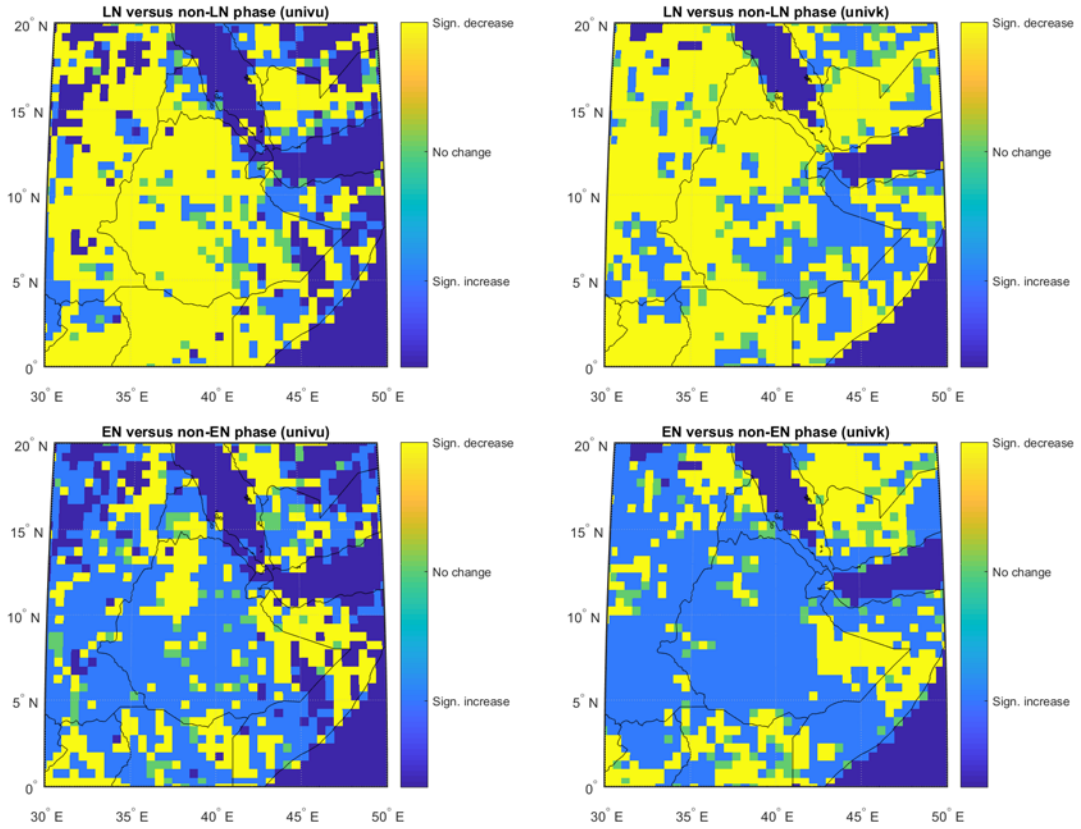

Figure 5.9 Spatial distribution of area with a significant increase, decrease or no change in frequency of drought months when comparing the El Niño years with the non El Niño years and the La Niña years with the

non La Niña years. Left: Sub-plots show the results for PCR-GLOBWB. Right: Sub-plots show the results for WaterGAP.

Pearson correlation coefficient values between the continuous JMA SST and the SSFI-1 are shown to be relatively low for Ethiopia (see Figure 5.10). Moreover, no significant spatial variation in the height of the correlation coefficient value was identified. Both the PCR-GLOBWB and WaterGAP values fluctuate around ~0.1-0.2. A significant spatial variation does exist when evaluating the optimal time-lag to be used to establish the correlations between JMA SST and SSFI-1. Both models show relatively long optimal time-lags for the central and south-eastern part of the country, whilst optimal lags are relatively shorter in the Northwest. Deviations exist between both models when looking at the far south-eastern region of Ethiopia. Here, WaterGAP indicates relatively long optimal time-lags for the correlation between the JMA-SST and the SSFI-1 whilst PCR-GLOBWB identifies significantly shorter optimal time-lags.

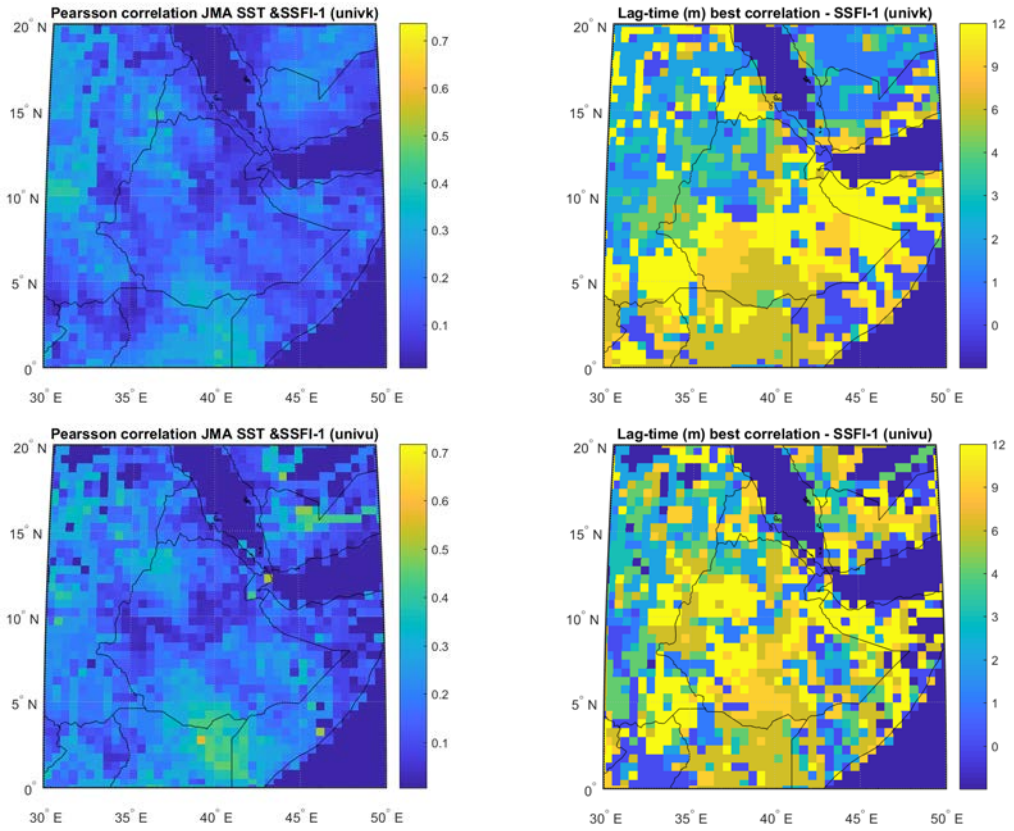

Figure 5.10 Spatial distribution of optimal Pearson correlation coefficient between continuous JMA SST values indicating ENSO conditions and the SSFI-1 drought indicator. Left: Sub-plots show the optimal correlation coefficient. Right: Sub-plots show the lag-time that corresponds to the best correlation coefficient found. Results for both the PCR-GLOBWB and WaterGAP are visualized.

5.3 Assessment of drought impact and risk platforms and datasets

5.3.1 Maps of overall drought impact and risk

Country scale maps are presented that are based on the Global map of drought risk from JRC (Carrão et al, 2016) (Figure 5.11). Although the presented indices of drought hazard, exposure, vulnerability, impact and risk are dimensionless factors based on an aggregation of information and data, they provide a good first impression of the drought risk situation in the country. For Ethiopia, drought hazard is relatively low in the central and western parts of the

country, while in the north, south and east some zones with medium to high drought hazards are shown. This does not fully match with the assessments of drought hazards that showed a higher number of drought hazard events at the country level (section 5.2.1). Exposure ranges from low to high and vulnerability is high across the entire country, which matches with the descriptive information of the country characteristics. The combination of varying levels of drought hazard and exposure, combined with high vulnerability, leads to impact and risk levels that range from low to high. Based on the number of registered drought events, this appears to be an underestimation of the actual drought impact and risk situation in Ethiopia. For an assessment of the spatial variability in the maps a detailed study including extensive collection of impact data is required.

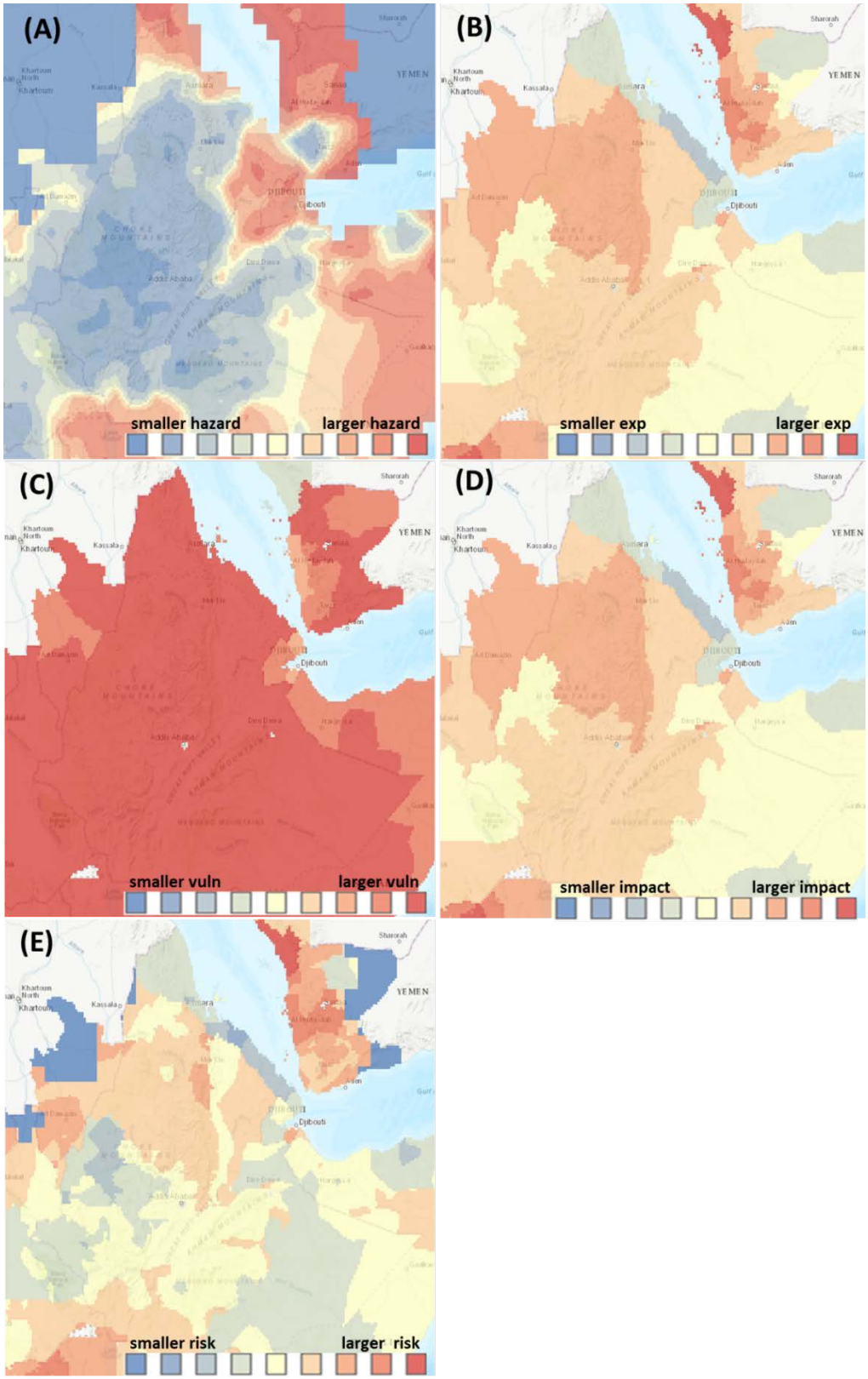

Figure 5.11 Maps from the Global map of drought risk developed by JRC showing the following indices: drought hazard (A), exposure (B), vulnerability (C), impact (exposure x vulnerability) (D), and risk (hazard x impact) (E).

5.3.2 Drought impact on population

The IWMI data portal provides maps with information related to drought impacts on population for all countries in the world: per capita mean annual river discharge, agricultural water crowding with respect to mean annual precipitation, and agricultural water crowding with respect to mean annual river discharge (Figure 3.15). For Ethiopia it shows that the annual discharge per person is diverse varying from medium-high in the areas bordering rivers to very low in the eastern part of the country. The amount of people that are dependent on one m^3 precipitation and one m^3 discharge water also varies widely from low to high. For the eastern part of the country this information is not available. The maps show some comparability with the drought impact and risk map from JRC (Figure 5.11). For an assessment of the spatial variability in the maps a detailed study including extensive collection of impact data is required. Impact data could consist of local data of actual reduction of water availability to the population and agriculture during historical drought periods as well as the effects of such levels of water shortage on economic revenues.

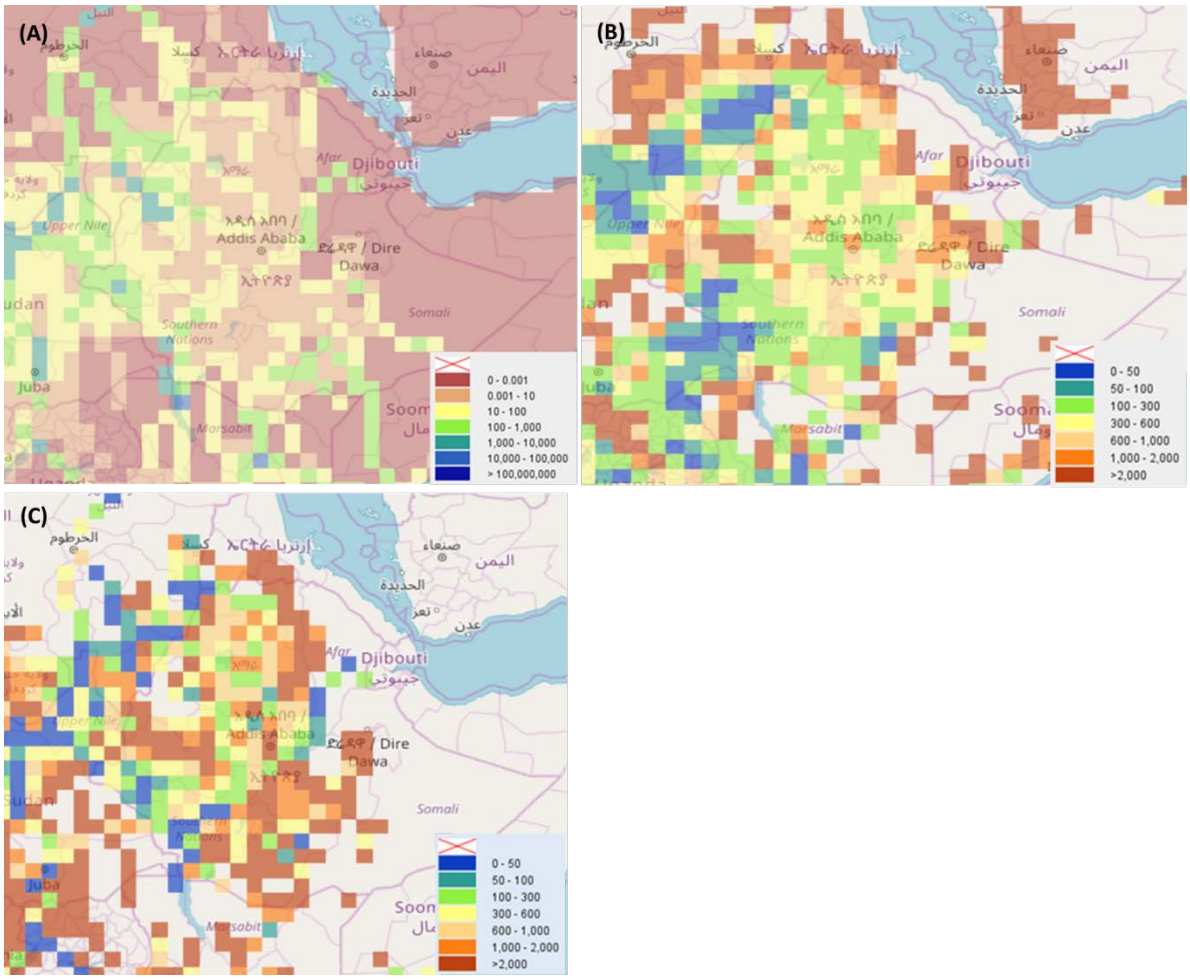

Figure 5.12 Maps providing impact (exposure/vulnerability) to population available from IWMI water data portal, from A to C: per capita mean annual river discharge (m^3 per person); agricultural water crowding with respect to mean annual precipitation (population m^3); agricultural water crowding with respect to mean annual river discharge (population m^3).

5.3.3 Impact on agriculture

Maps on historical agricultural drought impacts are provided by the online Aqueduct Water Risk Atlas (baseline water stress with respect to agriculture) and by the FAO-platform

"Agricultural Stress Index and precipitation anomalies" (Figure 5.13). Due to the difference in temporal aggregation periods, the maps cannot be compared. The spatial patterns of baseline agricultural water stress in the Aqueduct map shows little similarity with the impact map from JRC (Figure 5.11). The FAO-platform provides a map for the Agricultural Stress Index (ASI; % cropland affected by drought) for each year since 1985. For an assessment of the spatial variability in the maps a detailed study, including extensive collection of impact data, is required. Table 5.3 provides an overview of the years with coverage of approximately 25% the country or more with high to very high ASI levels and matching drought years based on registered droughts and the global drought hazard models (see section 5.2.1). According to the ASI maps, 9 out of 31-year monitoring periods show large areas with high levels of agricultural drought stress. Only 5 of these 9 years were listed as registered drought years and 4 of the 9 years were shown to be significant drought hazards by the global models.

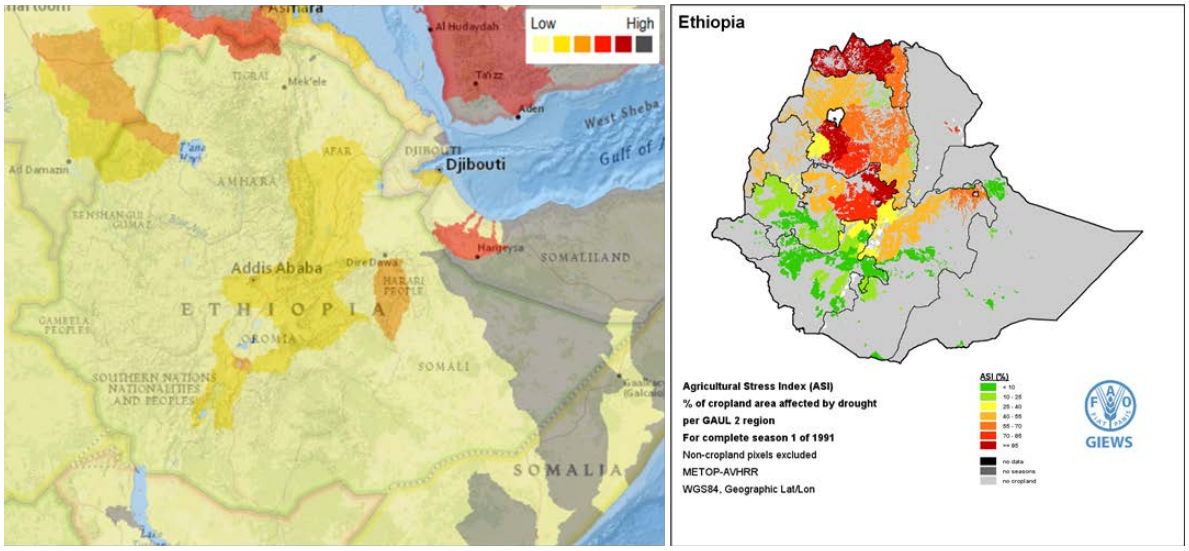

Figure 5.13 Maps on historical agricultural drought impacts. Left: Map from Aqueduct Water Risk Atlas providing baseline water stress with respect to agriculture; Right: Map from FAO-platform "Agricultural Stress Index and precipitation anomalies for a relatively dry year.

years with high ASI (S1)	Registered droughts	Hazard in global models
1984		x
1987	x	
1991		x
2002		
2008	x	(x)
2009	x	(x)
2011	x	
2012	x	
2015	N/A	N/A

Table 5.3 Years with high ASI values during first growing season covering 30% or more of the country (FAO platform[29]) compared to registered droughts and drought hazards determined with the global models (see section 5.2.1).

[29] *http://www.fao.org/giews/earthobservation/country/index.jsp?lang=en&code=ETH*

5.3.4 Impact on hydropower

The online Aqueduct Water Risk Atlas provides maps with baseline water stress with respect to electric power, which is (almost) identical to the map with baseline stress with respect to agriculture. For Ethiopia it can be observed that for a large part of the country the stress level is relatively low. The spatial patterns in the map are not in line with the map of overall drought impact from JRC (Figure 5.11). For an assessment of the spatial variability in the maps a detailed study including extensive collection of impact data is required. Impact data could consist of the location of hydropower plants and the actual reduction of water availability (eg. lowered reservoirs levels, reduced river discharge) to these plants during historical drought periods as well as the effects of such levels of water shortage on produced electricity and economic revenues.

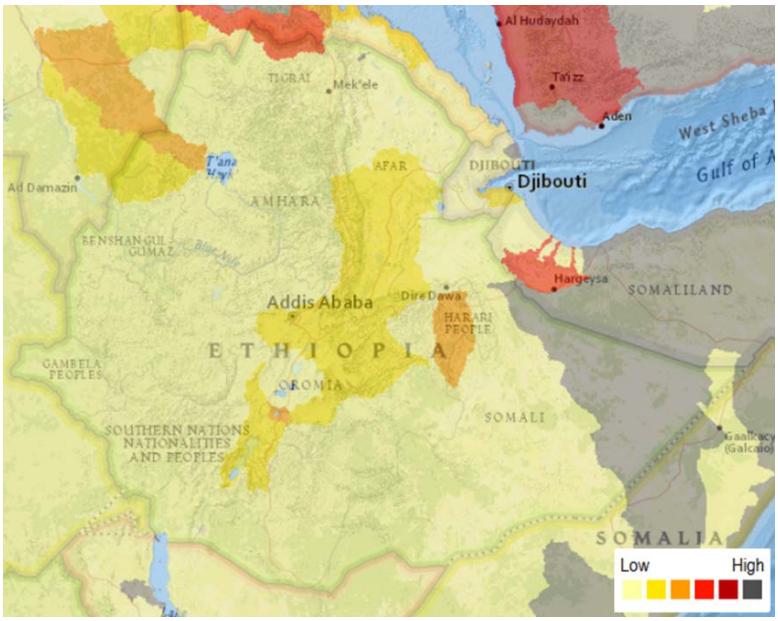

Figure 5.14 Map from the Aqueduct Water Risk Atlas providing baseline water stress with respect to electric power.

5.3.5 Impact to overall economy

A map presenting a socio-economic drought vulnerability index is available from the IWMI-portal, a default baseline water stress map is available from the Aqueduct Water Risk Atlas and a map showing a drought vulnerability index at the sub-basin level from the African Drought Observatory (all maps in Figure 5.15). The IWMI map shows a high level of socio-economic vulnerability but does not provide any spatial differentiation at the sub-national level. This is more or less similar to the vulnerability map from JRC (Figure 5.11). It can be observed that for a large part of the country the default water stress level on the Aqueduct map is relatively low, which is (almost) identical to the maps presenting baseline stress with respect to agriculture and electric power. The spatial patterns in the map are not in line with the map of overall drought impact from JRC (Figure 5.11). The map with the vulnerability index from the African Drought Observatory provides relatively detailed information, showing high vulnerability in the centre of the country, and low to medium high vulnerability in the surrounding areas. For an assessment of the spatial variability in the maps a detailed study including extensive collection of impact data is required.

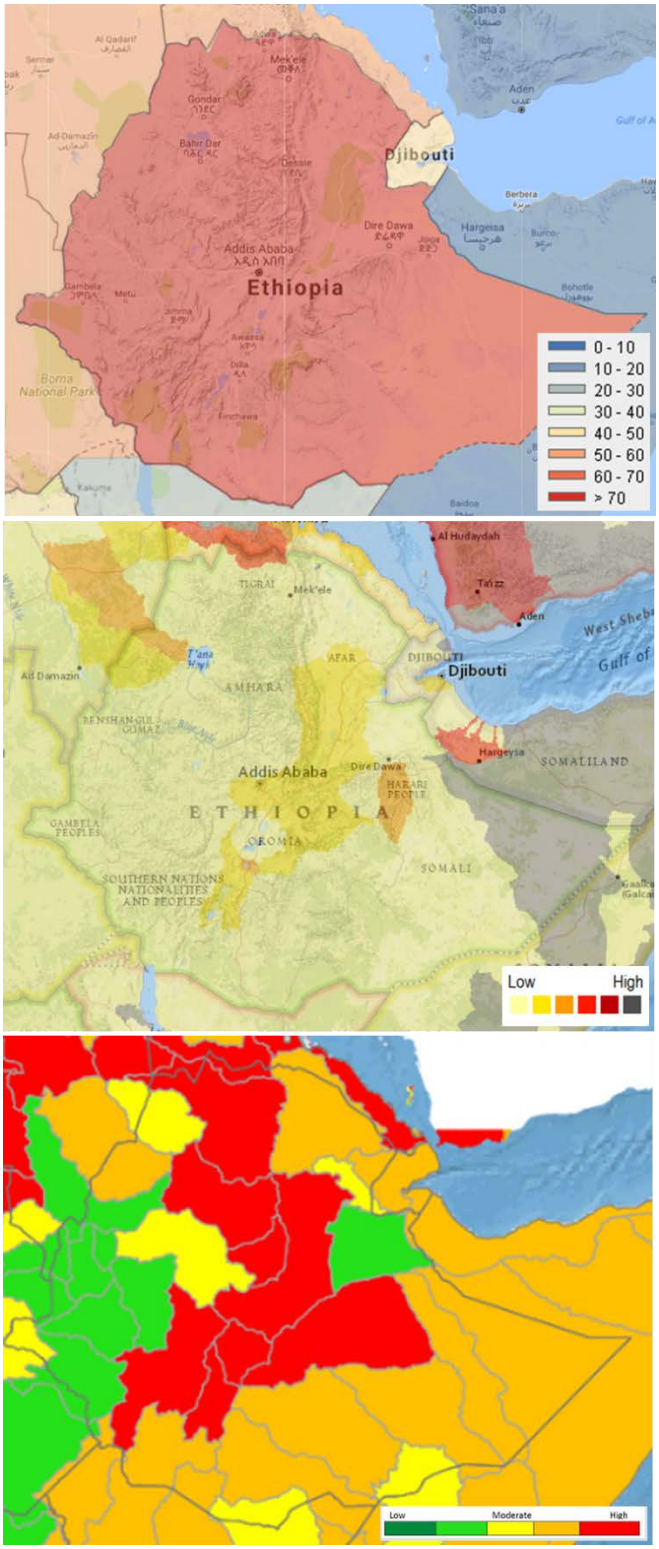

Figure 5.15 Maps with drought impacts on the overall economy from different online platforms. Top: Socio-economic drought vulnerability index from IWMI-portal; Middle: Baseline Water stress – Default form Aqueduct Water Risk Atlas (right); Bottom: Drought Vulnerability Index (sub-basin level) from African Drought Observatory.

5.3.6 Impact on municipal and industrial water needs

Various maps are available from the Aqueduct Water Risk Atlas that relates baseline water stress to industrial sectors (mining, food & beverage, chemicals, semi-conductor, oil and gas, mining, construction materials, textiles). However, there does not seem to be any variation in base line water stress for the different sectors. Also, no independent drought impact information for these industrial sectors was available for the case study countries. Hence, no further assessment of these impact maps was performed.

5.4 Evaluation of forecasting and monitoring systems

5.4.1 Current drought monitoring and forecasting

In Ethiopia, the National Meteorology Agency (NMA) provides weather forecast and early warnings on the adverse impacts of weather and climate (e.g., droughts and floods) by collecting, analysing, and studying atmospheric and earth observation data in Ethiopia. This climate information includes: daily weather report and forecast, 3-day weather assessment and forecast, ten-day forecast, monthly forecast, and seasonal forecast. The seasonal forecasts are provided for two rainy and one dry seasons. For the rainy seasons, a monthly update with the season's assessment (in-season progress report) is provided. The NMA mainly uses statistical forecasting methods that are based on empirical relationships between rainfall over specific parts of the country, which is coupled with several global (e.g., ECMWF, NOAA CPC, and IRI), regional (e.g. ICPAC) and local climate-based indices (e.g. Standardized Precipitation Index). The major planetary and synoptic systems climate systems that are operationally considered for monitoring and forecasting at NMA include:

- Evolution of monsoons;
- Vertical profiles of winds (both speed/magnitude and direction) at the earth's surface, at medium height from the earth surface (e.g. 500-hPa geo-potential height) and at upper air (e.g., 200-hPa geo-potential height);
- Madden-Julian Oscillation (MJO); (iv) Quasi Biennial Oscillation (QBO); (v)El Niño and Southern Oscillation (ENSO), (vi) Indian Ocean dipole (IOD), (vii) tropical storms/cyclones;
- Sea surface temperature (SST) gradients that have been derived from general circulation models using national, regional, and global products.

The climate forecasts information are produced by the NMA are provided through national radio, television and periodic national bulletins[30]. In addition, the NMA, as part of the regional IGAD (Inter-Governmental Authority on Development) Climate Prediction and Applications Centre (ICPAC), participates and produces seasonal climate prediction and early warning information using both statistical and dynamic climate forecasting methods[31]. This includes the Greater Horn of Africa Climate Outlook Forum (GHACOF). GHACOF that covers the countries in the region (i.e., Burundi, Djibouti, Eritrea, Ethiopia, Kenya, Rwanda, Sudan, Somalia, Tanzania and Uganda) is coordinated by the ICPAC in Nairobi, Kenya. Leveraging the GHACOF forum, ICPAC provides periodic/regular seasonal climate information for the region. The GHACOF statements are available at the ICPAC website[32] in a bulletin format reviewing the existing climate conditions over the GHA region and seasonal outlooks for the region's rainy seasons (e.g., the March to May, June to September, and October to December season). Highlights on the socio-economic climate impacts (e.g., impact on agriculture and vegetation condition) associated with the observed climate and seasonal outlooks are also provided in the bulletin.

[30] *http://www.ethiomet.gov.et/)*

[31] *http://www.icpac.net/index.php/climate-monitoring.html*

[32] *http://www.icpac.net/index.php/climate-monitoring/seasonal-forecasts.html*

5.4.2. Available operational systems

The global climate information products that are considered by the NMA and ICPAC include:

- ECMWF climate forecasts/products
  https://www.ecmwf.int/en/about/what-we-do/global-forecasts
- FEWS products for Africa and regions (e.g., East Africa)
  https://earlywarning.usgs.gov/fews/search/Africa
- The IRI probabilistic seasonal climate forecast
  http://iri.columbia.edu/our-expertise/climate/forecasts/seasonal-climate-forecasts/
- NOAA CPC: East Africa weather and climate (CFSV2 and NMME)
  http://www.cpc.ncep.noaa.gov/products/international/eafrica/eafrica.shtml
  http://www.cpc.ncep.noaa.gov/products/NMME/seasanom.shtml

A summary of the main characteristic of the available monitoring and forecasting systems is given in Table 5.4.

Table 5.4 Characteristics of seasonal drought monitoring and forecasting systems available in Ethiopia.

Characteristics	**NMA monitoring- and forecasting system**
Monitoring	Yes
Forecasting	Yes
Region/countries/areas	Ethiopia, Greater Horn of Africa region
Spatial resolution	Various including national and regional scale
Datasets used	Climate and satellite derived climate data (e.g., precipitation estimate) and regional and global climate products including stations (ground) observations, ECMWF products, NOAA GFS, and USGS/FEWS MODIS.
Software and tools used	N/A
Indices presented	Climate and satellite-derived indices such as SPI and NDVI
Reflective of impacts	Yes
Forecast horizon	Seasonal
Update frequency	Ten-daily and monthly
Accessibility of forecast	Freely accessible
Method of access	Radio, TV, and forecast bulletins through NMA website
Procedure / steps	Final climate products can be downloaded directly.
Resources required	Internet, TV, and Radio access
Post-processing	Weather assessment information periodically provided
Hit rate (estimation)	N/A

5.4.3 Predictability of droughts and potential for improvement

Studies suggest that the ENSO phenomenon is a main driver of interannual variability of seasonal precipitation in Ethiopia (Korecha and Barnston, 2007; Block and Rajagopalan, 2007; Tadesse, 1994). The predictability of droughts during the long rainy season (June–September) is governed primarily by ENSO, and secondarily reinforced by more local climate indicators near Africa and the Atlantic and Indian Oceans (Korecha and Barnston, 2007).

Operational rainfall forecasts using the analog method have been issued in Ethiopia since 1987. The NMA uses a statistical method based on analogue, multivariate ENSO index years for both long (summer) and short (spring) seasons (Diro et al., 2008). The outputs of this method are probabilistic categorical forecasts of regional Ethiopian rainfall. Rainfall anomaly patterns, including droughts, can be predicted with some skill within a short lead time of June-September based on emerging ENSO developments (Korecha and Barnston, 2007).

Even though the NMA performs routine evaluation of short- and long-term (seasonal) forecasts, there is no published documentation that indicates a comprehensive range of verification statistics to evaluate the accuracy of the forecasts in Ethiopia. However, several researchers (including the NMA experts) have studied the skill of seasonal forecasts in Ethiopia (Gleixner et al., 2017; Jury, 2014; Korecha and Sorteberg, 2013; Diro et al., 2008). For example, the evaluation of the performance of the forecast system for February–May and June–September rainy seasons over the period 1999–2011 showed that forecasts issued by the NMA have a weak positive skill for all eight regions of Ethiopia compared with climatology (Korecha and Sorteberg, 2013). This study suggested that the forecasting system has bias toward forecasting near-normal conditions and has problems in capturing droughts (below average rainfall events). However, the seasonal forecast has some positive skills in ranking the wet years of spring (February–May) season over the regions where there is high seasonal rainfall variability with significantly positive rank correlations for the above average rainfall years (Korecha and Sorteberg, 2013). Although the analogue method using ENSO years is skilful for some regions and seasons, it has little skill for the spring rains in the south of Ethiopia because of the fact that the ENSO signal is weaker during the spring (Diro et al., 2008). This shows that in addition to the existing analog method, the NMA should explore the possibility of improving the forecasts by using other dynamical and statistical forecast techniques that include the seasonal forecast information from available global modeling systems.

According to Jury (2007), early season forecasts from the coupled forecast system (CFS) are steadier than the European community medium range forecast (ECMWF) across the Ethiopian highlands. For example, in the period 1981–2006, the CFS and ECMWF April forecasts of June–August (JJA) rainfall achieved significant fit (r^2 = 0.27, 0.25, resp.), but ECMWF forecasts tend to have a narrow range with drought being under predicted (Jury, 2007). In a recent study, Gleixner et al. (2017) analyzed eleven dynamical prediction models (coupled general circulation models) and found that the summer rainfall prediction of the most skillful model from ECMWF has a correlation of 0.53 with observations. However, the majority of the 11 models studied here are not skillful (Gleixner et al., 2017). This also indicates further studies on global modeling systems are needed to understand the causes of instability in seasonal forecasts and develop bias correction for improved rainfall and temperature forecasting skills.

6 Results - Fiji

6.1 Drought risk related country characteristics

6.1.1 Introduction on the country

The Republic of Fiji is an island country in Melanesia in the South Pacific Ocean about 1,100 nautical miles northeast of New Zealand's North Island. Fiji is an archipelago of more than 330 islands, of which 110 are permanently inhabited, and more than 500 islets. The two major islands, Viti Levu and Vanua Levu, support 87% of the population of almost 920,000. The capital Suva is located on Viti Levu. About three-quarters of Fijians live on Viti Levu's coasts, either in Suva or in smaller urban centers like Nadi or Lautoka. Fiji has one of the most developed economies in the Pacific due to an abundance of forest, mineral, and fish resources. Today, the main sources of foreign exchange are its tourist industry and sugar exports. The main characteristics of Fiji are listed in Table 6.1.

Table 6.1 - Main characteristics of Fiji. (Source: SOPAC, 2007)

Geography	
Total Area	18,270 km^2
Land	18,270 km^2
Water	0 km^2
Highest Elevation	1,324 m
Land Use	
Arable	10.95%
Perm. Crop	4.65%
Other	84.4% (2005)
People	
Population	918 675 (July 2007 est.)
Population Growth Rate	1.394% (2007 est.)
Economy	
GDP per capita (PPP)	$6,200 (2006 est.)
Water Statistics	
Avg Rainfall	2000 - 3000 mm per annum

6.1.2 Hydrology and water resources

Surface water is used as the main source of supply for all major towns on the larger, high islands of Fiji. Some small, low lying islands rely exclusively on groundwater and rainwater. Contamination of the wells in the small islands may happen due to lack of sanitation and awareness of appropriate water health and sanitation practices. Surface water availability is a problem in some islands, which rely exclusively on groundwater. Rainwater harvesting using roof systems is widespread in Fiji but the limited risk perception of rural people may fail to take into account the possibility of extreme climate events and drought, which results in providing a small capacity of storage instead of a larger capacity. Some conflicts have occurred over surface water availability, in particular for irrigation. A considerable amount of potable water is lost in the water supply system as a result of background leakage and frequent bursts and several areas face problems with either too high or too low water pressure (SOPAC, 2007).

Groundwater extraction occurs on both the large islands and small low-lying islands, but the groundwater issues and challenges in these different physical environments differ. Groundwater is found in superficial and medium-depth strata on the larger islands of Viti Levu and Vanua Levu and some large islands, in either fractured rock or sedimentary formations. Significant groundwater deposits, such as the Nadi Valley coastal aquifer, on the large islands are available and are under pressure for development. Groundwater resources on small islands play a very different role. Some islands have shallow groundwater lenses in sand beds or coral formations, which lie on marine water and can be readily exhausted. The fragility of these groundwater lenses means that they need to be carefully managed[1].

6.1.3 Climate

Temperature records from Pacific Island observation stations show warming over the past 50 years, with trends mostly between 0.08 to 0.20°C per decade, consistent with global warming over this time. Unlike temperature, rainfall across the Pacific Islands displays large year-to-year and decade-to-decade changes in response to natural climate variability. Over the past 50 years, rainfall has increased northeast of the South Pacific Climate Zone (SPCZ) and declined to the south (Australian Bureau of Meteorology and CSIRO, 2011).

Based on global climate model projections, the Australian Bureau of Meteorology and CSIRO foresee increased rainfall within the SPCZ in the wet season in particular due to increased atmospheric moisture content in a warmer climate. Although authors mention that results of the climate scenarios should be interpreted with care, they indicate that a widespread increase in the number of heavy rain days (20–50 mm) in the Pacific is very likely, while droughts are expected to occur less often[2].

6.1.4 Drought history

In Fiji almost all droughts are associated with the El Niño phenomena, but not all El Niño occurrences lead to droughts. Table 6.2 provides an overview of the officially declared droughts between 1965 and 2000. Most El Niños start in the Southern Hemisphere autumn of the year listed in Table 6.2 and continue until the autumn of the following year. However, there are exceptions with events beginning later than normal or finishing earlier than normal. In Fiji, the National Disaster Management Office (NDMO) is the government agency that officially declares the state of drought (Fiji meteorological service, 2003).

Reported impacts of droughts include decreases in the production of sugar cane, rice, cotton, coconuts and pineapples as well as livestock mortality. Also, fire breakouts were reported and the forestry sector was adversely affected. In various drought periods a lack of drinking water supply occurred, mainly in rural areas, with associated health implications due to the reduced quality of the drinking water. Low stages of rivers during drought periods are reported to cause saline water intrusions. The economic impact of the damages due to the drought in 1998 was estimated by the World Bank (World Bank, 2000) to be between $275 million to $325 million Fijian.

Disaster data from EM-DAT (Figure 6.1Figure 6.1), shows a clear ENSO-dependency. The three strongest historic El Niño years (1982/1983, 1997/98 and 2015/16), appear associated with substantial drought afflicted populations: in 1982/183 31.000 people were affected, in 1997/1998 263.455 people and in 2015/2016 67.000 people.

Table 6.2 Overview of officially declared droughts included an indication of severity, association with El Niño phenomena, and specifics on the affected area. Source: Fiji meteorological service, 2003.

Period	Severe	El Niño	Affected area
1965	no	yes	Kabara (Lau island group) most affected
1966	yes	no	
1967	no	no	
1968	no	no	
1969-1970	yes	yes	
1972-1973	yes	yes	Kabara, Lau, Ono-I-Lau, and Lakeba most affected
1976-1978	yes	yes	Viti Levu and southern part of Lau island group most affected
1979-1980	no	no	
1982-1983	yes	yes	Whole of Fiji, but most extreme in west Viti Levu
1986-1987	yes	yes	Whole of Fiji, but most extreme in west Viti Levu
1992-1993	no	yes	Western Islands most affected
1997-1998	yes	yes	Whole of Fiji, but most extreme in western islands

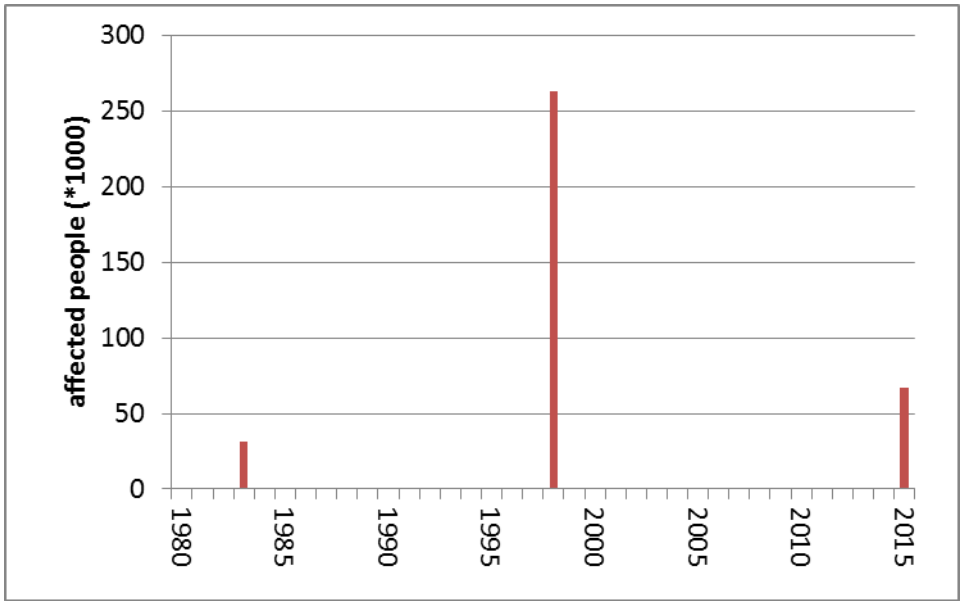

Figure 6.1 Drought events in Fiji recorded by EM-DAT.

6.2 Assessment of available drought hazard models

6.2.1 Comparison and validation of models at the country scale

For the relevant drought hazard indices available from the global datasets (section 2.2.1), graphs were produced of the percentage-area of the country experiencing drought conditions for three drought levels: moderately dry (index value below -1), severely dry (index value below -1.5) and extremely dry (index value below -2). All graphs are shown in Appendix A4). In these graphs, the registered droughts from EM-DAT and the Fiji Meteorological Service are plotted as well. Based on the graphs, the overlap of global drought hazard with reported droughts was assessed as well as the comparability of datasets and indices. SPI1 was left out of the comparison because the results are relatively spikey and could not be compared to

drought events at a yearly time scale. For Fiji, with its limited land area, results have to be interpreted with care. As can be viewed in the Figures in Appendix A4, the data in the graph show relatively coarse variations in percentage of the country in drought.

Table 6.3Table 6.3 gives an overview of the results for Fiji, showing that five of the seven reported droughts are very well detected by all drought hazard indices from the global datasets. However, the reported drought events from 1986 and 1997 were not found in any of the signals from the dataset-index combinations.

Table 6.3 Results of the country-scale assessment of globally available drought hazard dataset-index combinations. In the table, years with registered drought events are shown in black and years without registered drought events, but drought hazards shown by the dataset-index combinations are shown in red. Corresponding graphs can be found in Appendix A4.

drought events	Fiji Met Service-2	'83		'86	'87		'92	'93		'97	'98	Summary of hits			Summary of false alarms	
	EM-DAT (7)	'83	'85			'90			'96		'98	regist. events		global data		
	Global data											(+)	(+, +/-)	(+)	(+, +/-)	(+, +/-)
SPI 3	IRI	+	+/-	-	+	+	+	+	+	-	+	71%	71%	67%	100%	38%
	GLS	+	+/-	-	+	+	+	+	+	-	+	71%	71%	67%	100%	38%
	PRCGWB	+	+/-	-	+	+	+	+	+	-	+	71%	71%	67%	100%	38%
	WaterGap	+	+/-	-	+	+	+	+	+	-	+	71%	71%	67%	100%	38%
SPI 12	IRI	+	-	-	+	+	+	+	+	-	+	71%	71%	67%	67%	29%
	GLS	+	-	-	+	+	+	+	+	-	+	71%	71%	67%	67%	29%
	PRCGWB	+	-	-	+	+	+	+	+	-	+	71%	71%	67%	67%	29%
	WaterGap	+	-	-	+	+	+	+	+	-	+	71%	71%	67%	67%	29%
SPEI 3	GDM	+	+	-	+	+	+	+	+	-	+	71%	71%	100%	100%	38%
	PRCGWB	+	+	-	+	+	+	+	+	-	+	71%	71%	100%	100%	38%
	WaterGap	+	+	-	+	+	+	+	+	-	+	71%	71%	100%	100%	38%
SPEI 12	GDM	+	-	-	+	+	+	+	+	-	+	71%	71%	67%	67%	29%
	PRCGWB	+	-	-	+	+	+	+	+	-	+	71%	71%	67%	67%	29%
	WaterGap	+	-	-	+	+	+	+	+	-	+	71%	71%	67%	67%	29%
SSFI 1	PRCGWB	+	-	-	+	+	+	+	+	-	+	71%	71%	67%	67%	29%
	WaterGap	+	-	-	+	+	+	+	+	-	+	71%	71%	67%	67%	29%
Summary of hits	(+)	100%	19%	0%	100%	100%	100%	100%	100%	0%	100%	**71%**	--	**73%**	--	**30%**	--
	(+, +/-)	100%	75%	0%	100%	100%	100%	100%	100%	0%	100%	--	**71%**	--	**81%**	--	**32%**

In the 30-year period that was assessed, the global models indicated three other drought years, which were not registered as drought events by EM-DAT or the Fiji Meteorological Service. For 1985 and 1996 drought hazards were observed from all dataset-index combination. For 1985 the SPI3 and SPEI3 indices of all datasets showed more or less pronounced drought events. Except for this event in 1985, the comparability of the dataset-index combinations was very high showing either a pronounced drought or no drought.

6.2.2 Validation with local data

For Fiji only two GRDC measurement stations were available for this validation exercise, with a time-length of 24 months. Both measurement stations were, moreover, positioned, on one of the islands, Viti Levu (Figure 6.2Figure 6.2).

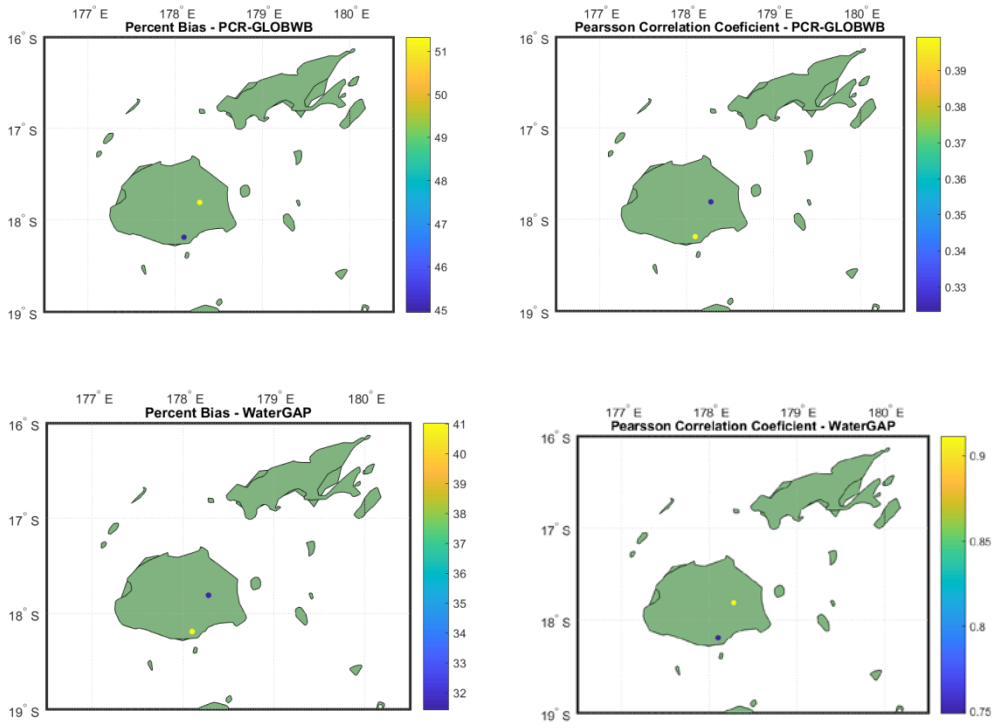

Figure 6.2 - Spatial distribution of GRDC measurement stations available for use in Fiji and their performance values for the percent bias, and the Pearson correlation coefficient.

Both PCR-GLOBWB and WaterGAP show an average performance in these stations, both when looking at the correlation coefficient as well as at the percent bias. For WaterGAP, correlation coefficients found ranged from 0.75 up to 0.91, whilst percent bias values varied from 31.4% up to 41.0%. PCR-GLOBWB's percent-bias values are in line with those of WaterGAP running between 44.9% to 51.3%. PCR-GLOBWB's performance on the correlation coefficient is, however, a little lower with values ranging from 0.32 to 0.40.

Hydrographs of both stations are plotted in Figure 6.3Figure 6.3. The hydrographs generally reflect well the difference in performance indicators between the two models, with WaterGAP performing much better overall. WaterGAP is generally able to catch the hydrological

seasonal and inter-annual variability, while PCR-GLOBWB shows more difficulties in expressing both peak- and low-flows.

The spatial distance between the two discharge measurement stations is, for this particular case, relatively small. Hence, when looking at the two hydrographs one can see that the two observation stations are being connected to the same grid-cell providing similar discharge estimates to both stations. In order to correctly deal with this, one should always account for the mismatch in spatial and/or temporal resolution between the modelled data used and the area or station of interest. In this particular case, coupling two discharge observation stations to a single discharge-cell does not provide much additional information. Usually, the most downstream station, or the station with the highest performance metrics, is used. In this particular case that would be station 5172200 (right sub-plot).

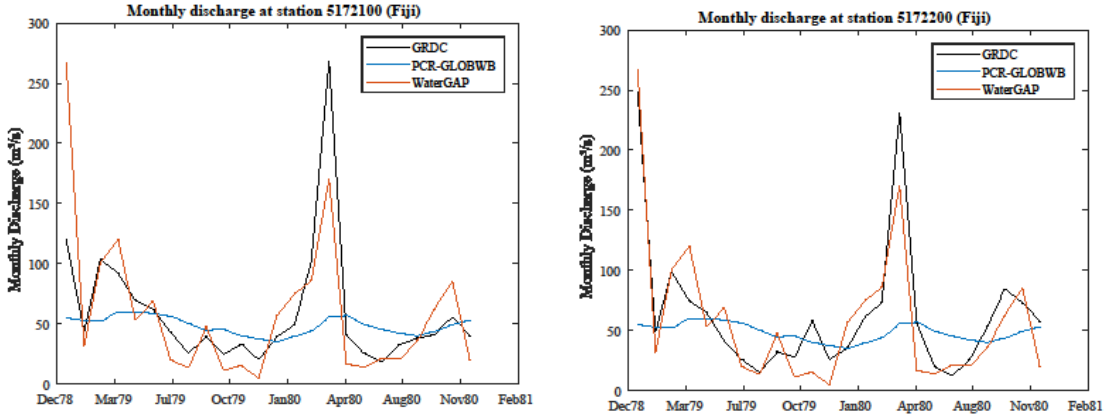

Figure 6.3 Hydrographs visualizing the performance of PCR-GLOBWB and WaterGAP relative to the historical observations.

6.2.3 ENSO analysis

For Fiji, the share of land area exposed to drought seems to be significantly lower during La Niña (LN) years compared to El Niño (EN) and Neutral (N) years, both for the SPI and SPEI and for most model runs and accumulation time-periods (see Figure 6.4Figure 6.4). On the other hand, EN years are shown not to result in elevated median values of the total land area exposed to drought, as compared to the neutral conditions. SSFI-1 values show an opposite signal for both WaterGAP and PCR-GLOBWB. Again, EN and N years seem to result in similar median values of exposure to drought whilst LN years indicate an elevated median drought exposure.

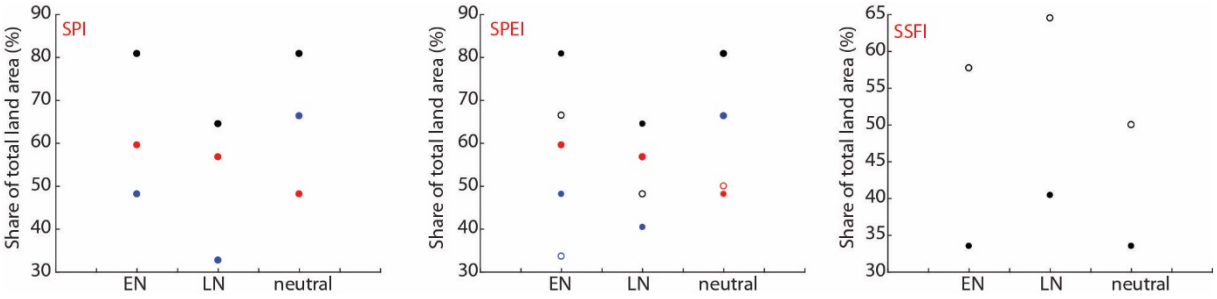

Figure 6.4 Area in drought in Fiji during El Niño (EN), La Niña (LN), or neutral years using the SPI, SPEI and SSFI drought indicator. The open symbols show the results for WaterGAP while the filled symbols show the results for PCR-GLOBWB. Different colors indicate the different accumulation periods used: 1 month (black), 3 months (blue) and 12 months (red).

Given Fiji only consists of a few grid-cells when using the global models, it is difficult to identify any significant spatial patterns. Nevertheless, we can see from the results visualized in Figure 6.5Figure 6.5 and Figure 6.6 that both models seem to be relatively consistent when looking at the change in drought frequency between EN and non-EN years or LN and non-LN years. Here, EN years indicate to lead to a significant decrease in drought frequency in most parts of Fiji. LN years, on the other hand, lead to increased drought frequency across a majority of the land area.

Correlation coefficient values between JMA SST and SSFI-1 are shown to be reasonably high for both WaterGAP and PCR-GLOBWB with correlation values around ~0.3-0.5 and ~0.5-0.7, respectively. Optimal lag times seem to lie around 6-9 months. Whilst PCR-GLOBWB does not make any spatial differentiation in optimal lag-time, WaterGAP indicates significantly lower optimal lag-times periods for the northern Island of Fiji at ~2-4 months.

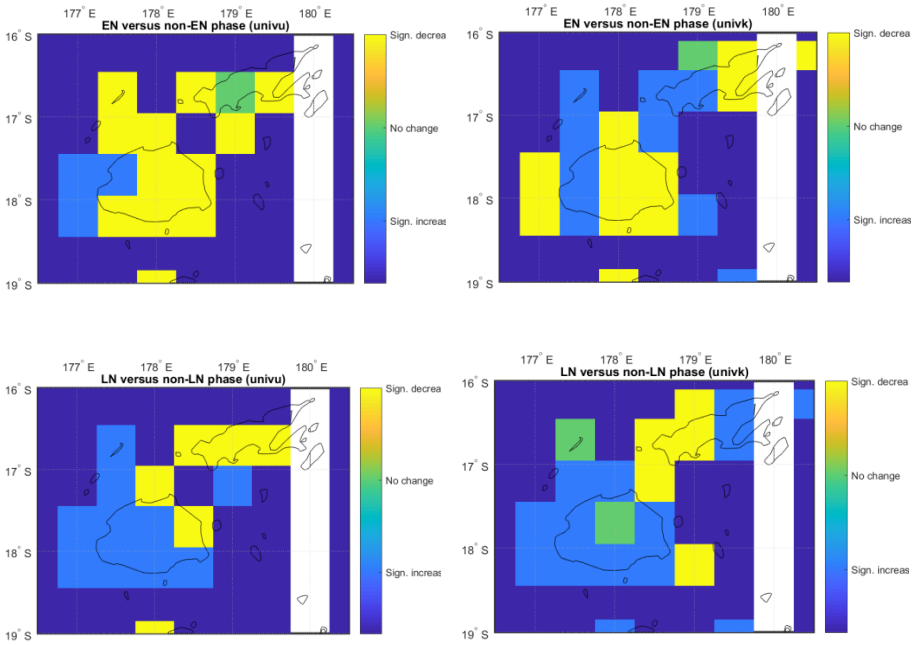

Figure 6.5 Spatial distribution of area with a significant increase, decrease or no change in frequency of drought months when comparing the El Niño years with the non El Niño years and the La Niña years with the no- La Niña years. Left sub-plots show the results for PCR-GLOBWB, right sub-plots show the results for WaterGAP.

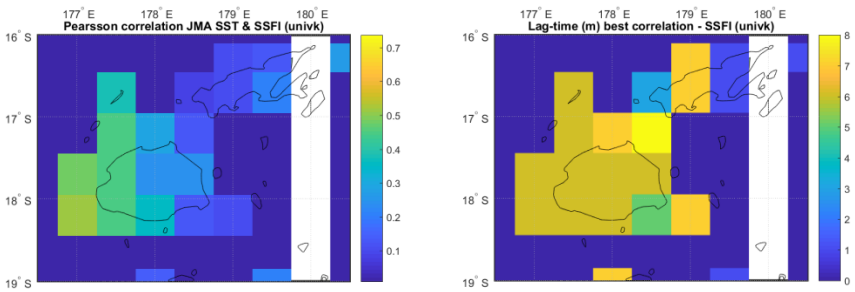

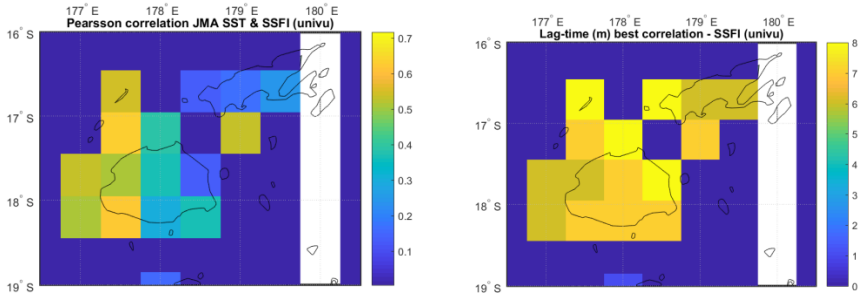

Figure 6.6 Spatial distribution of optimal Pearson correlation coefficient between continuous JMA SST values indicating ENSO conditions and the SSFI-1 drought indicator. Left sub-plots show the optimal correlation coefficient, right sub-plots show the lag-time that corresponds to the best correlation coefficient found. Results for both PCR-GLOBWB and WaterGAP are visualized.

6.3 Assessment of drought impact and risk platforms and datasets

6.3.1 Maps of overall drought impact and risk

Country scale maps based on the Global map of drought risk from JRC are not available for Fiji.

6.3.2 Drought impact on population

The IWMI data portal provides a map with information related to drought impacts on population for all countries in the world: per capita mean annual river discharge (Figure 6.7). For Fiji it shows that the annual discharge per person is generally low to medium at Viti Levu and somewhat higher at Vanua Levu.

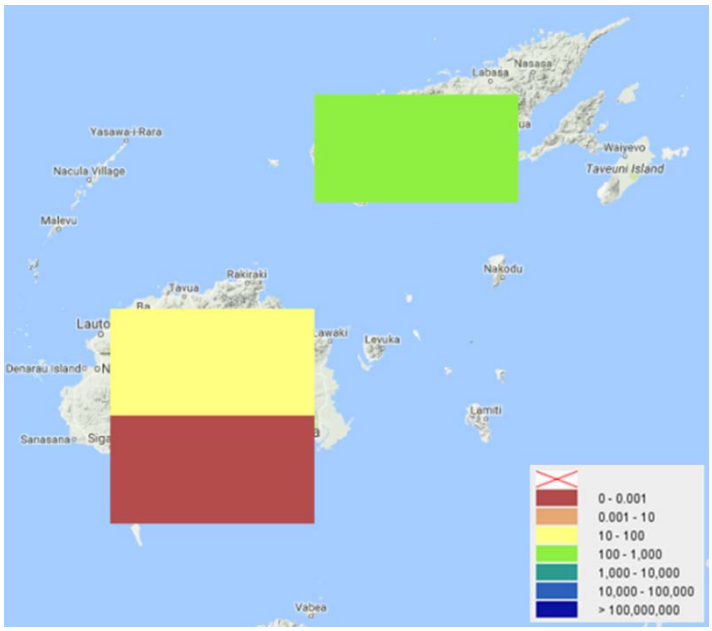

Figure 6.7 Map providing impact (exposure/vulnerability) to population available from IWMI water data portal: per capita mean annual river discharge (m^3 per person).

6.3.3 Impact on agriculture

Maps of historical agricultural drought impacts are provided by the FAO-platform “Agricultural Stress Index and precipitation anomalies” (Figure 6.8). This FAO-platform provides a map of

the Agricultural Stress Index (ASI; % cropland affected by drought) for each year since 1985. Table 6.4 provides an overview of the years with coverage of approximately 25% of the country, or more, with high to very high ASI levels and matching drought years based on registered droughts and from the global drought hazard models (see section 6.2.1). According to the ASI maps, 2 out of 31 years in the monitoring period show large areas with high levels of agricultural drought stress. None of these years were listed as a registered drought year, nor were they shown as significant drought hazard by the global models. This is not in agreement with the number of drought years that were registered for their impact on agriculture by the Fiji meteorological service in 1982/83, 1986/87, 1992/93, and 1997/98 (section 6.1.4).

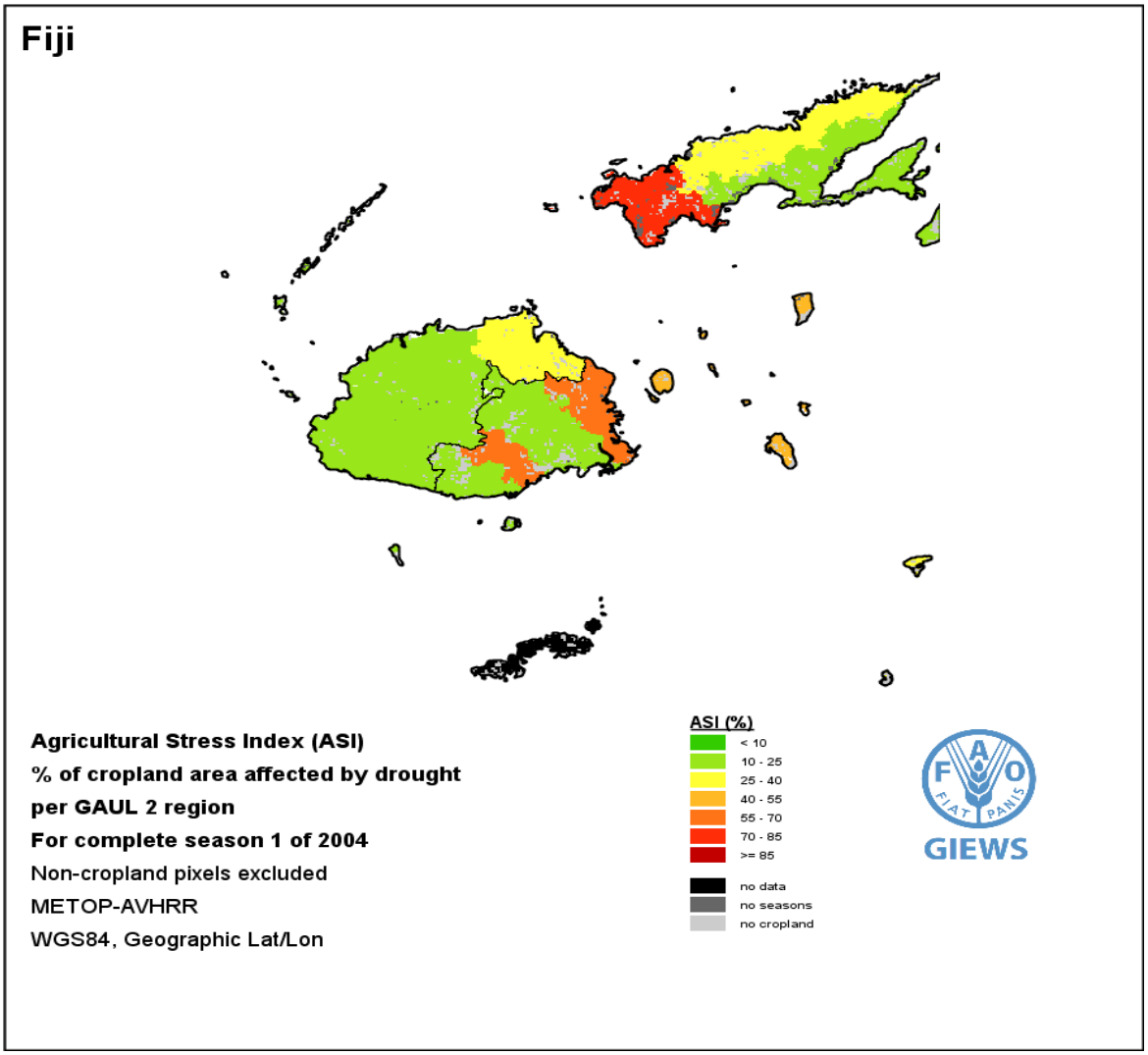

Figure 6.8 Map from FAO-platform "Agricultural Stress Index and precipitation anomalies for a relatively dry year.

years with high ASI (S1)	Registered droughts	Hazard in global models
2003	N/A	
2004	N/A	

Table 6.4 Years with high ASI values during the first growing season covering 30% or more of the country (FAO platform[33]) compared to registered droughts and drought hazards as determined by the global models (see section 6.2.1).

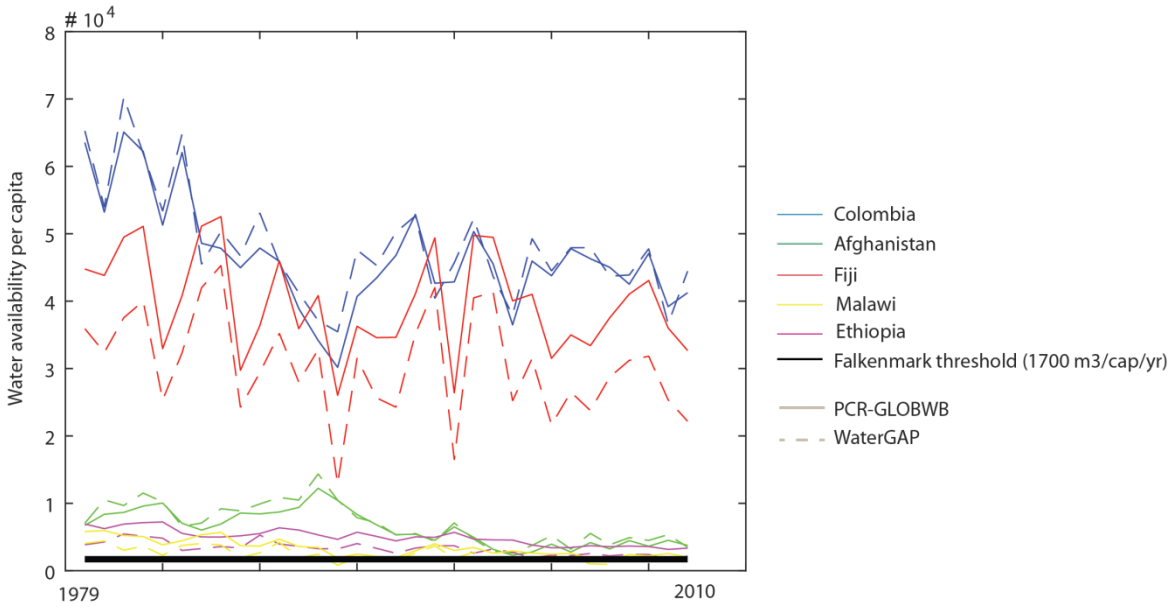

6.3.4 Impact on hydropower

Not available.

6.3.5 Impact on the overall economy

A map presenting a socio-economic drought vulnerability index is available from the IWMI-portal (Figure 6.9). The IWMI map shows a medium level of socio-economic vulnerability but does not provide any spatial differentiation at the sub-national level. This is not fully in-line with the country characteristics, as the Fiji meteorological service reported relatively high impacts during drought periods (section 6.1.4).

[33] *http://www.fao.org/giews/earthobservation/country/index.jsp?lang=en&code=FJI*

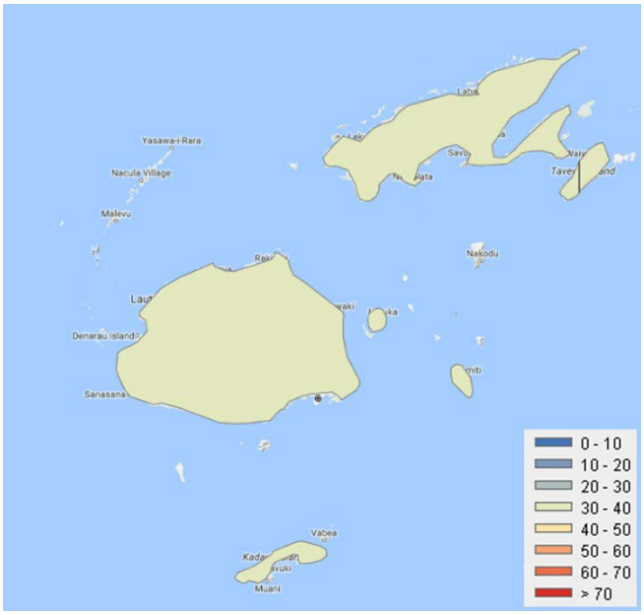

Figure 6.9 Map of the socio-economic drought vulnerability index from IWMI-portal.

6.3.6 Impact on municipal and industrial water needs

Various maps are available from the Aqueduct Water Risk Atlas that relates baseline water stress to industrial sectors (mining, food & beverage, chemicals, semi-conductor, oil and gas, mining, construction materials, textiles). However, there does not seem to be any variation in base line water stress for the different sectors. Also, no independent drought impact information for these industrial sectors was available for the case study countries. Hence, no further assessment of these impact maps was performed.

6.4 Evaluation of forecasting and monitoring systems

No information available.

7 Results - Malawi

7.1 Drought risk related country characteristics

7.1.1 Introduction to the country

Malawi is located in the southeast of the African continent and entirely landlocked by Zambia in the northwest, Tanzania in the northeast and Mozambique to the east, south and west[34]. Malawi is over 118,000 km^2 with an estimated population of 16,777,547 (July 2013). Table 7.1 provides an overview of the main characteristics of Malawi.

Table 7.1 - The main characteristics of Malawi.

Geography	
Total Area	118,484 km^2 [35]
Land	80% (94,787 Million km^2)
Water	20% (23,697 km^2)
Highest Elevation	3000 m
Land Use	
Arable	20.7%
Perm. Crop	1.18%
Other	78.14% (2014)[36]
People	
Population	16,777,547 Million (2013.)
Population Growth Rate	3.1 % (2010-2015)[37]
Economy	
GDP growth rate	5.6% (2014)
GDP per capita	482 USD 2016[38]
Water Statistics	
Lowlands Avg Rainfall	900 mm/year
Highlands Avg Rainfall	1400 -2200 mm/year

Malawi was colonized by the British from 1891 until 1953. In 1964 the country became independent and currently it is a multi-party democracy. It is one of the least developed countries of the world[39]. The countries main income originates from agriculture and the main part of the population lives in rural areas. The government highly relies on developmental aid. Life expectancy has dropped since the 1980s because of the spread of HIV/AIDS but is now starting to increase from 47-49 years in 2005 to over 60 years in 2015 (Reddy, 2016).

The country's topography is very heterogeneous. The Great Rift Valley runs from the north to the south through the country. The landscape around the valley consists of large plateaus at an elevation of around 800-1200m, but with peaks as high as 3000m. The country's climate

[34] *https://en.wikipedia.org/wiki/Malawi*

[35] *United Nations, 2013. (https://unstats.un.org/unsd/demographic/products/dyb/DYB2013/Table03.pdf)*

[36] *New-Agriculturist (http://www.new-ag.info)*

[37] *Data.un.org - CountryProfile*

[38] *Trading economics: https://tradingeconomics.com/malawi/indicators ; accessed date 22-05-18*

[39] *UN list of Least Developed Countries*

is tropical, but due to its high elevation temperatures are relatively low (McSweeney et al., 2010).

The country is densely populated and many farmers have to cultivate their crops on steep hillsides and often with inadequate soil and water conservation. Problems such as soil erosion and the resultant siltation of rivers and lakes are worsening, which is further increased by high levels of deforestation[40].

7.1.2 Hydrology and water resources

Malawi is relatively rich in water resources. Water is stored in the form of lakes, rivers and aquifers[41] with the largest lake being Lake Malawi. The availability of water resources is highly variable over the year – nearly 90% of the runoff occurs between December and June. The country is very vulnerable to risks related to droughts and floods RSMI, 2009.

There are two major drainage systems:

- The largest is the Lake Malawi system which includes most of the country (91%), which is part of the Zambezi River basin. The Shire River is the only outlet from the lake with an average flow of only 400 m^3/s.
- The Lake Chilwa system is shared with Mozambique. Lake Chilwa is an endorheic basin draining rivers from the eastern slopes of the Shire Highlands, the Zomba Plateau and the northern slopes of the Mulanje Massif. Large amounts of water are lost to evaporation.

There are two main aquifers in Malawi:

- The Precambrian weathered basement complex, which has a low yield (up to 2 l/s);
- The quaternary alluvial aquifers of the lakeshore plains and the Lower Shire valley, which are high yielding (up to 20 l/s) and thus a valuable groundwater resource.

Nearly all of Malawi's renewable water resources originate from within the country itself (approximately 17.28 km^3/year). Approximately 1 km^3/year originates from Mozambique.

7.1.3 Climate

The country's climate is tropical, but temperatures are relatively low due to its high elevation. In winter (JJA) temperatures drop to around 18-19˚C, and in the warmest months (September to January) temperatures range from 22-27˚C[85]. The rainfall amounts and patterns are mainly influenced by the Inter-Tropical Convergence Zone and the El Niño Southern Oscillation (ENSO). There is a large inter-annual variability in wet season rainfall. In southern Malawi the wet season normally lasts from November to February with around 150-300 mm rainfall per month, whereas in northern Malawi rainfall continues into March and April. The higher altitude regions receive the highest rainfall amounts. Temperature is projected to increase between 1.5 up and 5.0 degrees Celcius[74].

There is large uncertainty between models on projected change in annual rainfall ranging from -13% to +32%. Overall, the projections tend to show decreases for the dry season and increases for the wet season with more rain falling as heavy events in general[85]. Historical trends are hard to detect due to the large inter-annual variability.

[40] *New-Agriculturist (http://www.new-ag.info)*

[41] *FAO, AQUASTAT, Malawi, accessed date 11-08-2017*

7.1.4 Drought history

Table 7.2 provides an overview of the worst droughts events in Malawi up to 2009. Most recently, in 2016, Malawi was hit by a drought that affected most of the Southern part of Africa[42] and was considered to be the worst drought in 35 years[43,44]. In 2005 the drought conditions were so severe such that the country entered a food crisis and the government declared a national disaster. In addition, the 2006 wet season rainfall was still very low[85].

Table 7.2 - Worst drought events over Malawi over the period 1968-2008 derived from station data (obtained from RMSI (2009)).

Return Period	Year	November - March Rainfall (mm)	November - March SPI
40	1992	490	-2.89
20	1994	583	-2.00
10	2004	640	-1.52
5	2005	754	-0.62
2	1999	829	-0.07

The EM-DAT database summarizes the historic drought events in Malawi over the period 1990-2013 (Figure 7.1). In this period seven droughts were reported for Malawi: 1987, 1990, 1992, 2002, 2005, 2007, 2012 with 21,578,702 people affected in total over these years (Masih et al., 2014). Nearly all droughts occurred during ENSO years.

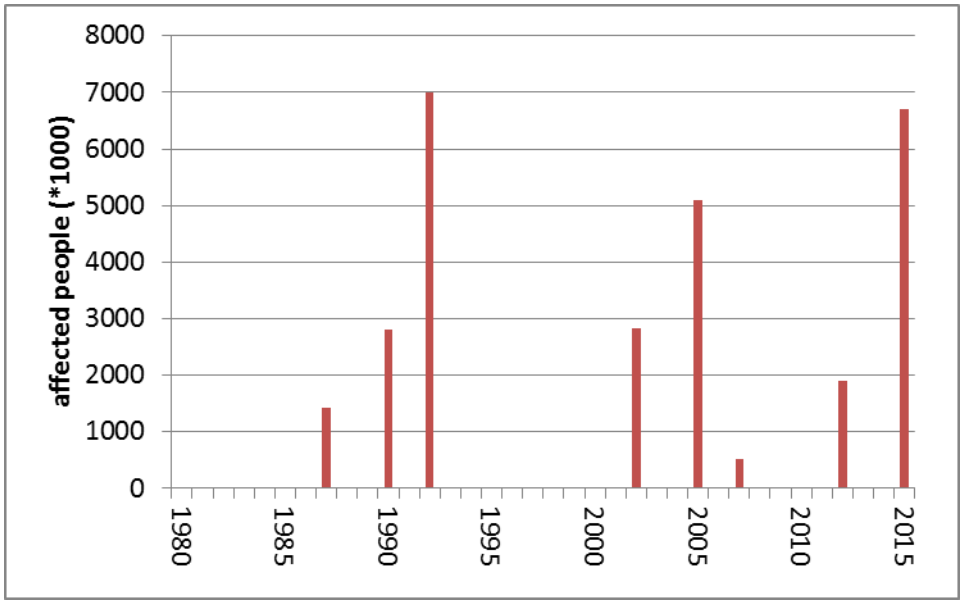

Figure 7.1 - Drought events in Malawi recorded by EM-DAT.

When droughts occur, Malawi suffers large losses because the country highly depends on its agricultural production, especially from tobacco and maize[45]. In 2009, RMSI conducted an assessment of Malawi's Economic Vulnerability related to disaster risk for the World Bank[72].

[42] *https://en.wikipedia.org/wiki/Malawi*

[43] *http://www.fews.net/southern-africa/malawi/key-message-update/march-2016*

[44] *http://www.fews.net/southern-africa/malawi/key-message-update/may-2016*

[45] *Pauw, K., Thurlow, J. and Van Seventer, D. Droughts and floods in Malawi, Assessing the economywide effects, IFPRI Discussion Paper 2010, pages: 34.*

They used daily rainfall data from 45 meteorological stations, which cover the 40 year period (1968 – 2008) to calculate the November-March rainfall totals and SPI values in order to identify droughts. The resulting droughts are meteorological droughts, thus (upstream) water use and management are not considered herein and may therefore not match up with the droughts as recorded in the EM-DAT database.

7.2 Assessment of available drought hazard models

7.2.1 Comparison and validation at the country scale

For the relevant drought hazard indices from the global datasets available (section 2.2.1), graphs were produced of the percentage-area of the country experiencing drought conditions for three drought levels: moderately dry (index value below -1), severely dry (index value below -1.5) and extremely dry (index value below -2). All graphs are shown in Appendix A5. In these graphs, the registered droughts from EM-DAT and RMSI are plotted as well. Based on the graphs, the overlap of global drought hazards with reported droughts was assessed as well as the comparability of the datasets and indices. SPI1 was left out of the comparison because the results are relatively spikey and could not be compared to drought events at a yearly time scale.

Table 7.3 gives an overview of the results for Malawi, showing that the reported droughts are not always well predicted by the drought hazard indices from the global datasets. For more than 50% of the calculated dataset-index combinations, the calculated drought hazard is not very pronounced or was barely visible, if at all. Dataset-index combinations that show a relatively good overlap with registered drought events are those that include the SPEI3 and SPEI12, as well as SSFI-1, based on the WaterGAP dataset.

Table 7.3 Results of the country-scale assessment of globally available drought hazard dataset-index combinations. In the table, years with registered drought events are shown in black and years without registered drought events but drought hazards shown by the dataset-index combinations, are shown in red. Corresponding graphs can be found in Appendix A5.

drought events	EM-DAT (7)	'87		'90		'92	'94			'99		'02	'04	'05		'07		'12	Summary of hits				Summary of false alarms	
	RMSI (5)																		regist. events		global data			
	Global data		'88		'91			'95	97/98		'00/01				'06		'11		(+)	(+, +/-)	(+)	(+,+/-)	(+)	(+, +/-)
SPI 3	IRI	+	+/-	-	+	+	+	+	+	+	+	-	+/-	+	+	-	+/-	-	50%	60%	71%	100%	50%	54%
	GLS	+	+/-	-	+	+	+	+	+	+/-	-	+/-	-	-	-	-	-	-	30%	50%	43%	57%	50%	44%
	PRCGWB	+	+/-	-	+	+	+	+	+	-	-	-	+/-	+	+	-	+/-	-	40%	60%	57%	86%	50%	50%
	WaterGap	+	+/-	-	+	+	+	+	+	+/-	-	-	+/-	+	+	-	+/-	-	40%	60%	57%	86%	50%	50%
SPI 12	IRI	+/-	+	-	+	+	+	+	+/-	+	+	+	-	+	+	-	-	-	50%	60%	71%	86%	50%	50%
	GLS	+	+	-	+	+	+	+	+	-	-	+	-	-	-	-	-	-	40%	40%	57%	114%	50%	67%
	PRCGWB	+/-	+	+/-	+	+	+	+	+	+	+	-	-	+	+	-	-	-	40%	60%	86%	86%	60%	50%
	WaterGap	+/-	+	+/-	+	+	+	+	+	+	+	-	-	+	+	-	-	-	40%	60%	86%	86%	60%	50%
SPEI 3	GDM	+	+	-	+/-	+	+/-	+	+/-	+	+	+/-	+/-	+	+	+/-	+/-	-	40%	80%	57%	100%	50%	47%
	PRCGWB	+	+	+/-	+/-	+	+/-	+	+	+	+/-	+/-	+/-	+	+	+	+	-	50%	90%	71%	100%	50%	44%
	WaterGap	+	+	+/-	+/-	+	+/-	+/-	+	+	+	+/-	+/-	+	+	+	+	-	50%	90%	57%	100%	44%	44%
SPEI 12	GDM	+/-	+	+/-	+	+	+	+	+/-	+	+	+	-	+	+	-	-	+/-	50%	80%	71%	86%	50%	43%
	PRCGWB	+/-	+	+/-	+	+	+	+	+	+	+/-	-	-	+	+	-	-	+/-	40%	70%	71%	86%	56%	46%
	WaterGap	+/-	+	+/-	+	+	+	+	+	+	+/-	-	+/-	+	+	-	-	+/-	40%	80%	71%	86%	56%	43%
SSFI 1	PRCGWB	-	+/-	-	+/-	+	+	+	+	+	+	-	-	+	+	-	-	+/-	40%	50%	57%	86%	50%	55%
	WaterGap	+	+/-	+	+/-	+	+	+	+	+	+	+/-	+/-	+	+	-	-	+/-	50%	80%	57%	86%	44%	43%
Summary of hits	(+)	56%	63%	6%	69%	100%	81%	94%	75%	75%	56%	19%	0%	88%	88%	13%	13%	0%	43%	--	65%	--	51%	--
	(+, +/-)	94%	100%	50%	100%	100%	100%	100%	100%	88%	75%	50%	50%	88%	88%	19%	38%	25%	--	67%	--	89%	--	49%

The comparability of the dataset-index combinations is limited. In the 30 year period that was assessed, the global models indicated seven other drought years, which were not registered as drought events by EM-DAT. For individual dataset-index combinations false alarm rates range between 43 and 50%. The dataset-index combination (GLS-SPI12) has a relatively high false alarm rate of 67%. For the years with registered drought events, the comparability of the droughts shown by the different dataset-index combinations was lower than for the drought years detected by the drought hazard indices from the global datasets.

7.2.2 Validation with local data

Malawi is well-covered with GRDC measurement stations. In total, 48 GRDC stations were available for use with an average time-series length of 95.1 months. The upstream catchment area of most stations is relatively small. As shown in Figure 7.2Figure 7.2 the observation stations available for use were equally distributed across the entire country.

Figure 7.2Figure 7.2 shows the results for both GHMs evaluated for the two performance metrics taking into account all available stations. Whereas correlation coefficient values are reasonably good for both PCR-GLOBWB (median: 0.56, 0.02-0.93) and WaterGAP (median: 0.70, 0.04-1) results for the percent bias indicate relatively large absolute deviations. WaterGAP has a median percent bias value of 130.7%, compared to PCR-GLOBWB, which gives a median percent bias value of 396.9%.

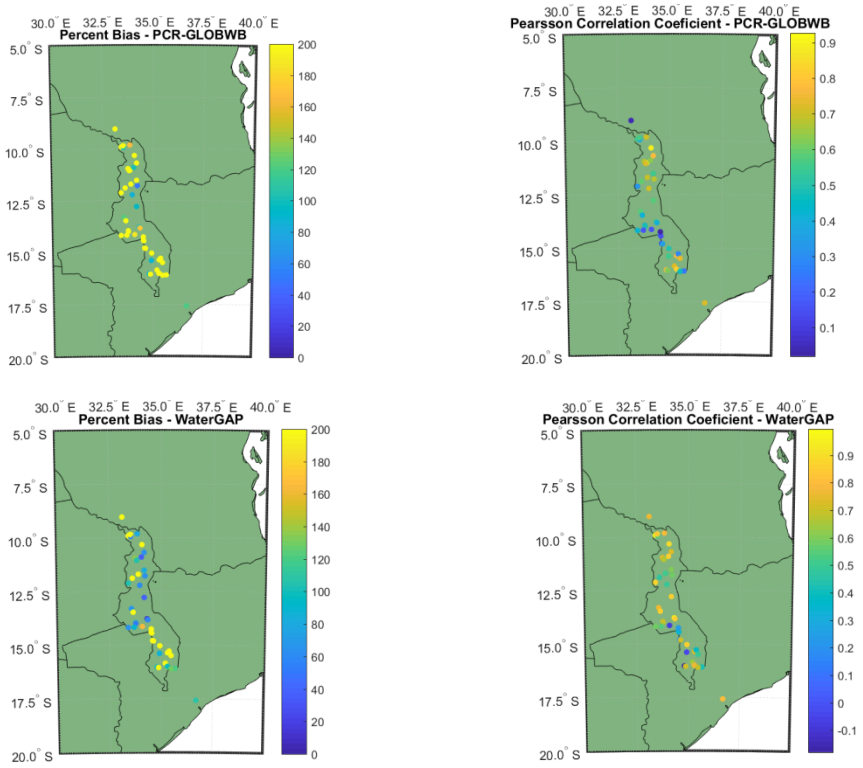

Figure 7.2 - Spatial distribution of GRDC measurement stations available for use in Malawi and their performance values for percent bias and the Pearson correlation coefficient.

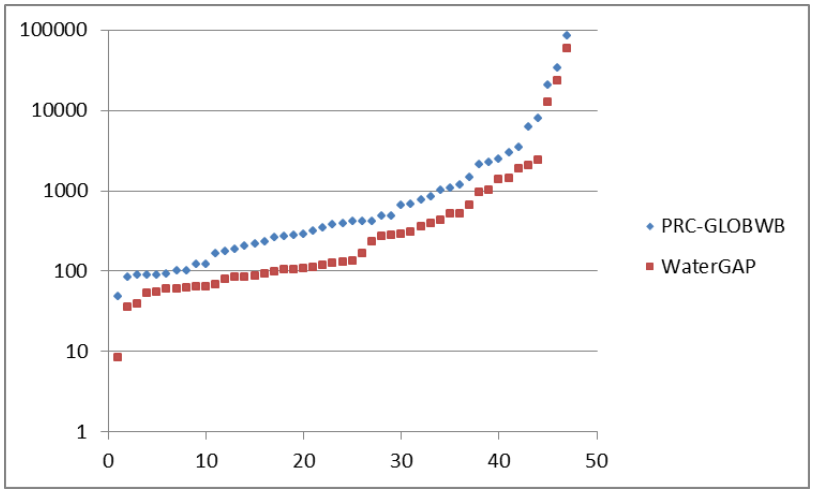

Figure 7.3 - Distribution of the percent bias values for both PCR-GLOBWB and WaterGAP. X-axis represents all stations available for analysis in Malawi. Y-axis represents the percent bias values. Note that the Y-axis is given in a logarithmic scale.

Figure 7.4Figure 7.4 shows for two selected stations the hydrographs indicating the performance of both models. Both models are generally able to resemble the historical hydrological conditions well, both when looking at the absolute values and its temporal pattern, for the station depicted in the left sub-plot. As a result, both the correlation coefficient and the percent bias values are relatively high for both models. With correlation coefficients of: 0.77 (WaterGAP) and 0.82 (PCR-GLOBWB). Percent bias values of 98.64% and 235.6% were found for WaterGAP and PCR-GLOBWB, respectively.

In constrast, both WaterGAP and PCR-GLOBWB have difficulties generating the very low discharges that were observed at the station depicted in the right sub-plot. Although the temporal pattern might be similar as reflected by reasonably good correlation coefficient values (WaterGAP: 0.59; PCR-GLOBWB: 0.49), both models significantly overestimate the absolute discharge levels with high percent bias values as result (WaterGAP: 1435.7%, PCR-GLOBWB: 2447.7%). Hydrographs for all other stations in Malawi are available as a supplement to this document.

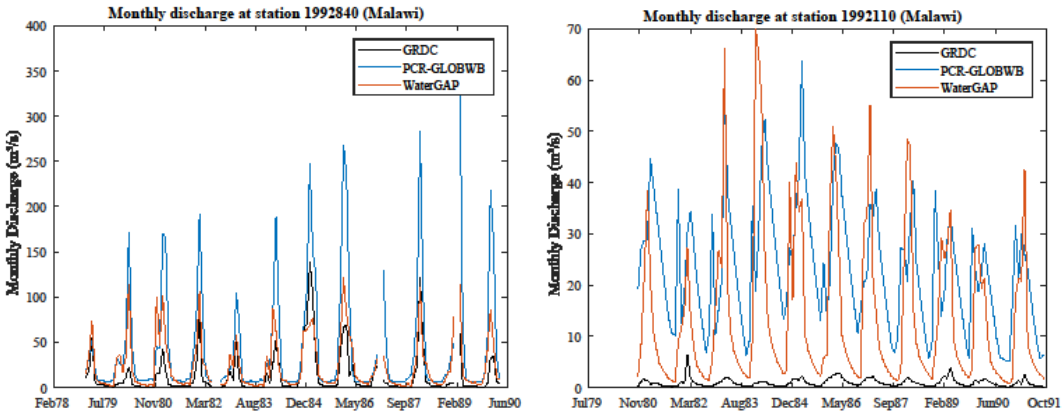

Figure 7.4 Hydrographs visualizing the performance of PCR-GLOBWB and WaterGAP relative to the historical observations at two selected stations.

7.2.3 ENSO analysis

For Malawi we find, finally, that when looking at the SPI and SSFI, the share of land area exposed to drought is generally high under neutral conditions and relatively lower during El Niño (EN) or La Niña (LN) years (see Figure 7.5Figure 7.5). For the SPEI drought indicators the figure is again more dispersed, with relatively long accumulation periods for both PCR-GLOBWB and WaterGAP showing that exposure to drought is relatively elevated during EN years and relatively lower during LN years. For shorter accumulation time-periods no consistent pattern exists between the two model runs. PCR-GLOBWB shows relatively higher drought exposure during LN compared to the EN and N years when using accumulation time-periods of 1 and 3 months. WaterGAP, on the other hand, indicates relatively lower median drought exposure during LN compared to EN and N years and depicts the N years as years with significantly elevated drought exposure.

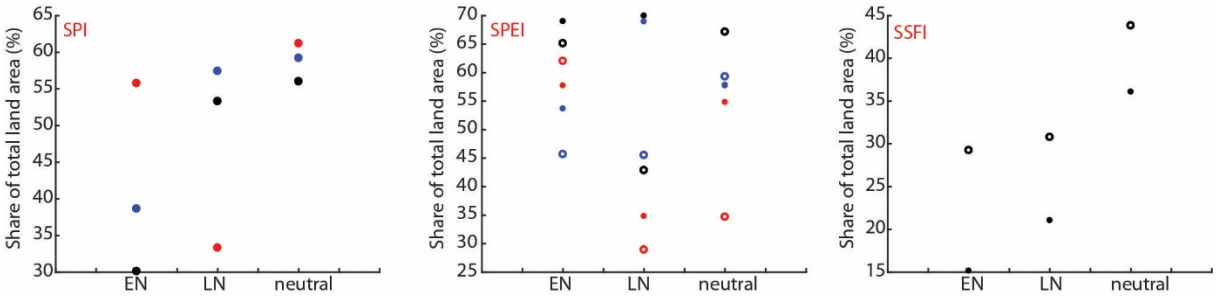

Figure 7.5 Area in drought in Malawi during El Niño (EN), La Niña (LN), or neutral years using the SPI, SPEI, and SSFI drought indicator. The open symbols show the results for WaterGAP while the filled symbols show the results for PCR-GLOBWB. Different colours indicate the different accumulation periods used: 1 month (black), 3 months (blue) and 12 months (red).

When looking at the spatial distribution of changes in drought frequency (Figure 7.6Figure 7.6) we find that for the whole country of Malawi the frequency of drought months seem to be significantly decreasing, both during EN and during LN, as compared to non-EN and non-LN years. This is in correspondence with the relatively high spatial exposure to drought during N years compared to EN and LN years depicted in the previous figure.

Both PCR-GLOBWB and WaterGAP show relatively low optimal correlation coefficient values for the entire country of Malawi at ~0.3-0.4 (see Figure 7.7). No significant spatial distribution was found in the optimal correlation coefficient values for either of the models. Optimal lag-times at which the best correlation coefficient values were found are relatively long for Malawi at ~6-12 months. For WaterGAP these optimal lag-times seem to be, moreover, relatively shorter (~6-9 months) as compared to the optimal lag-times found under PCR-GLOBWB (~9-12 months).

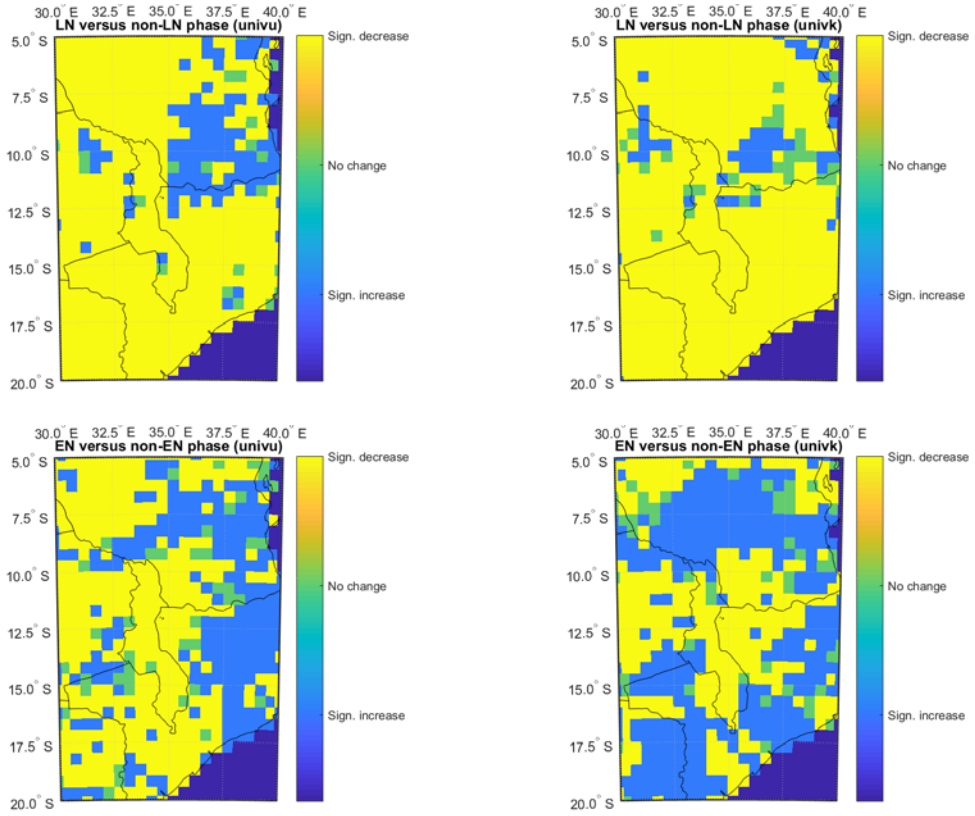

Figure 7.6 Spatial distribution of area with a significant increase, decrease or no change in frequency of drought months when comparing the El Niño years with the non-El Niño years and the La Niña years with the non-La Niña years. Left sub-plots show the results for PCR-GLOBWB, right sub-plots show the results for WaterGAP.

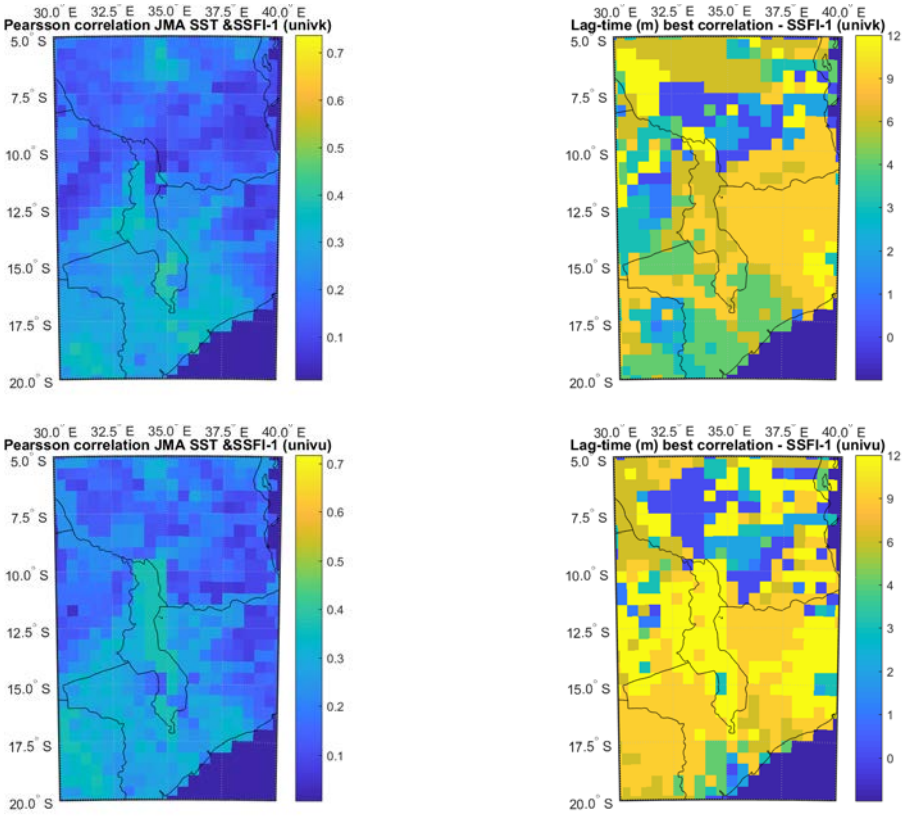

Figure 7.7 Spatial distribution of optimal Pearson correlation coefficient between continuous JMA SST values indicating ENSO conditions and the SSFI-1 drought indicator. Left sub-plots show the optimal correlation coefficient, right sub-plots show the lag-time that corresponds to the best correlation coefficient found. Results for both PCR-GLOBWB and WaterGAP are visualized.

7.3 Assessment of drought impact and risk platforms and datasets

7.3.1 Maps of overall drought impact and risk

Country scale maps are presented that are based on the Global map of drought risk from JRC (Carrão et al., 2016) (Figure 7.8). Although the presented indices of drought hazard, exposure, vulnerability, impact and risk are dimensionless factors based on an aggregation of information and data, they provide a good first impression of the drought risk situation in the country. For Malawi, the drought hazard is limited in large parts of the country, which is not in line with the assessments of drought hazards with global models and the descriptive information of the country characteristics. This difference is probably caused by the choice of the drought hazard index: for the JRC map the drought event is determined by means of the weighted anomaly of standardized precipitation index (WASP), while in the analysis for this comparative assessment we used SPI, SPEI and SSFI indices to estimate drought events.

Exposure and vulnerability are high to very high across the entire country, which is in line with the country information (e.g., low GDP, large part of population in rural areas, high dependency on agriculture and development aid). The combination of relatively low levels of hazard in large parts of the country and high exposure and vulnerability, leads to high drought impact and low to high risk levels.

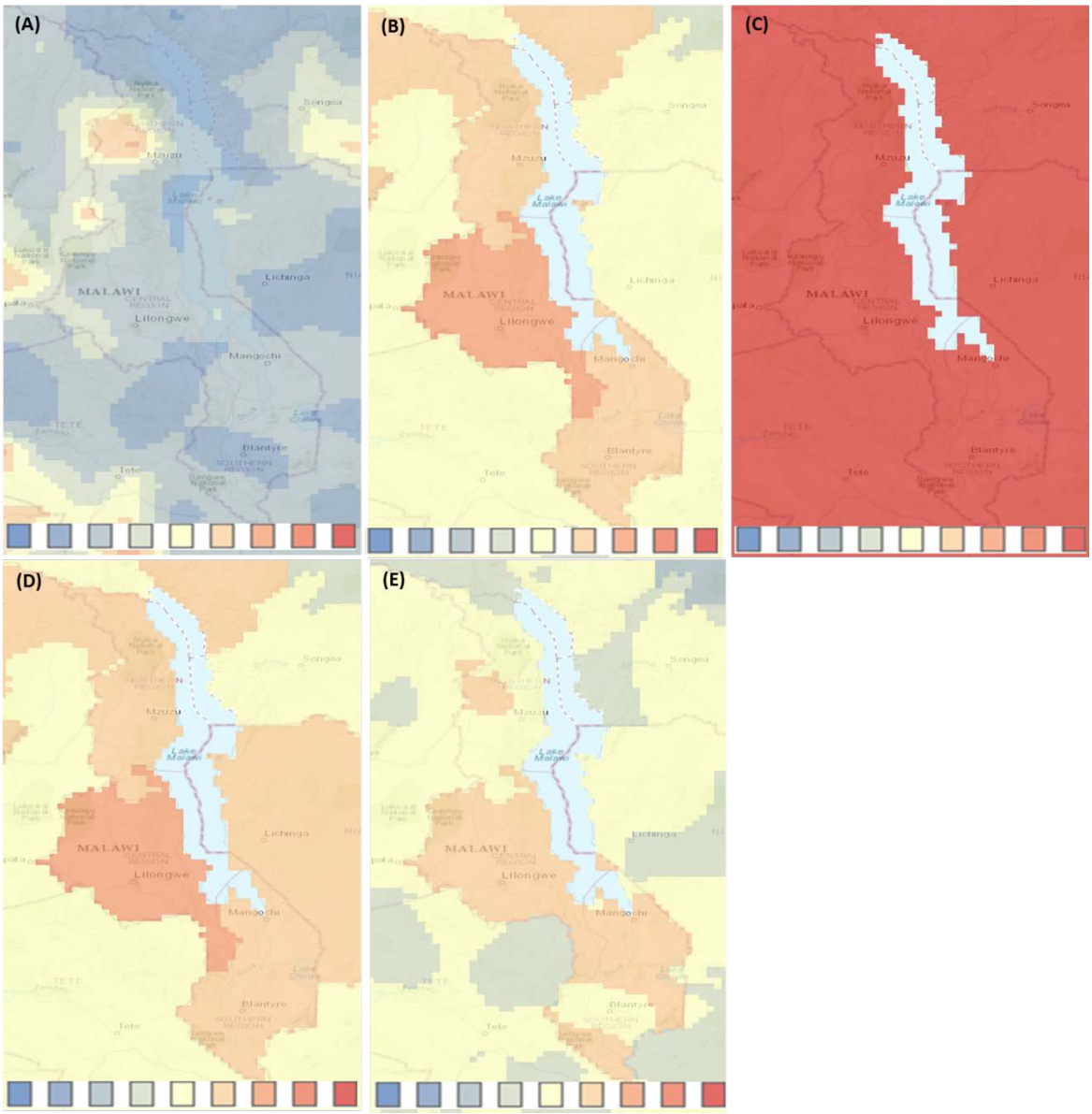

Figure 7.8 Maps from the Global map of drought risk developed by JRC (Carrão et al, 2016) showing the following indices: drought hazard (A), exposure (B), vulnerability (C), impact (exposure x vulnerability) (D), and risk (hazard x impact) (E).

7.3.2 Drought impact on population

Malawi is a densely populated country with extremely high rates of poverty. In 2016, the poorest 20% of Malawi's twenty-three million citizens existed on an income of approximately 70 cents a day based on World Bank data. This population is not spread evenly throughout the country but is densest in the southern region (near Blantyre) and along the western border with Zambia and Mozambique (near Lilongwe), which also tends to be drier and more strongly influenced by El Niño. These El Niño influences do not appear to be captured well by the PCR-GLOBWB and WaterGAP analyses shown in Figure 1.6, which generally show significant decreases in the chances of drought during El Niño years. On the other hand, estimates of exposure/vulnerability as presented in Figure 7.9Figure 7.9 (spatial patterns of the IWMI exposure maps) appears reasonably similar to surface water anomalies estimated

for the recent 2015-16[46]. Since runoff is a relatively small part of the hydrologic budget, rainfall deficits can be amplified, resulting in much larger relative runoff reductions. These values in 2015-16 were as low as 35% of a 1982-2015 baseline over Southern Africa. The IWMI exposure calculations provide a spatially coarse, but fairly realistic map of potential impacts.

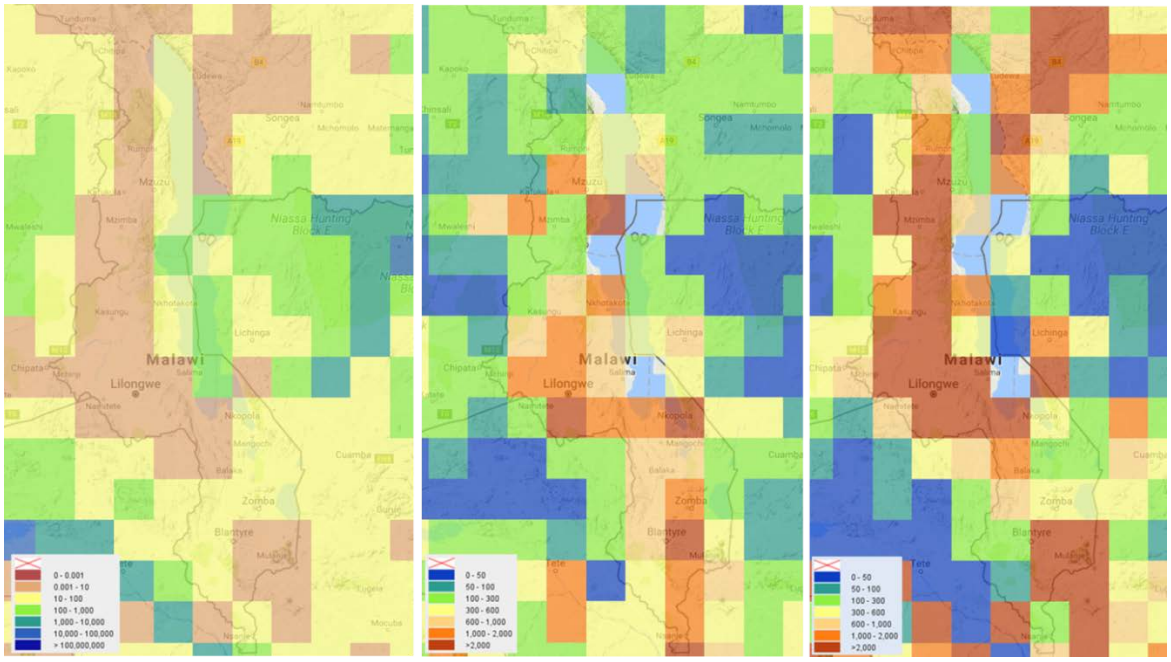

Figure 7.9 Maps providing impacts (exposure/vulnerability) on population as made available from the IWMI water data portal, from left to right: per capita mean annual river discharge (m^3 per person); agricultural water crowding with respect to mean annual precipitation (population m^3); agricultural water crowding with respect to mean annual river discharge (population m^3).

7.3.3 Impact on agriculture

Malawi's agricultural situation needs to be placed into historical context (Figure 7.10). Population has grown rapidly since the early 1980s, more than tripling by 2017. As a result, the per capita harvested area has declined by ~80%, from approximately 170 hectares per person in 1981 to around 100 hectares per person in 2017 (data: FAOSTATE, augmented with recent estimates from the US Department of Agriculture).

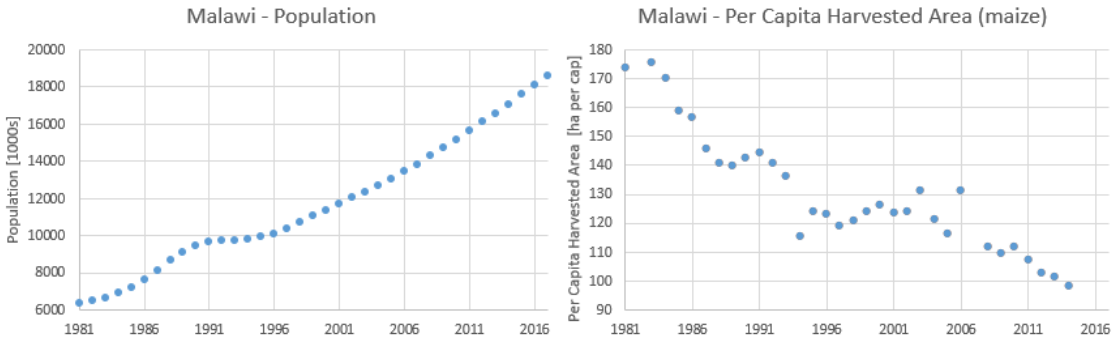

Figure 7.10 Malawi population and per capita harvested area.

[46] *https://www.fews.net/sites/default/files/documents/reports/FEWS%20NET_Southern%20Africa%202015_16%20Drought%20Map%20Book_20160318_0.pdf*

Over the same time period (1981-2016), yields for the main crop (maize) can be described as being relatively stationary over the 1981-2006 time period (Figure 7.11, left), with a marked increase being noted in most years after 2008. Combining population and maize production together, we can examine per capita cereal production (Figure 7.11, right). Overall, we can see that Malawi's per capita production has improved substantially since the 1980s and 1990s. We do find, however, a number of recent years with serious per capita production shortfalls: 1991/1992, 1992/1993, 2004/2005, 2014/15 and 2015/16.

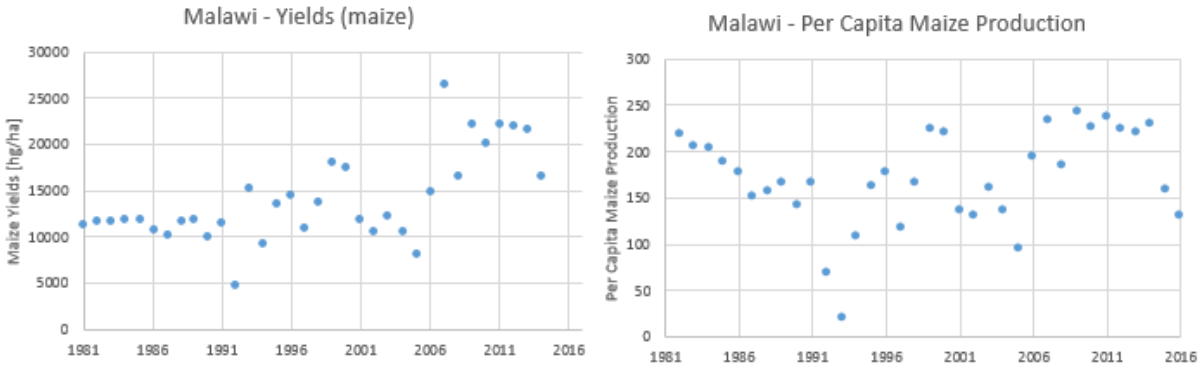

Figure 7.11 Malawi Maize Yields and Per Capita Maize Production

To support a forecast context, we can also express Malawi maize production in terms of detrended maize production estimates (Figure 7.12). As is common in many agricultural analyses, a linear trend was fit to the data, and this linear regression was used to remove the impacts of technological innovation and other non-climatic influences. This time series incorporates fluctuations in harvested areas and yields. We only show data since 1990, because the yield data show a suspicious lack of inter-annual variability in the 1980s (Figure 7.11, right). This time series indicates substantial multi-year episodes with suppressed yields. Note however that only some of these years are El Niño years. We will look at the predictability of these variations below.

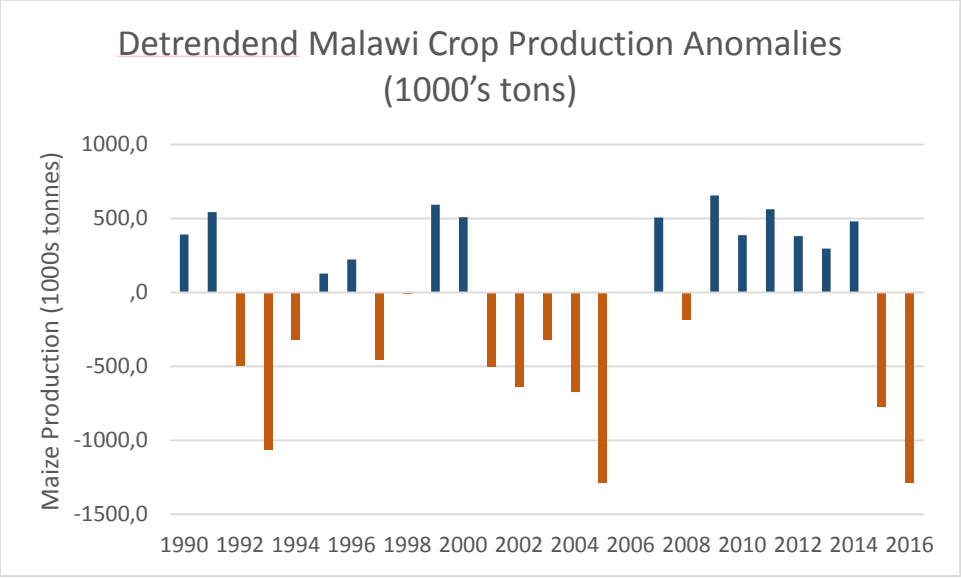

Figure 7.12 Detrended maize production anomalies.

This analysis, and prior FEWS NET analyses for the past 20 years, suggests that Malawi does experience periodic drought-induced crises that negatively impact yields, contribute to high cereal prices and help create very severe levels of food insecurity. For example, in 2016, some 5 million Malawi citizens required humanitarian assistance and were extremely food insecure. Malawi is a country with a dense population and complex topography and climate. As such, impact analyses will likely be very sensitive to the quality of the rainfall data used to drive the analyses. Maps such as the Aqueduct Water Risk Atlas baseline water stress with respect to agriculture (Figure 7.13) and baseline water stress with respect to hydropower (Figure 7.14) appear to underestimate the risks associated with severe drought events.

Hydrologic analyses by FEWS NET[47], focused on the 2015/16 drought, indicate large reductions in runoff and severe water stress. We find this stress associated with recent drought impacts identified in the EM-DAT data base and FEWS NET reports (2002, 2005, 2012, 2015). Some, but not all, of these years appear associated with below-normal maize production (2002, 2005, 2015/16; Figure 7.12). The Agricultural Stress Index, provided by the FAO platform, shows a good match with below-normal maize production (see Table 7.4 and Figure 7.13, right).

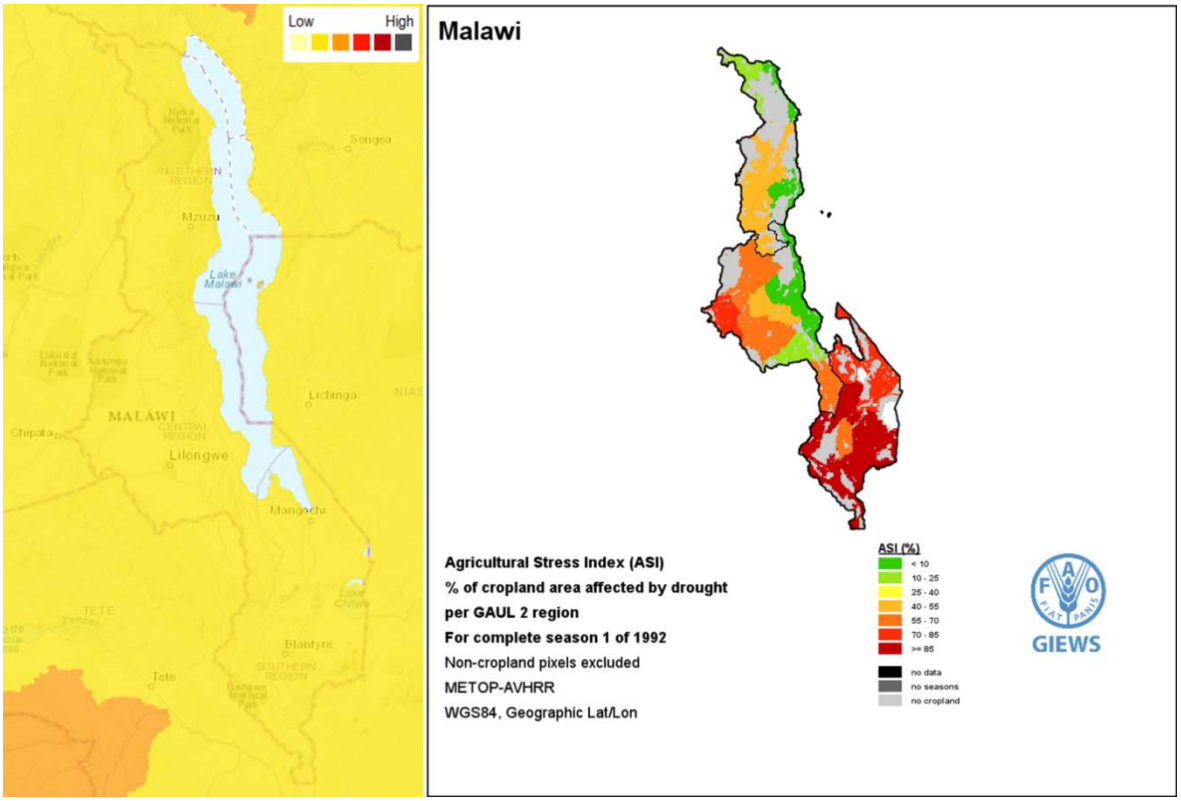

Figure 7.13 Maps of historical agricultural drought impacts. Left: Map from Aqueduct Water Risk Atlas providing baseline water stress with respect to agriculture; Right: Map from FAO-platform "Agricultural Stress Index and precipitation anomalies for a relatively dry year.

Table 7.4 Years with high Agricultural Stress Index (ASI) values during the first growing season covering 30% or more of the country (FAO platform[48]) compared to registered droughts and drought hazards

[47] *http://journals.ametsoc.org/doi/abs/10.1175/BAMS-D-16-0167.1*

[48] *http://www.fao.org/giews/earthobservation/country/index.jsp?lang=en&code=MWI*

determined with global models (see section 7.2.1). In 2004, the drought hazard from the global models was moderate (+/-).

years with high ASI (S1)	Registered droughts	Hazard in global models
1992	x	x
2003		
2004	x	(x)
2005	x	x
2006		x
2016	N/A	N/A

7.3.4 Impact on hydropower

The online Aqueduct Water Risk Atlas provides maps with baseline water stress with respect to electric power, which is very similar to the map with baseline stress with respect to agriculture. For Malawi it can be observed that for a large part of the country the stress level is relatively low. No spatial patterns can be observed.

Figure 7.14 Map from Aqueduct Water Risk Atlas providing baseline water stress with respect to electric power.

7.3.5 Impact on overall economy

Droughts modulate the economy of Malawi in many important ways. Overall, IWMI estimates that Malawi has a high level of socio-economic drought vulnerability (Figure 7.15, left) which seems in-line with recent history, analysis by FEWS NET and the World Food Programme, and recurrent severe humanitarian crises. Given fairly high levels of annual rainfall, it is possible that Malawi may have low levels of baseline water stress (Figure 7.15, middle), but reliance on average conditions may not be particularly informative from a disaster risk perspective. Estimates of Drought Vulnerability from the African Drought Observatory (Figure

7.15, right) indicate substantial variations across the country. The accuracy of these patterns requires further detailed analysis with additional information.

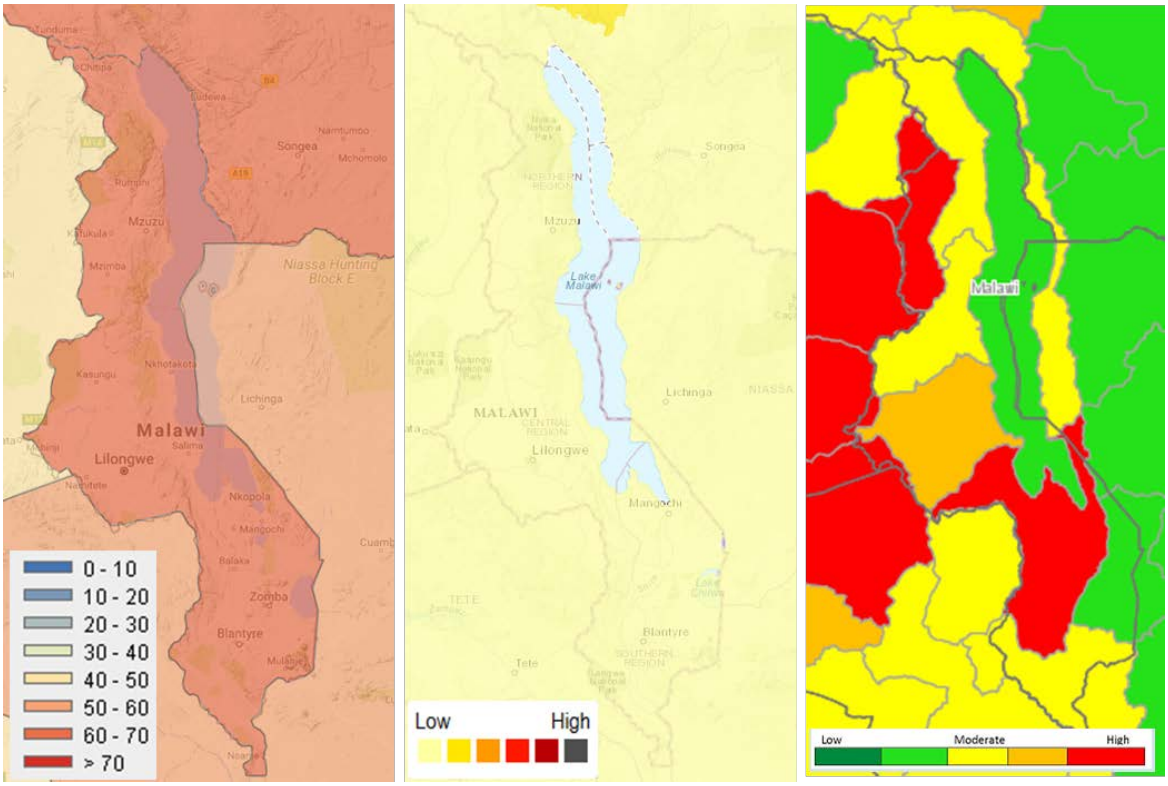

Figure 7.15 Maps with drought impacts on the overall economy from different online platforms. From left to right: Socio-economic drought vulnerability index from IWMI-portal; Baseline Water stress – Default from Aqueduct Water Risk Atlas; Drought Vulnerability Index (sub-basin level) from the African Drought Observatory.

Drought impacts agriculture, a key source of income, while also influencing the generation of hydropower (a direct economic benefit), which in turn supports additional industries. Droughts are associated with crop production deficits, which can in turn lead to cereal and food price increases. Figure 7.16 shows the recent year-to-year variations in Malawi's GPD, expressed as percent changes (Data source: World Bank). Recent (1993-2016) GDP changes in Malawi are very weakly correlated with detrended production anomalies (r=0.22) and January NINO3.4 SSTs (r=0.14).

We briefly examined newly available national retail maize price data (Figure 7.16) collected by FEWS NET at 12 markets located across Malawi. These are nominal prices and are not adjusted for inflation. The EM-DAT droughts reported in 2005/06, 2012 and 2015 are apparent in the data. The marked influence of the 2015/16 El Niño event is quite apparent. This may also emphasize the important non-local influence of El Niño events. By producing regional droughts across Southern Africa, ENSO events can modulate local food prices by creating both local crop production deficits and by supporting regional deficits that may also influence regional demand and regional food prices.

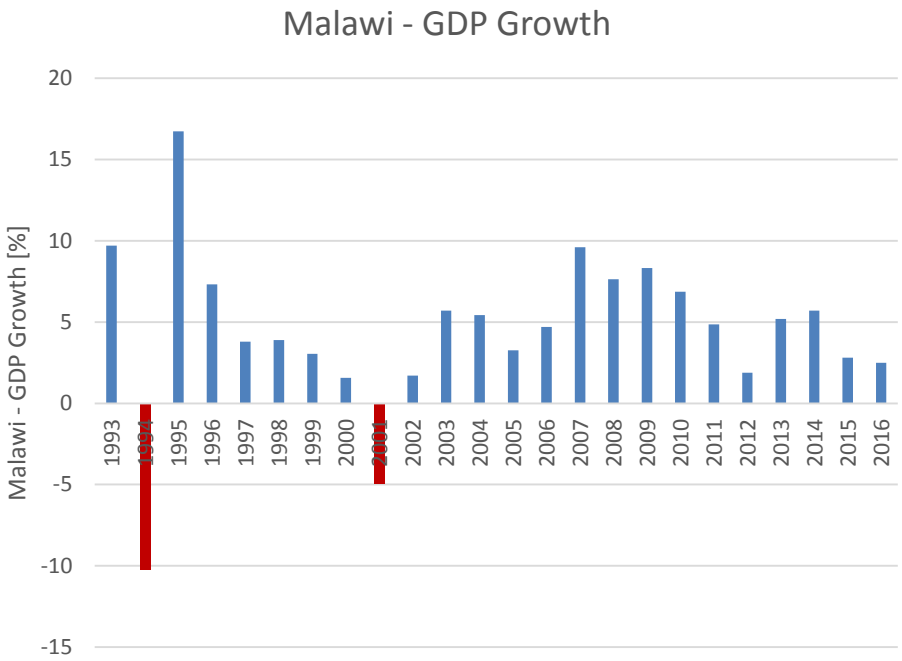

Figure 7.16 *Year-to-year changes in Malawi GDP, expressed in percentages.*

To explore the impact of droughts, we look at the change in 2007 to 2017 August-to-August maize prices, i.e. the maize price change from one dry season to the next. Analysis of the correlation between these variations and monthly CHIRPS data for Malawi indicates interesting monthly variation. January and March rainfall are very weakly correlated with changes in prices. February rainfall exhibits a strong (-0.7) inverse correlation with price changes. Presumably, mid-season drought in-phase with the main grain filling period for maize has a more substantial influence on yield deficits. Price increases are well correlated (r=-0.74) with detrended production anomalies (shown above). Knowing the maize price in February coupled with February CHIRPS rainfall results in a very strong predictive relationship for August prices during the following austral winter (August), with an R^2 valued of 0.83 with a substantial part of this predictability arising from the strong non-stationarity of Malawi cereal prices. Focusing rather just on the change between February price conditions and maize prices during the following August, we find a robust level of predictability (R^2=0.63), suggesting that price and precipitation monitoring systems, acting together, provide good advance warning of future price changes.

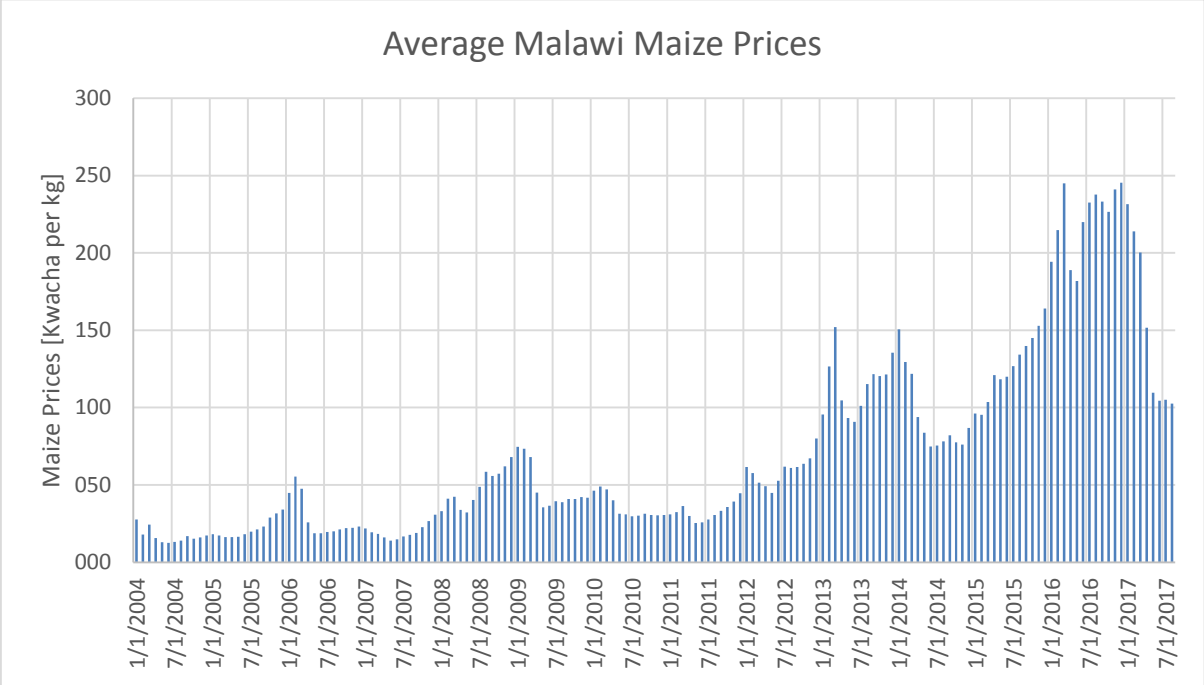

Figure 7.17 A time series of retail maize prices in Malawi, based on the average of 12 markets. Data provided by FEWS NET.

7.3.6 Impact on municipal and industrial water needs

Various maps are available at the Aqueduct Water Risk Atlas that compare baseline water stress to industrial sectors (mining, food & beverage, chemicals, semi-conductor, oil and gas, mining, construction materials, textiles). However, there does not seem to be any variation in baseline water stress for the different sectors. Also, no independent drought impact information for these industrial sectors was available for the case study countries. Hence, no further assessment of these impact maps was performed.

7.4 Evaluation of forecasting and monitoring systems

7.4.1 Current drought monitoring and forecasting

Forecasting in Malawi is primarily handled by the National Meteorological agency, which collaborates annually with the regional Climate Outlook Fora process. The Southern African Regional Climate Outlook Forum (SARCOF) is coordinated by the Southern African Development Community (SADC) Climate Services Centre (CSC) in Gabarone, Botswana. It covers all SADC Member States: Angola, Botswana, Democratic Republic of Congo, Lesotho, Madagascar, Malawi, Mauritius, Mozambique, Namibia, Seychelles, South Africa, Swaziland, Tanzania, Zambia and Zimbabwe. These climate forecasts are prepared on an annual basis, typically first appearing in September of each year.

Forecasts from the National Multi-model Ensemble (NMME) and the International Research Institute (IRI) are also consulted. Climate forecasts are used in conjunction with national rainfall monitoring to inform national bulletins[49] and the regional SADC agro-meteorological

[49] *http://www.metmalawi.com/bulletins/bulletins.php*

bulletins[50]. During the main growing season (October to April) these bulletins are updated on a monthly basis

7.4.2 Available operational systems

The GeoCOF and GeoCLIM tool
The GeoCOF tool, authored by CSC scientists and Tamuka Magadzire[51] is used to guide these forecasts, along with other statistical analyses. Statistical forecasts, based on ENSO conditions and Indian Ocean sea surface temperature anomalies are the primary inputs into these forecasts. These forecasts are updated during the course of the season and can be combined with observed precipitation to create a hybrid rainfall monitoring and prediction system.

The National Multi-Model Ensemble
The NMME (http://www.cpc.ncep.noaa.gov/products/NMME/) combines dynamic forecasts from 10 different coupled ocean-atmosphere models. These models and forecasts are updated monthly.

IRI probabilistic seasonal forecasts
These forecasts are produced based on logistic regression using a subset of the NMME models[52]. Empirical relationships between the NMME predictions and historical precipitation and temperature are used to guide tercile probability forecasts.

ECMWF forecasts
These are mentioned, but not evaluated since we lack access to the ECMWF forecasts.

A summary of the main characteristics of the available monitoring and forecasting systems is given in Table 7.5.

7.4.3 Model Evaluation and recommendation
Here we evaluated a simple statistical forecast, consistent with a GeoCOF analysis, based on observed September NINO3.4 sea surface temperatures (SSTs, 5°S-5°N, 170°E-120°W). We also examined climate forecasts from one of the NMME models, the Coupled Forecast System Version 2, using forecasts based on observed September SSTs. To simulate the IRI tercile estimation process, we also bias corrected the precipitation forecasts and then evaluated hit rates. We focused on predicting January-February-March rainfall in Southern Malawi (south of 14°S); the main growing season in the most drought sensitive part of the country.

As the 1981-2016 results show (Figure 7.18), a modest but useful negative tele-connection exists with ENSO SSTs. While the R^2 is quite low (24%), all severe droughts occurred in positive NINO3.4 seasons and all very wet years occurred during negative NINO3.4 seasons. The breakpoint for the bottom tercile of the observed rainfall is 588 mm. Using a simple regression predicting JFM precipitation using September SSTs only identifies 4 of the 12 dry years. The signature drought years of 1992 and 2005 are underestimated but were predicted to be below average.

[50] *http://www.sadc.int/news-events/newsletters/agrometerological-update/*
[51] *http://chg.geog.ucsb.edu/tools/geocof/*
[52] *http://iri.columbia.edu/our-expertise/climate/forecasts/seasonal-climate-forecasts/methodology/*

Table 7.5 - Characteristics of drought monitoring and forecasting systems available in Malawi.

	GeoCOF/ GeoCLIM tool	**National Multi-Model Ensemble**	**IRI probabilistic seasonal forecasts**	**ECMWF forecasts**
Monitoring	Yes	No	No	No
Forecasting	Yes	Yes	Yes	Yes
Region/countries/areas	Regional	Global	Global	Global
Spatial resolution	Regional	~1 degree	~1 degree	~1 degree
Datasets used	Observed SSTs Observed Rain	Initialized with Obs and reanalysis	NMME	Initialized with Obs
Software and tools used	GeoClim			
Indices presented	Rainfall amount, tercile probability	Rainfall anomaly and tercile probability	tercile probability	Rainfall amount
Reflective of impacts	Yes/no			
Forecast horizon	1-7 months	1-10 months	1-10 months	1-7 months
Update frequency	Can be monthly	monthly	monthly	monthly
Accessibility of forecast	Moderate	Easy	Easy	Moderate
Method of access	From SADC website	Online	Online	Online
Procedure / steps	Reported via Agromet reports	Updated automatically	Updated automatically	Updated automatically
Resources required	Human Expert w/ Computer	Minimal	Minimal	Minimal
Post-processing	Probabilistic Forecasts can be interpreted based on thresholds	Need to be downloaded for numerical analysis	Need to be downloaded for numerical analysis	Need to be downloaded for numerical analysis
Hit rate (estimation)	5 of 12 droughts	Always predicts drought due to dry bias	2 of 12 droughts	N.A.

We also examined the CFSv2 JFM forecasts for this region (Figure 7.19). The predicted rainfall is much lower than the observations, and very poorly correlated (R^2=0.05). The signature drought years are predicted to be below-normal, but so are the wettest years in the 1981-2016 record. Bias correcting the CFSv2 forecasts and estimating drought hit rates based on forecasts of less than 588 mm identified only 2 of the 12 droughts.

Assessment: While the skill associated with statistical models is modest for this region, there are evident changes in the underlying probability distributions supporting broad designation of 'average to above-average' and 'average to below-average' based SST conditions. These assessments can be refined as the rainy season progresses by incorporating observed rainfall and updating and refining SST-based forecast assumptions. While the NMME models can provide very valuable information about the evolution of large scale SST patterns, they likely lack local skill for this region and season.

This general lack of skill of the NMME is not localized to Malawi, or even Africa, but applies to most regions of the globe (Figure 7.20 and Figure 7.21Figure 7.21).

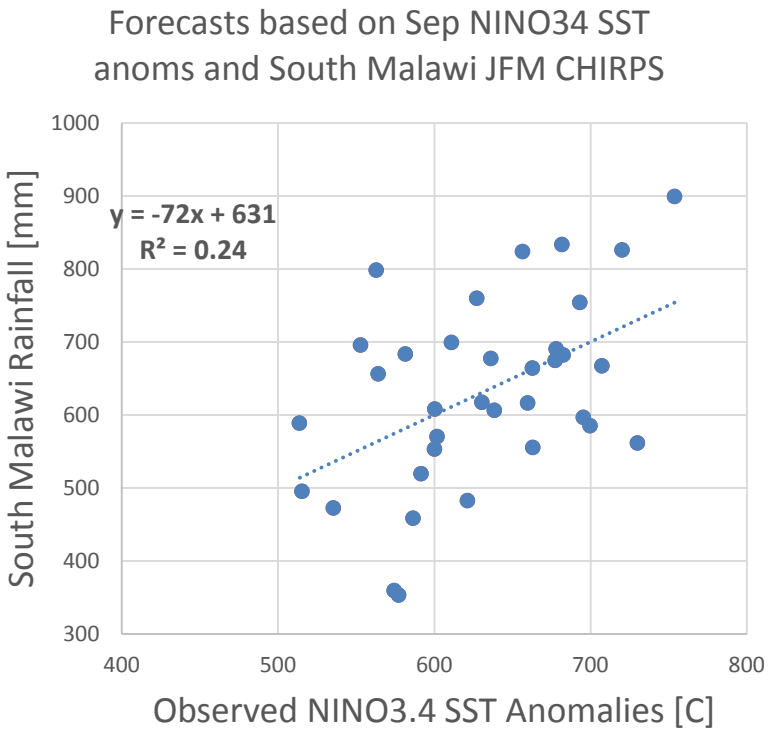

Figure 7.18 - Forecasts based on NINO3.4 SSTs

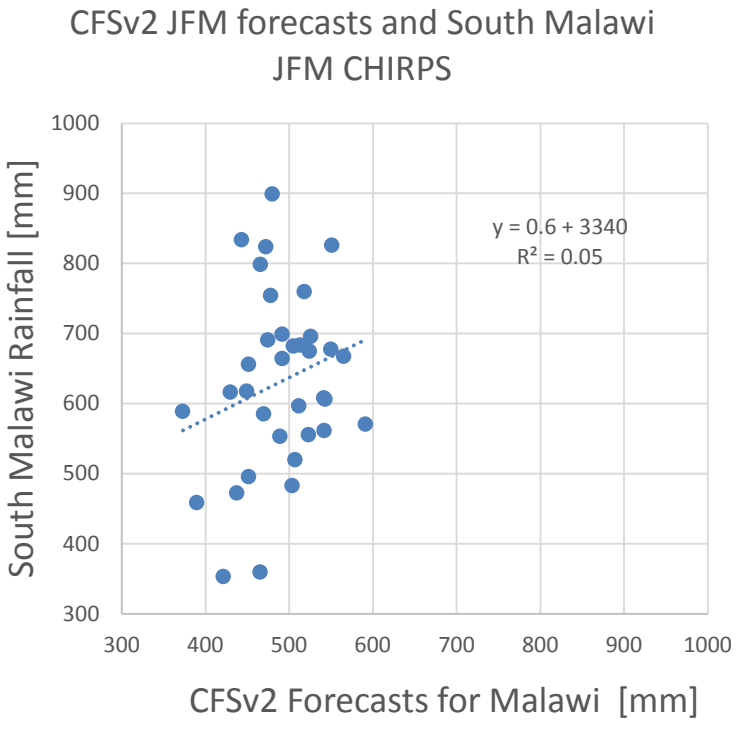

Figure 7.19 - Forecasts based on CFSv2 Model Simulations

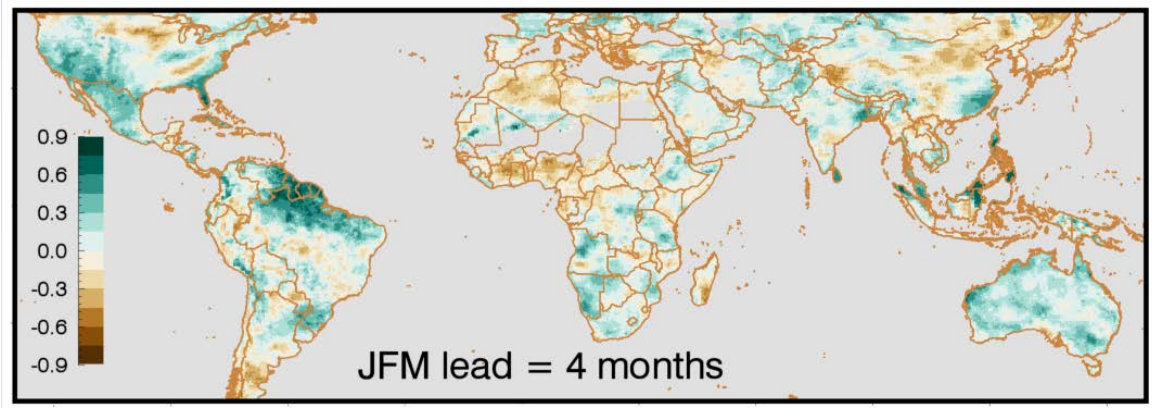

Figure 7.20 - 1982-2016 correlation between NMME ensemble average forecasts and CHIRPSv2

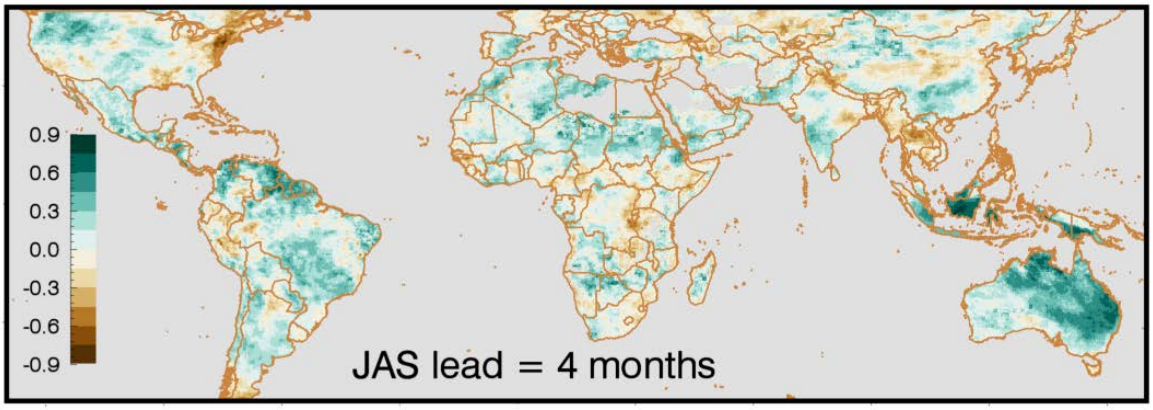

Figure 7.21 - 1982-2016 correlation between NMME ensemble average forecasts and CHIRPSv2

8 Conclusions and recommendations

8.1 Introduction

This chapter provides an overview of our conclusions and recommendations based on the quantitative and qualitative analyses that were conducted during this study. In the previous chapters of this report the results of the analyses were described for each case study country individually. Here the conclusions and recommendations are described for each aspect and method of drought risk analyses that was assessed in this study, thereby aggregating the findings from the five case study countries.

8.2 Country characteristics and reported droughts

A concise but complete description of drought related country characteristics is an important starting point for a drought hazard and risk assessment. In addition it reveals the existing level of drought context knowledge of the country and it provides much needed background information to interpret analyses results or for further drought risk assessments.

It is recommended to collect and describe the following aspects based on existing information and publications:

- Socio-economic country characteristics.
- Meteorological and hydrological characteristics (incl. inter- and intra-annual variability and the potential climatic teleconnections, like ENSO).
- Key characteristics of the natural environment (e.g., orography, river basins, soils) as well as the land use (systems).
- Water resources, water demand, and the relative water availability (level of water stress).
- Historical droughts and drought impacts.

8.3 Spatial time series analysis of global datasets

8.3.1 Comparison of global datasets

The various drought hazard indices from the global datasets showed varying correspondence to the registered drought events for the five case study countries (Table 8.1), ranging from a good match with registered events in (Afghanistan), a moderately good match (Fiji, Colombia) to a relatively poor match (Ethiopia, Malawi). Table 8.2 gives an overview of the dataset-index combinations that showed a good match with registered droughts for each of the case study countries. Based on this analysis, the SPEI3 index based on the WaterGAP dataset shows the best match with registered droughts, followed by SPEI3 and indices based on the Global Drought Monitor and PCR-GLOBWB datasets.

The comparability of dataset-index combinations in detecting droughts varies between the case study countries (Table 8.2). For Fiji, the comparability was very high with all models showing pronounced drought hazards for 5 out of the 7 registered droughts, while the other two registered droughts were not detected by any of the models. Also, for Afghanistan the comparability of the models for registered drought events was relatively high while for other models the comparability was limited for registered drought events. However, the dataset-index combinations for Ethiopia showed high comparability for non-registered drought hazards.

Table 8.1 Summary of registered and non-registered drought years, hit rates, false alarms, and comparability of dataset-index combinations.

	drought years		hit rate regist. droughts		hit rate non-regist. droughts		false alarm modeled droughts		comparability modeled drought hazards	
	registered	non-registered	(+)	(+, +/-)	(+)	(+, +/-)	(+)	(+, +/-)	registered	non-registered
Afghanistan	6	9	77%	97%	34%	60%	38%	47%	high	limited
Colombia	6	5	65%	83%	49%	93%	40%	48%	limited	limited
Ethiopia	12	8	35%	57%	77%	91%	60%	52%	limited	high
Fiji	7	3	71%	71%	73%	81%	30%	32%	high	high
Malawi	10	7	43%	67%	65%	89%	51%	49%	limited	limited

Table 8.2 Overview of dataset-index combinations that showed a (very) good hit rate with registered droughts shown as "+" signs. Also high and low false alarm rates are shown, shown as red (+) and (-). Intermediate false alarm rates are not shown.

	Global Land Surface		IRI data library		Global drought monitor		PCRGlobWB					WaterGap				
	SPI3	SPI12	SPI3	SPI12	SPEI3	SPEI12	SPI3	SPI12	SPEI3	SPEI12	SSF1	SPI3	SPI12	SPEI3	SPEI12	SSFI
Afghanistan	(+)		+ (+)		+	+	+		+	+		+		+	+	(-)
Colombia	(+)	(+)	+		+	+	+		+	+		+		+	+	
Ethiopia	(+)	(++)			(+)	(+)		(+)		(+)	(+)		(+)	+	(+)	
Fiji	+	+ (-)	+	+ (-)	+	+ (-)	+	+ (-)	+	+ (-)	+ (-)	+	(-)	+	+ (-)	+ (-)
Malawi		(+)	(+)	(+)	+	+	(+)	(+)	+	+	(+)	(+)	(+)	+	+	+

Interestingly, the dataset-index combinations assessed in this project showed more/other drought hazards than were registered. The false alarm rates of dataset-index combinations was on average 45% (Table 8.1). This was particularly the case for Ethiopia and Malawi where many false alarms were modelled by the dataset-index combinations, while for Fiji the false alarm rates are relatively low (Table 8.2). The dataset-index combination GLS-SPI3 and GLS-SPI1-2 resulted in a high level of false alarms for 3 out of the 5 case study countries, while the false alarm rate for WaterGAP-SSFI was relatively low. The overestimation of drought hazards can have various causes. The dataset-index combinations may overestimate the drought conditions in the country, perhaps due to the critical threshold values set for the drought hazard indices. There can also be a mismatch in the timing of the modelled drought hazards and the registered events. This can be caused by an error in the models, but it is also likely that a drought event is registered (a year) later than the drought hazard occurs due to the time-lag of the impacts of drought events. Moreover, the modelled droughts only represent the hazard aspect of drought risk, while for the registered droughts the exposure and vulnerability to drought are also important. Hence, a drought does not necessarily have to result in adverse impacts.

Unfortunately, at the time this research was performed, no global spatio-temporal datasets were available online that enabled us to assess other types of drought than meteorological drought and hydrological drought. It is however recommended that a similar analysis is made for agricultural drought and socio-economic drought if and when such datasets become available.

8.3.2 Validation with local time series

Using the two global models in the different country scale case studies to validate its results with local time-series we do not find large consistent differences in performance. No single

best model exists across all case study countries or even within each case study country. Selection of the model used depends very much on the particular region and the specific purpose of use, e.g. for drought monitoring and detection (here variability is the most important factor) or water resources management (here the absolute biases in discharge estimates are the most important factor).

Overall, the global models are relatively better in representing the correlation coefficient (i.e. having the relative variability right) rather than estimating the absolute values correctly. Having such knowledge at hand, the global models can be safely applied in drought event detection and monitoring but should be handled with care when applying them for water resources management purposes. This is especially true for the PCR-GLOBWB, which generally overestimates water resources availability across all case studies investigated. This, in turn, results in an underestimation of water resources scarcity conditions. When using global models for water resources management purposes, absolute estimates need to be bias corrected towards local observations. Long-term mean water resources availability of WaterGAP have been calibrated/validated towards long-term mean discharge estimates. Therefore, WaterGAP is performing relatively better when looking at the absolute biases.

In this report we used open-source discharge observations to validate the global models with. Since the time-length of these discharge observations is usually too short we have not performed a validation on droughts. This would require 30 years of data availability in both observations and models. Instead, we evaluated the correlation coefficient and bias ratio of discharge estimates. Together these indicators give, nevertheless, a good insight into the ability of the models to represent the variability and absolute estimates. Future research could look into other data-sources to allow for a validation of other drought indicators as well, for example datasets that are able to represent historical potential evapotranspiration.

8.3.3 ENSO analysis

For most case study countries we find significant differences in drought frequency and exposure between El Niño (EN)/La Niña (LN) phases, and neutral or non-EN/-LN phases correlation. Despite the significant anomalies in drought frequency and exposure, we do not always find a strong correlation between the continuous drought indicator values and the JMA SST index. In the case of Colombia we found high correlations and relatively short optimal lag times. Correlations for Fiji and Afghanistan were moderate while low correlations were found for Ethiopia and Malawi. High correlation results indicate that a relatively large part of the variability in drought conditions can be associated to ENSO variability, more specifically to ENSO variability represented by the JMA SST index, Low correlation results indicate that the identified variability in drought conditions cannot be explained merely by variations in the JMA SST; here drought variability is the result of a composite of actors. This is the case for example for Ethiopia and Malawi.

Whereas the country-scale anomalies are shown to be consistent across the two models investigated when looking at the meteorological drought indicators (SPI, SPEI), the results differ in most case studies for the SSFI indicator. This can be explained by the differences in routing routines and calibration between the two models and the level of variability incorporated within the two models. Looking at the spatially explicit anomalies in exposure and the spatial patterns of correlation we do see, however, that for most case studies investigated that both models show a similar spatial pattern and that the choice of model does not significantly affect the outcomes.

In this assessment we only coupled the exposure to drought with the ENSO signal. However, ENSO is part of an ocean–atmospheric climate variability system that constitutes many more subregional systems and local circulation patterns (e.g., Indian monsoon, Pacific/North America pattern, North Atlantic Oscillation, East Atlantic/West Russia pattern, Scandinavia pattern), which modulate the ENSO signal (Hannaford et al., 2011). Future research should therefore look into the sensitivity of drought exposure to combinations of these systems, especially in areas that provide a relative low ENSO signal. In addition, a more detailed analysis into the influence of large-scale oscillation patterns on the regional exposure of droughts, focusing more specifically on the different time/space intervals for different parts of the case study countries would provide more insight into the local to regional sensitivity of the case study countries to ENSO driven variability.

8.4 Assessment of drought impact and risk platforms and datasets

Five available online platforms and datasets were assessed for their capacity to provide spatial drought impact and/or risk information:

- Global map of drought risk (JRC)
- IWMI water data portal
- Aqueduct Water Risk Atlas
- FAO Agricultural Stress Index and precipitation anomalies
- African Drought Observatory

The online platforms and datasets providing impact and risk information based on historical data were compared with information from the country descriptions and, where possible, with each other. A general weakness of the analysis is the lack of adequate impact data, impeding a more sophisticated quantitative approach. Also, drought impact and risk could not be assessed for each sector, because of a lack of global drought modeling tools or other resources for specific sectors. Hence, the analysis resulted in a bias towards drought impact and risk to the population, the agricultural sector and the overall economy. Below, a description of the pros and cons of each of the impact/risk platforms and datasets is provided based on our qualitative analyses.

- The advantage of the *global map of drought risk* from JRC is that the relative share of hazard, exposure, and vulnerability in the final maps of impact and risk is clear. The impact estimates seem logical compared to country information available, however, the findings cannot be verified at the level of spatial detail provided due to a lack of local impact information. A disadvantage is that the impact and risk for the various sectors are not specified per sector. In addition, the estimated drought hazard does not always seem to be in line with country information on droughts and the drought analysis based on the global models in the report.

- The advantage of the maps provided by the *IMWI water data portal* is that they provide impact information at a relatively high spatial detail. The impact estimates seem logical compared to country information available for most countries; however, verification at the level of spatial detail provided is not possible due to a lack of local impact information. A disadvantage is that the impact information is not readily available for many sectors, if at all.

- The advantage of the *Aqueduct Water Risk Atlas* is that it relates baseline water stress to the important sectors (agriculture, hydropower, mining, food & beverage, chemicals, semi-conductor, oil and gas, mining, construction materials, textiles). Unfortunately, there does not seem to be (any) variation for the different sectors; all maps appear to be the same or very similar to the default baseline water stress map. In addition, the water

stress information is not always in line with country information or with the other impact/risk models.

- The advantage of the *FAO platform* with agricultural stress indices is the high resolution and the spatial time scale of years, enabling a detailed assessment of historical agricultural droughts. However, verification at the level of spatial detail provided is not possible due to a lack of local impact information. A comparison at the country scale shows that the information at the FAO platform is often in line with registered (agricultural) droughts, but in many cases agricultural impact is missed (e.g., Fiji case).

- The maps from the *African Drought Observatory* could only be evaluated for two case study countries (Ethiopia and Malawi). The advantage of these maps is that they provide information at the sub-basin level. However, the accuracy of the drought vulnerability patterns provided requires further detailed analysis with additional information that was currently not available. Another disadvantage is that no specifications per impact category / sector are provided.

An important general observation during this project was the *unavailability of data about drought related impacts for relevant impact categories on a sub-national scale*. As a result, actual validation of the maps from the online platforms and datasets was not possible. For Malawi, an analysis of national and sub-national agricultural data could be made available based on information from FEWS NET. However, also in the case of Malawi, drought impact data on hydro-power and data on other relevant impact categories were not available. It is advised that a *separate investigation* is started to develop a methodology for collection of sub-national drought impacts in the main sectors and that effort is put into building a database for such data (historic impacts as well as exposure and vulnerability information). In a follow-up of this study the efforts of the Sendai Framework for Disaster Risk Reduction (2015-2030), such as the Disaster Information Management System[53], could also be included.

Another general observation is the diversity of approaches, underlying data and spatial scales that are used to create and present impact and risk in the maps available at online platforms and datasets. This diversity makes it virtually impossible to carry out a meaningful comparison. It is recommended that more uniformity in drought impact and risk indices and visualisation is promoted in order to increase comparability of products. Moreover, this will probably increase the level of understanding and utilization of the drought impact and risk information.

Finally, it is recommended that information about actual drought impacts is added to the (existing) online portals and databases. By doing this the quality and relevance of the impact and risk maps (which are often a product of map layers of hazard, exposure and vulnerability) can be demonstrated, thereby increasing their reliability and use. It is however very well possible that such data is not available and collection of impact information is required first.

8.5 Qualitative assessment of forecasting and monitoring products

For the five focus countries we provide a qualitative analysis of the existing drought monitoring and forecasting systems. The *key conclusions* of the analysis are as follows:

- Of the five countries analysed, drought monitoring and forecasting systems are most limited in Afghanistan. Thus far the only source of monitoring and forecasting products

[53] *https://www.desinventar.net/DesInventar/*

in Afghanistan is through FEWS NET. Our review identifies that although drought related literature is limited for Afghanistan, results of the existing studies are promising for developing a drought monitoring/forecasting system, as they indicate some potential predictability.

- From the five countries analysed we found that the drought monitoring and forecasting systems are most mature in Ethiopia, which has multiple systems in place through national agencies such as National Meteorology Agency (NMA), regional agencies such as IGAD-ICPAC (Inter-Governmental Authority on Development Climate Prediction and Applications Centre) and International agencies such as FEWS NET and IRI.

- Likewise, the Instituto de Estudios Ambientales y Meteorlogía (IDEAM) and SADAC are responsible for providing drought monitoring and forecasting information in Columbia and Malawi, respectively.

- In general, most of the national and regional monitoring systems in the case study countries rely on FEWS data products among other products, and forecasting systems combine consensus forecasts (based on local experts assessments and statistics e.g., the GHACOF process for Ethiopia) with forecasts from global dynamical forecasts such as NMME and ECMWF.

- Despite several global scale drought monitoring and forecasting systems exist, it is found that these systems are most mature in the countries where there are one or more national or regional agencies tasked with providing monitoring and forecasting information and where there are national or regionally focused versions of the global datasets.

Based on this assessment, the following *recommendations* are provided for starting up or improving drought detection/early warning and forecasting systems:

- Appoint one or, preferably, several national and regional agencies with providing monitoring and forecasting information to authorities and the public. A strong national or regional agency mandated to provide operational drought monitoring and early warning products, is key. Countries can improve their system or set-up a forecasting and early warning system by committing resources towards the implementation of a national/regional climate service agency. In addition, international agencies should work towards supporting such agencies and capacity building efforts.

- It is important that governments commit to multi-year collaboration so that the operational demonstration of monitoring and forecasting products has been realized and make sure that local agencies have the skill and infrastructure they need to keep the system operationally sustainable.

- In case there is a lack of understanding of the climate and drought sensitivity and exposure to different sectors, it is important that research is conducted to assess the drought characteristics and the level of drought predictability for a given country or region.

- Global systems are extremely valuable as they provide first cut monitoring and early warning product for the national and regional agencies, without them spending their computational resources. They can work with the global systems-based products and revise/refine based on their local products and expertise. Consensus forecasts could be

combined with a national or regionally focused version of the global dynamical forecast datasets. A global system also makes sense as drought events are often linked to global and/or regional phenomenon that may be beyond the borders of the case study country. Here it is important that local/regional agencies have knowledge as well as easy and smooth access to global products.

- Monitoring and forecasting products should be developed in close collaboration with the local/regional agencies. The agencies should be provided with the right tools, skills and datasets needed so they can best utilize their local expertise on monitoring and early warning. Assistance from (foreign) experts could be requested to set up and/or improve drought detection and forecasting systems.

- Importantly, drought detection and monitoring systems should connect closely to the questions and needs of local/regional agencies and other stakeholders. In doing so, data and derivative products from such a system can be packaged into usable impact information.

References

ADB (2014). Disaster Risk Management Overview. Supplementary Appendix A, Northern Flood-Damaged Infrastructure Emergency Rehabilitation Project (RRP AFG 48326), Asian Development Bank, Manila.

Australian Bureau of Meteorology and CSIRO, 2011. Climate Change in the Pacific: Scientific Assessment and New Research. Volume 1: Regional Overview. Volume 2: Country Reports.
Awulachew, S. B., and Yilma (2007). Water resources and irrigation development in Ethiopia, Iwmi.

Bhattacharyya, K.; Azizi, P. M.; Shobair, S. S.; Mohsini, M. Y. 2004. *Drought impacts and potential for their mitigation in southern and western Afghanistan.* Working Paper 91. Colombo, Sri Lanka: International Water Management Institute.

Bouwman, A. F., Kram, T., and Klein Goldewijk, K., Netherlands Environmental Assessment Agency (MNP), Bilthoven, 2006.

Bierkens, M.F.P. and L.P.H. van Beek (2009): Seasonal predictability of European Discharge: NAO and Hydrological Response Time. J. Hydrometeor, 10, 953–968.

Carrão, H., G. Naumann, P. Barbosa (2016) Mapping global patterns of drought risk: an empirical framework based on sub-national estimates of hazard, exposure and vulnerability. Glob. Environ. Chang., 39 (2016), pp. 108-124, 10.1016/j.gloenvcha.2016.04.012.

Cheng Y., Tang, Y., and Chen, D.: Relationship between predictability and forecast skill of ENSO on various time scales, J. Geophys. Res., 116, C12006, doi:10.1029/2011JC007249, 2011.

Davey, M. K., Brookshaw, A., and Ineson, S. (2014). The probability of the impact of ENSO on precipitation and near-surface temperature. Climate Risk Management, 1, 5-24.

Deltares, 2018. Global inventory of drought hazard and risk modeling tools and resources. D.M.D. Hendriks, P. Trambauer, M. Mens, M. Faneca Sànchez, S. Galvis Rodriguez, H. Bootsma, C. van Kempen, M. Werner, S. Maskey, M. Svoboda, T. Tadesse, T. Veldkamp. Deltares report 11200758-002.

Dutra, E., W. Pozzi, F. Wetterhall, F. Di Giuseppe, L. Magnusson, G. Naumann, P. Barbosa, J. Vogt, and F. Pappenberger. 2014. “Global Meteorological Drought – Part 2: Seasonal Forecasts.” Hydrology and Earth System Sciences 18 (7): 2669–78. doi:10.5194/hess-18-2669-2014.

Fiji meteorological service, 2003. List of droughts that have occurred in Fiji from 1965 to 2000. Information Sheet No. 126.

Funk, C., a. Hoell, S. Shukla, I. Bladé, B. Liebmann, J. B. Roberts, F. R. Robertson, and G. Husak. 2014. “Predicting East African Spring Droughts Using Pacific and Indian Ocean Sea Surface Temperature Indices.” Hydrology and Earth System Sciences Discussions 11 (3): 3111–36. doi:10.5194/hessd-11-3111-2014.

Government of Afghanistan (2011). Afghanistan Strategic National Action Plan (SNAP) for Disaster Risk Reduction: Towards Peace and Stable Development.
GWP-SA (2014). Summary Report of the Need Assessment Survey on the Development of South Asian Drought Monitoring System (SA DMS). Global Water Partnership – South Asia, Battaramulla, Sri Lanka.

Lehner, B., Döll, P., Alcamo, J. et al. Climatic Change (2006) 75: 273. https://doi.org/10.1007/s10584-006-6338-4

Habib, H. (2014). Water related problems in Afghanistan. *International Journal of Educational Studies, 1*(3), 137–144.

Harris, I., Jones, P.D., Osborn, T.J. and Lister, D.H. (2014), Updated high-resolution grids of monthly climatic observations – the CRU TS3.10 Dataset. Int. J. Climatol., 34: 623–642. doi:10.1002/joc.3711.

Hoell, A., Funk, C. and Barlo M. (2015). The Forcing of Southwestern Asia Teleconnections by Low-Frequency Sea Surface Temperature Variability during Boreal Winter. Journal of Climate, DOI: 10.1175/JCLI-D-14-00344.1.

IFRC (2013). International Disaster Response Law (IDRL) in Afghanistan, International Federation of Red Cross and Red Crescent Societies, Geneva.

International Business Publications, 2013. Afghanistan Country Study Guide – Volume 1. Strategic information and developments (2013) International Business Publications, USA. Washington DC USA – Afghanistan.

Keyantash, John & National Center for Atmospheric Research Staff (Eds). Last modified 08 Mar 2018. "The Climate Data Guide: Standardized Precipitation Index (SPI)." Retrieved from https://climatedataguide.ucar.edu/climate-data/standardized-precipitation-index-spi.

Klein Goldewijk, K. and van Drecht, G.: HYDE 3: Current and historical population and land cover, in: Integrated modelling of global environmental change. An overview of IMAGE 2.4, edited by: Kumar, A., Hu, Z. Z., Jha, B., & Peng, P. (2017). Estimating ENSO predictability based on multi-model hindcasts. Climate Dynamics, 48(1-2), 39-51.

Liu, J., Yang, H., Gosling, S. N., Kummu, M., Flörke, M., Pfister, S., ... & Alcamo, J. (2017). Water scarcity assessments in the past, present, and future. *Earth's Future*, *5*(6), 545-559.
Ludescher, J., Gozolchiani, A., Bogachev, M. I., Bunde, A., Havlin, S., and Schellnhuber, H. J.: Very early warning of next El Niño, P. Natl. Acad. Sci. USA, 111, 2064–2066, oi:10.1073/pnas.1323058111, 2014.

Masih, I., S. Maskey, F.E.F. Mussá, P. Trambauer (2014) A review of droughts on the African continent: a geospatial and long-term perspective. Hydrol. Earth Syst. Sci., 18, 3635–3649, 2014. doi:10.5194/hess-18-3635-2014.

McKee, T. B., N. J. Doesken, and J. Kleist, 1993: The relationship of drought frequency and duration of time scales. Eighth Conference on Applied Climatology, American Meteorological Society, Jan17-23, 1993, Anaheim CA, pp.179-186.

McPhaden, M.J., S.E. Zebiak, M.H. Glantz (2006) ENSO as an Integrating Concept in Earth Science. Science, 314(5806), 1740–1745, 2006.

McSweeney, C., M. New, G. Lizcano, and X. Lu (2010) The UNDP Climate Change Country Profiles: Improving the Accessibility of Observed and Projected Climate Information for Studies of Climate Change in Developing Countries. Bulletin of the American Meteorological Society. https://doi.org/10.1175/2009BAMS2826.1.

Muhammad, A. (2011). Drought Characterization Using Remote Sensing and Ground Data in Amudarya Basin. MSc Thesis WSE-HWR 11.01, UNESCO-IHE, Delft.
Nasery, M. T (2017). Estimation of Flow Duration Curves for use in Hydropower Development for ungauged or partially gauged subbasins in the Kabul River basin, Afghanistan. A report based on the MSc thesis WSE-HWR 17.13, UNESCO-IHE, Delft.

Naumann, G., P. Barbosa, L. Garrote, A. Iglesias, J. Vogt (2014) Exploring drought vulnerability in Africa: an indicator based analysis to be used in early warning systems. Hydrol. Earth Syst. Sci., 18 (2014), pp. 1591-1604.

Palmer, W. C. (1965). Meteorological drought. U.S. Weather Bureau Research Paper 45, 58 pp. Available online by the NOAA National Climatic Data Center at:
http://www.ncdc.noaa.gov/temp-and-precip/drought/docs/palmer.pdf

Poveda, G., a. Jaramillo, M.M Gil, N. Quiceno, and R. Mantilla. 2001. “Seasonality in ENSO Related Precipitation, River Discharges, Soil Moisture, and Vegetation Index (NDVI) in Colombia.” Water Resources Research 37 (8): 2169–78. doi:10.1029/2000WR900395.

Poveda, Germán, Diana M. Álvarez, and Óscar a. Rueda. 2011. “Hydro-Climatic Variability over the Andes of Colombia Associated with ENSO: A Review of Climatic Processes and Their Impact on One of the Earth’s Most Important Biodiversity Hotspots.” Climate Dynamics 36 (11–12): 2233–49. doi:10.1007/s00382-010-0931-y.

Poveda, Germán, Diana M. Álvarez, and Óscar a. Rueda. 2011. “Hydro-Climatic Variability over the Andes of Colombia Associated with ENSO: A Review of Climatic Processes and Their Impact on One of the Earth’s Most Important Biodiversity Hotspots.” Climate Dynamics 36 (11–12): 2233–49. doi:10.1007/s00382-010-0931-y.

Qureshi, A.S. (2002). Water Resources Management in Afghanistan: The Issues and Options. Working Paper 49, Pakistan Country Series No. 14, International Water Management Institute (IWMI).

Reddy, K.S. (2016), Global Burden of Disease Study 2015 provides GPS for global health 2030, The Lancet, DOI: http://dx.doi.org/10.1016/S0140-6736(16)31743-3.

RSMI (2009) Malawi: Economic Vulnerability and Disaster Risk Assessment.

Schepen, Andrew, Q. J. Wang, and David E. Robertson. 2012. “Combining the Strengths of Statistical and Dynamical Modeling Approaches for Forecasting Australian Seasonal Rainfall.” Journal of Geophysical Research Atmospheres 117 (20): 1–9. doi:10.1029/2012JD018011.

SOPAC, 2007. Integrated Water Resources Management programme's Diagnostic Reports (SOPAC, 2007)

Telesca, L., M. Lovallo, I. Lopez-Moreno and S. Vicente-Serrano, 2012: Investigation of scaling properties in monthly streamflow and Standardized Streamflow Index time series in the Ebro Basin (Spain). Physica A: Statistical Mechanics and its Applications, 391(4): 1662–1678. DOI: 10.1016/j.physa.2011.10.023. (For more information on this paper, please contact the IDMP HelpDesk).

Trambauer, P., M. Werner, H. C. Winsemius, S. Maskey, E. Dutra, and S. Uhlenbrook. 2015. “Hydrological Drought Forecasting and Skill Assessment for the Limpopo River Basin, Southern Africa.” Hydrology and Earth System Sciences 19 (4): 1695–1711. doi:10.5194/hess-19-1695-2015.

UN-WATER, W. (2004). National Water Development Report for Ethiopia Addis Ababa, Ethiopia, United Nations Educational, Scientific, and Cultural Organization.

Van Beek, L. P. H.(2007) PCR-GLOBWB model description. Integration of GFS Data with PCR-GLOBWB using FEWS. WL | Delft Hydraulics Rep. 18 pp. [Available online at http://vanbeek.geo.un.nl/suppinfo/vanbeek2007a.pdf]. Google Scholar"

Veldkamp, T.I.E. , S. Eisner, Y.Wada, J.C.J.H. Aerts, P. J. Ward (2015) Sensitivity of water scarcity events to ENSO-driven climate variability at the global scale. Hydrol. Earth Syst. Sci., 19, 4081–4098, 2015. doi:10.5194/hess-19-4081-2015.

Vicente-Serrano S.M., Santiago Beguería, Juan I. López-Moreno, (2010) A Multi-scalar drought index sensitive to global warming: The Standardized Precipitation Evapotranspiration Index - SPEI. Journal of Climate 23: 1696-1718.

Vicente-Serrano, S. M., López-Moreno, J. I., Gimeno, L., Nieto, R., Morán-Tejeda, E., Lorenzo-Lacruz, J., & Azorin-Molina, C. (2011). A multiscalar global evaluation of the impact of ENSO on droughts. Journal of Geophysical Research: Atmospheres, 116(D20).

Viste, E., et al. (2013). "Recent drought and precipitation tendencies in Ethiopia." Theoretical and Applied Climatology 112(3-4): 535-551.

Viste, E. D. Korecha, A. Sorteberg (2013) Recent drought and precipitation tendencies in Ethiopia. Theoretical and Applied Climatology, Volume 112, Issue 3–4, pp 535–551

Wada, Y., van Beek, L. P. H., and Bierkens, M. F. P.: Modelling global water stress of the recent past: on the relative importance of trends in water demand and climate variability, Hydrol. Earth Syst. Sci., 15, 3785–3808, doi:10.5194/hess-15-3785-2011, 2011a.

Wada, Y., van Beek, L. P. H., Viviroli, D., Dürr, H. H.,Weingartner, R., and Bierkens, M. F. P.: Global monthly water stress: 2. Water demand and severity of water stress, Water Resour. Res., 47, W07518, doi:10.1029/2010WR009792, 2011b.

Wang-Chun Lai, A., Herzog, M., & Graf, H. F. (2018). ENSO Forecasts near the Spring Predictability Barrier and Possible Reasons for the Recently Reduced Predictability. Journal of Climate, 31(2), 815-838.

Wells N, Goddard S and Hayes MJ (2004) A self-calibrating Palmer Drought Severity Index. Journal of Climate 17, 2335-2351. doi:10.1175/1520-0442.

Wondie M. and Terefe T., (2016). Assessment Of Drought In Ethiopia By Using Self Calibrated Palmer Drought Severity Index (ScPDSI). International Journal of Eng. and Management VOL.7 (2): 108-117.

World Bank, 2000. Economic Implications of Climate Change in Two Pacific Country Locations Case Study of Tarawa, Kiribati and Viti Levu, Fiji. World Bank – Pacific Region.

World Bank, 2012. Analisis de la gestión del riesgo de desastres en Colombia. Ana Campos G., Niels Holm-Nielsen, Carolina Díaz G., Diana M. Rubiano V., Carlos R. Costa P., Fernando Ramírez C. y Eric Dickson (Banco Mundial – GFDRR). Marzo, 2012.

World Bank, 2014. Islamic Republic of Afghanistan Agricultural Sector Review. Revitalizing Agriculture for Economic Growth, Job Creation and Food Security. June 2014. Report No: AUS9779. Report No: AUS9779.
http://documents.worldbank.org/curated/en/245541467973233146/pdf/AUS9779-REVISED-WP-PUBLIC-Box391431B-Final-Afghanistan-ASR-web-October-31-2014.pdf

Appendix A – Country scale analysis of Global Models

A1. Figures Afghanistan

Figure A1.1 – Meteorological drought index SPI1 based on IRI data library (top), based on PCR-GLOBWB (middle), and based on WaterGAP (bottom) for Afghanistan. Grey stars indicate drought events recorded by EM-DAT and other sources (Deltares, 2016).

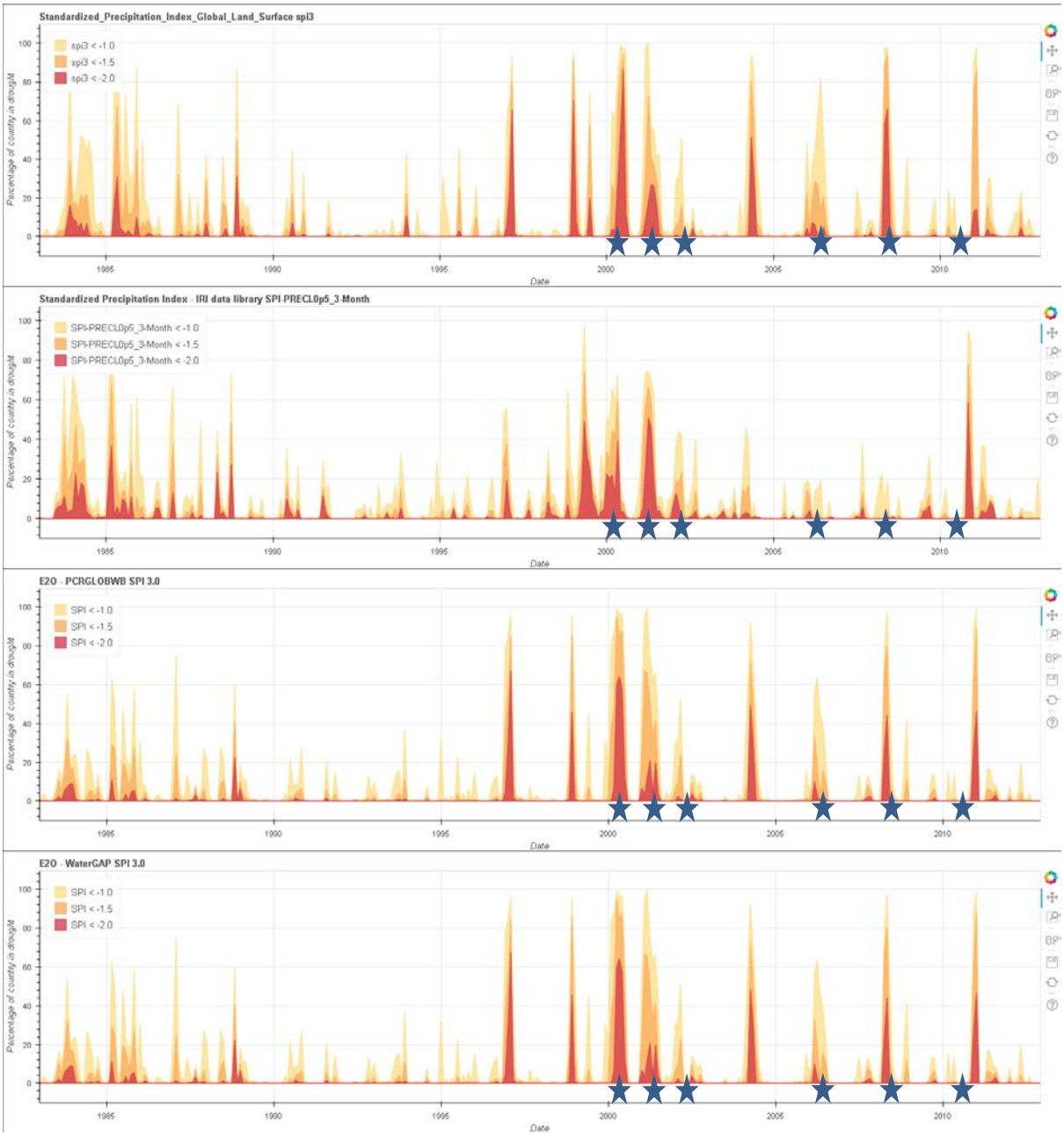

Figure A1.2 – Meteorological drought index SPI3 based on Global Land Surface (top), based on IRI data library (second), based on PCR-GLOBWB (third), and based on WaterGAP (bottom) for Afghanistan. Grey stars indicate drought events recorded by EM-DAT and other sources (Deltares, 2016).

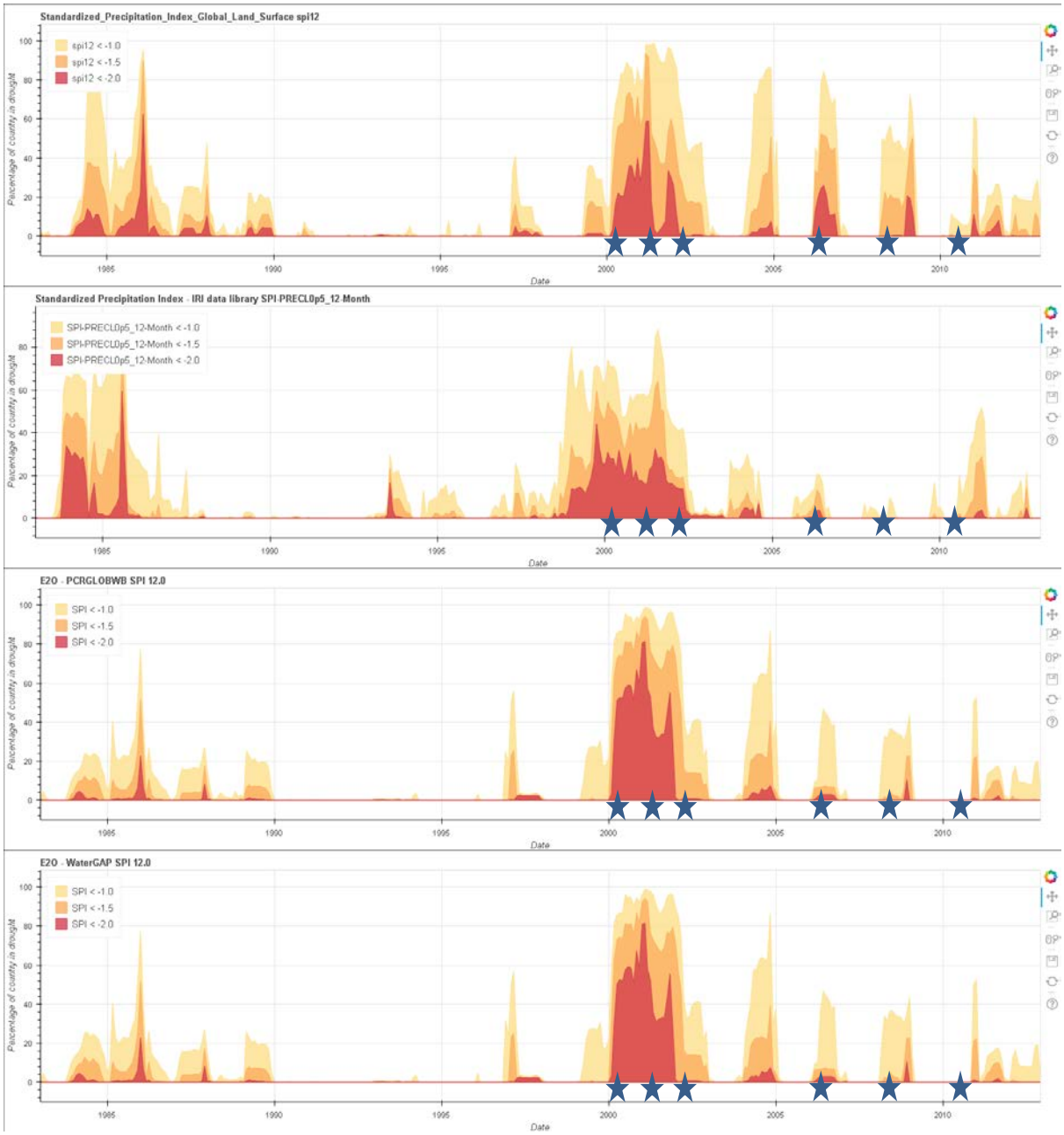

Figure A1.3 – Meteorological drought index SPI12 based on Global Land Surface (top), based on IRI data library (second), based on PCR-GLOBWB (third), and based on WaterGAP (bottom) for Afghanistan. Grey stars indicate drought events recorded by EM-DAT and other sources (Deltares, 2016).

Figure A1.4 – Meteorological drought index SPEI1 based on Global Drought Monitor (top), based on PCR-GLOBWB (middle), and based on WaterGAP (bottom) for Afghanistan. Grey stars indicate drought events recorded by EM-DAT and other sources (Deltares, 2016).

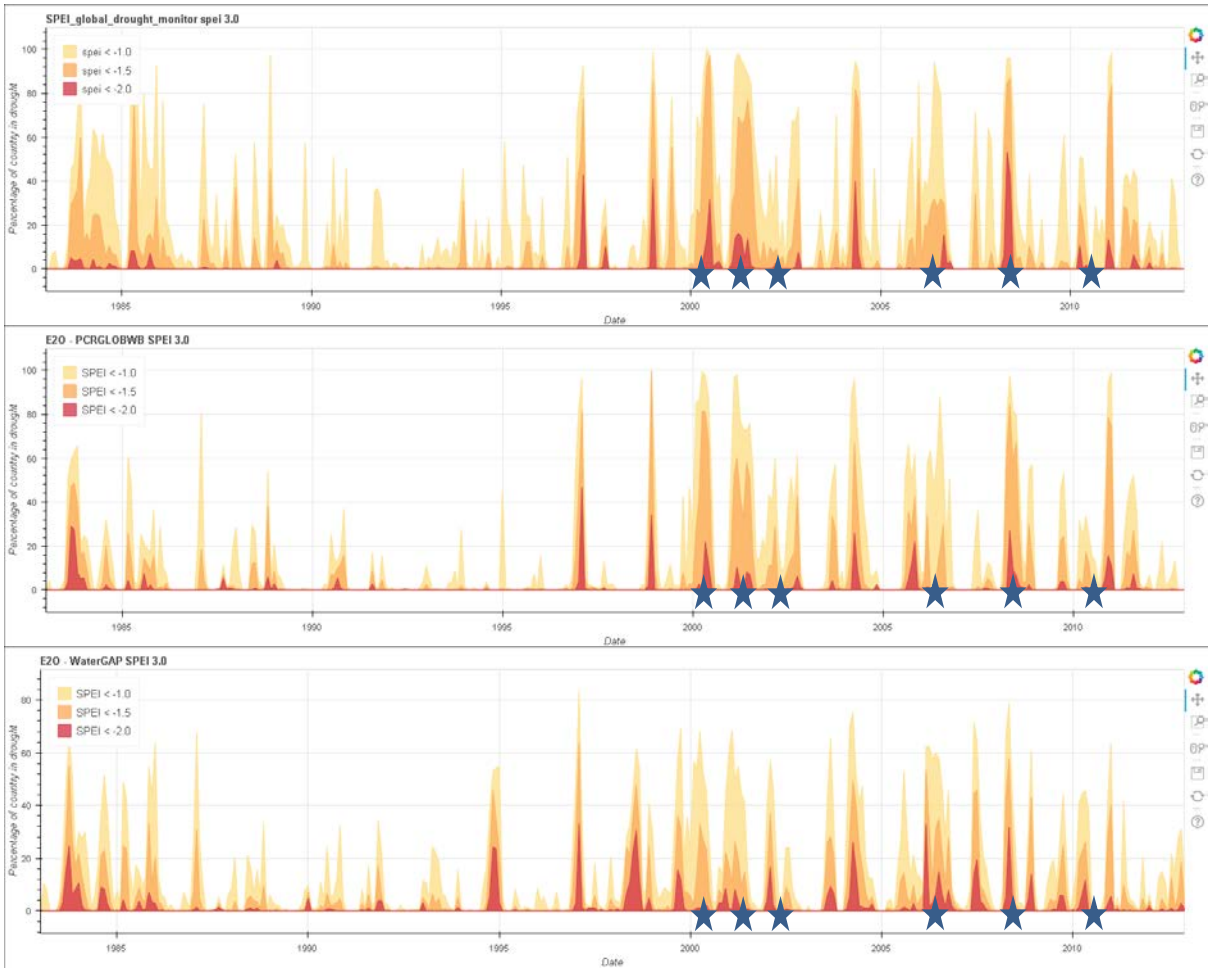

Figure A1.5 – Meteorological drought index SPEI3 based on Global Drought Monitor (top), based on PCR-GLOBWB (middle), and based on WaterGAP (bottom) for Afghanistan. Grey stars indicate drought events recorded by EM-DAT and other sources (Deltares, 2016).

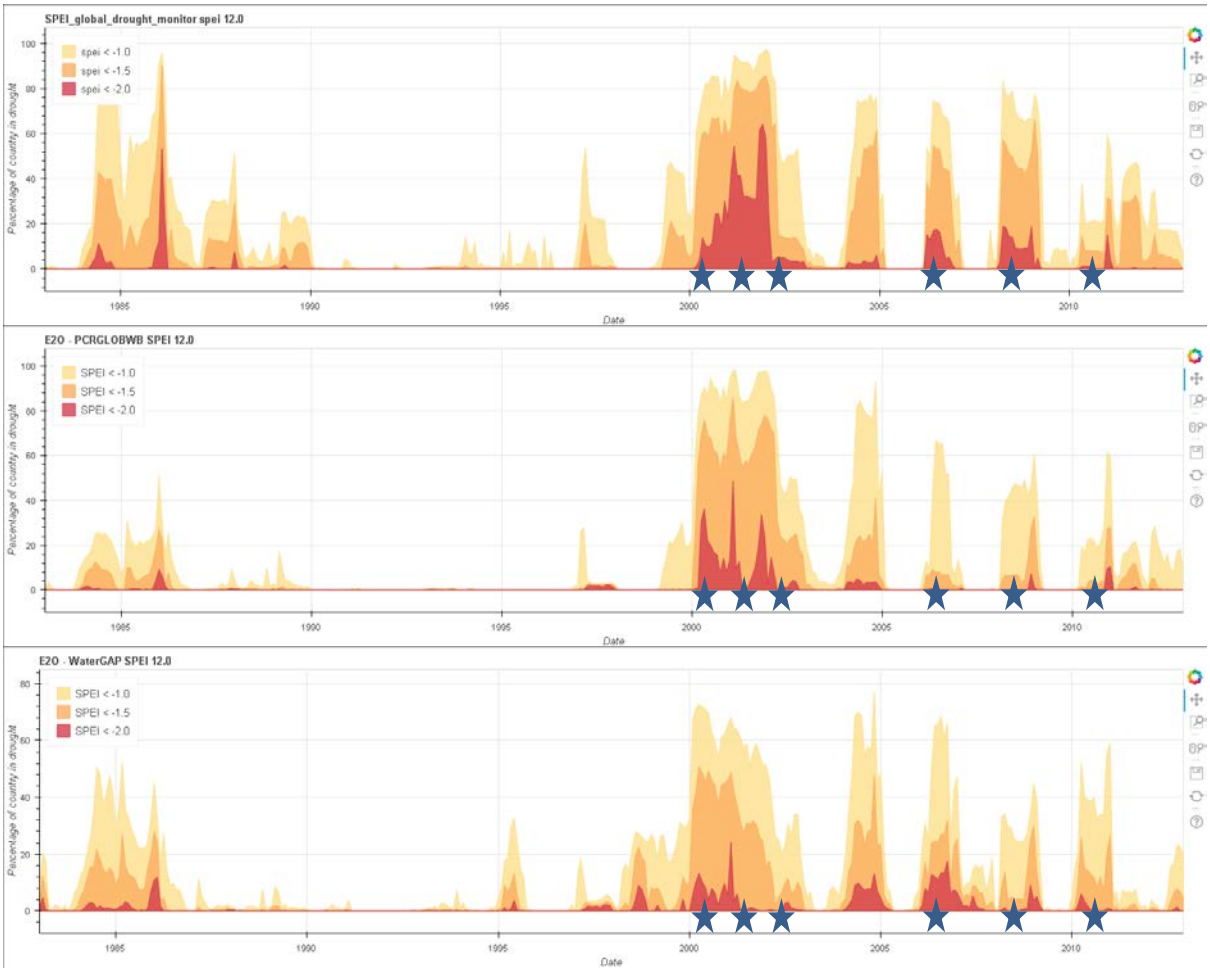

Figure A1.6 – Meteorological drought index SPEI12 based on Global Drought Monitor (top), based on PCR-GLOBWB (middle), and based on WaterGAP (bottom) for Afghanistan. Grey stars indicate drought events recorded by EM-DAT and other sources (Deltares, 2016).

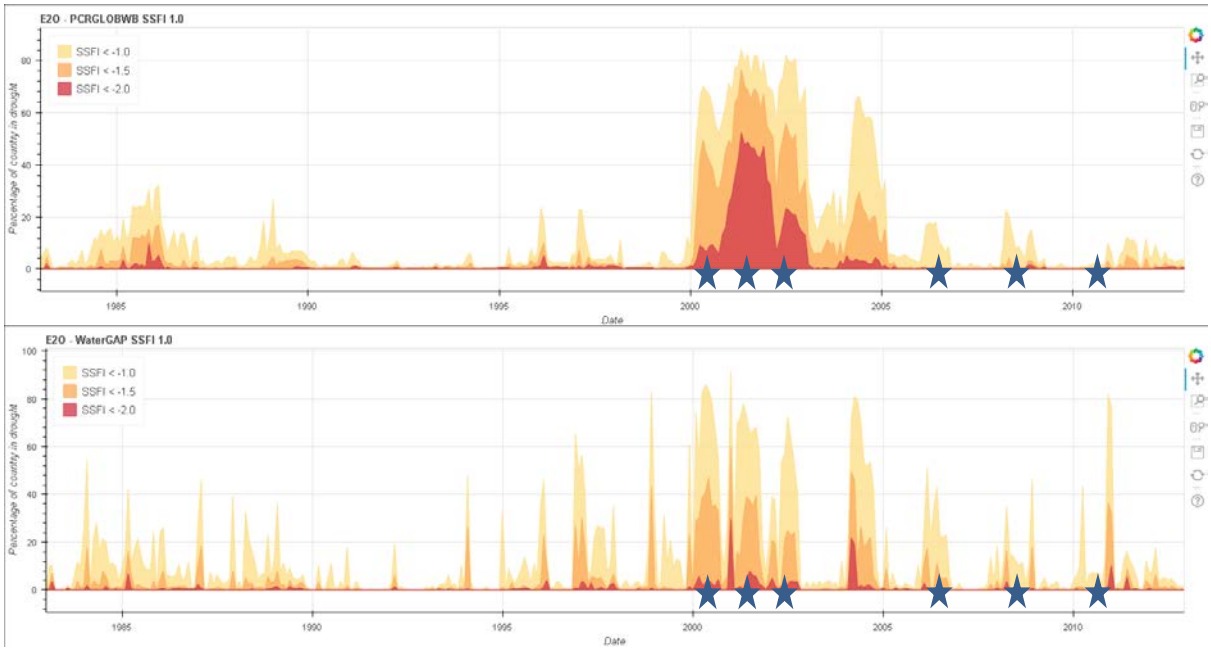

Figure A1.7 – Hydrological drought index SSFI-1 based on based on PCR-GLOBWB (top) and based on WaterGAP (bottom) for Afghanistan. Grey stars indicate drought events recorded by EM-DAT and other sources (Deltares, 2016).

A2. Figures Colombia

Figure A2.1 – Meteorological drought index SPI1 based on IRI data library (top), based on PCR-GLOBWB (middle), and based on WaterGAP (bottom) for Colombia. Grey dots indicate drought events recorded by IDEAM; Grey triangles indicate drought events recorded by EM-DAT and IDEAM.

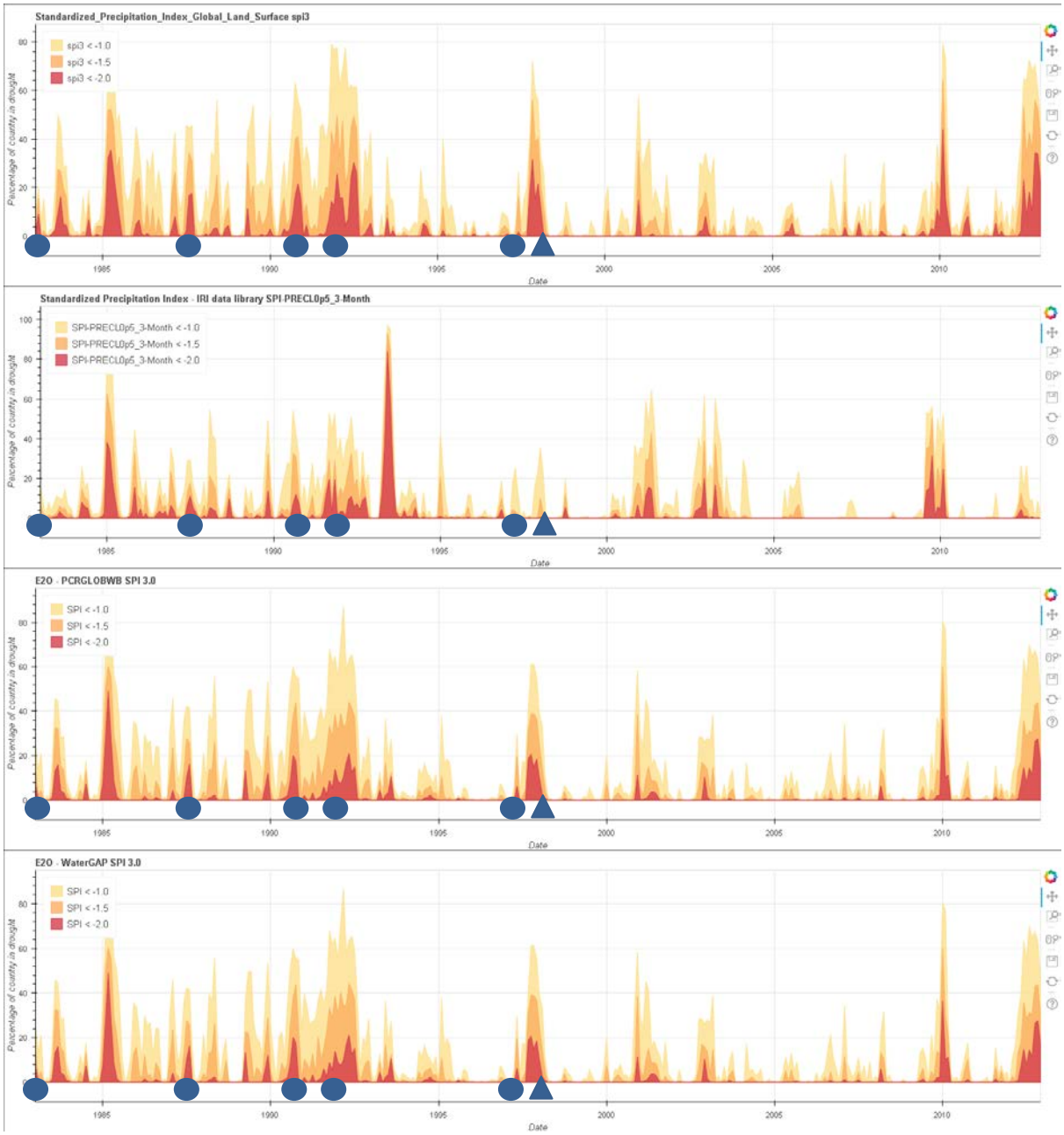

Figure A2.2 – Meteorological drought index SPI3 based on Global Land Surface (top), based on IRI data library (second), based on PCR-GLOBWB (third), and based on WaterGAP (bottom) for Colombia. Grey dots indicate drought events recorded by IDEAM; Grey triangles indicate drought events recorded by EM-DAT and IDEAM.

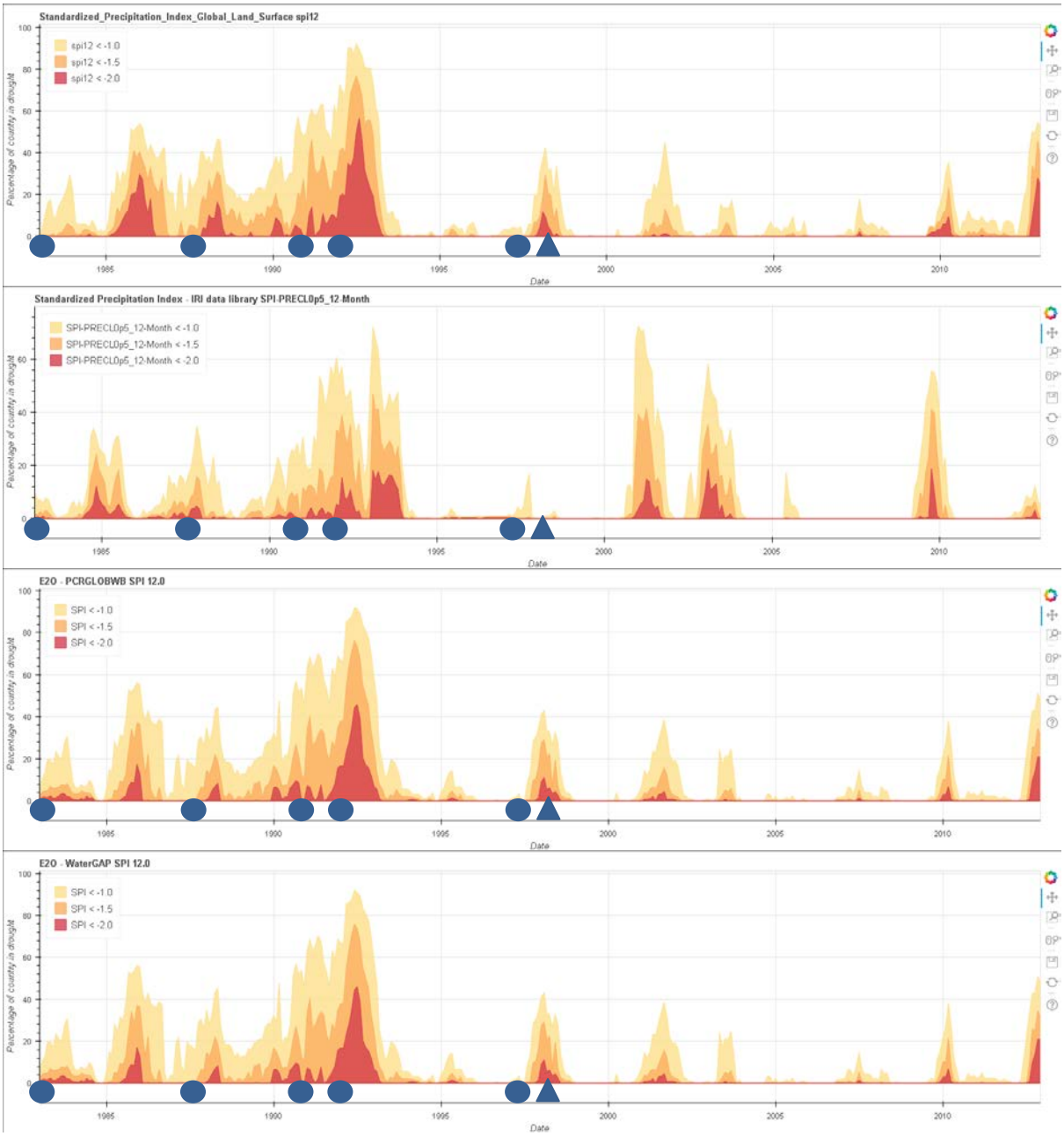

Figure A2.3 – Meteorological drought index SPI12 based on Global Land Surface (top), based on IRI data library (second), based on PCR-GLOBWB (third), and based on WaterGAP (bottom) for Colombia. Grey dots indicate drought events recorded by IDEAM; Grey triangles indicate drought events recorded by EM-DAT and IDEAM.

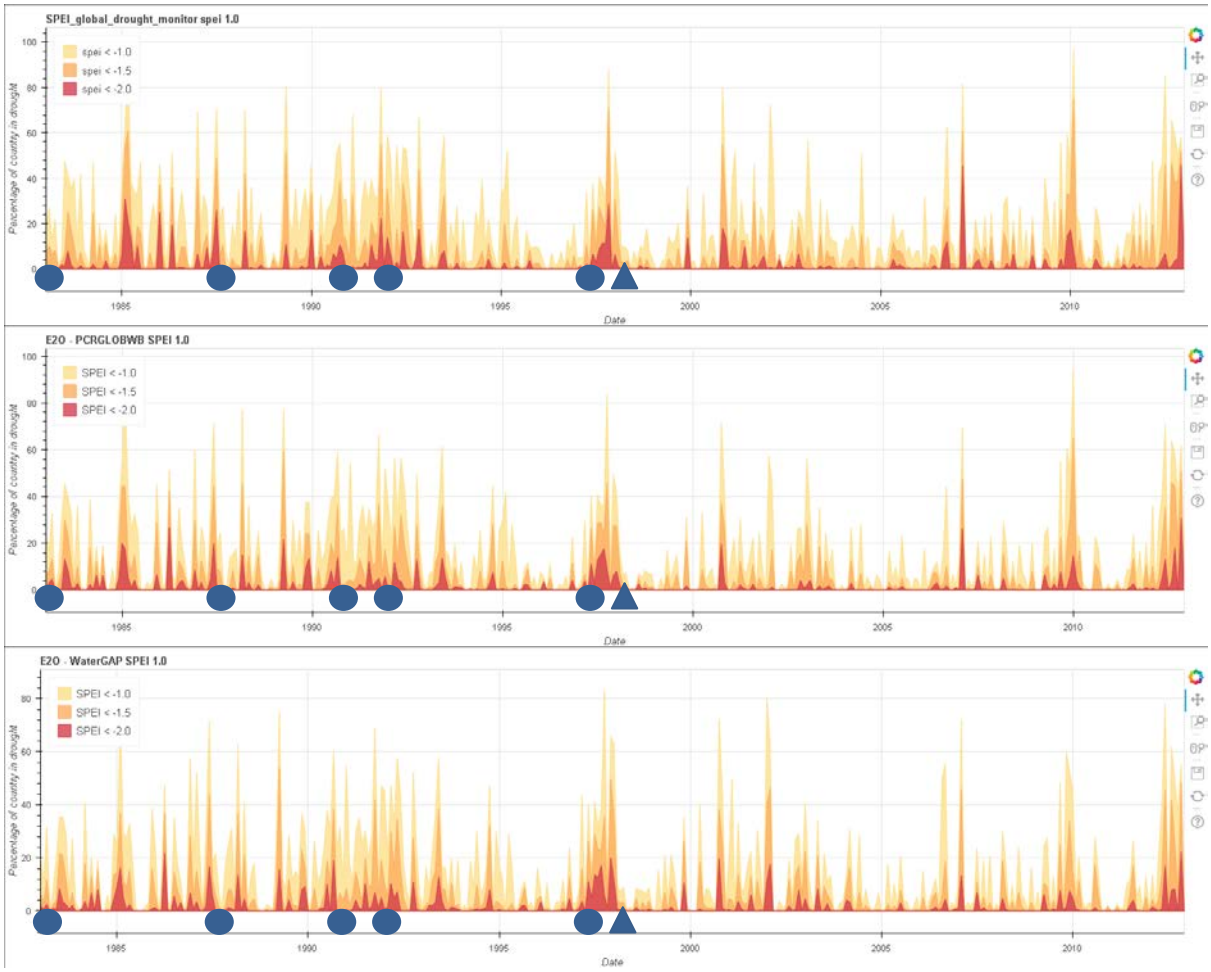

Figure A2.4 – Meteorological drought index SPEI1 based on Global Drought Monitor (top), based on PCR-GLOBWB (middle), and based on WaterGAP (bottom) for Colombia. Grey dots indicate drought events recorded by IDEAM; Grey triangles indicate drought events recorded by EM-DAT and IDEAM.

Figure A2.5 – Meteorological drought index SPEI3 based on Global Drought Monitor (top), based on PCR-GLOBWB (middle), and based on WaterGAP (bottom) for Colombia. Grey dots indicate drought events recorded by IDEAM; Grey triangles indicate drought events recorded by EM-DAT and IDEAM.

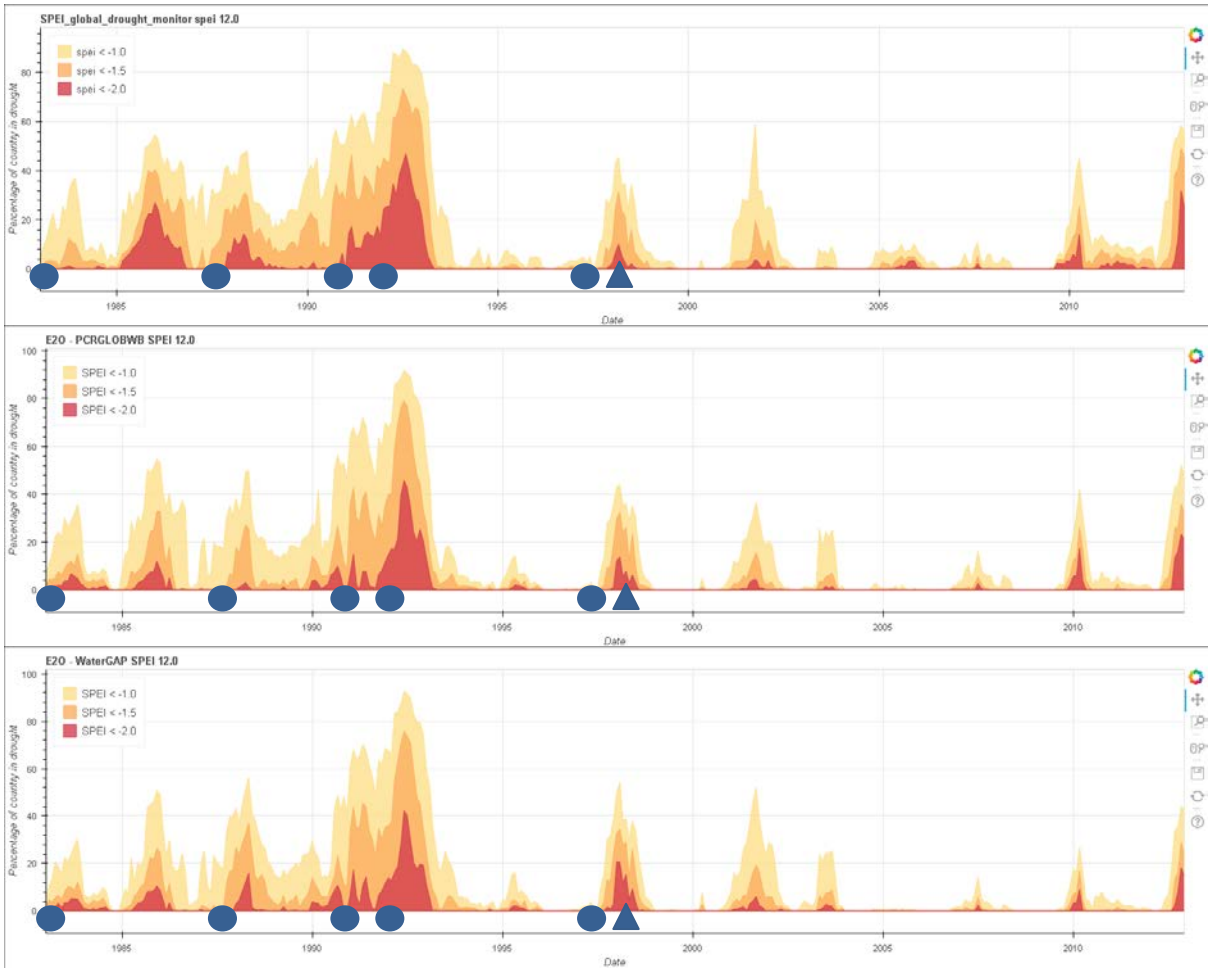

Figure A2.6 – Meteorological drought index SPEI12 based on Global Drought Monitor (top), based on PCR-GLOBWB (middle), and based on WaterGAP (bottom) for Colombia. Grey dots indicate drought events recorded by IDEAM; Grey triangles indicate drought events recorded by EM-DAT and IDEAM.

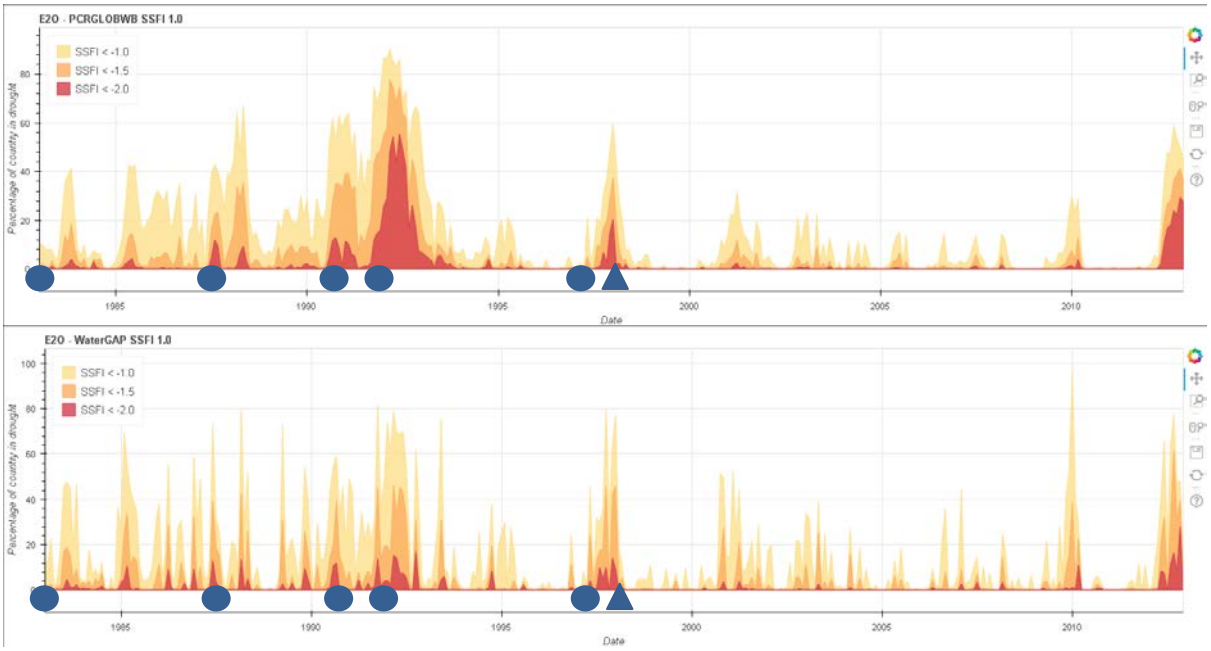

Figure A2.7 – Hydrological drought index SSFI-1 based on based on PCR-GLOBWB (top) and based on WaterGAP (bottom) for Colombia. Grey dots indicate drought events recorded by IDEAM; Grey triangles indicate drought events recorded by EM-DAT and IDEAM.

A3. Figures Ethiopia

Figure A3.1 – Meteorological drought index SPI1 based on IRI data library (top), based on PCR-GLOBWB (middle), and based on WaterGAP (bottom) for Ethiopia. Grey stars indicate drought events recorded by EM-DAT.

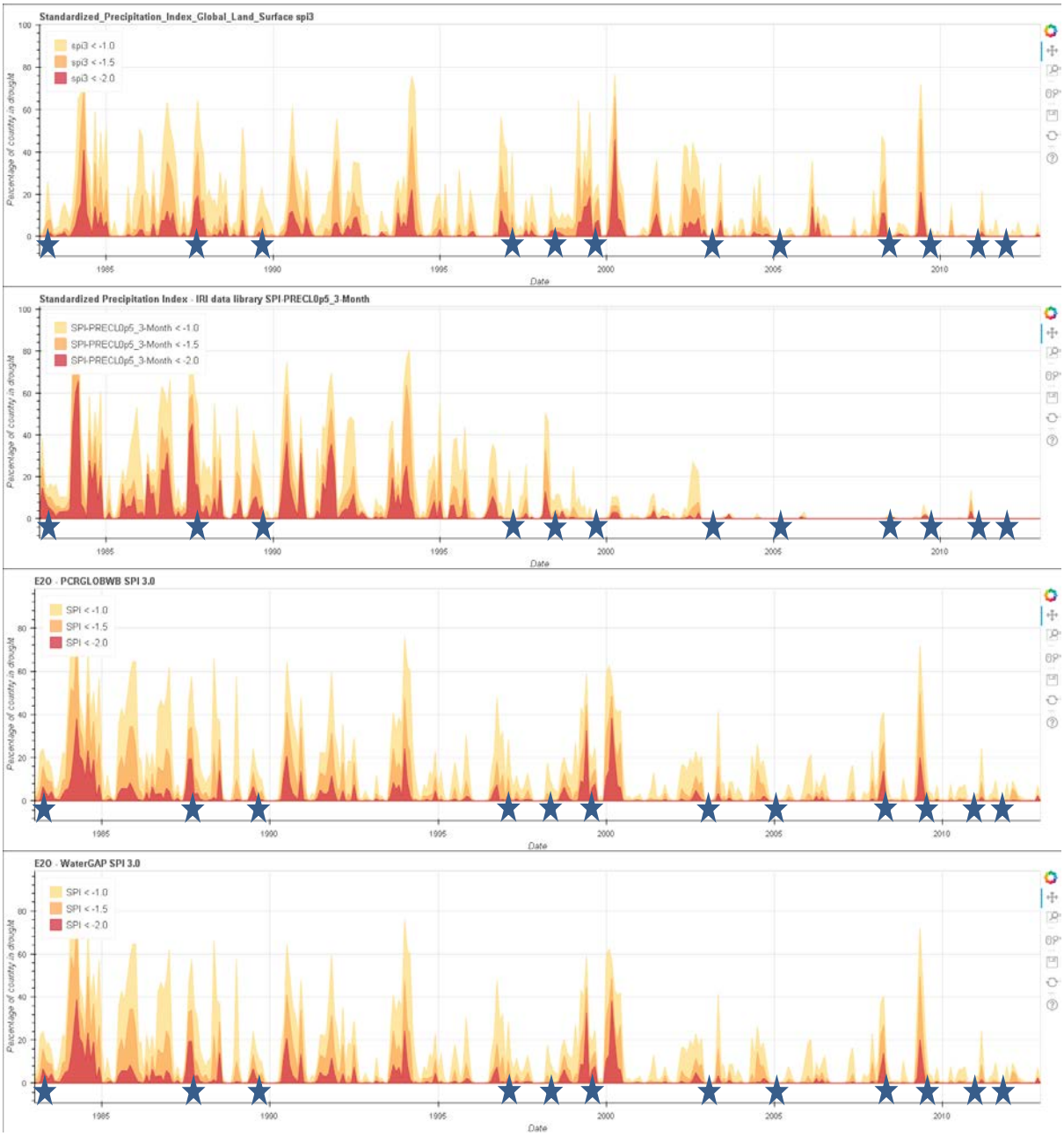

Figure A3.2 – Meteorological drought index SPI3 based on Global Land Surface (top), based on IRI data library (second), based on PCR-GLOBWB (third), and based on WaterGAP (bottom) for Ethiopia. Grey stars indicate drought events recorded by EM-DAT.

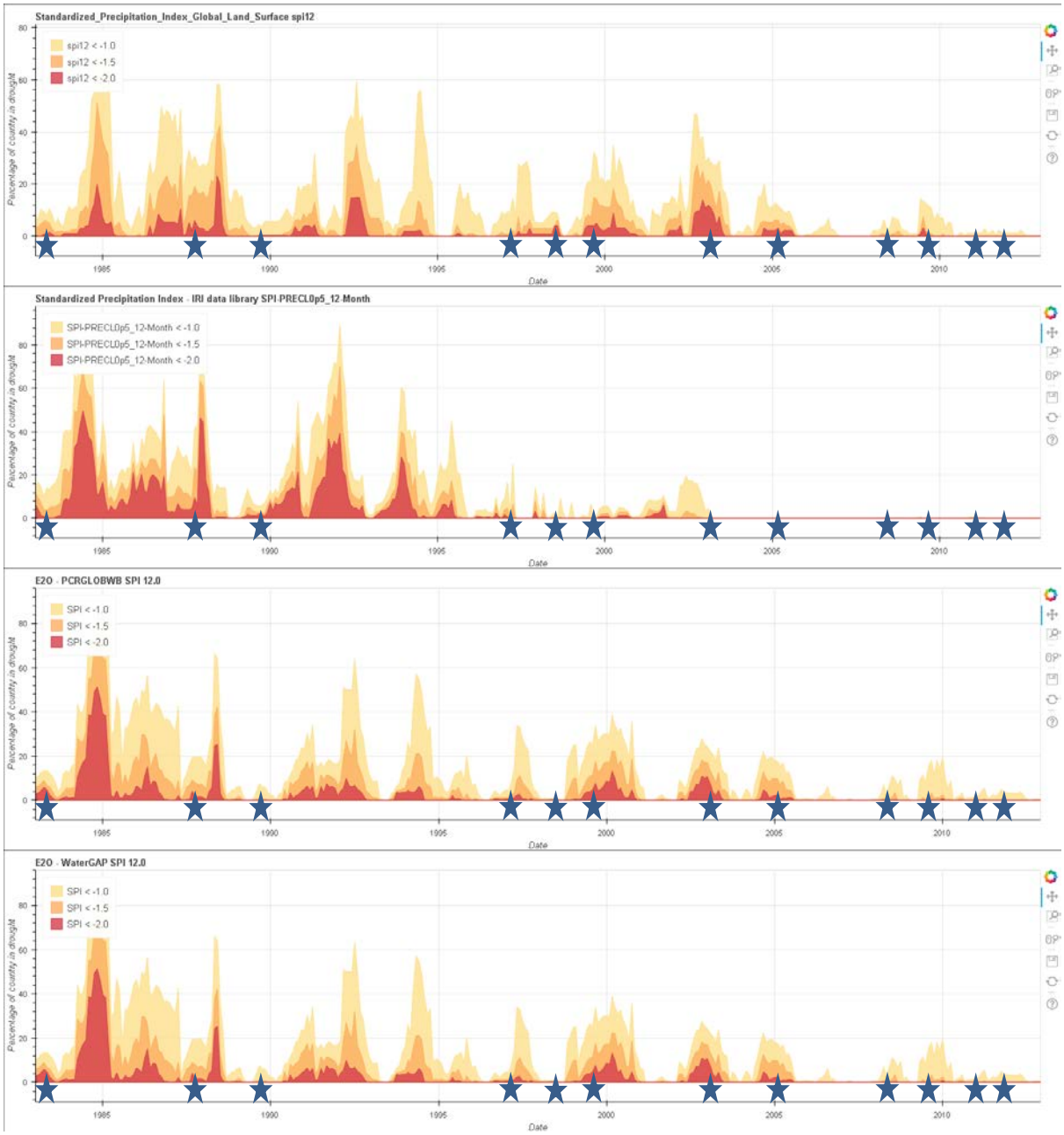

Figure A3.3 – Meteorological drought index SPI12 based on Global Land Surface (top), based on IRI data library (second), based on PCR-GLOBWB (third), and based on WaterGAP (bottom) for Ethiopia. Grey stars indicate drought events recorded by EM-DAT.

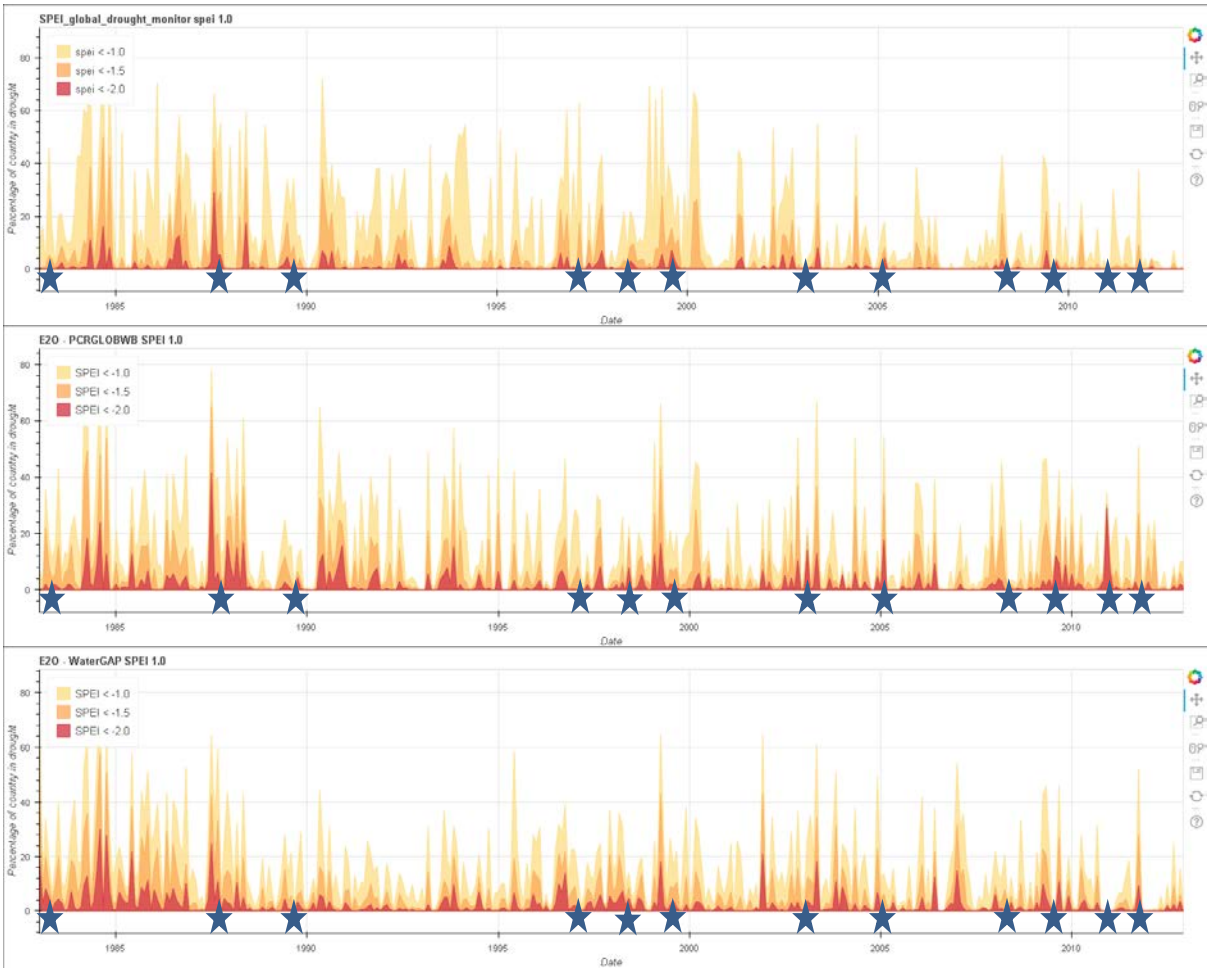

Figure A3.4 – Meteorological drought index SPEI1 based on Global Drought Monitor (top), based on PCR-GLOBWB (middle), and based on WaterGAP (bottom) for Ethiopia. Grey stars indicate drought events recorded by EM-DAT.

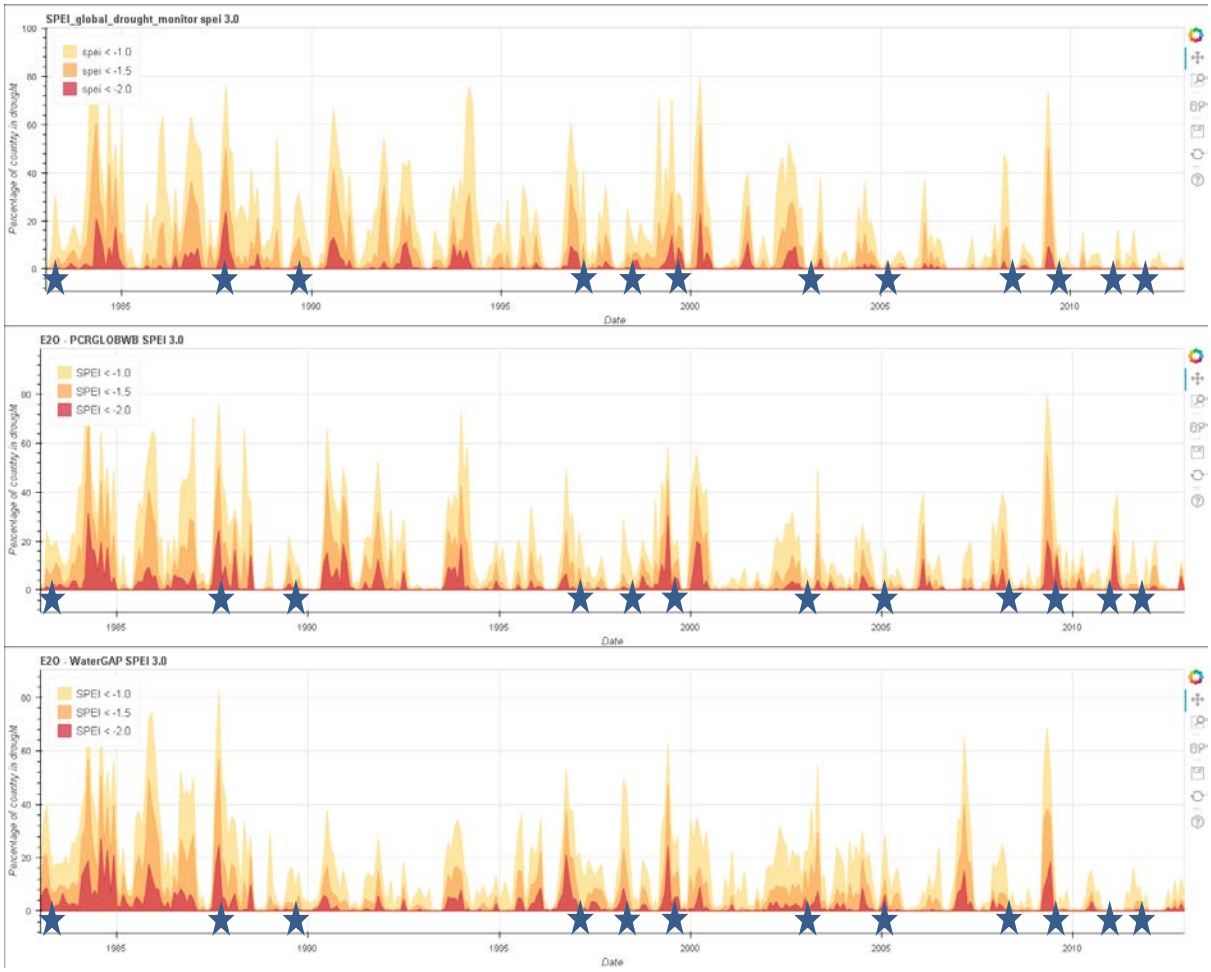

Figure 3.5 – Meteorological drought index SPEI3 based on Global Drought Monitor (top), based on PCR-GLOBWB (middle), and based on WaterGAP (bottom) for Ethiopia. Grey stars indicate drought events recorded by EM-DAT.

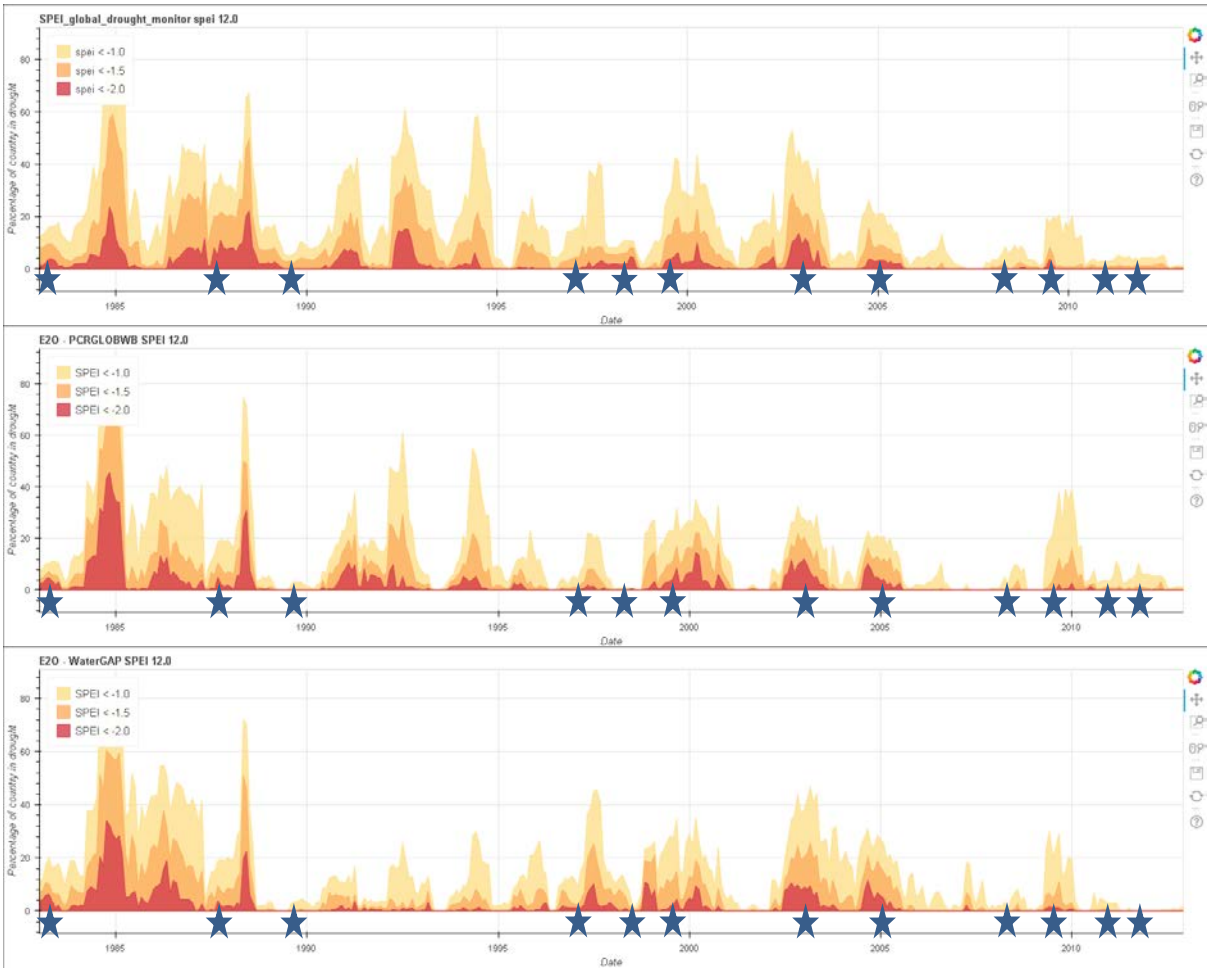

Figure A3.6 – Meteorological drought index SPEI12 based on Global Drought Monitor (top), based on PCR-GLOBWB (middle), and based on WaterGAP (bottom) for Ethiopia. Grey stars indicate drought events recorded by EM-DAT.

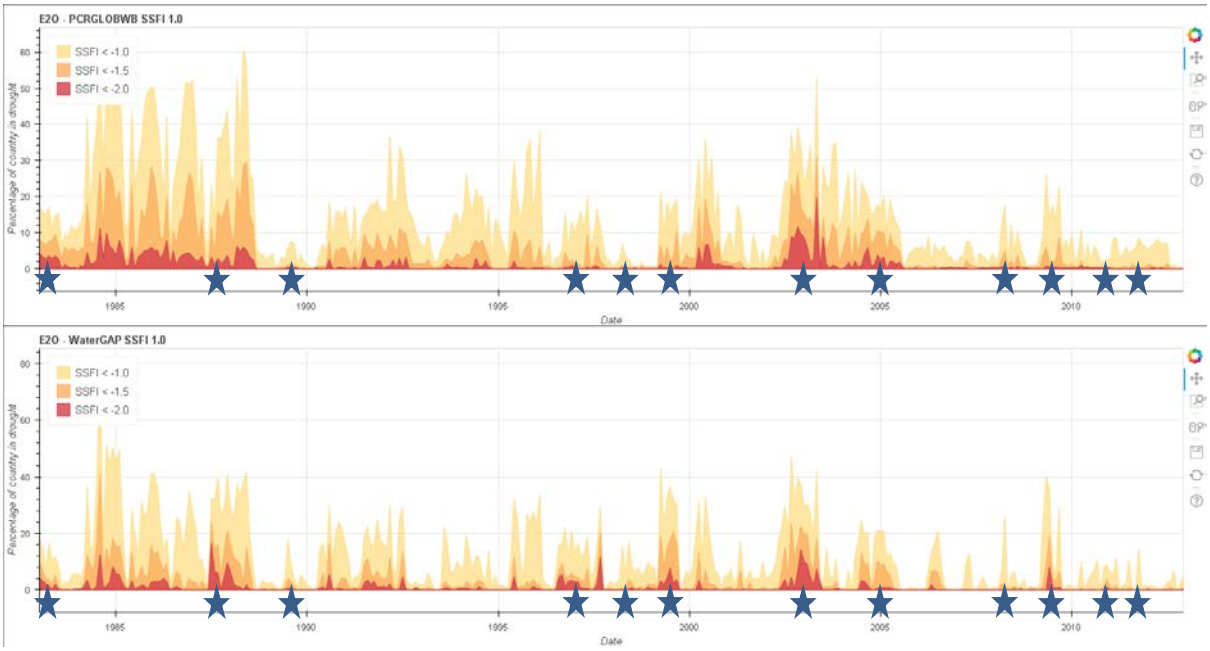

Figure A3.7 – Hydrological drought index SSFI-1 based on based on PCR-GLOBWB (top) and based on WaterGAP (bottom) for Ethiopia. Grey stars indicate drought events recorded by EM-DAT.

A4. Figures Fiji

Figure A4.1 – Meteorological drought index SPI1 based on IRI data library (top), based on PCR-GLOBWB (middle), and based on WaterGAP (bottom) for Fiji. Grey dots indicate drought events recorded by Fiji meteorological service; Grey triangles indicate drought events recorded by EM-DAT and Fiji meteorological service.

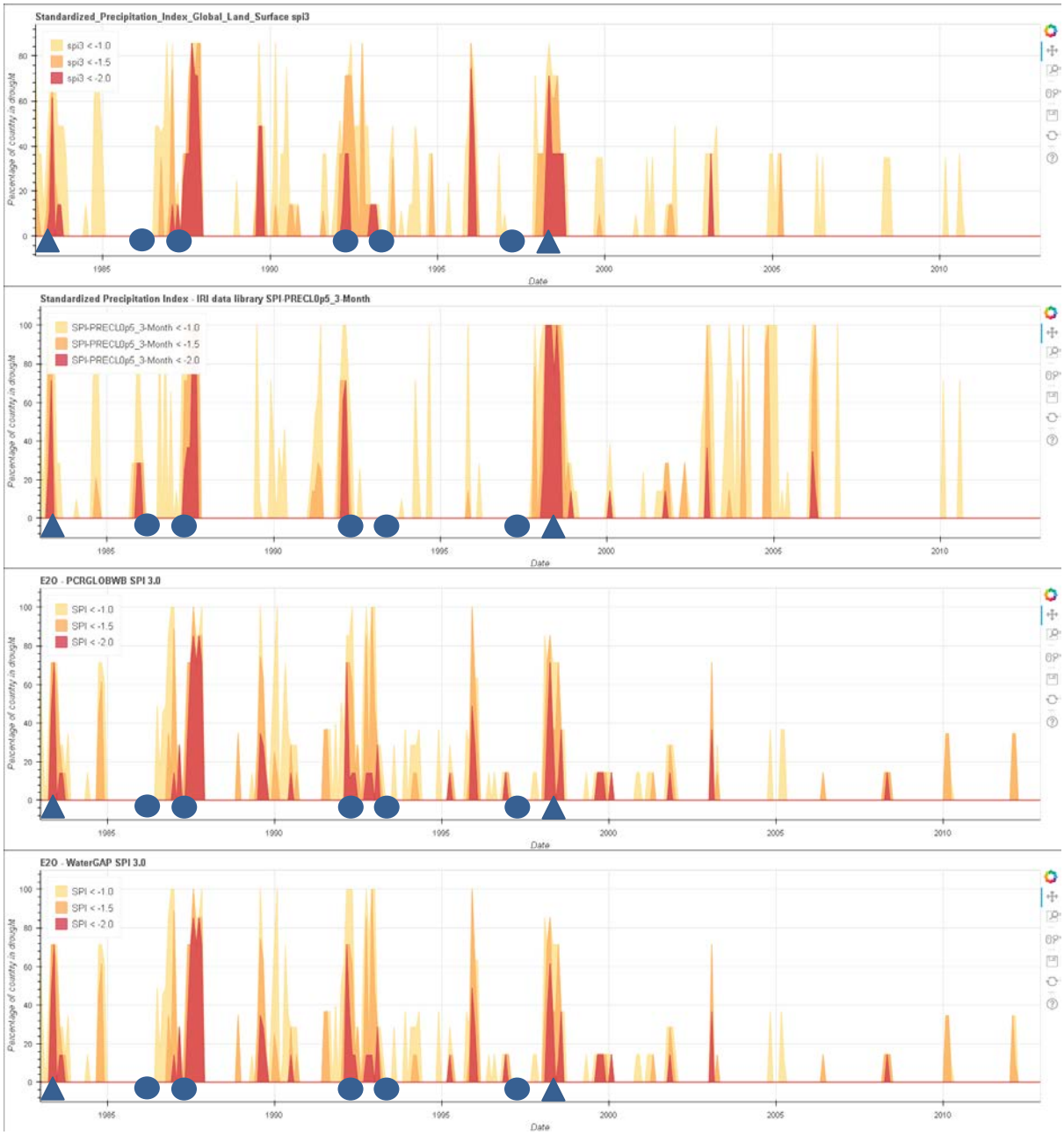

Figure A4.2 – Meteorological drought index SPI3 based on Global Land Surface (top), based on IRI data library (second), based on PCR-GLOBWB (third), and based on WaterGAP (bottom) for Fiji. Grey dots indicate drought events recorded by Fiji meteorological service; Grey triangles indicate drought events recorded by EM-DAT and Fiji meteorological service.

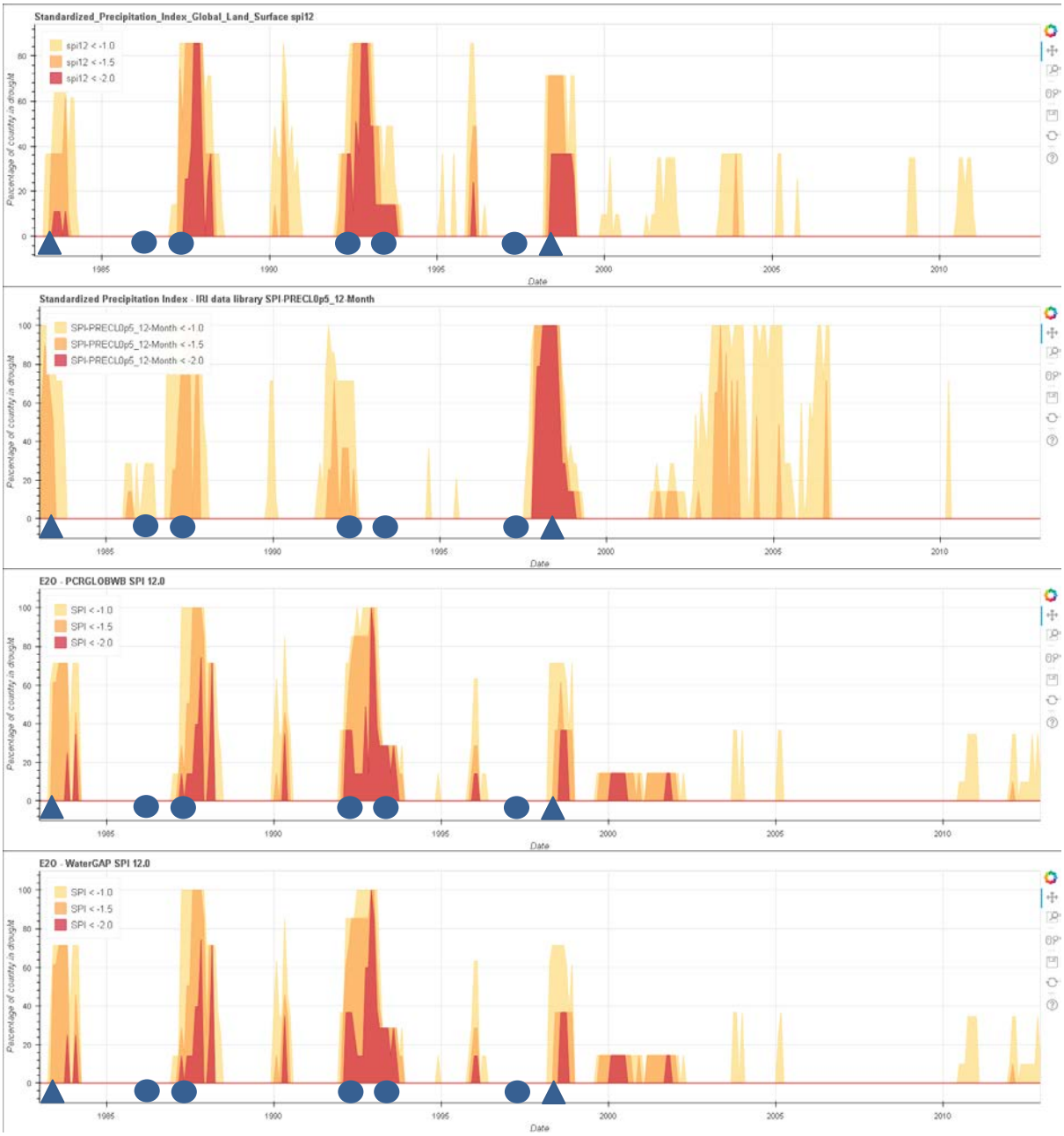

Figure A4.3 – Meteorological drought index SPI12 based on Global Land Surface (top), based on IRI data library (second), based on PCR-GLOBWB (third), and based on WaterGAP (bottom) for Fiji. Grey dots indicate drought events recorded by Fiji meteorological service; Grey triangles indicate drought events recorded by EM-DAT and Fiji meteorological service.

Figure A4.4 – Meteorological drought index SPEI1 based on Global Drought Monitor (top), based on PCR-GLOBWB (middle), and based on WaterGAP (bottom) for Fiji. Grey dots indicate drought events recorded by Fiji meteorological service; Grey triangles indicate drought events recorded by EM-DAT and Fiji meteorological service.

Figure A4.5 – Meteorological drought index SPEI3 based on Global Drought Monitor (top), based on PCR-GLOBWB (middle), and based on WaterGAP (bottom) for Fiji. Grey dots indicate drought events recorded by Fiji meteorological service; Grey triangles indicate drought events recorded by EM-DAT and Fiji meteorological service.

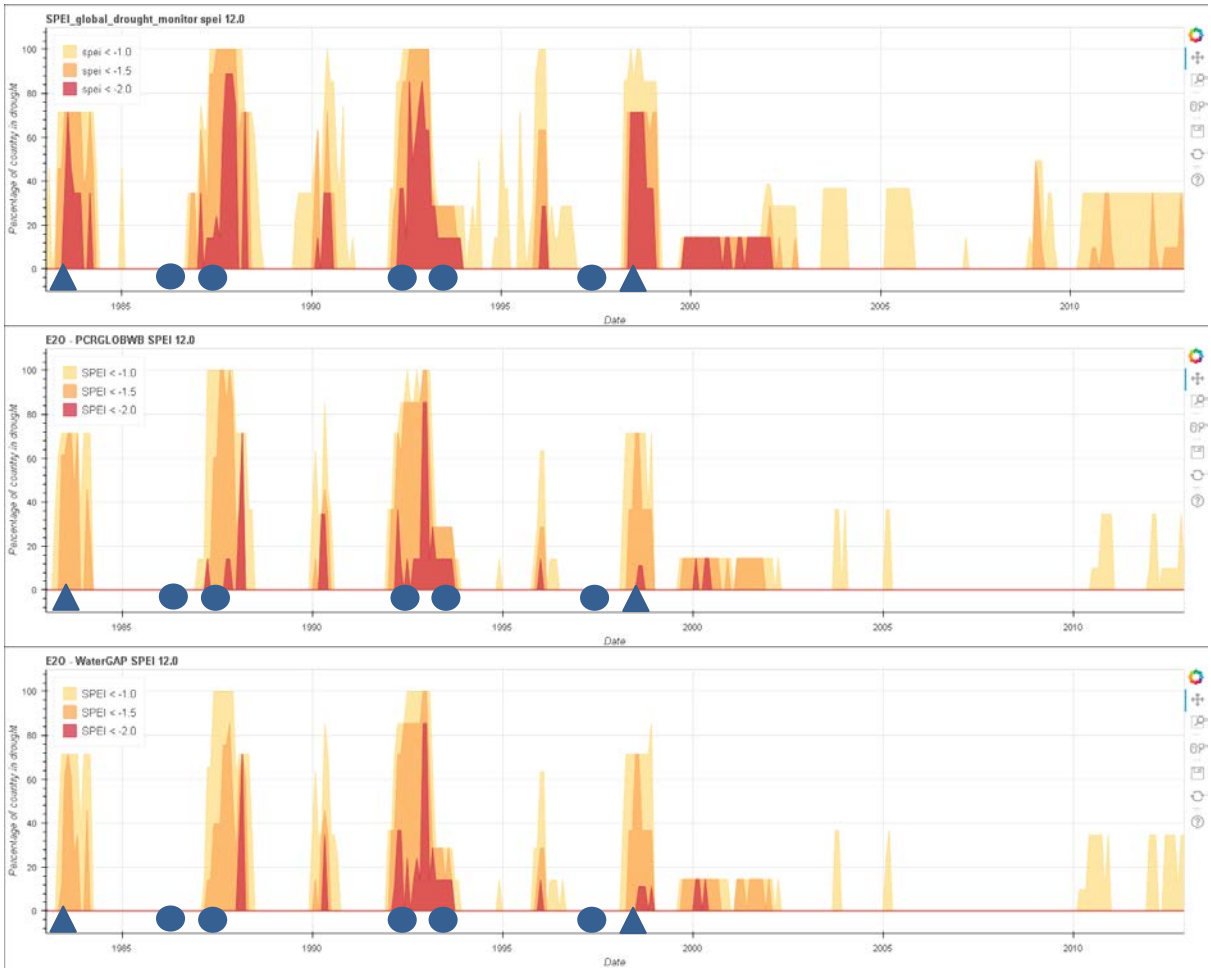

Figure A4.6 – Meteorological drought index SPEI12 based on Global Drought Monitor (top), based on PCR-GLOBWB (middle), and based on WaterGAP (bottom) for Fiji. Grey dots indicate drought events recorded by Fiji meteorological service; Grey triangles indicate drought events recorded by EM-DAT and Fiji meteorological service.

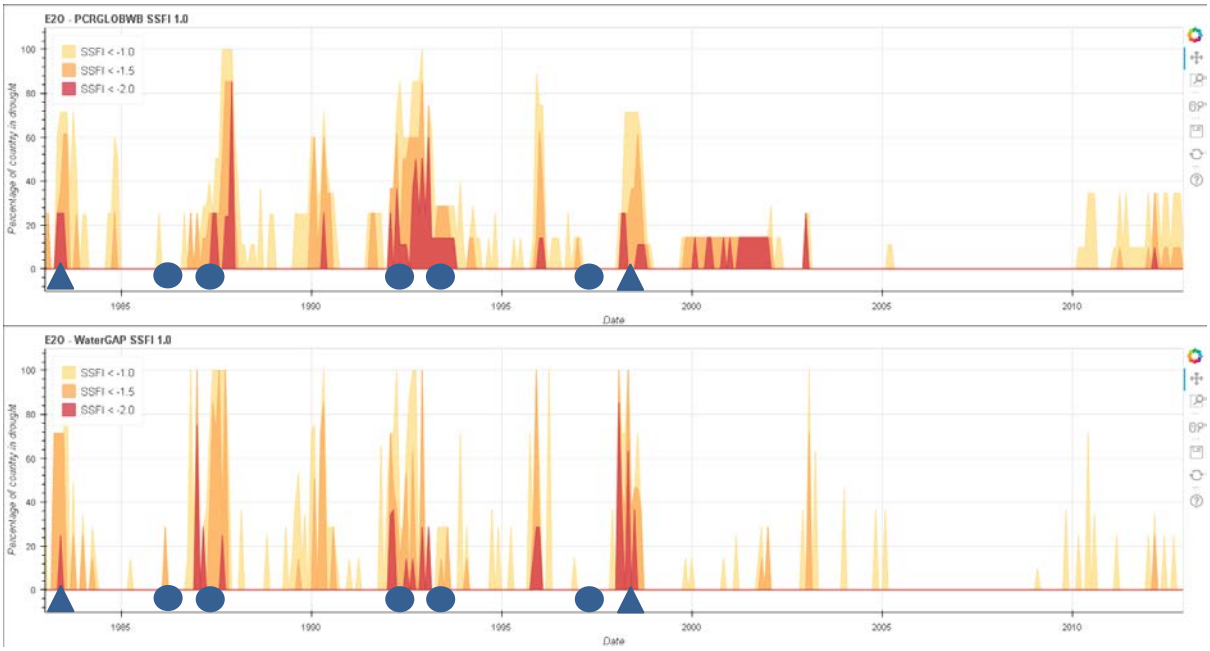

Figure A4.7 – Hydrological drought index SSFI-1 based on based on PCR-GLOBWB (top) and based on WaterGAP (bottom) for Fiji. Grey dots indicate drought events recorded by Fiji meteorological service; Grey triangles indicate drought events recorded by EM-DAT and Fiji meteorological service.

A5. Figures Malawi

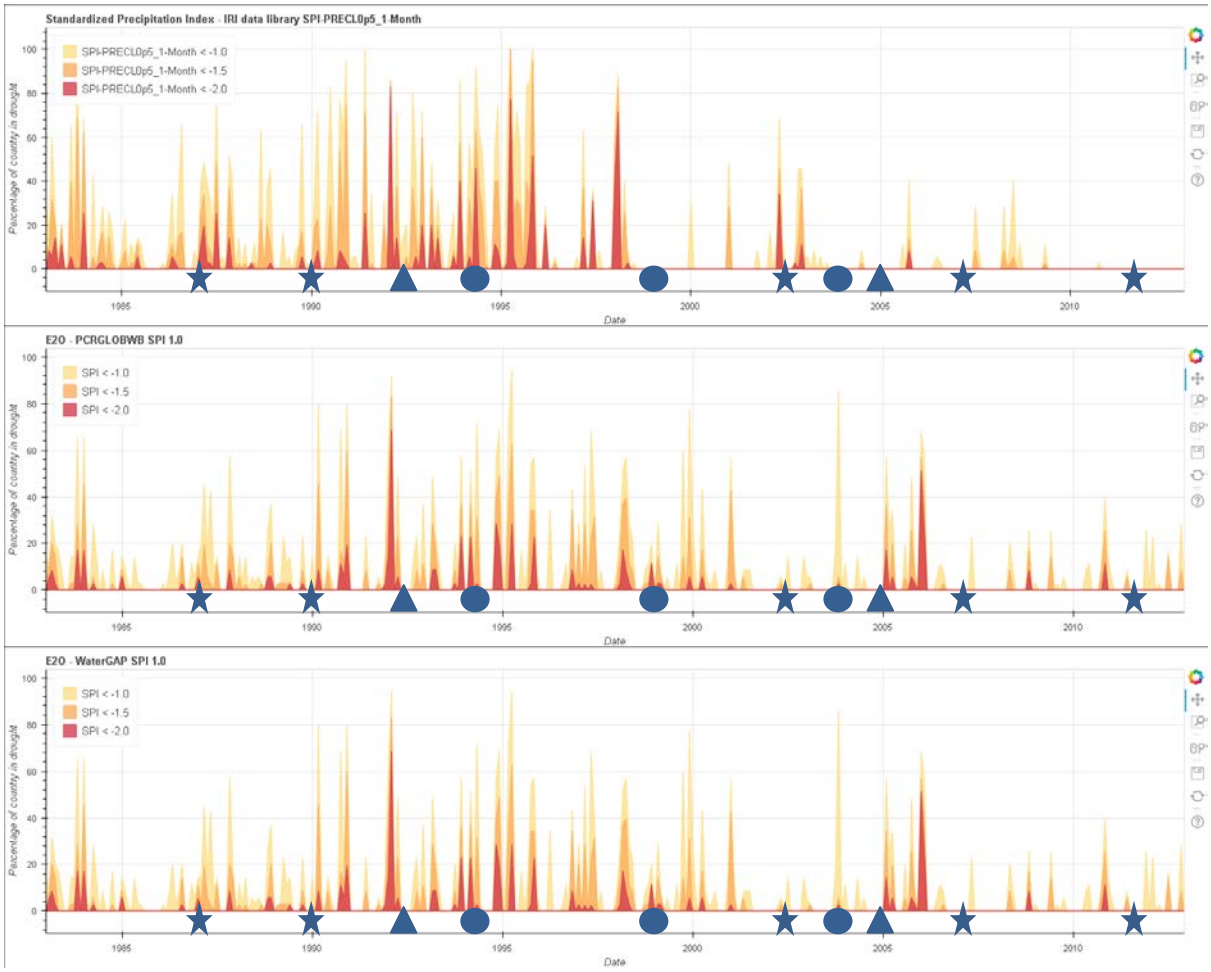

Figure A5.1 – Meteorological drought index SPI1 based on IRI data library (top), based on PCR-GLOBWB (middle), and based on WaterGAP (bottom) for Malawi. Grey stars indicate drought events recorded by EM-DAT; Grey dots indicate drought events recorded by RMSI; Grey triangles indicate drought events recorded by EM-DAT and RMSI.

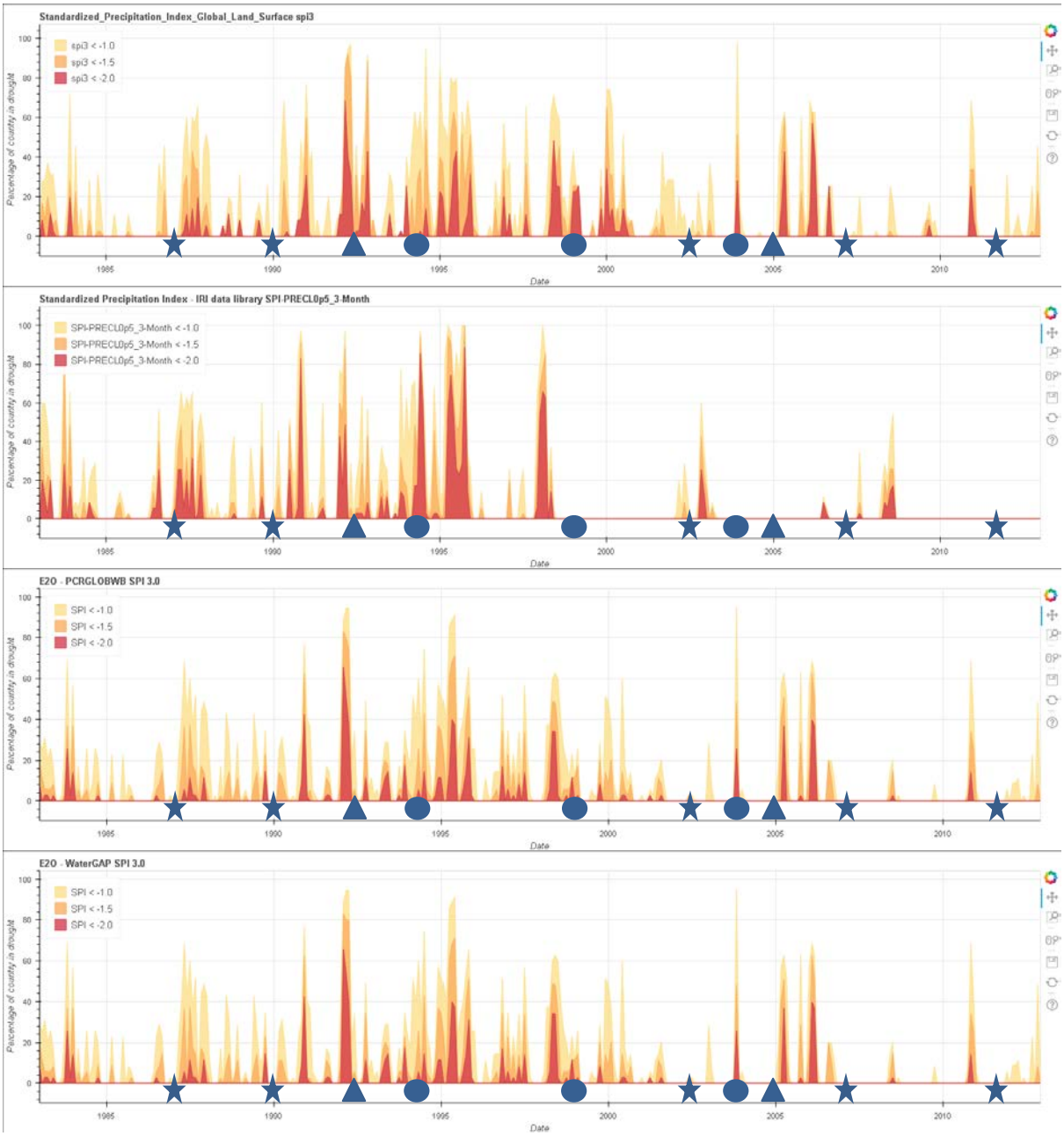

Figure A5.2 – Meteorological drought index SPI3 based on Global Land Surface (top), based on IRI data library (second), based on PCR-GLOBWB (third), and based on WaterGAP (bottom) for Malawi. Grey stars indicate drought events recorded by EM-DAT; Grey dots indicate drought events recorded by RMSI; Grey triangles indicate drought events recorded by EM-DAT and RMSI.

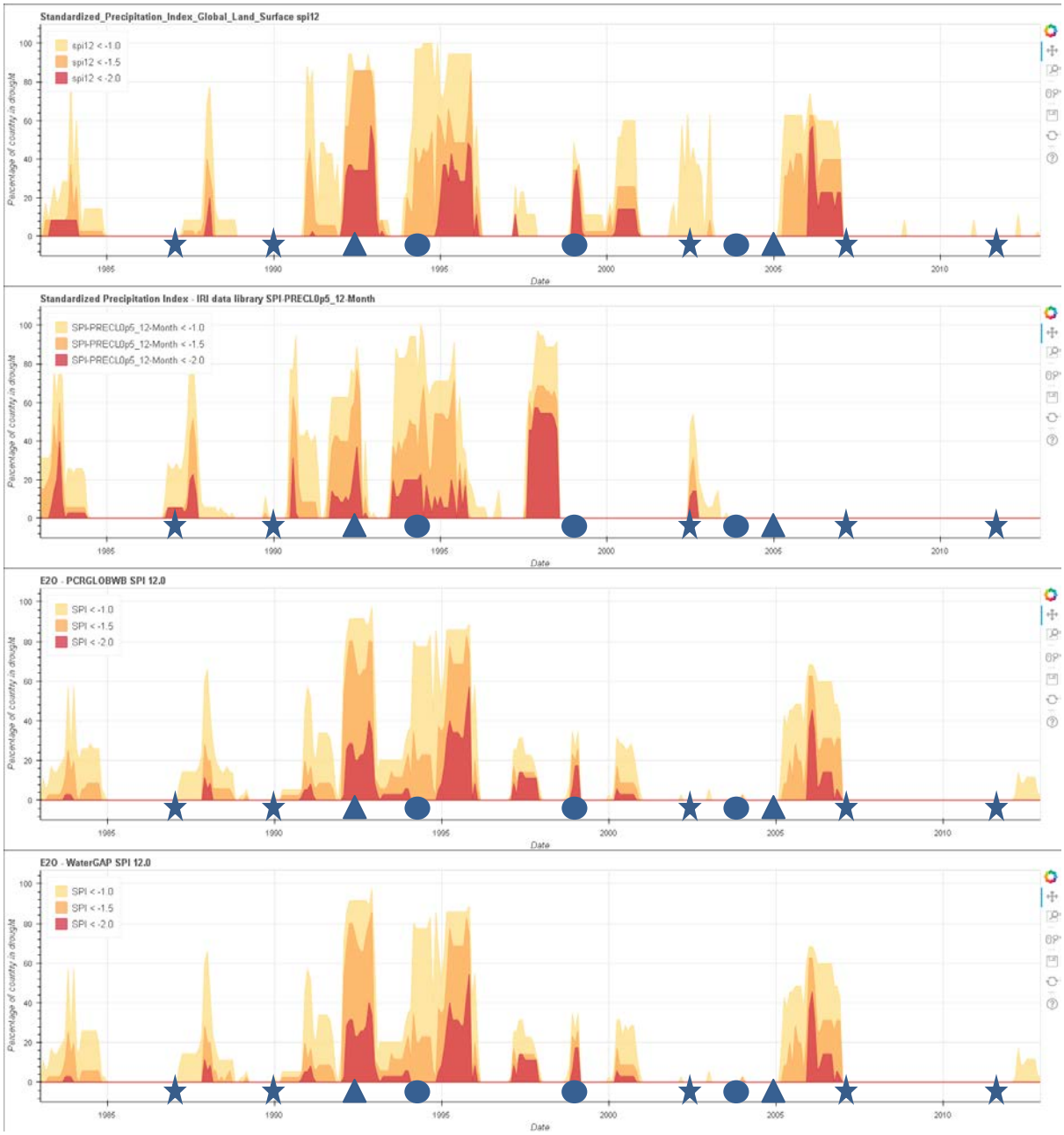

Figure A5.3 – Meteorological drought index SPI12 based on Global Land Surface (top), based on IRI data library (second), based on PCR-GLOBWB (third), and based on WaterGAP (bottom) for Malawi. Grey stars indicate drought events recorded by EM-DAT; Grey dots indicate drought events recorded by RMSI; Grey triangles indicate drought events recorded by EM-DAT and RMSI.

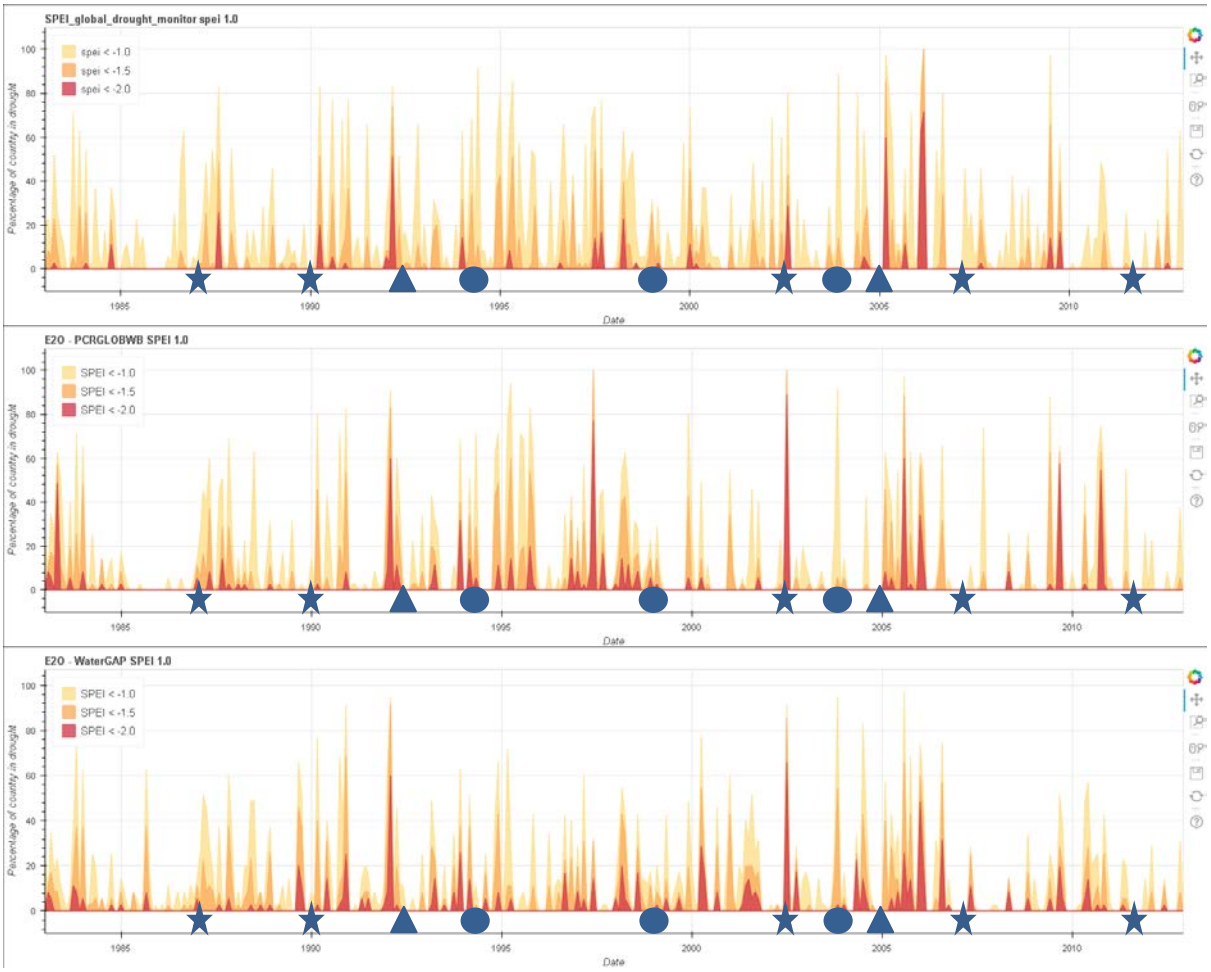

Figure A5.4 – Meteorological drought index SPEI1 based on Global Drought Monitor (top), based on PCR-GLOBWB (middle), and based on WaterGAP (bottom) for Malawi. Grey stars indicate drought events recorded by EM-DAT; Grey dots indicate drought events recorded by RMSI; Grey triangles indicate drought events recorded by EM-DAT and RMSI.

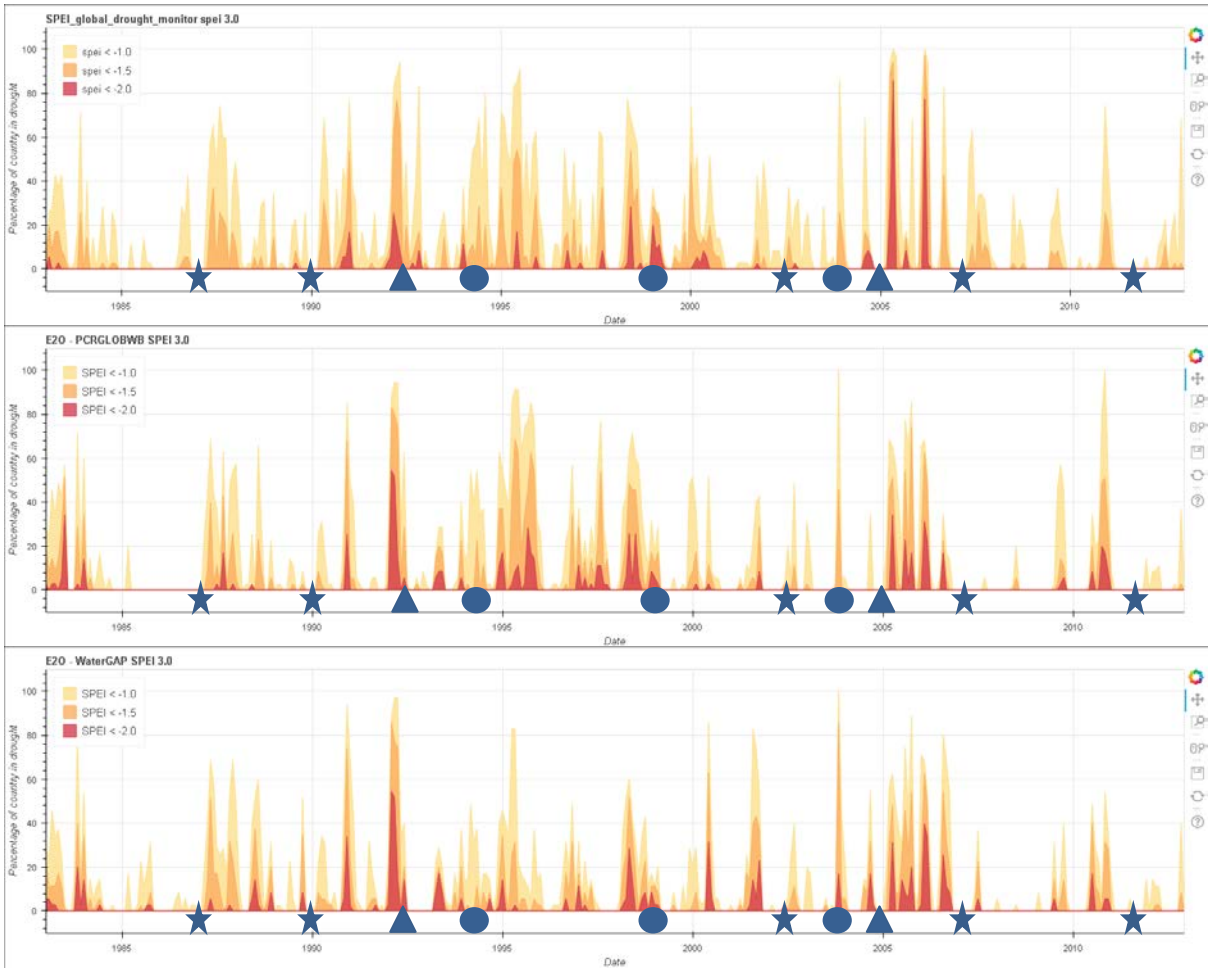

Figure A5.5 – Meteorological drought index SPEI3 based on Global Drought Monitor (top), based on PCR-GLOBWB (middle), and based on WaterGAP (bottom) for Malawi. Grey stars indicate drought events recorded by EM-DAT; Grey dots indicate drought events recorded by RMSI; Grey triangles indicate drought events recorded by EM-DAT and RMSI.

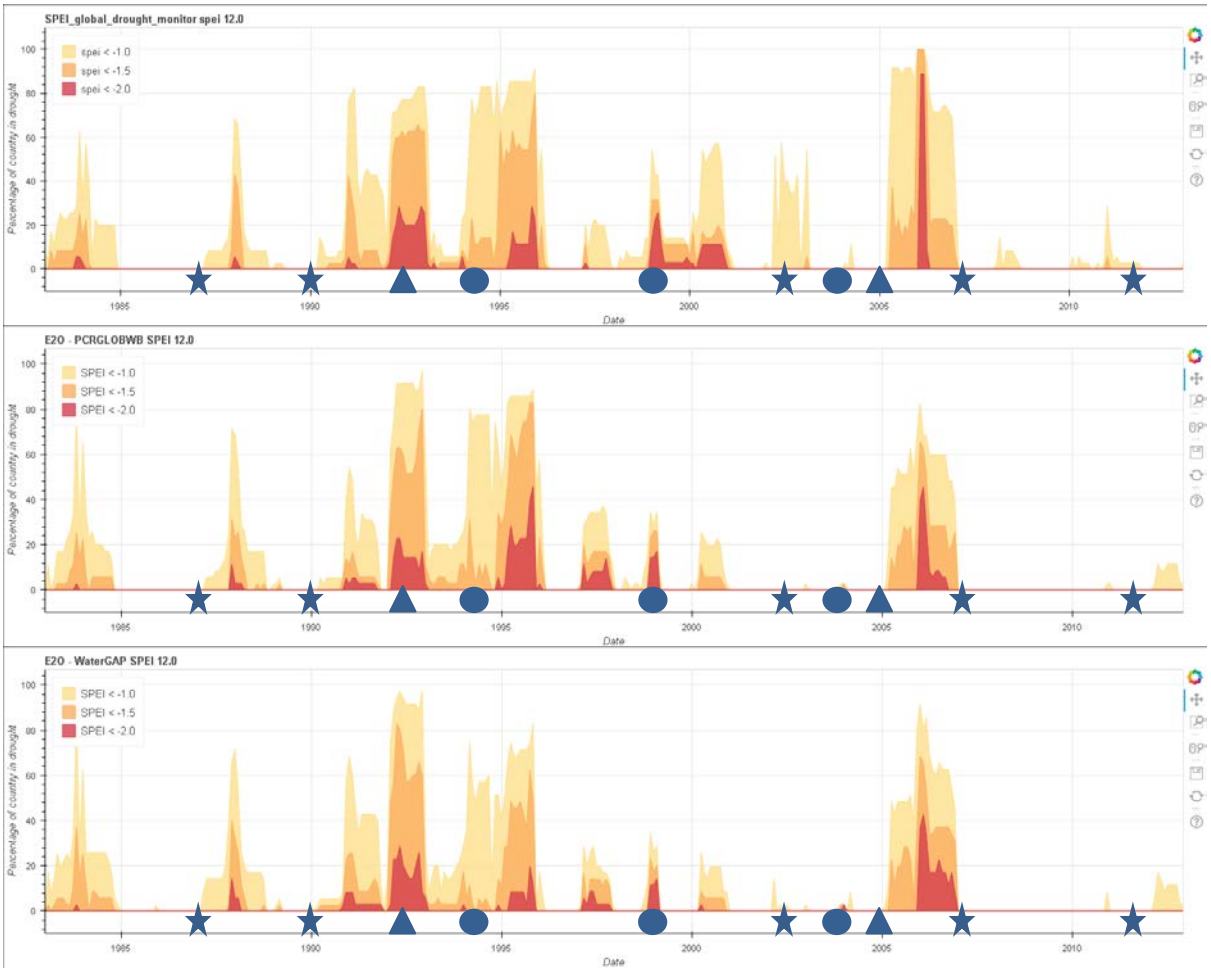

Figure A5.6 – Meteorological drought index SPEI12 based on Global Drought Monitor (top), based on PCR-GLOBWB (middle), and based on WaterGAP (bottom) for Malawi. Grey stars indicate drought events recorded by EM-DAT; Grey dots indicate drought events recorded by RMSI; Grey triangles indicate drought events recorded by EM-DAT and RMSI.

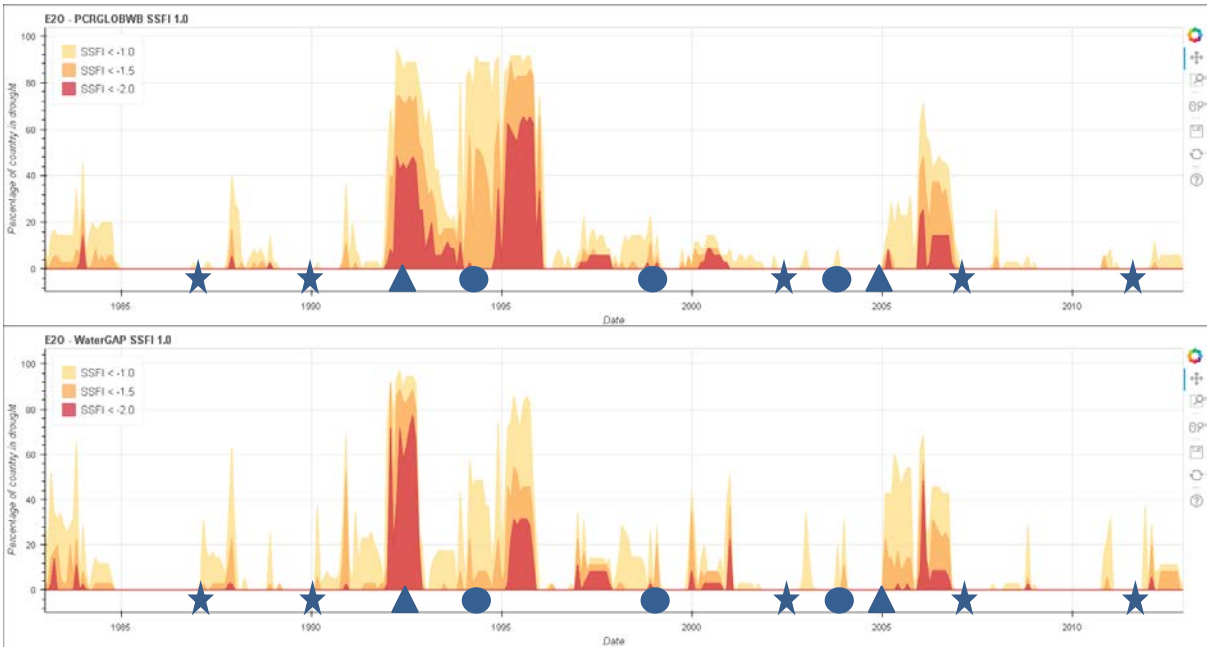

Figure A5.7 – Hydrological drought index SSFI-1 based on based on PCR-GLOBWB (top) and based on WaterGAP (bottom) for Malawi. Grey stars indicate drought events recorded by EM-DAT; Grey dots indicate drought events recorded by RMSI; Grey triangles indicate drought events recorded by EM-DAT and RMSI.